DOCTORAL DISSERTATION

博士論文

SLAKING AND DEFORMATION BEHAVIOR OF MUDSTONE

泥岩のスレーキングと変形挙動

14 WA 901
ANDIUS DASA PUTRA
（アンディウス　ダサ　プトラ）

Graduate School of Urban Innovation
Yokohama National University

YOKOHAMA - JAPAN
2018

SLAKING AND DEFORMATION BEHAVIOR OF MUDSTONE

by
ANDIUS DASA PUTRA

Supervisor
Assoc. Prof. MAMORU KIKUMOTO

A DOCTORAL DISSERTATION

Submitted to

Graduate School of Urban Innovation
Yokohama National University

in partial fulfillment of the requirements for the degree of

Doctor of Philosophy (PhD)

March 2018

DOCTORAL DISSERTATION

SLAKING AND DEFORMATION BEHAVIOR OF MUDSTONE

Dissertation approved:

Assoc. Prof. Mamoru KIKUMOTO
Academic Supervisor

Prof. Kazuo KONAGAI
Committee Member

Prof. Kimitoshi HAYANO
Committee Member

Assoc. Prof. Akira HOSODA
Committee Member

Assoc. Prof. Cui YING
Committee Member

Abstract

Slaking is a mechanical–hydraulic process in which geomaterials disintegrate or crumble when subjected to wetting and drying cycles; mudstone is particularly susceptible to this process. This paper presents an experimental, theoretical and numerical approaches to explore and get a better understanding of slaking behavior of mudstones and the mechanical consequences using a comprehensive set of experimental data obtained through accelerated slaking tests and newly developed one-dimensional compression slaking tests and triaxial slaking tests. The results of X-ray fluorescence (XRF) analysis, X-ray diffraction (XRD) analysis and scanning electron microscopy (SEM) are also used to elucidate the effects of mineral content and morphology texture on the slaking characteristics of crushed mudstone. The XRD test result showed a large amount of quartz mineral and clay mineral. Paid attention to the clay smectite (montmorillonite, saponite and nontronite) contents is necessary since smectite is one of expandable mineral. It significantly affects the physical weathering process to generate the fine particles. The linear correlation between the smectite mineral content and breakage parameter (B_r) has been proven that increasing the smectite content tends to increase the potential physical disintegration. As known, instead of physical weathering, the chemical weathering process also occurs even though it takes times during the process. It can be concluded that the slaking phenomenon on mudstone is induced by the physical weathering mechanism that occurs during the wetting and drying cycle applied, especially during the wetting phase which is then gradually followed by the chemical weathering mechanism. The dimension of intra-granular pores was involved to generate the physical weathering process, which has the same tendency with the smectite mineral content. Preliminary tests revealed that evolution of grading due to slaking causes irreversible change in the mechanical properties of crushed mudstone attributable to variation in packing density. Moreover, the evolution of grading during compression can increase the compressibility of crushed mudstone, with wetting and drying cycles causing significant compression despite the effective stress remaining constant.

A newly developed one-dimensional compression slaking test and triaxial slaking had been performed to explore the slaking behavior and its mechanical consequences. The potential large deformation can be reduced by conducting the high-stress level at the beginning and unload it. The remolded mudstone material which is packed in medium density still exhibited the progressive deformation when the slaking cycle started. The anisotropic behavior as a failure behavior occurs during wetting and drying cycle applied.

A proposed constitutive model for granular materials within the framework of elastoplastic had been developed by considering particle crushing phenomenon (Kikumoto, et.al, 2010). Extent the constitutive model to accommodate the particle size changes due to slaking cycles on mudstone are needed to obtain appropriate comprehension of their behavior. By considering the particle size distribution transformation caused by slaking cycles, this paper has established the development of an elastoplastic constitutive model incorporate the evolution law of grading state index (I_G) which considering the effect of crushing as well as the slaking phenomenon simultaneously.

Keywords: mudstone, slaking, weathering mechanism, stress-strain, failure deformation

Acknowledgement

In the name of Allah, the Most Gracious and the Most Merciful.

Alhamdulillah, all praises to Allah SWT for the strengths and His blessings in completing this dissertation. Special appreciation goes to my academic supervisor, Assoc. Prof. Mamoru KIKUMOTO for the continuous support and supervision during my Ph.D course and related research, for his patience, motivation, and immense knowledge. His guidance helped me in all the time of research and writing of this dissertation. I could not have imagined having a better advisor and mentor for my Ph.D course.

Besides my supervisor, I would like to thank the rest of my dissertation committee: Prof. Kazuo KONAGAI, Prof. Kimitoshi HAYANO, Assoc. Prof. Akira HOSODA and Assoc. Prof. Cui YING, for their insightful comments and encouragement, but also for the hard question which incented me to widen my research from various perspectives.

My sincere thanks also goes to Dr. Hiroyuki KYOKAWA, who teach me how to conduct the appropriate laboratory test and give me a chance to discuss with his student at Tokyo University. Without his support, it would not be possible to conduct a better experimental research. I thanks to my “senpai” and “kouhai” for the stimulating discussions and teach me how to make a simulation with my limited knowledge of computer language, for the sleepless nights we were working together before deadlines, and for all the fun we have had in the last four years. Further appreciation is also extended to the Research Center of Yokohama National University for providing the equipment to perform X-ray fluorescence, X-ray diffraction and Scanning Electron Microscope (SEM).

Last but not the least, I would like to thank my family: my beloved wife Nining PURWASIH, my sons Muhandis Bayu ADJIE, Dwikashinta Purwanda PUTRA, Abqari Althof Wianda PUTRA, my parents in heaven and to my brothers and sister for supporting me spiritually throughout writing this dissertation and my life in general. Great thanks to Indonesia Endowment Fund for Education (LPDP), Ministry of Finance Republic of Indonesia for financial support and the University of Lampung for the valuable support and give me a chance to take this opportunity.

TABEL OF CONTENT

Abstract
Acknowledgement
Table of content
List of Tables
List of Figures

Chapter 1 Introduction 1
1.1. Background 1
1.2. Sedimentary soft rocks: mudstones and shales 3
1.3. Objectives 8
1.4. The outline of dissertation 9

Chapter 2 Literature Review 11
2.1. The mechanisms of slaking 11
2.2. The slaking durability 15
2.3. Physical disintegration of mudstone particle 16
2.4. Mechanical consequences of mudstone induced by slaking 17

Chapter 3 The chemical and physical properties of mudstones 21
3.1. Introduction 21
3.2. X-ray fluorescence test (XRF test) 23
3.3. X-ray diffraction analysis (XRD test) 25
3.4. Scanning Electron Microscope (SEM) analysis 33
3.5. Summary 37

Chapter 4 Slaking Resistance 39
4.1. Introduction 39
4.2. Methods and Materials 40
4.2.1. Accelerated slaking 40
4.2.2. The Breakage Parameter (B_r) by Hardin 42
4.2.3. Chemical and Mineralogy Analysis 43
4.2.4. SEM and morphology analysis 44

4.3. Result and Discussion 44
4.3.1. Accelerated Slaking on Mudstone 44
4.3.2. The clay minerals content after acceleration slaking test 53
4.3.3. The morphology appearance 59
4.4. Summary 65

Chapter 5 One Dimensional Compression Slaking: Deformation behavior 68
5.1. Introduction 68
5.2. One Dimensional compression slaking test 69
5.2.1. Compression pressure system 69
5.2.2. Modified Confining Cylinder for slaking cycle 70
5.2.3. Wetting and drying cycles 71
5.3. Test Procedure of one dimensional compression slaking 71
5.3.1. Specimens preparation 71
5.3.2. Vertical loading test 73
5.3.3. Slaking cycles test 73
5.3.4. Particle Size Distribution after one-dimensional compression slaking test 73
5.4. Result and discussion of one-dimensional compression slaking test 75
5.5. The Effect of Relative Density (D_r) on Slaking Characteristics 83
5.6. The countermeasure effort to minimize the potential deformation due to slaking behavior 87
5.6.1. The effect of fine grain on slaking behavior 87
5.6.2. The effect of wetting and drying history on slaking behavior 89
5.6.3. The effect of loading/unloading history on slaking behavior 93
5.7. Summary 95

Chapter 6 Triaxial Slaking: Failure behavior 97
6.1. Introduction 97
6.2. Double Cell Triaxial System for Slaking 100
6.3. Calibration of the double cell triaxial system 102
6.4. Triaxial Slaking 103
6.4.1. Sample preparation 104
6.4.2. Triaxial slaking 104
6.5. Result and Discussion 107
6.6. Summary 113

Chapter 7 A Constitutive model of slaking and deformation behavior 114
7.1. Introduction 114
7.2. A constitutive model of saturated over-consolidated soil 116
7.3. A constitutive model by considering of grading change 120
7.4. Results and Discussion 122
7.4.1. Parametric studies 122
7.4.2. Validation of the proposed model 124
7.4.3. The applicability of proposed model 128
7.5. Summary 132

Chapter 8 Conclusion and Recommendation 134
8.1. Conclusion 134
8.1.1. The chemical and physical properties effect to the slaking on mudstone 134
8.1.2. The slaking resistance induced by wetting and drying cycle 135
8.1.3. One dimensional compression slaking test 136
8.1.4. Triaxial slaking test 136
8.1.5. A propose constitutive model by considering the particle size distribution changes due to slaking cycles 137
8.2. Recommendation 138

LIST OF TABLES

Table 1. Engineering problems caused by the weathering of sedimentary rocks in Japan (Chigira & Oyama, 1999)

Table 2. Estimates of slake durability and long-term material behavior based on the rate of change of strength (R) value (compiled with data from Santi & Higgins, 1998; Santi, 1995)

Table 3. Particle shape after accelerated slaking test

Table 4. The Nou mudstone properties

Table 5. The initial void ratio (e_i) and relative density (D_r) of Nou mudstone

Table 6. The initial void ratio (e_i) and relative density (D_r) of Nou mudstone during one-dimensional compression slaking test

Table 7. The initial parameter to observe the effect of fine grains on slaking behavior

Table 8. General properties of geomaterials

Table 9. Constitutive Parameters of the Kakegawa Mudstone and Kobe Mudstone

LIST OF FIGURES

Figure 1. The earth-construction disaster due to the existence of mudstone
Figure 2. The locations of mudstone specimen tested in this study
Figure 3. The Miyazaki mudstone specimen with the diameter 2.00-0.85 mm
Figure 4. Research flow chart of slaking and deformation behavior
Figure 5. The relation of water content of a mudstone to relative humidity free energy (Nakano, 1967)
Figure 6. (A) Shale sample, (B) Macro-pore with water and air pressure, (C) Air and water forces at the air-water interface in a macro-pore (Vallejo & Murphy, 1999)
Figure 7. Stress-strain relationship of Mercia mudstone weathering zone 1, 3 and 4 (drained, cell pressure 68.95 kPa) showing change from brittle to plastic behavior as weathering process (after Chandler 1969 in Hobbs, et.al, 2002)
Figure 8. The stress-shear displacement-volume change relationship (90% compaction degree) (Yoshida & Hosokawa, 2004)
Figure 9. Relationship between number of wetting and drying cycles (N) and increment vertical displacement during wetting (Sharma, 2012)
Figure 10. Delayed failure due to slaking (Nakano et.al., 1998)
Figure 11. The initial chemical elements of mudstone as the result of XRF test.
Figure 12. Data base interpretation of mineralogy content of Kobe mudstone
Figure 13. The PDXL analysis result against Kobe mudstone, Kakegawa mudstone and Hattian Bala mudstone
Figure 14. The XRD patterns of three kinds of mudstone to observe the smectite mineralogy content (dash-line red box magnified)
Figure 15. The XRD patterns of crushed mudstone regarding the clay mineral content
Figure 16. The summary of mineralogy composition against mudstone specimen
Figure 17. SEM images showing the surface texture of mudstone specimens at two different magnifications (×50 and ×500)
Figure 18. SEM image showing the surface texture of Toyoura sand at two different magnifications (×150 and ×500)
Figure 19. The size of intragranular pores of mudstone specimen
Figure 20. The Rock density of mudstone specimens
Figure 21. The mudstone specimen for accelerated slaking test (NEXCO-110-2012)
Figure 22. Change in particle size accumulation curve and definitions of B_r parameters
Figure 23. Variation in particle size distribution during accelerated slaking
Figure 24. Particle size distribution D_{10}, D_{50} and D_{90} corresponding to the percentages 10%, 50%,

and 90% of particle after accelerated slaking test
Figure 25. Correlation between Breakage parameter (B_r) and the particle size diameter at D_{50}
Figure 26. Grain crushing ratio (H) against Slaking ratio (S)
Figure 27. The XRD patterns of clay mineralogy content of Kobe, Kakegawa and Hattian Bala mudstone before and after accelerated slaking test
Figure 28. Changes of clay mineralogy content of mudstone and shale materials after accelerated slaking test
Figure 29. A variation of smectite mineral content during accelerated slaking test
Figure 30. The effect of smectite content as an expansive clay mineral to the weathering process based on the breakage parameter (B_r)
Figure 31. A variation of illite and quartz content after chemical reaction between smectite and kaolinite
Figure 32. The combining percentage of pyrite as the main mineral on the process oxidation and smectite as an expansive clay to the weathering mechanism
Figure 33. The effect of oxidation of pyrite mineral combining with the expansive potential of smectite content on the process of weathering of mudstone
Figure 34. Air entrapment may occur by short–circuit of macro-pore (a), in a rough macro-pore (b) and by condensation of water in pore accesses (c)
Figure 35. The morphology surface appearance of mudstone specimens after slaking with magnification of x500
Figure 36. The tendency relationship between the diameter of intra-granular pores and breakage parameters (B_r)
Figure 37. The relationship between mudstone density (ρ_d), smectite mineral content and breakage parameter (B_r) correspond to slaking behavior on mudstone
Figure 38. The mechanism of weathering and the subsequent cementation process of mudstone
Figure 39. Photograph of One Dimensional Compression Slaking apparatus
Figure 40. Schematic diagram of one dimensional compression slaking test assembly
Figure 41. Change in particle size accumulation curve by particle crushing and slaking and definitions of I_G and B_r parameters
Figure 42. Change in particle size of Kakegawa mudstone during one-dimensional compressive slaking testing
Figure 43. Change in particle size of Kobe mudstone during one-dimensional compressive slaking testing
Figure 44. Change in particle size of Hattian Bala mudstone during one-dimensional compressive slaking testing
Figure 45. Change in compressive properties and particle size of Kobe mudstone during one-dimensional compressive slaking testing

Figure 46. Change in compressive properties and particle size of Kakegawa mudstone during one-dimensional compressive slaking testing
Figure 47. Change in compressive properties and particle size of Hattian Bala mudstone during one-dimensional compressive slaking testing
Figure 48. Change in compressive properties and particle size of Toyoura sand during one-dimensional compressive slaking testing
Figure 49. Relationship between wetting and drying cycles and the maximum and minimum void ratio of Kakegawa mudstone
Figure 50. Relationship between wetting and drying cycles and the maximum and minimum void ratio of Hattian Bala mudstone
Figure 51. Relationship between wetting and drying cycles and the maximum and minimum void ratio of Toyoura sand
Figure 52. The variation of λ_s (slaking) and Δe (compression) during one dimensional compression slaking test
Figure 53. Changes in particle size distribution due to variation in void ratio and relative density during one dimensional compression slaking test
Figure 54. The breakage parameter (B_r) of each case to check the effect of initial void ratio (e_i) and relative density (D_r) on slaking behavior
Figure 55. Change in compressive properties and particle size of each case to observe the effect of initial void ratio and relative density
Figure 56. The volumetric compression behavior of Nou mudstone under one-dimensional compression slaking test
Figure 57. Effects of Non-Plastic Fines particles on Minimum and Maximum Void Ratios
Figure 58. Changes in the particle size curve of the Nou Mudstone in the one-dimensional compression slaking test by adding fine grains material
Figure 59. Compression characteristics and particle size change in Nou Mudstone one-dimensional compression slaking test (fine particle addition)
Figure 60. Decrease of void ratio due to addition of fine particle on Nou mudstone
Figure 61. Changes in the particle size distribution of Nou Mudstone due to initial wetting and drying cycles (the wetting and drying history)
Figure 62. Compression characteristics and particle size change in one-dimensional compression slaking test of Nou mudstone under conditions of wetting and drying cycle history
Figure 63. Changes in particle size distribution of Nou Mudstone in one-dimensional compression slaking test under stress history condition
Figure 64. Compression characteristics and particle size change in one dimensional compression slaking test of Nou mudstone under stress history condition
Figure 65. Schematic devices of Triaxial slaking

Figure 66. Double Cell Triaxial system devices and water level control
Figure 67. Principle calculation of volume change in double cell triaxial slaking system
Figure 68. The water level change inside the inner cell as representative of the volume changes of soil specimen
Figure 69. State reference of water level during compression and expansion stage of soil specimen
Figure 70. The result of B-check to confirm specimen saturated
Figure 71. Calibration of volumetric strain measurement by burette and inner cell
Figure 72. A schematic overview of triaxial slaking testing
Figure 73. Schematic of E/P regulator for Axial Pressure and Cell Pressure
Figure 74. The photograph of triaxial specimen preparation
Figure 75. Changes in particle size distribution during triaxial slaking testing on mudstone
Figure 76. Change in compressive properties and strain behavior of Kobe mudstone during triaxial slaking testing
Figure 77. Change in compressive properties and strain behavior of Kakegawa mudstone during triaxial slaking testing
Figure 78. Change in compressive properties and strain behavior of Hattian Bala mudstone during triaxial slaking testing
Figure 79. Volume change characteristic due to slaking cycle of Kobe mudstone with different deviatoric stress
Figure 80. Volume change characteristic due to slaking cycle of Kakegawa mudstone with different deviatoric stress
Figure 81. Volume change characteristic due to slaking cycle of Hattian Bala mudstone with different deviatoric stress
Figure 82. State Boundary Surface including Normal Consolidation Line (NCL) and Critical State Line (CSL)
Figure 83. Description of response to Over-Consolidated Soil based on the concept of the sub-loading state boundary
Figure 84. Change in the specific volume of over-consolidated soil considering change in particle size
Figure 85. The effect of material parameter on the proposed model related to crushing stress (p_{ci}) and crushing resistance (p_r)
Figure 86. Validation of the proposed model based on the one-dimensional compression slaking test result of Kakegawa mudstone
Figure 87. Validation of the proposed model based on the one-dimensional compression slaking test result of Kobe mudstone
Figure 88. Validation the model based on triaxial slaking test result of Kobe mudstone

Figure 89. Validation the model based on triaxial slaking test result of Kakegawa mudstone
Figure 90. The diagram contour of relationship between accelerated slaking parameter (λ_s) in accordance with grading state index (I_G) and number of slaking cycle (n) for Kakegawa mudstone (a) and Kobe mudstone (b)
Figure 91. Parametric study of the parameter (λ_s) that represents of acceleration slaking under σ_v' = 1256 kPa
Figure 92. The Distribution of compressibility parameter (Δe) based on varying the parameter λ_s, p_r and σ_v'
Figure 93. The volumetric compression behavior during the loading and unloading stress and followed by the three slaking cycles

Chapter 1

Introduction

1.1. Background

An appropriate attention should be paid when the sedimentary soft rocks such as mudstones, siltstones, tuffs, shales and other clay-bearing rocks was considered in earth construction works. Sedimentary soft rocks cannot be classified as hard rocks or soft soils in terms of their behavior and show an intermediate behavior between the soils-rocks. The performance of ground fills derived from such materials is closely related to the strength and durability of the individual rock fragments. Once disturbed or weathered, some of these materials retain the mechanical characteristics of the original material, but others degrade within a time frame that is relevant to the long-term performance of earthen structures such as embankments (Figure 1) and cut slopes (Walkinshaw & Santi, 1996; Botts, 1998; Santi, 2006; Vallejo & Pappas, 2010). This has already led to numerous problems being encountered in the construction of embankments or cut slopes through mudstone or shale formations (Shamburger et al., 1975; Hopkins & Beckham, 1998), as well as the many embankments in Japan that are constructed using crushed mudstone. One of these embankments, located on the Tomei expressway in Makinohara district, failed during the Surugawan earthquake in 2009, with subsequent field investigation and analysis identifying the primary cause to be slaking of the mudstone (Yasuda et al., 2012).

Landslides occurring on tertiary sedimentary rocks are also of great interest in places where such deposits are widely exposed, as the bedrock or mudstone in such cases has usually been weathered and gradually weakened into landslide clay. When subjected to repeated wetting and drying cycles, granular fills derived from mudstones and shales tend to develop a finer grain size through slaking, which also reduces the stiffness and strength of the material and can lead to structural instability. This makes it necessary to understand fully the weathering process and the changes in the physical and mechanical characteristics of geomaterials derived from weak rocks such as mudstones, especially when it comes to studying the long-term

stability problems of slopes (Bhattarai et al., 2006). The slaking of weak rocks has been extensively studied experimentally (Nakano, 1967; Franklin & Chandra, 1972; Moriwaki, 1974; Vallejo et al., 1993; Yoshida et al., 2002; Yoshida & Hosokawa, 2004; Yasuda et al., 2012) through slake-durability tests (Franklin & Chandra, 1972) and other similar tests, in which number of wetting and drying cycles are applied under unconfined conditions to evaluate the weathering resistance of granulated shales, mudstones and siltstones. This has demonstrated that slaking cycles significantly affect the degradation process and evolution of particle size distribution in such rocks (Sadisun et al., 2005; Gautam & Shakoor, 2013).

(a) A failure of highway embankment of Tomei expressway in Japan due to Surugawan earthquake

(b). A large settlement of Haliwen-Haekesak road in Indonesia due to landslide after heavy rainfall

Figure 1. The earth-construction disaster due to the existence of mudstone.

The U.S. Office of Surface Mining developed a classification system of strength–durability based on jar-slake tests and free swell and point load tests and insisted upon its effectiveness through the results of applying the system and the slake-durability tests to 116 samples (Welsh et al., 1991). Meanwhile, loading tests such as one-dimensional compression and unconfined compression tests performed on weak rocks with varying degrees of slaking have revealed that peak strength is significantly reduced not only by soaking (Yoshida & Hosokawa, 2004; Schaefer & Birchmeir, 2013), but also by cyclic wetting and drying (Botts, 1998; Yasuda et al., 2012; Rocchi & Coop, 2015). Several studies have discussed the effects of various mineralogical, chemical, physical and mechanical properties on the weathering characteristics of weak-rocks. These studies have shown: expansive clay minerals have a dominant effect on the weathering of sedimentary rocks (Moriwaki, 1974; Chigira & Oyama, 1999; Bhattarai et al., 2006; Schaefer & Birchmeir, 2013); compression of the pore air entrapped in the macro-pores within the rock particles has a significant effect on the mechanism of slaking (Moriwaki, 1974; Vallejo et al., 1993); and the dissolution of the cementing agents into pore water is also considered to be a cause of slaking (Surendra et al., 1981).

The mechanism of the pore air compression within intragranular pores was further studied and the dominant effects of the roughness of the pore boundaries and the diameter of the pores on the resistance of particles against slaking as well as crushing have been pointed out (Vallejo et al., 1993; Vallejo & Murphy, 1999). Particle characteristics such as the grading of weak rock tend to evolve in response to slaking induced by wetting and drying, and this will ultimately affect the mechanical behavior, as the material after slaking is quite different from the original material. Weak rocks may lose their strength or stiffness through slaking, as this usually results in a decrease in the particle size. Such variation in mechanical characteristics during slaking can directly affect the deformation and failure behavior of the ground; however, so far, most studies have only looked at the role of slaking in the evolution of the particle size distribution or the change in behavior. Shima & Imagawa (1980) conducted cyclic wetting and drying tests on soft rock fragments under confined conditions and Pappas & Vallejo (1997) conducted static-compression-creep tests, in which time-dependent deformation of non-durable shales due to water absorption was measured under confined conditions. However, there has still been little discussion of the deformation behavior that is directly induced by slaking.

1.2. Sedimentary soft rocks: mudstones and shales

Sedimentary soft rocks are formed from sediment grains deposited by water, wind or ice. They are always formed in layers, called “beds” or “strata”, and quite often contain fossils.

Sedimentary rocks have covered about 60% of the continents and most of the ocean floor (Blatt et, al., 1980). Sedimentary rocks are composites of pre-existing rocks that have been weathered and eroded, or pieces of once-living organisms. Most fossils are found in sedimentary rocks of which there are three main types: sandstone, limestone, and shale/mudstone. Most of these rocks started as sediments carried in fluid, that were deposited as the current slowed. When the sediments are buried and dried, they become cemented to form rock. Most sedimentary rocks become cemented together by minerals and chemicals or are held together by electrical attraction; some, however, remain loose and unconsolidated.

Pettijohn (1975) suggests that the average shale or mudstones contains about two parts silts and one part is clay. It is likely that the grain size of fine-grained rocks varies widely. Texturally, clay is defined as all material finer than 4 microns; silt ranges in size from 4 to 63 microns; sand ranges from 63 microns to 2mm. The sizes of fine, unconsolidated particles can be determined by using an experimental method, which are based mainly on measuring the settling velocity of particles in water (Boggs, 2006). These methods cannot be used to measure the grain sizes of particles in mudstones and shales, which generally cannot be disaggregated to yield individual particles. The sizes of grains in consolidated rocks can be measured by using an electron microscope; however, this is an expensive procedure that is seldom done. Dewhurst, et.al (1998) stated that mudstones are fine-grained sedimentary rocks composed of silt and clay, commonly between 25% and 75% of clay or silt. Grain size is up to 0.0625 millimeters (0.00246 in) with individual grains too small to be distinguished without a microscope. Mudstones are found in deep sea environments as well as on continental margins and comprise about 70% of the volume of sedimentary basins around the world.

Mudstones are not well understood yet because of large variations in their mechanical and transport behavior unlike sandstone that have long been the subject to research. The high compressibility and low permeability of mudstones contribute to overpressure around the world (Broichhausen et al., 2005). Overpressure drives fluid flow in the subsurface, which impacts solute mass transport and heat transfer. Overpressure can cause slope instabilities such as submarine landslides that in turn can cause tsunamis, which can be fatal to highly populated coastal areas. Related to the mineral contents, clay minerals, fine-size micas, quartz, and feldspars are the most abundant minerals in mudstones or shales. A variety of other minerals may occur in these rocks in minor quantities, including zeolites, iron oxides, heavy minerals, carbonates, sulfates, and sulfides, as well as fine-size organic matter. Because of the difficulties involved in petrographic analysis of fine sediments, most investigators have concentrated on the clay mineralogy of shales, which can be determined fairly-easily by X-ray diffraction

(XRD) methods. Quantitative to semiquantitative determination of fine quartz, feldspars, and other minerals in shales can be made also by X-ray diffraction methods (Suryanarayana and Norton, 1998), with a scanning electron microscope equipped with an energy-dispersive X-ray unit (Goldstein et al., 2003), or with an electron probe microanalyzer (Reed and Romanenko, 1995). Also, quartz, feldspars, and other non-clay minerals can be separated from clay minerals in shales by chemical techniques (Blatt et al., 1982), allowing these non-clay minerals to be studied more effectively by petrographic methods.

In this study, the mudstone specimens were derived from eleven locations from different places in Japan, namely, Kakegawa, Kobe, Takasaki, Akita, Okinawa, Miyazaki, Nou, Jouetsu, Suzuka, Fujieda and Shimizu districts. Others mudstone specimen also derived from Pakistan, Indonesia and Australia. The Hattian Bala mudstone was sourced from a natural dam site located 3.5 km upstream of the Karli River, which is a tributary of the Jhelum River in Azad Jammu and Kashmir, Pakistan (Figure 2a). This natural dam was formed after the 2005 Kashmir earthquake, but was subsequently breached on 9 February 2010 (4 years and 4 months later) owing to rainfall following drought (Sattar et al., 2011). The Indonesia mudstone was obtained from the Krui city, West Lampung, Lampung Province (Figure 2b) due to several failures of embankment occurs. Meanwhile, the Australia shale was derived from the area near of Sydney (Figure 2c). The mudstone locations from Japan shown in Figure 2(d). Most of mudstone specimen were obtained from several highway embankments in Japan that consisted mainly of crushed mudstone. The Kakegawa mudstone was picked from an embankment located between the Kikugawa interchange and Fukuroi interchange on the Daiichi Tokai (Tomei) expressway and originated from the Hijikata formation of the Pliocene age, Neogene period. It is similar for Fujieda mudstone which has derived from the same formation and age with Kakegawa mudstone. The Kobe mudstone is a sedimentary rock found in the Kobe layer from the late Eocene to early Oligocene age and was sampled from an embankment on the Shin–Tomei expressway. The Takasaki mudstone was taken from an embankment located between the Fujioka interchange and Yoshii interchange on the Joetsu expressway, and which originated from the Yoshii layer of the Miocene age, Neogene period. The Akita mudstone is a sedimentary rock of the Pliocene age, Neogene period to early Pleistocene age, Quaternary period, and was taken from the Tentokuji formation near the Nihonkai–Tohoku expressway. The Okinawa mudstone is a rather uniform and silty mudstone that was sourced from a marine sedimentary layer of the late Miocene to Pliocene age, Neogene period. The Shimizu mudstone is a crushed sedimentary rock consisting of sandstone, mudstone and pudding stone that originated from the Hamaishidake group, and which was used for the construction of

embankments in the Chubu Odan expressway. The Jouetsu mudstone and Nou mudstone are mudstones which derived from near area of Nihorikai-Tohoku expressway. Suzuka mudstone was derived from the area near of Ise expressway. It was suspected that the failure of embankment due to the existence of weathering rock. Miyazaki mudstone was derived near of Higashi-Kyushu expressway and made by formation Shimanto belt at the Pliocene age.

(a) The location of Hattian Bala mudstone, Pakistan

(b) The location of Krui mudstone, Indonesia

(c) The location of Australia shale, Sydney, Australia

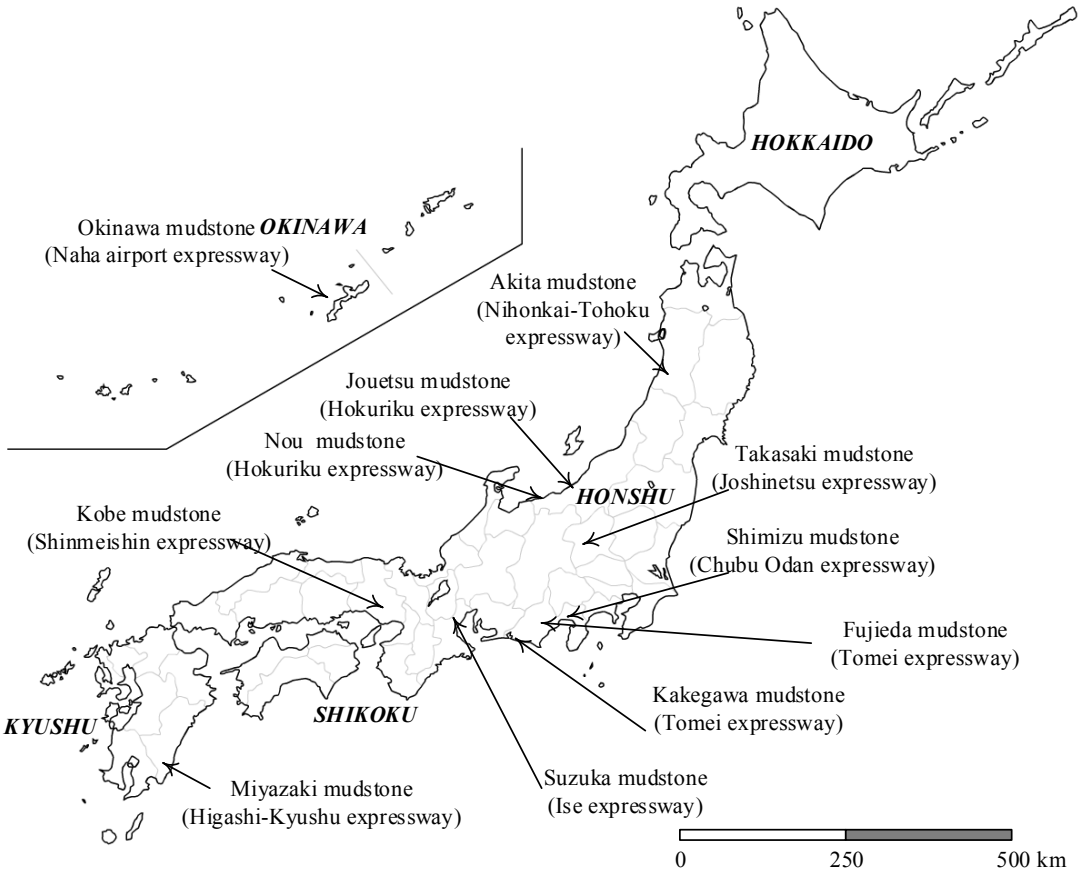

(d) The locations of mudstones specimen in Japan

Figure 2. The locations of mudstone specimen tested in this study

One sample of morphology texture of mudstone specimen is shown in Figure 3. Through the microscope photography, the morphology texture of Miyazaki mudstone texture could be seen after magnified for 500 times.

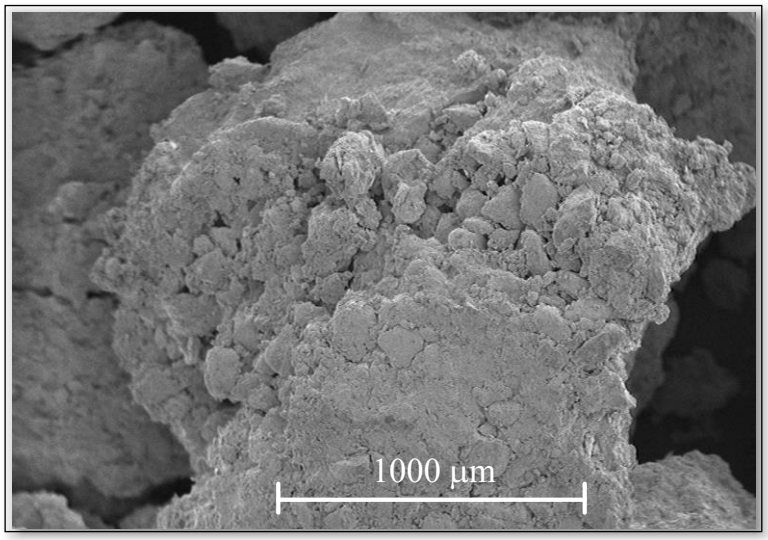

Figure 3. The Miyazaki mudstone specimen with the diameter 2.00-0.85 mm

1.3. Objectives

As mentioned, the increase of the geotechnical issues in the earth construction field due to widely used of mudstone are still necessary to be studied further. The large deformation on the highway embankment is one of issue due to slaking phenomena of mudstone. Slaking is a mechanical–hydraulic process in which geo-materials disintegrate when subjected to wetting and drying cycles; mudstone is particularly susceptible to this process. Mudstone as one of the geo-weathering rocks are intermediate in behavior between rock and soil, and they tend to transgress from rock-like to soil-like materials within relatively short time frames when involved with water (Botts, 1998). Even though many researchers have been devoted to studying the issues related to the deformation due to slaking phenomena of mudstone, but the proper comprehension of this issue is still needed. The main objectives of this study are to explores the slaking behavior of mudstone and their mechanical consequences related to the evolution grading changes. The mechanisms of weathering have been studied by performing the X-ray fluorescence test (XRF), X-ray diffraction test (XRD), Scanning Electron Microscope test (SEM) and the accelerated slaking test based on NEXCO standard procedure (NEXCO-110-2012). The slaking resistance during accelerated slaking test was presented as the particle size distribution changes and plotted into the graph, at the same time the slaking ratio (*S*) at the end of slaking was calculated. During the accelerated slaking test, the photograph of every stage of wetting and drying was documented as well. Next, two devices

had developed to realize the main objectives of this study. The newly one-dimensional compressive slaking test is developed to address the evolution of grading based on the stress–strain relationship that develops during slaking. Slaking and its direct effect on the deformation behavior were investigated, wherein the effective stress is held constant during wetting and drying cycles in order to observe the volumetric behavior that occurs in response to slaking.
To evaluating the failure deformation due to slaking of mudstone, the triaxial which provided with wetting and drying cycle was performed and the particle size distribution changes after the test was observed. Finally, a constitutive model is proposed which can take slaking into consideration by describing the evolution of an appropriate grading index due to slaking, and then link this to reference packing density.

1.4. The outline of dissertation

The outline of the dissertation is organized into 8 chapters. C**hapter 1** present the background of this study related to the geotechnical issues caused by mudstone material which has used widely as a material in the earth construction project. The slaking and deformation behavior of mudstone is necessary to be studied further to minimize the potential risks of earth construction failure in the future. In addition, a constitutive model is proposed by describing the evolution of an appropriate grading index due to slaking. As a guidance, the short research flow chart is present in this chapter.

Chapter 2 presents a summary review of relevant literature to strengthen the methodology and updating the current issues related to mudstone and weathering rocks. In addition, the recent efforts on the experimental study to observe the mudstone behavior are reviewed.

Chapter 3 presents a summary result of the mineral content of mudstone based on the XRF test and XRD test. The chemical constituent and mineral content are investigated to understand the weathering mechanism of mudstone. The microscope photography was performed to check the morphology texture and the possibility of the existence of intra-granular pores which has a potential to decrease the strength.

Chapter 4 presents the effect of weathering mechanism of mudstone to the particle size distribution changes under the accelerated slaking test. The mechanisms of weathering divided into two types are physical weathering and chemical weathering. The tendency relationship among chemical constituent, mineral content, morphology texture, intragranular pores and the grading changes were analyzed.

Chapter 5 presents the slaking and its mechanical consequences in one-dimensional compression condition. This chapter is paid attention to the grading change due to constant

stress and deformation after wetting and drying cycles. The evolution law of grading state index is one important parameter to be proposed in a constitutive model.

Chapter 6 presents the failure deformation behavior of mudstone due to slaking. The volumetric strain is measured using the double cell. The anisotropic behavior is expected to obtain at the end of this experiment as one of the slaking behavior of mudstone.

Chapter 7 presents a proposed constitutive model by extends the elastoplastic model that considers the particle-crushing phenomenon to accommodate the particle size change, due to slaking phenomenon on mudstone in the same framework as the particle size crushing phenomenon. The validation of the constitutive model against one-dimensional compression slaking and triaxial slaking tests were performed as one of the important outcomes from this chapter. The validation result will reveal of reproduce-ability of the constitutive model.

Chapter 8 the last chapter summarizes the substantial results obtained from this study regarding the mechanism of weathering process during wetting and drying cycle applied, the deformation and failure behavior due to slaking and a propose constitutive model by extent the particle crushing phenomenon.

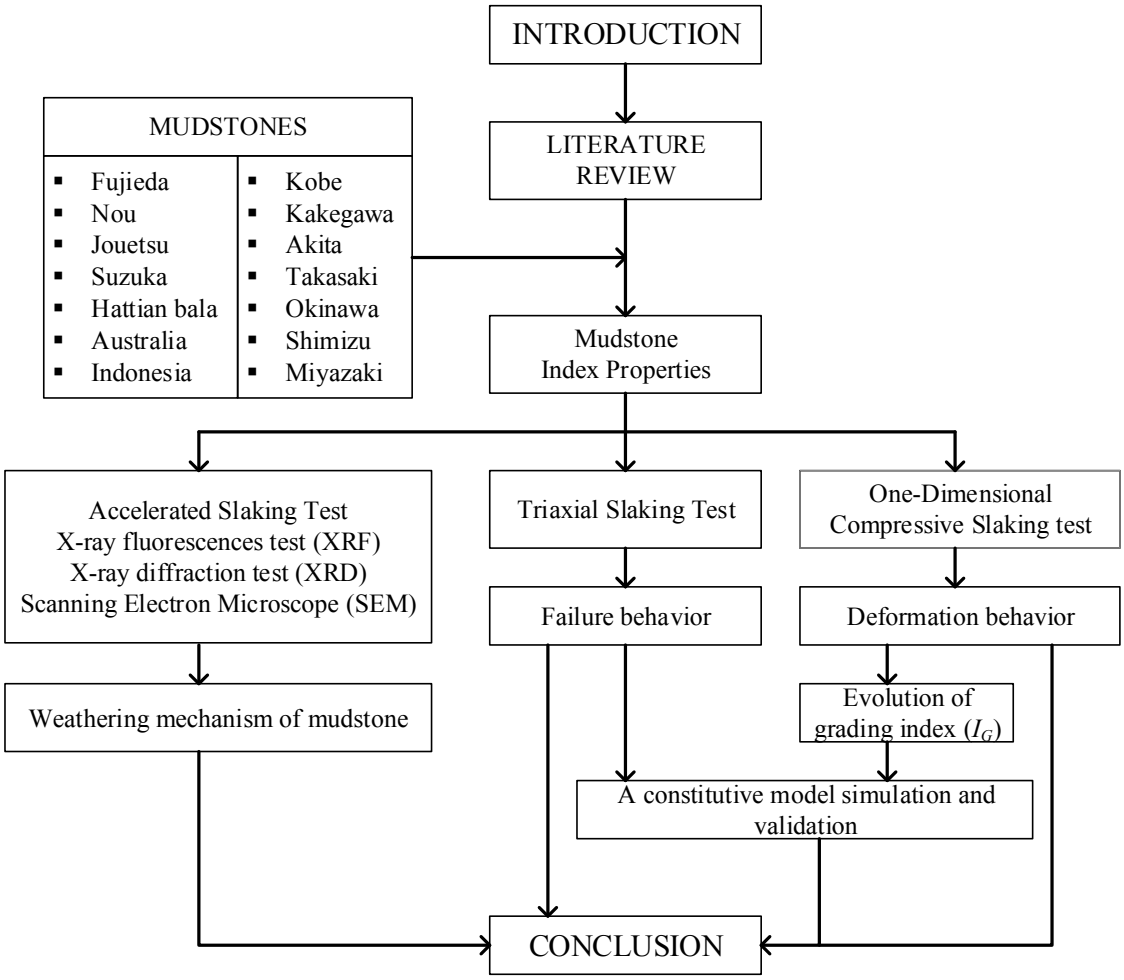

Figure 4. Research flow chart of slaking and deformation behavior

Chapter 2

Literature Review

As disclosed in the first chapter, number of research or studies regarding the investigating and observing slaking behavior of mudstones or shales had been performed for many years ago. A brief overview of existing literature on slaking behavior on many aspects and research works related to the mudstone are reviewed in this chapter. The definition of mudstone and the weathering mechanism of mudstone materials will be investigated by reviewing and concluding the result from the published journals. The chemical and physical properties associated with the mechanism of weathering during wetting and drying applied on mudstone are presented as well in this chapter. Since the particle size disintegration as an evolution of grading and decrease of strength due to slaking is one of the main parameters in this study, then it is become important to be reviewed.

2.1. The mechanisms of slaking

The term of slaking usually implies the phenomena of material “disintegration” or “crumble” observed when dried or undisturbed specimens of mudstone or shale are encountered with water. Most slaking is assumed to result from the disruption of diagenetic bonds and the release of stored strain energy (Bjerrum, 1967). Some clays, mudstone and shales at natural water content slake when immersed in water. However, if these materials are first dried and then rewetted, wetting and drying induced slaking can occur. In accordance with slaking experiment, the tendency for sedimentary rocks to weathered, soften, and slake upon drying and rewetting has been well documented. The degradation causes the material to soften and lose strength, possibly leading to slope failures. According to the softening of mudstone, Skempton (1964) noted that strength losses up to 80% in some deposits after it. Nakano (1967) during observing the mechanism of deterioration of bedrock (mudstone) in landslide zones has found that softening material is mainly due to the amounts of Gibbs' free energy evolved when hydrogen-bond is formed between originally adsorbed water molecules and newly adsorbed ones around

clay particles (Figure 5). After that, he was applied several monotonic torsional shears on crushed rocks under saturated condition reveal an enormous loss of strength due to water-induced granular decomposition.

Slaking mechanism in terms of pore-air compression. At the process of wetting and drying, when mudstone become dry, the air was drawn into macro-pores and a high suction pressure develops. As a result, it will increase shear stress and resistance of the individual fragments based on the high contact pressures. The bulk of the voids are filled with air under extreme desiccation conditions. When the mudstones immersed to the water and the water pulled in to each macro-pore, as a result, capillary forces developed due to suction, and the air that originally filled the micropores will be subjected to compression. Tensile failure of mineral skeleton along the weakest lanes may occur as a result of which the significant surface area to be exposed increase.

The air pressure developed in the macro-pores depends on the capillary pressures, which themselves are related to the surface tension of the water (Terzaqhi, 1937; Taylor and Spears, 1970; Seedsman, 1986) and the pore radius (Vallejo, et. al., 1993). Figure 6 exhibit the mechanism of the pore air compression within intragranular pores was further studied and the dominant effects of the roughness of the pore boundaries and the diameter of the pores on the resistance of particles against slaking as well as crushing have been pointed out (Vallejo et al., 1993; Vallejo & Murphy, 1999).

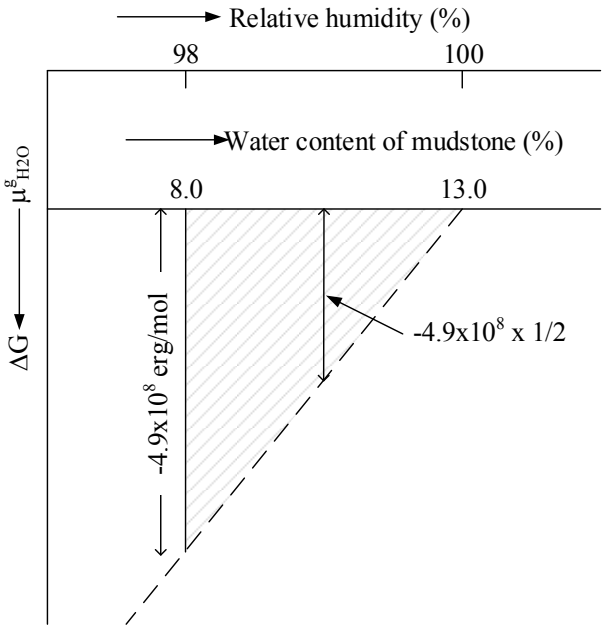

Figure 5. The relation of water content of a mudstone to relative humidity free energy (Nakano, 1967)

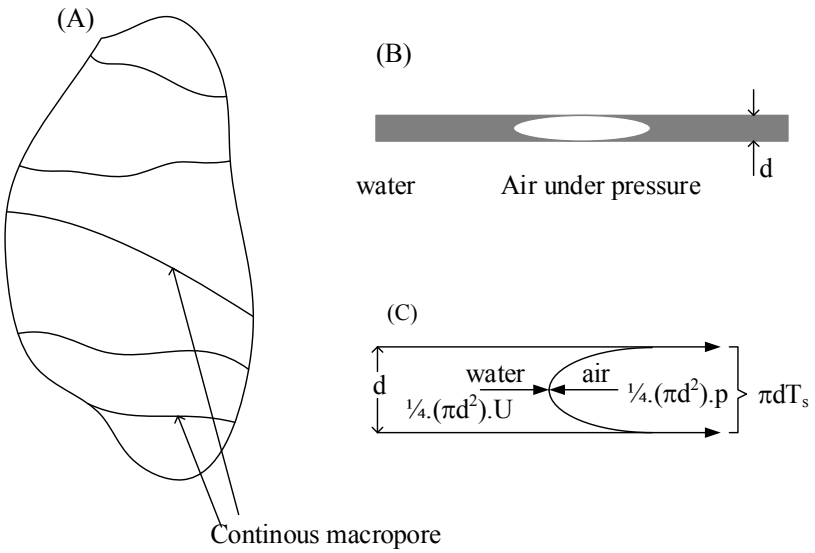

Figure 6. (A) Shale sample, (B) Macro-pore with water and air pressure, (C) Air and water forces at the air-water interface in a macro-pore (Vallejo & Murphy, 1999)

Weathering in over-consolidated clays and clay shale has been observed to be a significant process due to the mode of deposition and the bonding from diagenesis, especially in outcroppings. One of the largest and most problematic clay shales in the United States is the Pierre Shale Formation (Fleming et al. 1970). The strength reduction from the peak to residual strength is a source of the stability problems associated with these materials. Initial fissuring results from rebound in clay shales and leads to clay swelling, strain softening and weathering (Brooker and Peck, 1993).

A lot of the previous work on residual strength has focused on the mechanical aspects with less emphasis on the role of the more dynamic, physicochemical effects on residual strength. While the mineralogy mechanisms are well known, very few studies on clay shale have been conducted to analyze the role of physic-chemical occurrences on the strength loss. Nakano (1970) presented evidence that some materials will not slake if the water content remains above a certain threshold. The weathering processes in sedimentary rocks is an important concern include the significant progress regarding the identification of chemical content, physical appearance and/or combination of physical-chemical alteration mechanisms (Taylor and Smith, 1986; Seedsman, 1986; Taylor, 1988; Olivier, 1990; Vallejo and Murphy, 1999). Indeed, changes in mechanical properties during the test cannot be separated from the mineralogy or chemical contents and physical appearance. The mineralogy, geochemistry and physical and mechanical properties of rocks from four weathering profiles of Miocene to Pleistocene mudstones and sandstones in Japan showed that chemical weathering of sedimentary rocks is characterized by sequential reaction between percolating groundwater and rock-forming minerals. Pyrite, a common mineral contained in sedimentary rocks, is

especially important in these sequential reactions. Pyrite is oxidized by oxygen coming from the ground surface and sulfuric acid is generated at the base of the oxidized zone. The sulfuric acid, in turn, dissolves rock-forming materials to make a dissolved zone (Chigira & Oyama, 1999). The summarized of the previous studies of the weathering of sedimentary rocks and engineering geological problems caused by the weathering in Japan is tabulated in Table 1.

Table 1. Engineering problems caused by the weathering of sedimentary rocks in Japan (Chigira & Oyama, 1999)

Damage or process studied	Loaction	Formation	Age	Rock type	References
Heaving by sulfate	Fukushima	Taira Fm.	Miocene	Marine mudstiones	Oyama et.al (1996)
Exfoliation of stone sculpture by sulfate	Chiba	Miura Group	Miocene	Marine tuffaceous sandstones and tuff breccia	Seki & Sakai (1987)
Exfoliation of stone sculpture by sulfate	Fukushima	Tatsunokuchi Fm.	Pliocene	Tuff and mudstone	Seki et.al (1987)
Concrete footing damage by sulfate	Miyazaki	Miyazaki Group	Pliocene	Marine mudstone	Kobayashi (1982), Takaya (1983)
Weathering	Niigata	Yamaya Fm. Of Uonoma Group	Pliocene	Marine sandstone	Chigira (1988b)
Weathering	Niigata	Haizume Fm.	Pleistocene	Marine mudstone	Chigira (1988a, 1990)
Weathering	Hokkaido	Toyonikawa Fm.	Miocene	Marine sandstone and conglomerate cemented by zeolite	Chigira and Sone (1991)
Weathering	Chiba	Kakinokidai Fm.	Pleistocene	Marine mudstones	Shidahara et.al (1994)

The accelerate slaking has been observed to be dependent on the mineralogy and physic-chemical behavior, especially in materials with high activity clay minerals (Perry and Andrews 1984; Kikumoto et.al, 2016). Moriwaki and Mitchell (1977) investigated several factors that mainly affect the slaking phenomenon. They classified into four common kinds of slaking are dispersion slaking due to the Na-Kaolinite content is abundant, swelling slaking in response to volume changes of Na-Montmorillonite, body slaking when Ca-Kaolinite and Ca-Illite are abundant and surface slaking which has any correlation with the Ca-Montmorillonite content in the specimens. It can be concluded that the type of slaking was strongly controlled by clay mineralogy and the concentration of exchangeable sodium ions. Since mudstones contain a lot of clay minerals, their intrinsic slaking behavior will be significantly affected by the amount and type of the constituent clay minerals in a particle. Mitchell (1993) identifies three

mechanisms that lead to slaking: dispersion of soil particles, swelling caused by stress relief and water absorption and tensile stresses resulting from compression of entrapped air as water is absorbed.

2.2. The slaking durability

Landslides occurring on tertiary sedimentary rocks are also of great interest in places where such deposits are widely exposed, as the bedrock or mudstone in such cases has usually been weathered and gradually weakened into landslide clay. When subjected to repeated wetting and drying cycles, granular fills derived from mudstones and shales tend to develop a finer grain size through slaking, which also reduces the stiffness and strength of the material and can lead to structural instability. This makes it necessary to understand fully the weathering process and the changes in the physical and mechanical characteristics of geomaterials derived from weak rocks such as mudstones, especially when it comes to studying the long-term stability problems of slopes (Bhattarai et al., 2006). The slaking of weak rocks has been extensively studied experimentally (Nakano, 1967; Franklin & Chandra, 1972; Moriwaki, 1974; Vallejo et al., 1993; Yoshida et al., 2002; Yoshida & Hosokawa, 2004; Yasuda et al., 2012) through slake-durability tests (Franklin & Chandra, 1972) and other similar tests, in which a number of wetting and drying cycles are applied under unconfined conditions to evaluate the weathering resistance of granulated shales, mudstones, and siltstones. This has demonstrated that slaking cycles significantly affect the degradation process and evolution of particle size distribution in such rocks (Sadisun et al., 2005; Gautam & Shakoor, 2013). The U.S. Office of Surface Mining developed a classification system of strength–durability based on jar-slake tests and free swell and point load tests and insisted upon its effectiveness through the results of applying the system and the slake-durability tests to 116 samples (Welsh et al., 1991).

Santi (1998) improved the method to observe the durability of slaking by proposing three kinds of jar slake tests. These methods are aimed to improve reproducibility, reduce the level of effort required and better correlate the test to actual slaking characteristics. This kind of jar slakes test method reduce the test variability by one-third and offering a substantial improvement in consistency. The durability of weak rocks is an important parameter describing geomaterials susceptibility to breakdown upon exposure to water or during construction. While laboratory methods have been developed to measures durability, but there is no correlation between laboratory results and simple field test have been determined (Table 2). The field of parameters can predict slake durability with acceptable accuracy. The

recommended field tests, in order of desirability, are slake ratio index, jar slake, hammer rebound and NGI "Q" value (Santi, 1998; Santi & Higgins, 1998).

Table 2. Estimates of slake durability and long-term material behavior based on the rate of change of strength (R) value (compiled with data from Santi & Higgins, 1998; Santi, 1995)

(R) value (Jar slake category)	Slake durability	Slake Index	Long-term treatment*)
1	0 – 15	75 – 100	Soil
2	15 – 25	40 – 90	Soil
3	25 – 40	25 – 70	Very poor rock
4	40 – 55	5 – 30	Poor, yet durable rock
5	55 – 70	5 – 15	Good to fair rock
6	70 - 100	0 - 10	Good to fair rock

2.3. Physical disintegration of mudstone particle

Particle characteristics such as the grading of weak rock tend to evolve in response to slaking induced by wetting and drying, and this will ultimately affect the mechanical behavior, as the material after slaking is quite different from the original material. By means of triaxial testing over an extended range of pressures, Coop & Lee (1993) concluded that for a variety of sands of different mineralogy there was a unique relationship between the amount of particle breakage that occurred on shearing to a critical state and the value of the mean normal effective stress. The identification of a unique critical state line was then used as the basis for a critical state framework for sands at both large strains and small (Jovicic & Coop, 1997) and for the analysis of the behavior of geotechnical structures in sands, such as driven piles (Klotz & Coop, 2001). The approach had much in common with the state parameter framework of Been & Jefferies (1985). The implied assumption in the framework was that at the critical state a sand would reach a stable grading at which the particle contact stresses would not be sufficient to cause further breakage. An alternative assumption, based on the work by Chandler (1985) for material with deformable grains and implemented by Baharom & Stallebrass (1998) for soils with breakable grains, is that a critical state reached in the triaxial apparatus represents a balance between volumetric compression arising from particle breakage and volumetric dilation from particle rearrangement. Luzzani & Coop (2002) identified that there was some doubt, particularly at higher stress levels, as to whether samples did reach a true constant-volume state in triaxial tests and therefore whether the particle breakage had completely ceased. To investigate this further they carried out ring shear tests on two sands, one with a quartz and

one a carbonate mineralogy. In both cases particle breakage was found to continue to strain very much higher than those reached in the triaxial apparatus, so confirming the hypothesis that any constant-volume state observed in a triaxial test must be the result of counteracting components of volumetric strain and not because a stable grading has been reached. However, the displacements or strains that were achievable in their tests were insufficient to see whether the soil would eventually reach a stable grading or not. For tests on the carbonate sand at one stress level a constant ratio was found between volumetric strain and the amount of particle breakage as quantified with relative breakage, Br, defined by Hardin (1985), suggesting that the volumetric strain would cease only when particle breakage is discontinued. At this state, it was expected that a stable grading reached. Through improved testing techniques it has proved possible to reach higher displacements in the ring shear apparatus, allowing an investigation to be made of the evolution of grading at even larger strains, so identifying whether or not a stable grading reached the limit . As for most of the tests presented by Luzzani & Coop (2002), a carbonate sand has been used for this study, to maximize the breakage and so minimize the strains that would be required to reach a constant grading, should it exist. However, the patterns of behavior are likely to be applicable to sands of other mineralogy, although it is still not possible to reach the even higher strains that would be required to confirm the conclusions presented here for a quartz sand. Luzzani & Coop (2002) also restricted their investigation to one initial grading and loose samples at higher stress levels, so that the carbonate sand was starting from an initial state that was on its normal compression line, or limiting compression curve (Pestana & Whittle, 1995). Kikumoto et.al., (2010) had been proposed a constitutive model by extended the Severn-Trent sand model to include the effects of particle breakage. Severn-Trent sand is frictional hardening Mohr-Coulomb which described within a kinematic hardening, bounding surface frame work. The constitutive behavior of granular materials descripted that the evolution of limiting states with changing particle size distribution due to particle crushing described through a grading state index. It can be applied to observe the physical weathering due to the variation in stresses, temperature and hygroscopic behavior and chemical weathering.

2.4. Mechanical consequences of mudstone induced by slaking

Weak rocks may lose their strength or stiffness through slaking, as this usually results in a decrease in the particle size. Such variation in mechanical characteristics during slaking can directly affect the deformation and failure behavior of the ground. Pappas & Vallejo (1997) conducted static-compression-creep tests, in which time-dependent deformation of non-

durable shales due to water absorption was measured under confined conditions. In line with engineering advances, several studies had been performed to understanding the mechanical consequences due to slaking phenomenon. Hayano et.al (1997) performed a series of small unload-reload cycles was applied on rectangular prismatic of mudstone specimen to define elastic and plastic deformation properties at intermediate loading stages under triaxial test. Very large bedding errors were observed at both the top and bottom ends and at the lateral surfaces of specimens during isotropic compression, and at the ends during triaxial compression. Local strains showed approximately isotropic deformation during isotropic compression. Hobbs, et.al (2002) related to the weathering state of mudstones, it has a significant effect on their strength and deformability when measured in a series of experimental laboratory. After Chandler (1969), in case of Mercia mudstones, the result of the test shown the shape of stress strain relationship where essentially brittle behavior for weathering zone I material becomes entirely plastic behavior for zone 4 material (Figure 7). During the test, it was difficult to obtained undisturbed specimens to test for strength and durability, as an estimation it was made from the result of in-situ standard penetration test N-value.

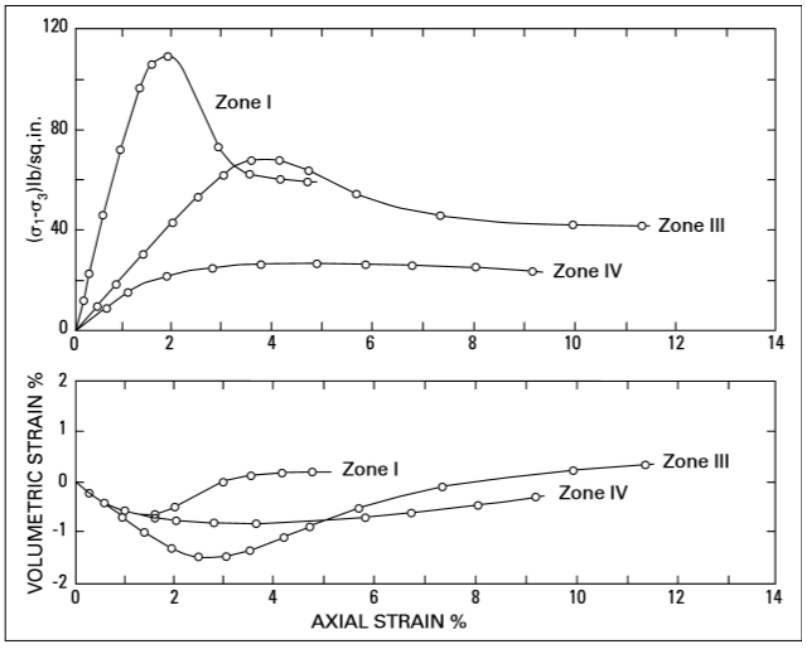

Figure 7. Stress-strain relationship of Mercia mudstone weathering zone 1, 3 and 4 (drained, cell pressure 68.95 KPa) showing change from brittle to plastic behavior as weathering process (after Chandler 1969 in Hobbs, et.al, 2002)

Yoshida and Hosokawa (2004) performed the impressive staged compression-immersion-direct shear test conducted on the compacted samples of crushed mudstone. Figure 8 exhibit the result from the compressive and shear behavior were analyzed with concern to cementation

effects. Compression behavior of the compacted samples was influenced significantly by the compaction degree. Immersion phase caused an additional compression and reduction in shear stress. Moreover, immersion also reduced significantly the peak shear strength parameter. A series of direct shear test under the different stress ratio and consolidated specimen was performed. A constant shear loading and ended with monotonic shear load was applied after third wetting to observe shear strength and deformations characteristics. Sieve analysis also performed to investigate the changes in particles size distribution and degradation index. As the result, the significant creep shear deformation could be found in the first wetting process. However, the amount of creep shear deformation during wetting is decreased with a step of the drying and wetting cycles. Almost equal vertical deformation occurs in each wetting step if the water content of the specimen before wetting becomes quite smaller.

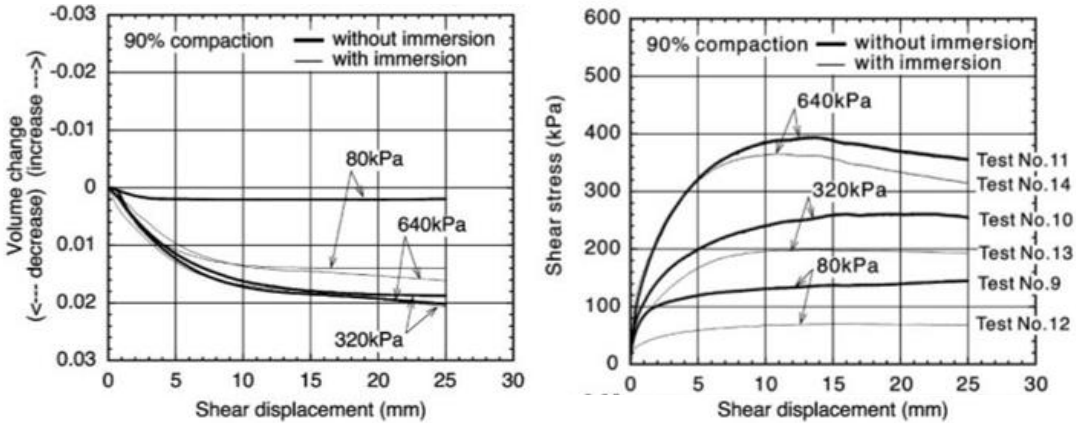

Figure 8. The stress-shear displacement-volume change relationship (90% compaction degree) (Yoshida & Hosokawa, 2004)

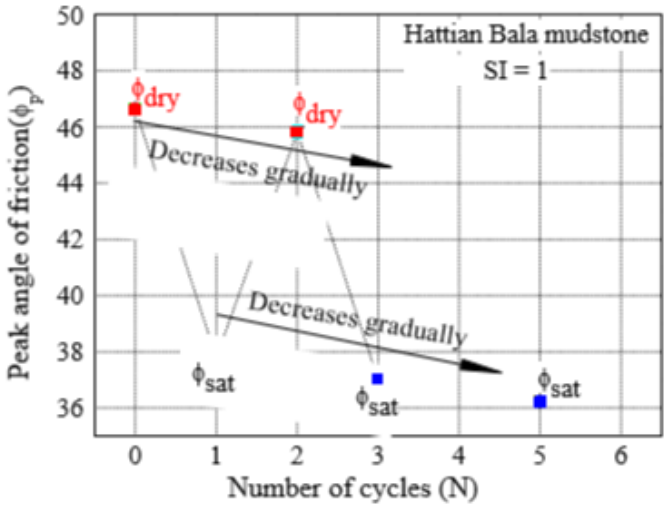

Figure 9. Relationship between number of wetting and drying cycles (N) and increment vertical displacement during wetting (Sharma, 2012)

Moreover, a 20% reduction in the peak shear strength for the cyclic wetting and drying was obtained compared to the dry condition test (Figure 9). Similarly, about 3% more particles crushing of the mudstones samples after cyclic wetting and drying is found (Sharma, 2012).

The effect of compaction during construction of the embankment regarding shales or mudstone geomaterial was observed to evaluate the potential slaking (Yoshida et. al, 2002 and Vallejo & Pappas, 2010). In addition to compaction, slake durability tests which number of wetting and drying cycles is given under unconfined condition also performed to evaluate the weathering resistance of weak rocks as shales, mudstones, and siltstones. It is pointed out that the slaking cycles significantly affect the degradation process and the evolution of the particle size distribution curve of the rocks (Santi, 2006; Sadisun et.al, 2005; Gautam and Shakoor, 2013; Kikumoto, et.al, 2016).

Nakano et.al, (1998) has performed a series of triaxial tests to interpret the mechanism of slaking behavior in terms of elasto-plastic mechanics, the saturated mudstone is first idealized as a heavily over-consolidated clay. For describing the shear behavior of a heavily over-consolidated clay, Asaoka et.al (1997) applied the sub-loading surface concept developed by Hashiguchi & Ueno (1977) and Hashiguchi (1993) to the original Cam-clay (Schofield and Wroth, 1968). The essentials of the sub-loading surface Cam-clay model are summarized. By using this mode, a series of soil-water coupled finite deformation analyses to simulate the pre- and the post-failure behavior of a heavily over-consolidated triaxial specimen are obtained. It was revealed that the occurrence of slaking is relatively easy and fast in unsaturated mudstone particles when compared with the saturated conditions (Figure 10).

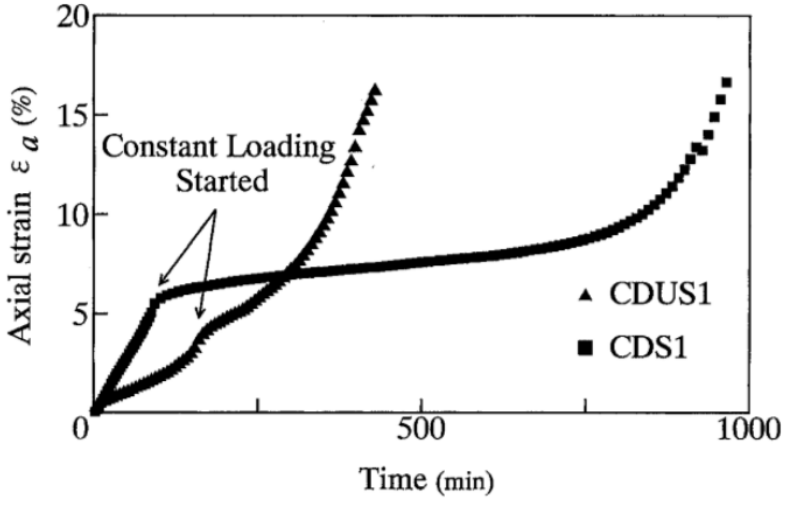

Figure 10. Delayed failure due to slaking (Nakano et.al., 1998)

Chapter 3

The chemical and physical properties of mudstones

3.1. Introduction

In the first chapter in this study has mentioned that almost 60% of the continents and most of the ocean floor was covered by the sedimentary soft rocks. Sedimentary rocks are formed by the accumulation of sediments. There are three basic types of sedimentary rocks. Clastic sedimentary rocks such as breccia, conglomerate, sandstone, siltstone, shale and mudstone are formed from mechanical weathering debris. Chemical sedimentary rocks, such as rock salt, iron ore, chert, flint, some dolomites, and some limestones, form when dissolved materials precipitate from solution. Organic sedimentary rocks such as coal, some dolomites, and some limestones, form from the accumulation of plant or animal debris. Mudstone as one of the sedimentary soft rocks was widely used as the material of earth construction since available in the large quantities. Meanwhile, an increase in number of geotechnical issues occurs since mudstone was very prone and tends to change from rock-like to soil-like during contact with water, especially the cycle of wetting and drying. Alternate wetting and drying of mudstone can be very important factor in weathering, a process known as slaking. Two types of disintegration of mudstones may be possible, a minor disintegration and a major disintegration. The minor disintegration is caused by slaking and the major disintegration is initiated by splitting in two or more large pieces of about equal size.

In terms of geology, there is two categories of weathering processes. Physical weathering and chemical weathering. Physical weathering is the breakdown or disintegration of rocks and minerals by a physical or mechanical process. Some of the forces are originates within the rock while others are applied externally. The applies stresses lead to strain and eventually to rupture (Ollier, C., 1969). Physical weathering involves the mechanical breakdown of rock into smaller particles by the exertion of stresses sufficient to strain end eventually split it

(Clowes & Comfort, 1987). Variety of factors introduce physical weathering, but the decisive role is played by those initiating mechanical movement of rock particles, which disturbs the mechanical bond between the rock constituents. These factors of physical weathering are related to a large extent by climate. Chemical weathering has a deeper penetrative capacity and its impact is defined by a radical transformation of rocks. This type of weathering consists the effect of various atmospheric factors; oxygen, carbon dioxide, air moisture and the active organic substances. The major reactions causing chemical weathering are as oxidation, hydration, dissolution and hydrolysis. Oxygen presence in the volume of water is capable to converting many minerals into oxides and thus oxides further converted into hydroxides. This process is termed as oxidation wherein weathering residue becomes in red color due to the formation of iron oxide. The main agent responsible for chemical weathering reactions is water and weak acids formed in water.

Related to the mudstone as one of sedimentary rocks, the chemical weathering of mudstone is extremely recommended to observe in geological engineering projects since the mechanical properties of these materials are fully determined by the extent of weathering, and due to some of the process are weathered extremely decreasing the strength of the construction. As mentioned before, the chemical weathering of mudstone was influenced by the water, in which the oxidation of pyrite, a common rock forming in sedimentary soft rocks is very important (Chigira, 1990; Chigira & Oyama, 1999). Pyrite has been identified as an important mineralogy in chemical weathering process due to it is oxidized easily to produce the sulfuric acid, which in turn leaches the rock-forming minerals and causes degradation or disintegration of rocks, as a result, the geotechnical issues is a rise rapidly (Taylor, 1988; Pye & Miller, 1990; Chigira & Oyama, 1999; Bahlburg & Dobrzinski, 2009). One of slaking phenomenon is attributed to the compression of entrapped air in the pores when water enters as a result of capillary suction. This entrapped air in the pores exerts tension on the solid skeleton, causing the material to fail in tension. The pore air compression is the predominant slaking mechanism in composed primarily of non-expansive clay minerals such as kaolinite (Moriwaki, 1974; Vallejo, et al., 1993). Clay surface hydration by ion adsorption has been suggested as another mechanism that causes slaking through the swelling of montmorillonite clays (Andres, et.al, 1980; Vallejo, et al., 1993). The removal of cementing agents from the geo-materials by groundwater dissolution is also considered to be a mechanism that causes slaking.

Many researchers interested in the weathering process related to the slaking phenomenon on mudstone and their changes in chemical, mineral and physical properties (Matsukura and Yatsu, 1982; Chigira & Oyama, 1999; Bhattarai et al., 2006; Schaefer & Birchmeir, 2013;). Related

to the mineralogy content, the weathering behavior is controlled by the mineralogy content such as quartz and clay mineralogy (Dhakal, et.al, 2002; Sadisun, et.al, 2005; Santi, 2006). The alter of chemical and physical properties of mudstone during the weathering processes was triggered by the environmental activities as well. According to this, it is necessary to evaluate the durability of mudstone against weathering and their effect on the chemical and physical properties. To enhance the understanding of weathering behavior of mudstone, this chapter attempts to indicate the chemical constituent, mineralogy and morphology texture of mudstone. The x-ray fluorescence (XRF test) and x-ray diffraction (XRD test) methods were prepared to obtain the chemical properties and scanning electron microscope to observe the morphology texture of mudstone surfaces.

3.2. X-ray fluorescence test (XRF test)

X-ray fluorescence or XRF is a non-destructive test method. XRF is typically used for bulk analyses of larger fractions of geological materials to investigate the chemical component or composition of rocks, minerals and sediments. XRF is widely used methods for chemical analysis element, due to it is easy to use and relatively low cost compare to the other methods with same purposes. The crushed mudstone specimen for XRF test was prepared with the diameter between 2.0-0.85 mm. Figure 11 exhibit a qualitative analysis result of the X-ray fluorescence method of mudstone specimens. It was exhibited that the mudstone contains high concentration of silicon (Si), iron (Fe), aluminum (Al), sulfur (S), calcium (Ca), potassium (K), titanium (Ti) and low concentration of sodium (Na), chlorine (Cl) and strontium (Sr). The major elements contained in the mudstone specimen are in order of Si, Fe, Al, Ca, K, Na and Mg. It indicates that the major constituent material of mudstone was based on crystalline element (Ollier, 1969). Based on those chemical elements, the arrangement of mudstone mineralogy content is formed. If one looks at mudstones of various ages, it is observed that Tertiary and younger mudstones consist mostly of smectites and mixed layer clays.

In the older mudstones, illite is the dominant clay mineral, and in early Paleozoic and older rocks less than 10% of the clay minerals are smectite clays. This is likely due to diagenetic processes that convert the smectites to illite over time. Such a conversion would involve the release of elements like Si, Ca, Na, Mg, and Fe from the clays. Most of these released elements likely remain in the mudstone and crystallize to form quartz, chlorite, albite, calcite, dolomite, siderite, and ankerite, which are all minerals that occur in mudstones. Many of these minerals may in fact be products of diagenesis.

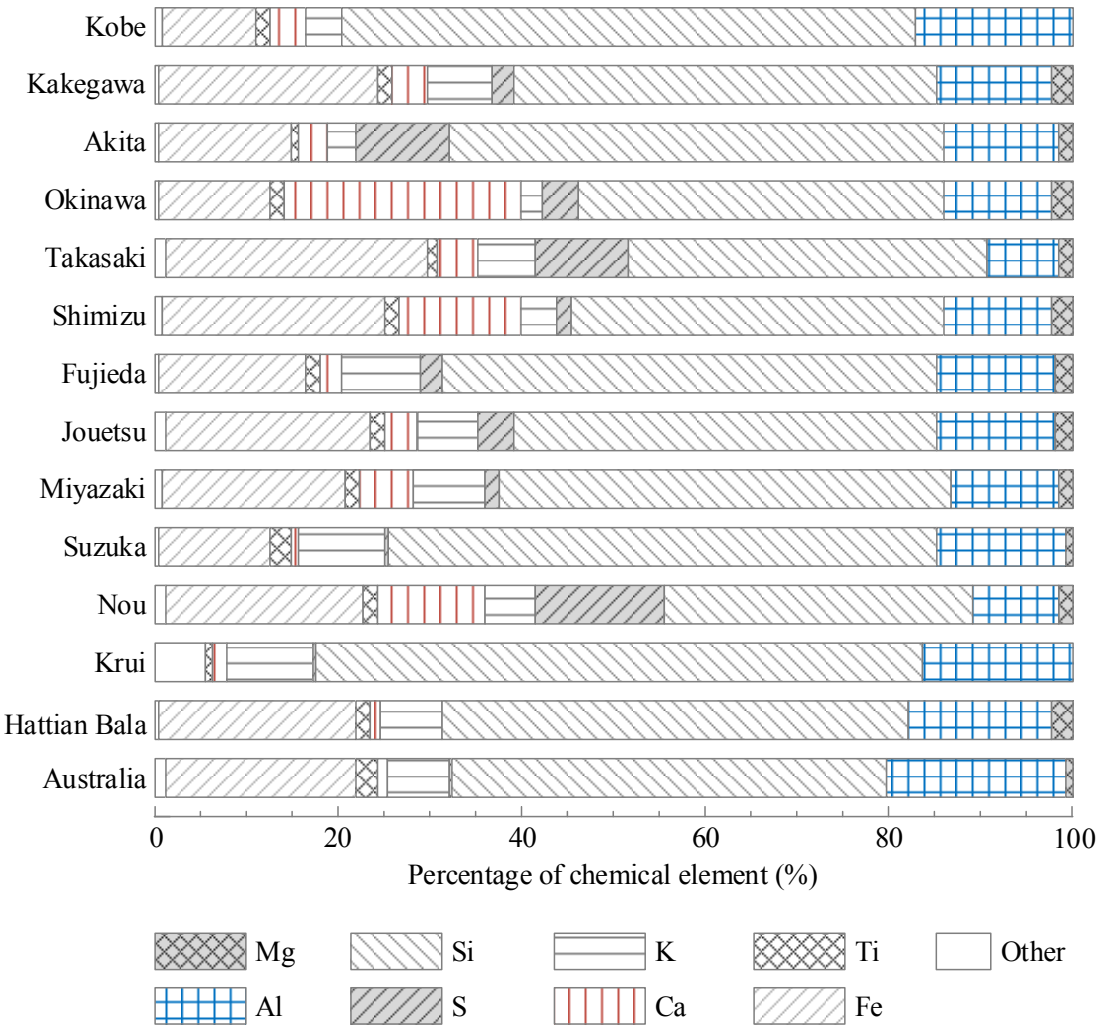

Figure 11. The initial chemical elements of mudstone as the result of XRF test.

The result of the test also indicate that the major crystalline phase of sand is quartz, the phase of clay is illite, while silt is represented by silica, aluminum, and calcium. The cementing reaction due to existences of silica and aluminum has brought to the pozzolanic characteristics. Silicon dioxide is a manifestation of quartz or non-clay material, while alumina and iron are manifestations of clay material. Related to mineralogy content, the smectite content is very identic to the mudstone characteristics and manifestation of clay material (Yao, 1993; Lee, et.al, 2007; Peltonen, et.al, 2008). The total amount of alumina and iron concentration tend to be used to justify the smectite content on mudstone or weathering rock material.

In common, clay mineral of mudstone consists of kaolinites, smectites and illites. Kaolinites [$Al_2Si_2O_5(OH)_4$] are formed in warm moist climates where Ca, Na, and K ions are leached and removed in solution during the weathering process. Smectites are expanding clays and might be expand by taking in water between layers. Montmorillonite [$(½Ca, Na)_{0.7}(Al,Fe,Mg)_4Si,Al)_8O_{20}(OH)_4.nH_2O$] is a good example. These clays form from

weathering of Fe -Mg rich igneous and metamorphic rocks in temperate climates. Illite [$K_{1-1.5}Al_4Si_{7-6.5}Al_{1-1.5}O_{20}(OH)_4$] are formed by weathering of feldspars in temperate climates and by alteration of smectite clays during diagenesis.

3.3. X-ray diffraction analysis (XRD test)

X-ray diffraction or XRD test is a method to identify of minerals in rocks and soils. It provides detailed information about the atomic structure of crystalline substances. The bulk of the clay fraction of many soils is crystalline, but clay particles are too small for optical crystallographic methods to be applied. Therefore, XRD has long been a mainstay in the identification of clay-sized minerals in soils. However, its usefulness extends to coarser soil fractions as well. X-ray diffraction analysis can be conducted on single crystals or powders. The XRD test in this study will be devoted to X-ray powder diffraction (Reynolds, 1989). X-ray diffraction (XRD) analyses for mineral composition were conducted with Rigaku Ultima-IV powder diffractometer in the Research Center of Yokohama National University. Scans were collected using Cu-K_β radiation over a 2theta (2θ) range from 2°- 90°. The acceleration of scans was set around 10 minutes. Mineral phases were identified using the PDXL software package, which allows identification of minerals containing specific elements.

The simplest preparation procedure is to grind the specimen into a powder fine enough to mount in the focal plane of the diffractometer. However, the minerals occurring in clay fractions are often very different in nature from minerals that dominate the coarser fractions. Grinding the whole specimen makes it difficult to detect and identify the clay sized minerals due to dilution and other confounding effects of the coarser components. This is a disadvantage because the clay-sized minerals often have a disproportionate effect on chemical and physical properties of soils. Thus, if the objective is an effective characterization of all minerals, it is best to analyze individual particle size fractions separately. Bulk mineralogy of mudstone was determined from powder samples using XRD test and analyzed by using the software package of PDXL analysis. PDXL analysis is a software to analyze the XRD pattern based on the data base interpretation of each component mineralogy. Figure 12 are the interpretation of Kobe mudstone mineralogy as a sample of analysis result from PDXL software. PDXL provided with the database, therefore every mineral content has their own interpretation.

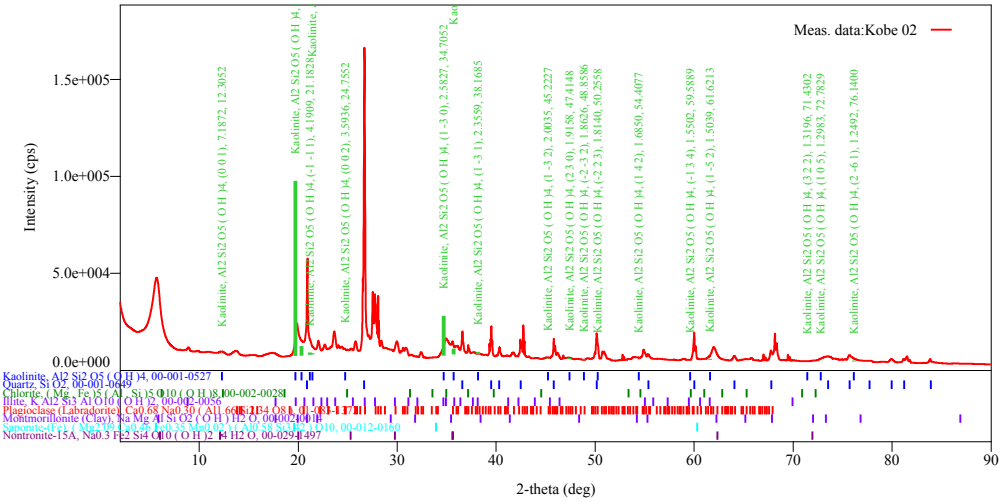

(a) Kaolinite

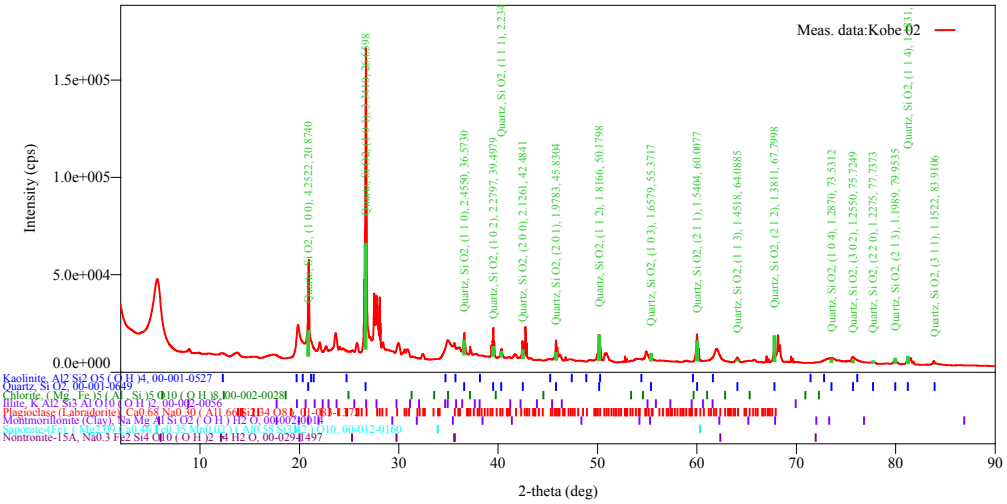

(b) Quartz

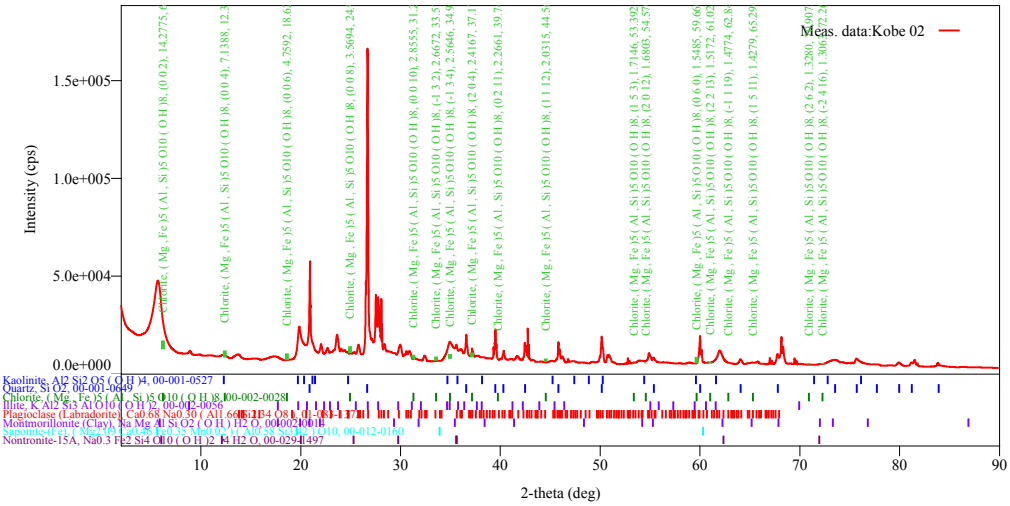

(c) Chlorite

Figure 12. (continued)

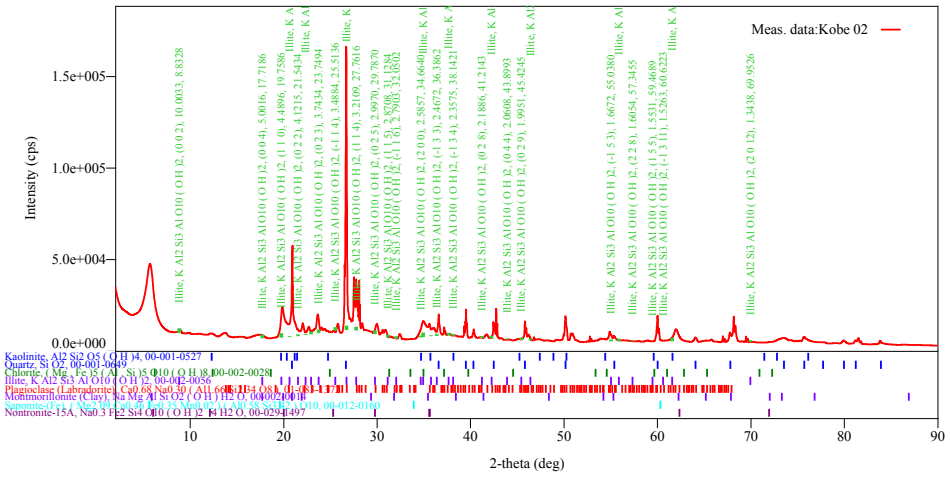

(d) Illite

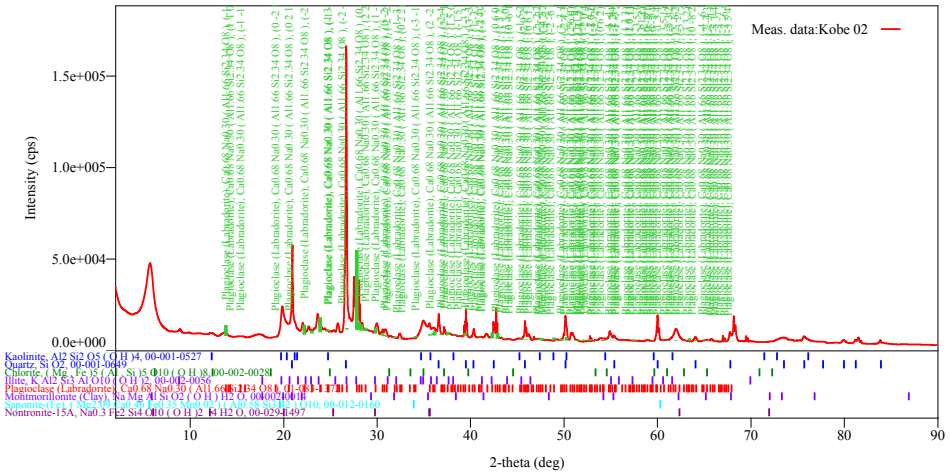

(e) Plagioclase

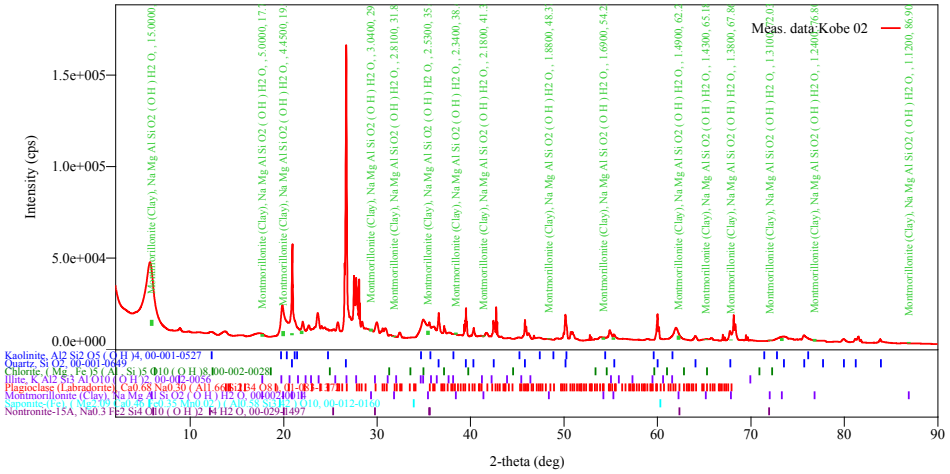

(f) Montmorillonite

Figure 12. (continued)

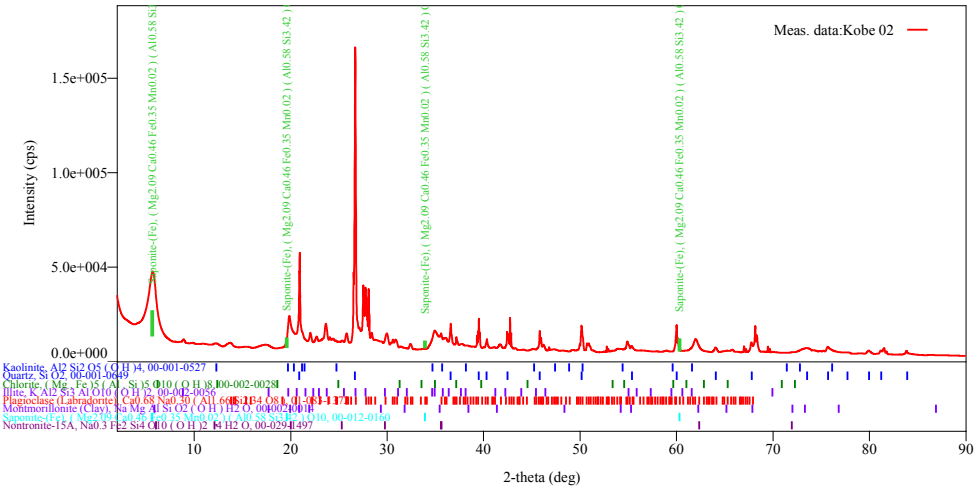

(g) Saponite

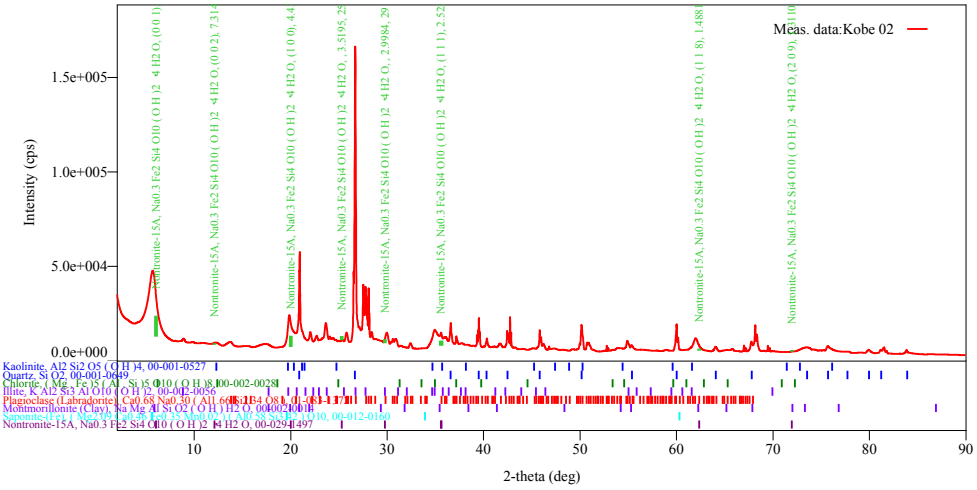

(h) Nontoronite

Figure 12. Data base interpretation of mineralogy content of Kobe mudstone

The XRD pattern result of Kobe, Kakegawa and Hattian Bala mudstone was exhibit in Figure 13. Based on the pattern of XRD test, the mudstone material has an identical pattern to determine the mudstone specimen. According to XRD test result and the analysis of mineral content, the mudstone specimen consists of clay mineral and quartz mineral. The quartz minerals are abundant mineral in mudstone, making up over 70%, nevertheless, the quartz is not exactly mineral (Nelson, 2013). The XRD patterns of Kobe, Kakegawa, and Hattian Bala mudstone are almost identical, which the quartz minerals are the dominant mineral and small amount of clay mineral content. Even the small amount of clay mineral content, it is necessary to observe the slaking behavior of the mudstone. The dash box red line is part of XRD pattern to investigate the clay mineral content such as smectite or montmorillonite content. The magnifying of this pattern exhibited in Figure 14. As a part of XRD pattern which is paid attention to investigate the clay mineral content, it was found that the mudstone specimen has

a clay mineral content such as smectite (montmorillonite, saponite and nontronite), illite and kaolinite.

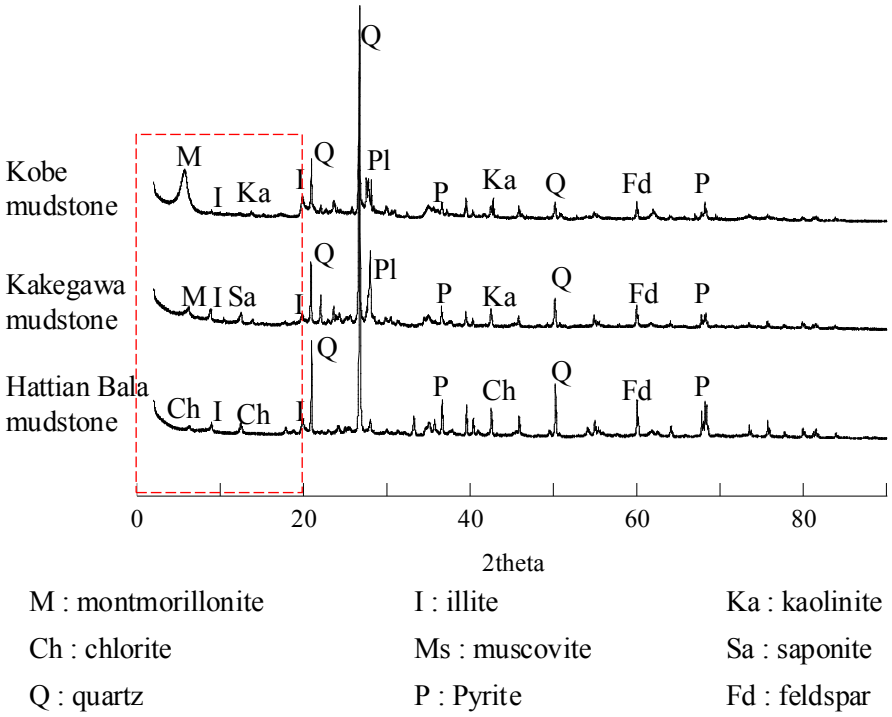

Figure 13. The PDXL analysis result against Kobe mudstone, Kakegawa mudstone and Hattian Bala mudstone

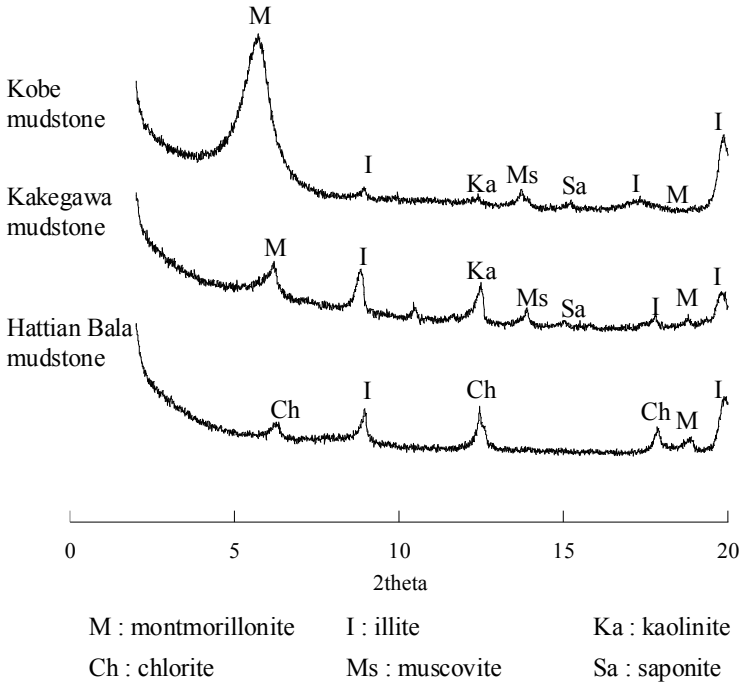

Figure 14. The XRD patterns of three kinds of mudstone to observe the smectite mineralogy content (dash-line red box magnified)

The XRD pattern of mudstone specimens to investigate the clay mineral content especially the expandable clay content (smectite) has shown the identical pattern (Figure 15). It was indicated that the XRD pattern of mudstone specimen in this study shown the characteristics and compare to the Toyoura sand, the pattern is totally different. And once more, it was proven that the samples in this study are mudstone, except for Australia shale and Krui. The Krui mudstone was suspected that not exactly mudstone since the pattern more approach to the shale. Furthermore, this pattern was clearly different with the specimen that does not have a clay mineral content such as Toyoura sand. For the Australian shale and Krui mudstone, even the pattern of XRD testing result shows a bit different pattern in the initial degrees, but the clay mineral content still exists with the high clay mineral content is kaolinite.

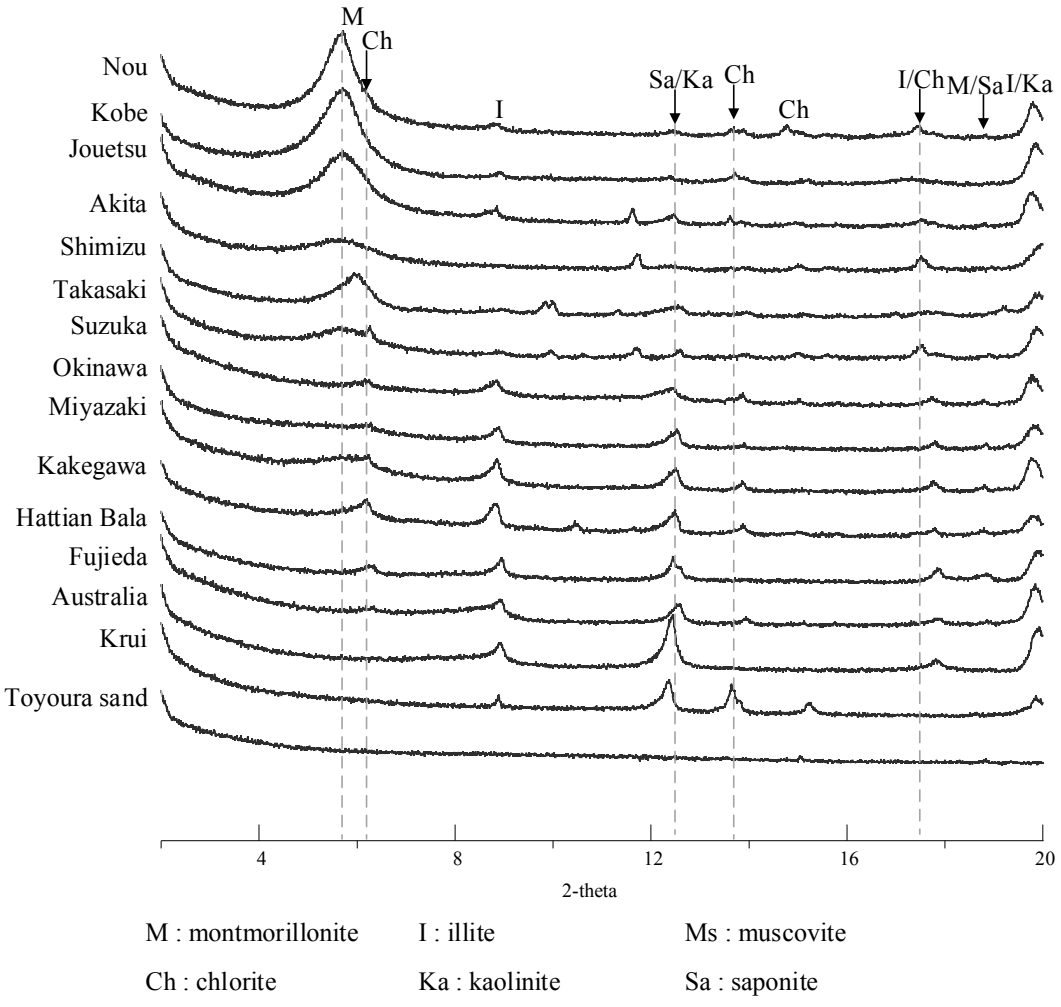

Figure 15. The XRD patterns of crushed mudstone regarding the clay mineral content

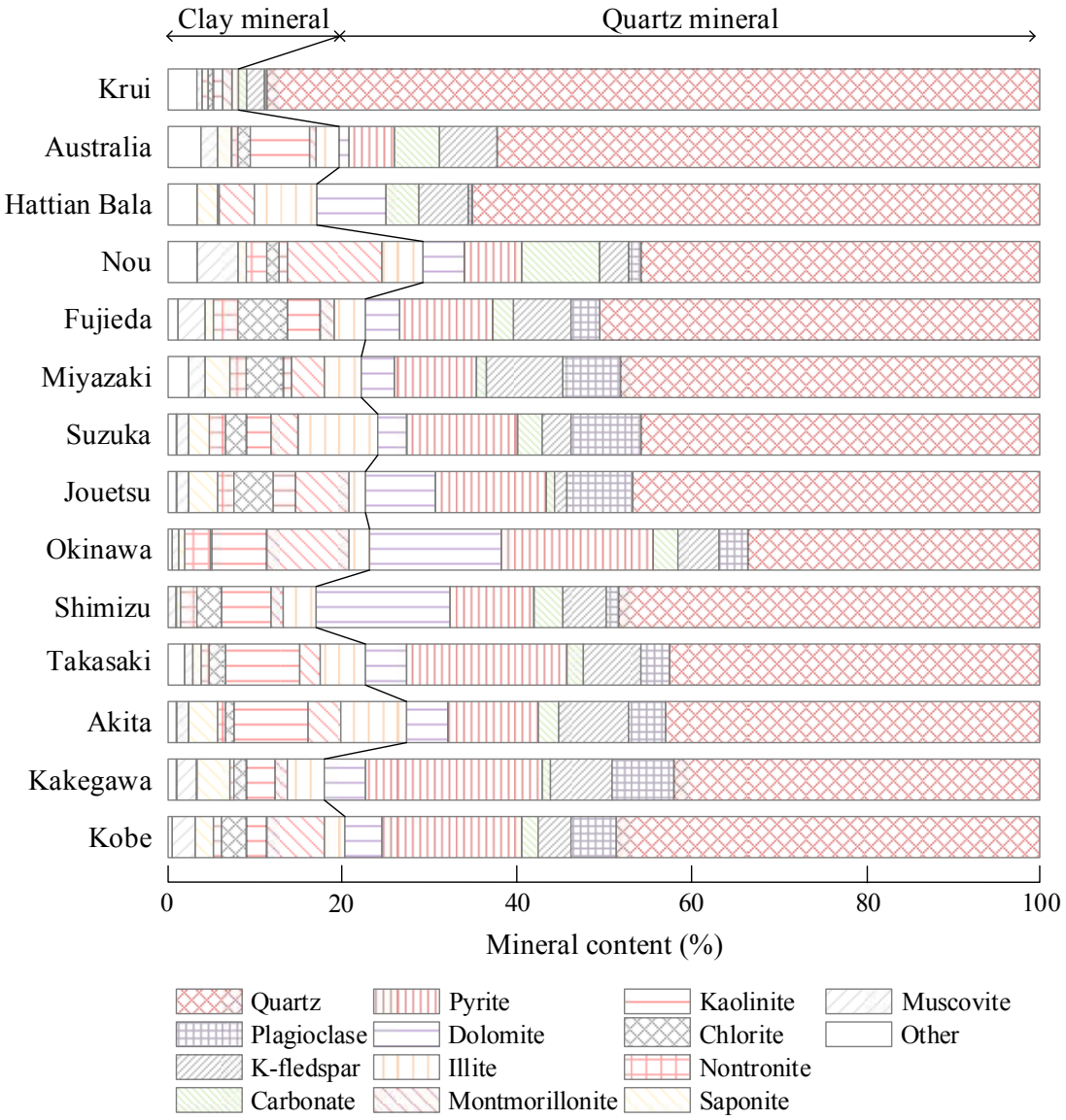

Figure 16. The summary of mineralogy composition against mudstone specimen

The summary of XRD test result in Figure 16, shows that the clay minerals were primarily mixed-layer clays as well as minor amounts of illite, kaolinite, chlorite, muscovite and smectite (montmorillonite, nontronite, saponite). Meanwhile, quartz mineral as the non-clay mineral was observed to be highly heterogeneous, with a significant amount of quartz, plagioclase, K-feldspar, carbonates, pyrite and dolomite. The major non-clay mineral is quartz in average is 49.79% and followed by Pyrite of 13.19% in average and the major clay-mineral content is illite in average of 5.7% and the second is kaolinite. Regarding, the smectite minerals, including montmorillonite and bentonite, have the most dramatic shrink-swell capacity, and known as expansive.

Expansive soils contain minerals such as smectite clays that are capable of absorbing water. When they absorb water, they increase in volume. The more water they absorb, the more their

volume increases. Expansive soils will also shrink when they dry out. This shrinkage can reduce the strength capacity to support of buildings or other structures and result in damaging subsidence. Fissures in the soil can also develop. These fissures can facilitate the deep penetration of water when moist conditions or runoff occurs. This produces a cycle of shrinkage and swelling that places repetitive stress on structure. In the field, expansive clay soils can be easily recognized in the dry season by the deep cracks, in roughly polygonal patterns, in the ground surface. The zone of seasonal moisture content fluctuation can extend from 30-40 feet deep. This creates cyclic shrink/swell behavior in the upper part of soil column, and cracks can extend to much greater depths than imagined by most engineers. Since mudstone has a smectite mineral, then appropriate understanding regarding the weathering mechanism caused by smectite content. In order to understand the weathering mechanism due to the mineral content, it is important to understand the process that might be triggering those mechanisms. First, it was mentioned that pyrite content is quite important in these sequential of weathering of mudstone. The oxidation process on pyrite by oxygen coming from the ground surface and sulfuric acid is generated at the base of the oxidized zone. The sulfuric acid, in turn, dissolves rock-forming materials to make a dissolved zone (Chigira & Oyama, 1999). The transformation of pyrite at the oxidation process (Russel & Parker, 1979; Dixon et al., 1982; and Chigira, 1990) causes the sulfuric acid is produced according to the formulae (Vear & Curtis, 1981; Berner & Berner, 1987). This is a critical chemical reaction; the oxidation of pyrite and subsequent growth of secondary sulfates in the mudstones causes crystal growth and resultant volume change. Sulfate as oxidation products of pyrite are humidity or water sensitive and can change chemistry hourly. Oxidation of pyrite is a chemical reaction that results in crystal growth of various sulfates, expansion and volume change at or near the site of pyrite and release of mild sulfuric acid and iron. The chemical reaction of pyrite oxidation of mudstones specimen shown below:

$$2FeS_2 + CaCO3 + 6O_2 + 3H_2O \rightarrow FeCa(SO_4) + 3H_2SO_4 + CO_2 + Fe$$

The crystal structures of sulfates are larger than that of pyrite, and this increase in volume can be substantial. Due to the process of oxidation pyrite, it will make the chlorite transform to be part of smectite.

In addition, the transformation mineral of smectite to be illite occurred during wetting and drying process. It was related to the ion K+ of feldspar.

$$Al_2Si_4O_{10}[OH]_2.\ nH_2O + KAlSi_3O_8 \rightarrow KAlSi_3O_{10}[OH]_2 + 4SiO_2 + nH_2O$$

(smectite) (K-feldspar) (illite) (quartz)

$2K^+ + 3Al_2Si_4O_{10}[OH]_2\ nH_2O \rightarrow 2KAl_3Si_3O_{10}[OH]_2 + 6SiO_2 + 2H^+ + 3nH_2O$

Ion K+ (smectite) (illite) (quartz)

Experimental transformation of muscovite following additions of magnesite and dolomite have been studied. Formation of layer silicates such as smectite, serpentine, some mixed-layer phases and other minerals is shown to be a function of the composition of the starting materials, temperature and run duration. It is established that phlogopites are formed from muscovite, respectively, under Mg-bearing hydrothermal conditions. Some causes of variations in the composition of serpentines at elevated temperature as a function of the composition of hydrothermal media are given. These data may be used to explain the main characteristics of clay mineral formation from muscovite-bearing sedimentary rocks during their alteration in post diagenetic and metasomatic processes.

3.4. Scanning Electron Microscope (SEM) analysis

The existences of intragranular pores of the crushed mudstones were explored through Scanning Electron Microscope (SEM). The images of each specimen were taken by two magnification images. The low-magnification images present on the left-hand side and the high-magnification images present on the right-hand side in Figure 17. The images certainly exhibit that mudstone particle is in fact an aggregate of randomly shaped, clay-sized particles that produce a rough surface texture. Several different mechanisms of the slaking of weak rocks have been pointed out in the past studies. One of the slaking mechanisms is attributed to the compression of air entrapped in the intragranular pores of the particles (Moriwaki, 1974). Vallejo et al. (1993) and Vallejo & Murphy (1999) studied the effect of the geometry of the intragranular pores and revealed that the size of the pores and the roughness of the pore boundaries have dominant effects on the resistance of particles against slaking. The surface characteristics of the crushed mudstones with dimension of 2.00-0.85mm were explored through SEM. The low-magnification images of each specimen on the left-hand side in Figure 17 clearly demonstrate that each particle is in fact an aggregate of randomly shaped, clay-sized particles that produce a rough surface texture. This surface texture can be better seen in the higher magnification images on the right-hand side in Figure 17. Note that with the particles of the Kobe and Okinawa mudstone there is a particularly pronounced accumulation of tiny particles, with apparent intragranular pores appearing to form within each bulk particle. In comparison, the surface texture of the Takasaki, Akita and Shimizu mudstone looks relatively smoother, but is still rougher than the Toyoura sand presented in Figure 18.

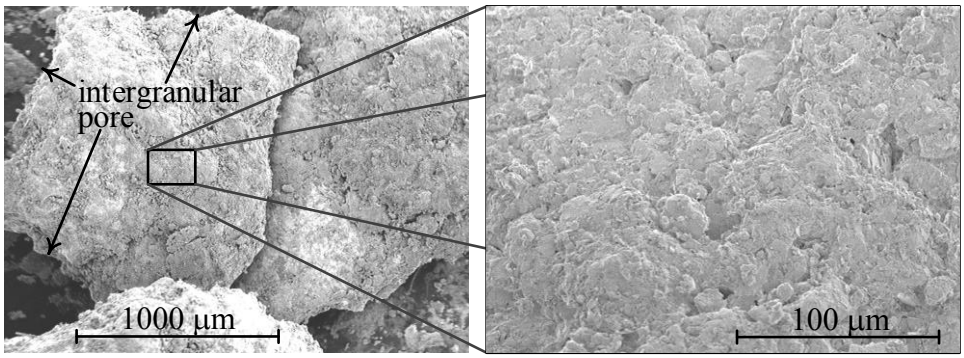

(a) Kakegawa mudstone

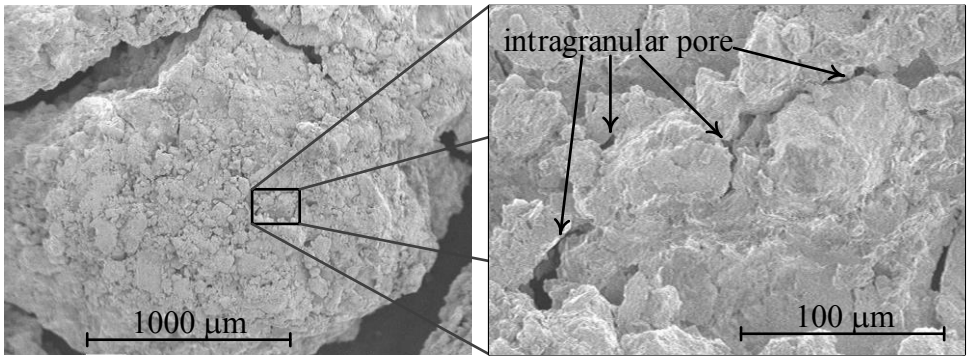

(b) Kobe mudstone

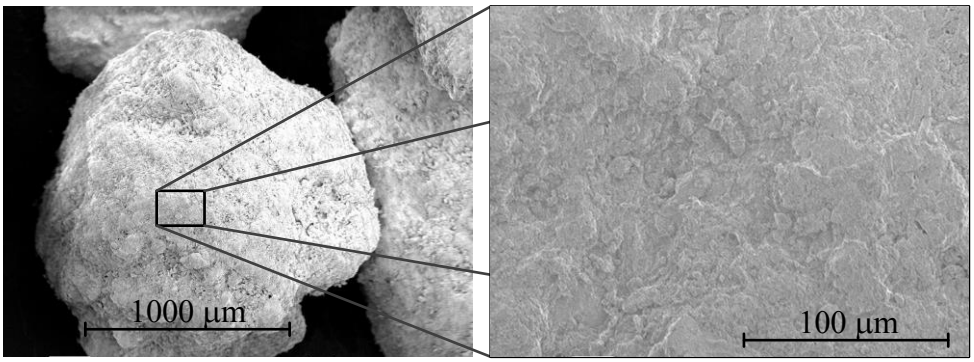

(c) Takasaki mudstone

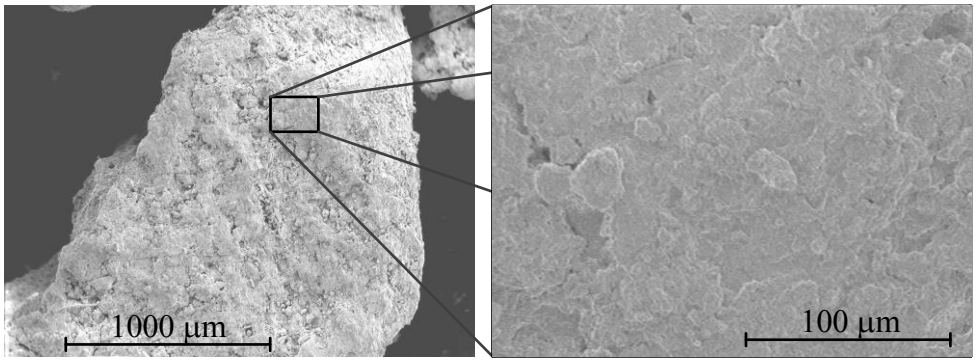

(d) Akita mudstone

Figure 17. (continue)

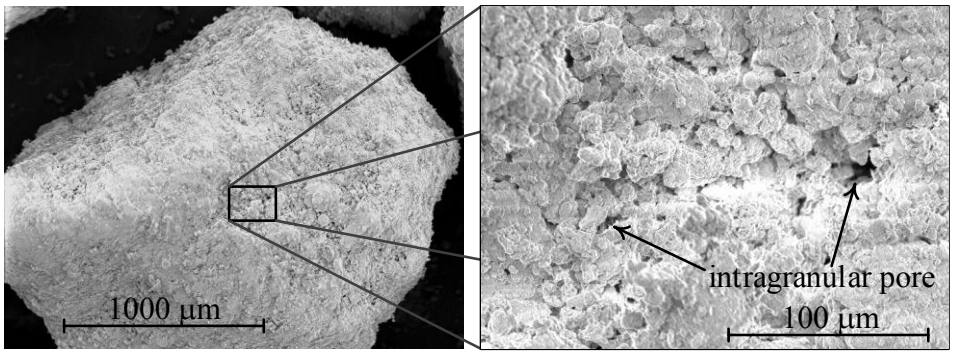

(e) Okinawa mudstone

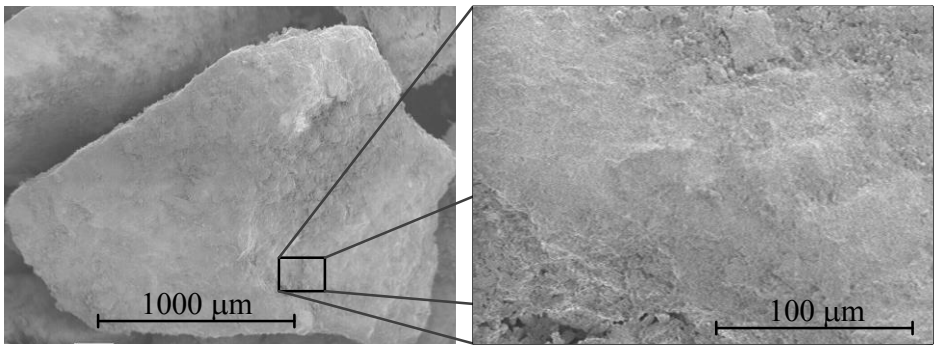

(f) Shimizu mudstone

Figure 17. SEM images showing the surface texture of mudstone specimens at two different magnifications (×50 and ×500)

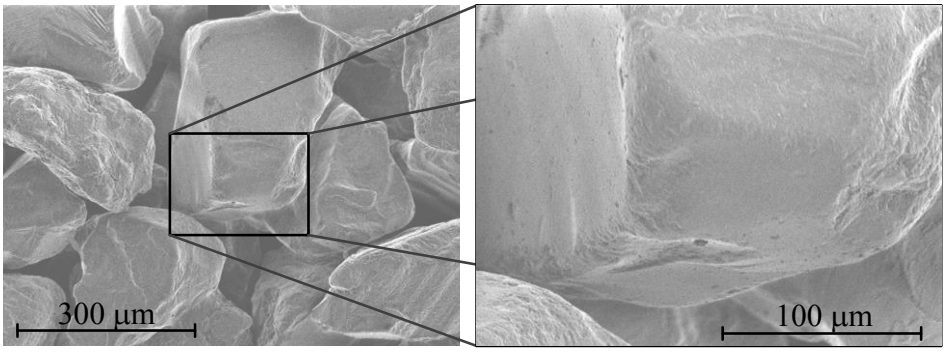

Figure 18. SEM image showing the surface texture of Toyoura sand at two different magnifications (×150 and ×500)

Vallejo and Murphy (1993) was performed the procedure to investigate and measure the mean of intragranular pore diameters of each mudstone specimen compared with their slaking behavior. In this study a slightly different procedure was performed to check the diameter of intragranular pores. First, an area is determined based on the magnified photo of mudstone specimen, then the mean diameter of intragranular pores inside the determine area is measured.

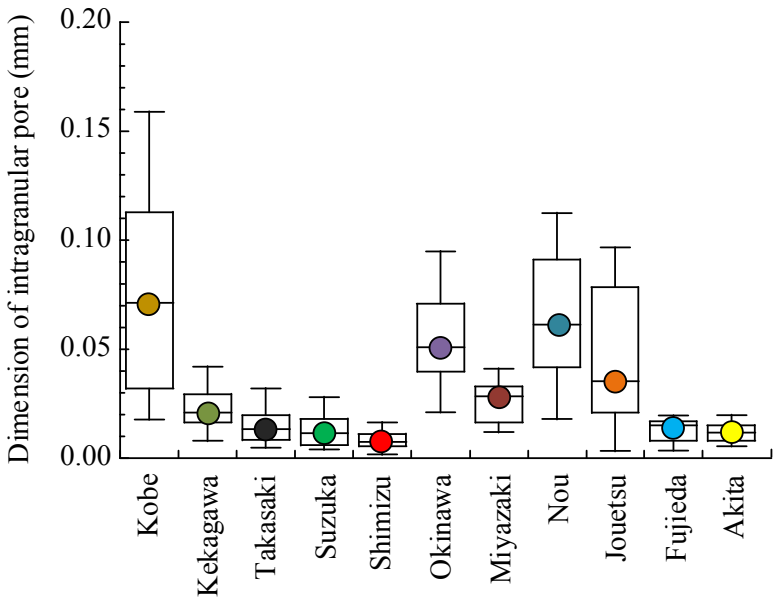

Figure 19. The size of intragranular pores of mudstone specimen

The mean diameter on intragranular pore was transposed into the diameter of circle which equal to the circumference. Considering the random data of diameter of intragranular pores, the mean and quartile parameter of diameter pores was calculated and presented in Figure 19. However, this procedure of measurement seems to be quite arbitrary but at least provides an early overview of the weathering mechanism due to the presence of intragranular pores.

Mudstone density in this study was measured by using glass bead method. This method is designed for oddly-shaped samples such as sandstone, shale, and mudstone. The other procedure to check the density of oddly-shaped samples is weighing into the water. But since mudstone is very sensitive when in contact with water, then this method is not considered or not recommended to be used. Several initial tests were performed to determine the number of tamping and layer of glass bead against solid rocks such as obsidian. The density of obsidian as a reference to determine the number of blows and layer to produce the same density. Based on these tests, the density of mudstone should be performed by dividing the height of glass bead inside the stainless-steel chamber into 10 layers and each layer should blow for 15 times. The density of mudstone in this study was checked for three samples of each specimen and the result exhibited in Figure 20. Akita mudstone has the lowest density compared to other specimen, despite it has a very small dimension of intragranular pores. Based on the existence of pore dimensions, Akita mudstone should have a high density, but in this case encountered an irregularity.

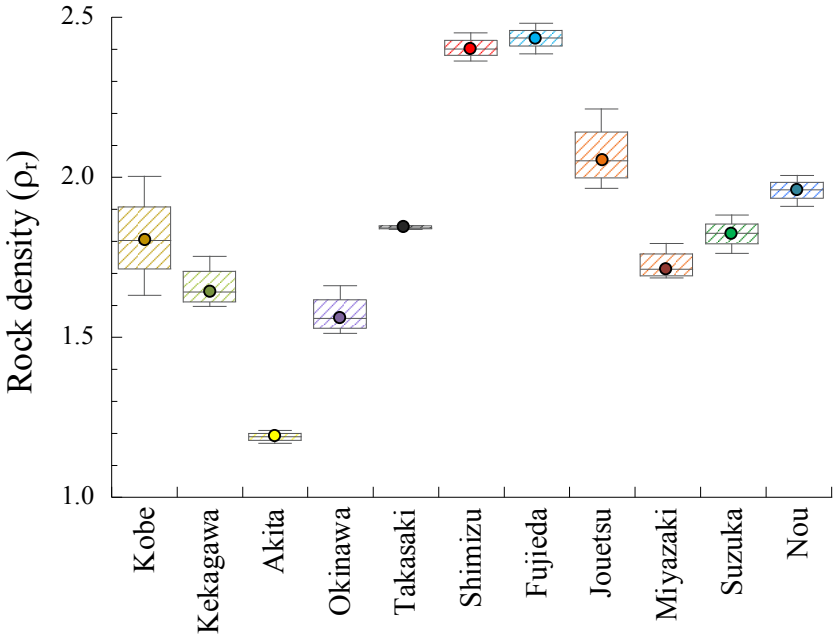

Figure 20. The Rock density of mudstone specimens

3.5. Summary

The mudstone specimen in this study was made up of Neogene to Pliocene period. The major constituent of chemical element consists of silicon (Si), iron (Fe) and aluminum (Al). It might indicate that the major constituent material of mudstone was based on crystalline element. Most of these released elements likely remain in the mudstone and crystallize to form quartz, chlorite, albite, calcite, dolomite, siderite, and ankerite, which are all minerals that occur in mudstones. Many of these minerals may in fact be products of diagenesis. It was indicated that the major crystalline phase sand is quartz, the phase of clay is illite, while silt is represented by silica, aluminum, and calcium.

The smectite clay minerals, montmorillonite has the most dramatic shrink-swell capacity, and known as expansive. Expansive soils contain minerals such as smectite clays that are capable to absorb the water by ion Ca^{+} and expand the particle by ion Na^{+}. When they absorb water, they increase in volume. The more water they absorb, the more their volume increases. Expansive soils will also shrink when they dry out. In the field, expansive clay soils can be easily recognized in the dry season by the deep cracks, in roughly polygonal patterns, in the ground surface. The Pyrite content is quite important in these sequential of weathering of mudstone. Pyrite is oxidized by oxygen coming from the ground surface and sulfuric acid is generated at the base of the oxidized zone. The sulfuric acid, in turn, dissolves rock-forming materials to make a dissolved zone (Chigira & Oyama, 1999). The transformation of pyrite at the oxidation process causes the sulfuric acid. This is a critical chemical reaction; the oxidation

of pyrite and subsequent growth of secondary sulfates in the mudstones causes crystal growth and resultant volume change. Oxidation of pyrite is a chemical reaction that results in crystal growth of various sulfates, expansion and volume change at or near the site of pyrite and release of mild sulfuric acid and iron. The existence of intragranular pores are indicated based on microscope photograph of mudstone specimen. It might be useful since one of the weathering mechanism was indicated by existence of pores. However, it is an arbitrary summarize regarding the existence of intragranular pore affect the weathering process. Further investigation needed by checking the rock density of mudstone specimen and compare with the size of intragranular pores.

Chapter 4

Slaking Resistance

4.1. Introduction

Soils or rocks material originating from the chemical decomposition do not undergo any sorting in their grading and therefore well graded. Their structure or composition may be influenced by weathering in one feature or more such as grading size changes, mineral composition and morphology of particle. Every feature and their effects on the mechanical behavior has got an attention in the past. Related to the mudstone specimen in this study, the weathering process due to slaking can induce a rapid transformation of rock material to become a soil particle, especially occur on the sedimentary soft rock. In terms of geology or civil engineering, the state of this process was known as durability index and related to the slaking cycle is commonly known as slake durability index. The slake durability index is very common to check or observe the transformations of sedimentary soft rocks such as shale, mudstone, and sandstones (Vallejo, 1993; Santi, 1998; Czerewko & Cripps, 2001). Weathering process in over-consolidated clays and clay shales has been observed to be a significant process due to the mode of deposition and the bonding from diagenesis. In United states, one of the largest and most problematic clay shales is the Pierre Shale Formation (Fleming et al. 1970). The decrease of strength from the peak to residual strength is a source of the stability problems associated with these materials. Initial fissuring results from rebound in clay shales and leads to clay swelling, strain softening and weathering (Brooker and Peck 1993). Much of the past work on residual strength has focused on the mechanical aspects with less emphasis on the role of the more dynamic, physicochemical effects on residual strength. The durability behavior of these sot rocks is responsible for slope stability problems due to rapid slope degradation by the loss of strength of the surface material, unexpected additional settlements and failures of embankments, long term loss of intact strength affecting the stability of underground. Due to this behavior, several issues on earth construction such as deformation

on the embankment and landslides problem are necessary to understand better. Cano, et al. (2017) was performed the slake durability tests to evaluate the degradation of marble calcareous rocks by the Potential Degradation Index (PDI). The changes of changes in the fragment size distribution curves obtained from the material retained in the drum after each slake durability test cycle, up to a total of five cycles. The Preliminary results of in situ weathering suggest the existence of a clear relation between the different classes of degradation stated by the PDI, the behavior of the fragments retained in the drum along the slake durability test cycles, the slaking behavior under natural climatic conditions and the weathering behavior patterns and rates observed at weathered profiles in the field. It has been mentioned that wetting and drying cycle was the main factor to weathering of sedimentary rock, such as mudstone or shale. The accelerated slaking test is a test to describe the resistance of rock specimen against the wetting and drying cycles. In this chapter, attempts to obtain a conclusion related to the slaking resistance associated with the mechanisms of weathering. The parameter disintegration of mudstone material during the wetting and drying cycles in the accelerated slaking test would be analyzed by considering the breakage parameter (Hardin, 1985). Meanwhile, the result from XRD test, XRF test and the microscopic photograph of SEM result would be used to explore the mechanisms of weathering of mudstone specimen after a number slaking cycles in accelerated slaking test applied.

4.2. Methods and Materials

The term weathering is understood as all changes of physical or chemical nature occurring in a rock as a response to its interaction with the environment, and that modifies the rock's deformability, strength and permeability characteristics (Marques, 1992; Marquez, et.al, 2010). Weathering mechanisms are the processes that act upon a rock or a mineral in response to new environmental conditions and tend to cause break down. Finally, durability defines the ease with which a rock weathers, or its susceptibility to weathering processes. As mentioned in introduction, there is two types of processes cause rock weathering: physical disintegration and chemical decomposition. Both have complementary effects and occur together in natural systems, although it is convenient to consider them as separate agents of rock weathering for facilitate discussion. Physical disintegration is considered as the dominant process because it occurs faster than chemical decomposition and produces more free surfaces (Taylor and Cripps, 1987).

4.2.1. Accelerated slaking

Several authors have performed the slake durability test by using the standard testing method

developed by Franklin and Chandra (1972) and recommended by the International Society for Rock Mechanics (ISRM, 1981) and standardized by the American Society for Testing and Materials (ASTM, 1990). Meanwhile, the accelerated slaking test based on the NEXCO standard (NEXCO-110-2012) was performed in this study. The crushed mudstone particles with a diameter of 9.5 to 37.5 mm were oven-dried and then placed in a single layer in a container (Figure 21). The weight of mudstone specimen and picture of the specimen was documented as an initial state. In the wetting process, distilled water was poured into the container until the sample was fully submerged, and the sample was then kept at a constant temperature of 20°C for 24 h. In the drying process, water was thrown away from the container while taking care to retain the original arrangement of particles, after which the specimen was oven-dried for 24 h at a temperature of 110±5°C. A picture of each specimen was taken after each wetting and drying process, with this being repeated until a prescribed number of cycles was reached. After the last cycle, the particle size distribution of each specimen was determined by sieving analysis (JGS, 2009), whereby the specimens were sieved in a fully dried condition using a horizontal circular movement without any tapping impulse. Five cycles of wetting and drying were applied to each of mudstone specimen. The graphic of particle size distribution after accelerated slaking test is needed to calculate the breakage parameter of mudstone specimen. As an objective in this study, the breakage parameter is one important parameter to explore the physical disintegration due to slaking behavior of mudstone related to the mechanism of weathering, slaking durability and intragranular pores.

Figure 21. The mudstone specimen for accelerated slaking test (NEXCO-110-2012)

4.2.2. The Breakage Parameter (B_r) by Hardin

Consider the shear strength of granular materials, to be dependent upon the basic friction angle and dilatancy during shearing (Taylor, 1948 and Rowe, 1962). It is shown that the shear strength increases with increasing the dilatancy, which tends to decrease with increasing confining pressure. Lee and Seed (1967) exhibited that, under high pressure, the shear strength of sand increased while the dilatancy decreased. They attributed this observation to particle crushing and rearrangement during shearing. Miura and O-hara (1979) indicated that particle breakage could be significant for low-strength granular materials such as decomposed granite, even under low confining pressure. McDowell et al. (1996) discussed the existence of the limiting particle size based on the concept of fractals, but this quantity is not always a fractal. In addition, the particle size properties themselves can be defined based on another scalar quantity, but when describing constituent relationships, it is convenient to define I_G that increases monotonically from 0 to 1. Meanwhile, Hardin (1985) proposed the relative crushing ratio B_r as an index of crushing quantity that identical with I_G. B_r is, as shown in Figure 22(b), given as the ratio of the area *ABCD* and *ABCE*, and the change in B_r. However, even when particle size crushed and slake, B_r does not reach 1 realistically, and the relative crushing ratio B_r does not consider the limiting particle size. Hence, it is inconvenient to use it for constituent modeling as a state variable of particle size. Although both indices take a value from 0 to 1, Hardin's breakage parameter *Br* does not incorporate the idea of limiting or critical grading. There is, however, considerable experimental evidence for a limit on grading before the *Br* reaches 1, with the results presented here suggesting that the change in grading during wetting and drying can be described by the grading index I_G in a similar way to particle crushing. Based on the particle size distribution curve after wetting and drying cycles, the breakage parameter (*Br*) value will be analyzed.

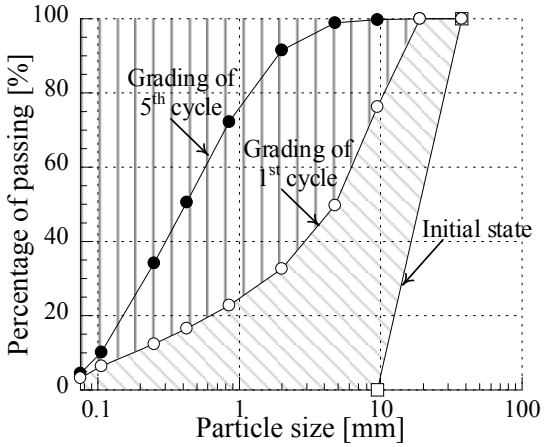

(a) The sample of curve of particle distribution to determine breakage parameter (B_r)

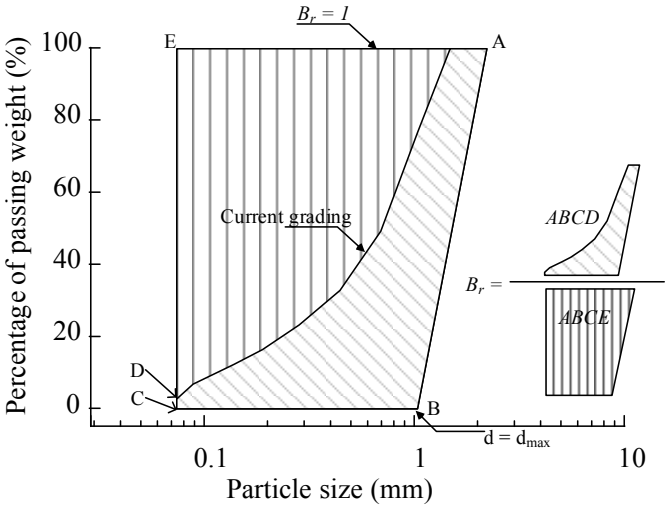

(b) Hardin's Breakage parameter (B_r)

Figure 22. Change in particle size accumulation curve and definitions of B_r parameters

4.2.3. Chemical and Mineralogy Analysis

X-ray fluorescence (XRF) and x-ray diffraction (XRD) analyses used both bulk samples and size fractions to determine the composition of the material. Bulk, silt, and sand mineralogy was obtained from random-oriented mount samples mounted in the XRD unit and analyzed at a speed of 2θ (two theta) per minute with copper K-beta radiation. Cutting edge and beam stopper was used during conduct the XRD test to minimize the error and interference from unnecessary mineralogy element. The Bragg Brentano configuration had been used during conduct the XRD test. The configuration of the Bragg-Brentano diffractometer is very simple, but the lattice constants can be determined at the precision of five significant numbers by using this type of diffractometers. Since Bragg-Brentano diffractometers have been used for a long time, the errors of the instrument have already been studied in detail. It is known that significant deformation of observed diffraction peak profile is caused by spectroscopic profile of the specific x-ray, axial divergence aberration, flat-specimen aberration and sample-transparency aberration. Minerals were identified by a computerized package PDXL analysis. The oriented-mounted samples intensify the (001) reflections and reduce (hk0) reflections by removing non-platy minerals, dispersing clay minerals into individual colloidal particles, and laying the clay particles flat (Moore and Reynolds 1997). The filter transfer method, as recommended by Moore and Reynolds (1997), was used to transfer the material to a filter. The type of clay mineral is identified by the characteristic expansion, contraction, or collapse of the clay mineral's d-spacing. XRF test, as mentioned in the previous chapter, the energy dispersive X-ray fluorescence spectrometer irradiates the sample with X-rays and measures the energy (wavelength) and intensity of the generated fluorescent X-rays to determine the

type and content of the elements comprising the sample. The X-ray fluorescence spectrometry permits the non-destructive elemental analysis of solid, powder, and liquid samples as well as rapid, non-destructive testing for harmful elements in printed circuit boards and other electronic devices. The XRF and XRD test are performing to the mudstone specimen after the accelerated slaking cycle performed.

4.2.4. SEM and morphology analysis

Scanning electron microscope or SEM is one methods to analysis the quality of morphology in soils and rock surface appearance. Dry samples are required for analysis in the vacuum environment of the scanning electron microscope (SEM). The freeze-drying technique was used to obtain relatively undisturbed samples. A sample from each mudstone specimen after accelerated slaking cycle was prepared. The size of diameter particle was selected between 2.00 - 0.85 mm. The surface morphology of mudstone specimen will observe on five random points on the surface mudstone particle and compare to the initial surface condition before accelerated slaking applied.

4.3. Result and Discussion

4.3.1. Accelerated Slaking on Mudstone

This study has an interesting research on the evolution of grading induced by weathering mechanism on mudstone. An extensive study of a disintegrated weathering rock of mudstone was carried out under accelerated slaking test procedure (NEXCO-110-2012). The particle size distribution and mineral content include the morphology texture were characterized for each mudstone specimen and the results will be discussed later. The cumulative distributions of the particle size changes of mudstone specimen under accelerated slaking test shown in Figure 23. According to the test result, the Kobe, Jouetsu and Nou mudstone (Figure 23), which reveals that the mudstone particle was clearly disintegrated after the first cycle applied and more than 80% of the particles (by weight) were smaller than 9.5 mm. This percentage of particles smaller than 9.5 mm increased to approximately 100% after five cycles of wetting and drying, yet the maximum grain size remained almost the same. The particle size distribution became a straight line in a semi-logarithmic plot of particle size against the percentage of finer particle by weight, and so the uniformity coefficient was apparently increased. The sequential photographs presented in Figure 23 confirm that slaking occurred after the wetting and drying cycles, with the fracture and crumble of some particles becomes the finer grains, while other particles remained intact. It is apparent from the accelerated slaking test results for the other

mudstone specimens in Figure 23 (e) to (g) that, although a change in particle size distribution occurred with all mudstone types, the magnitude of this change in grading was notably different.

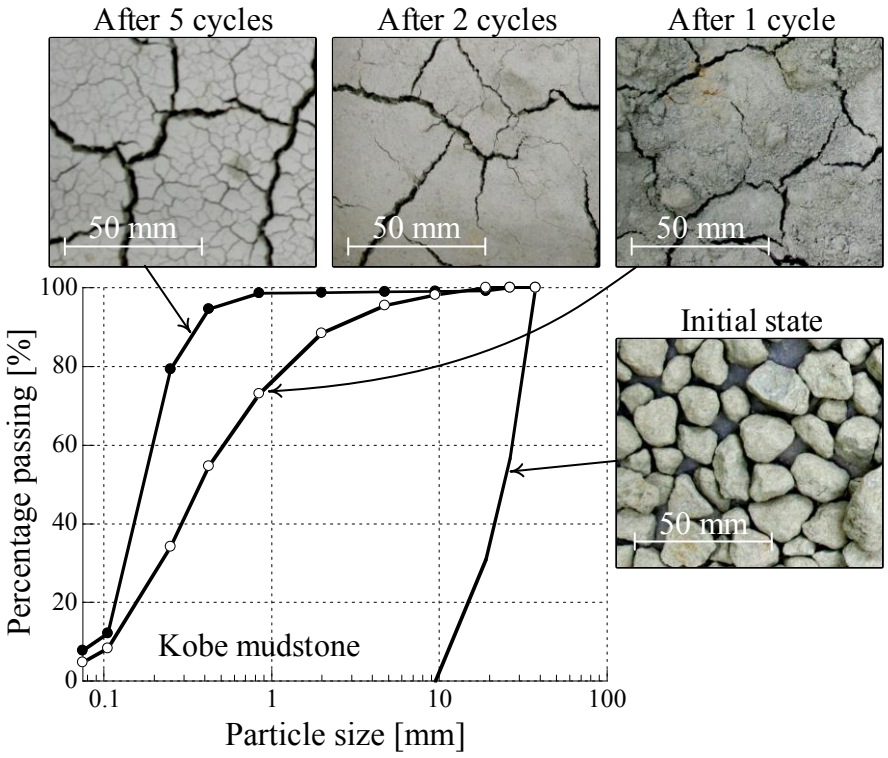

(a) Kobe mudstone

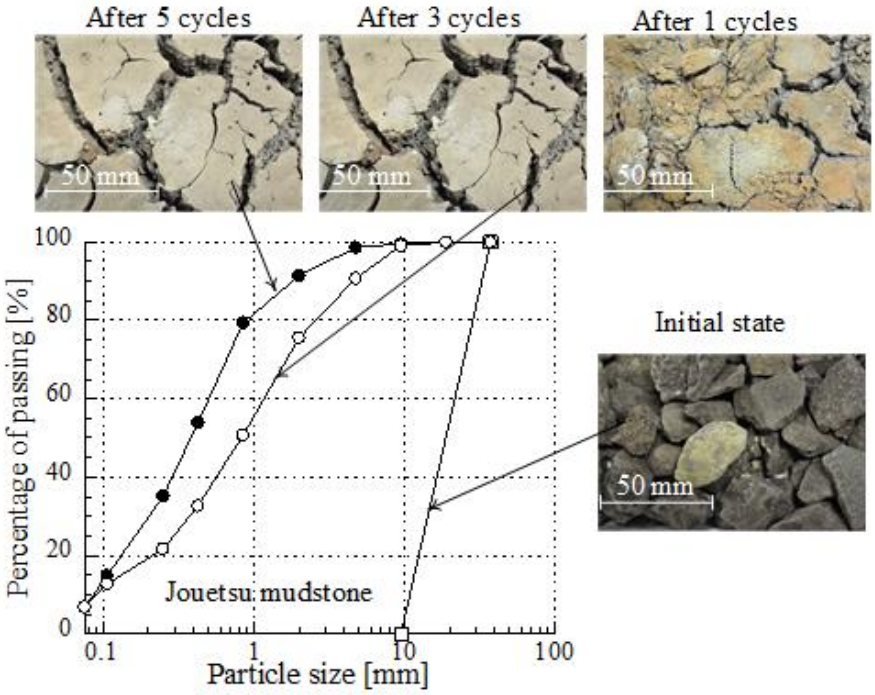

(b) Jouetsu mudstone

Figure 23. (continue)

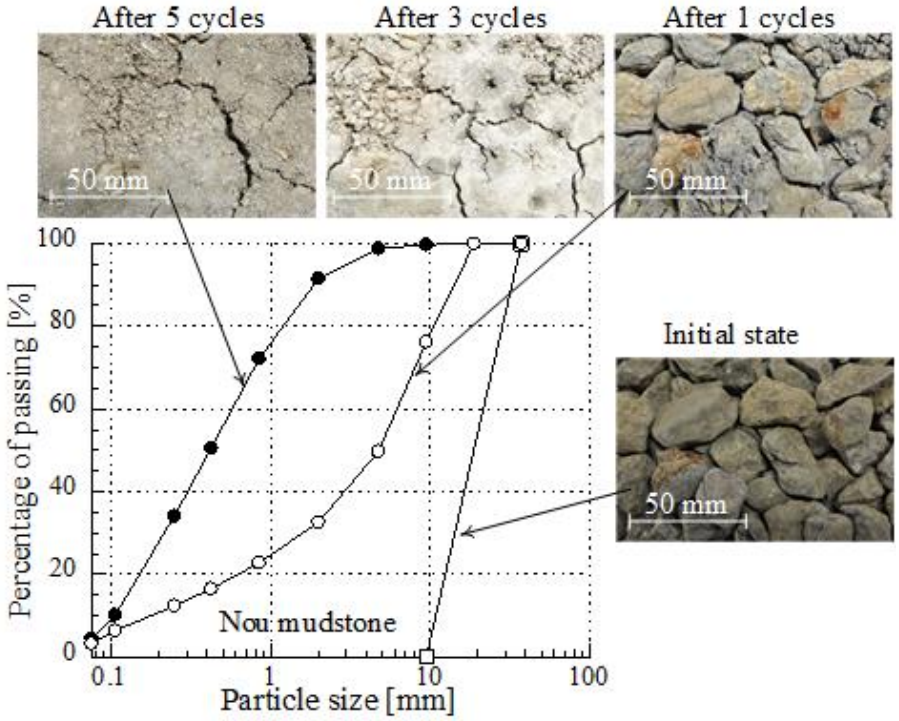

(c) Nou mudstone

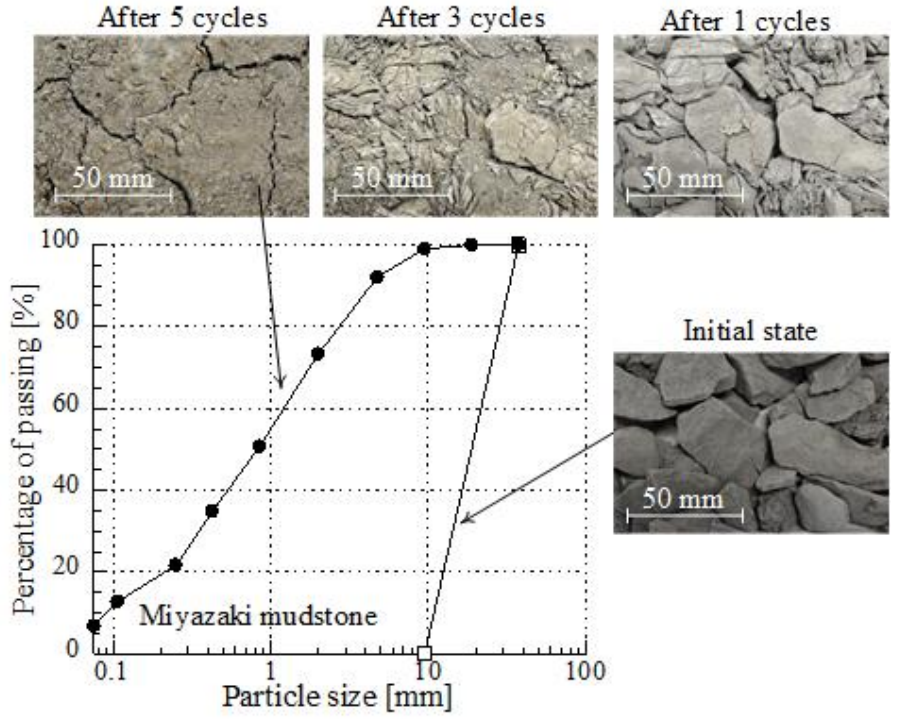

(d) Miyazaki mudstone

Figure 23. (continue)

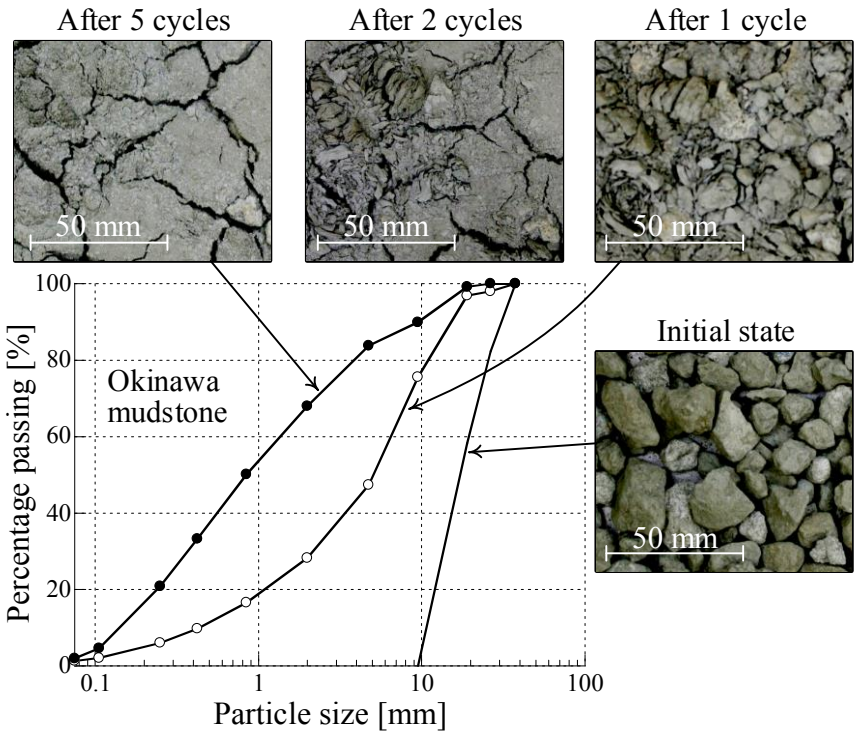

(e) Okinawa mudstone

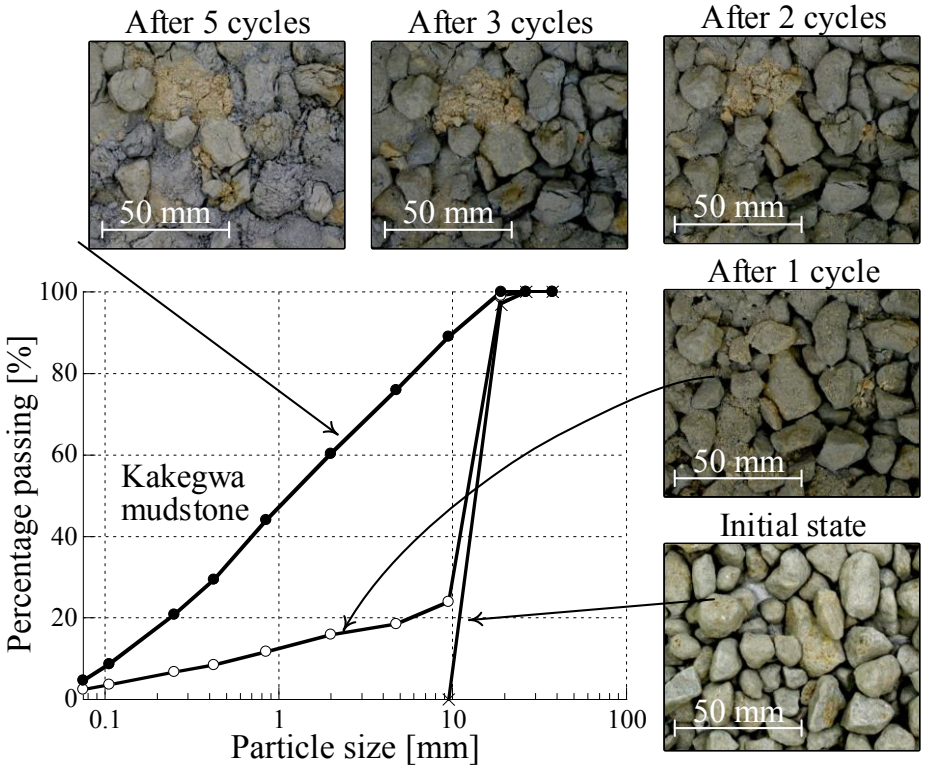

(f) Kakegawa mudstone

Figure 23. (continue)

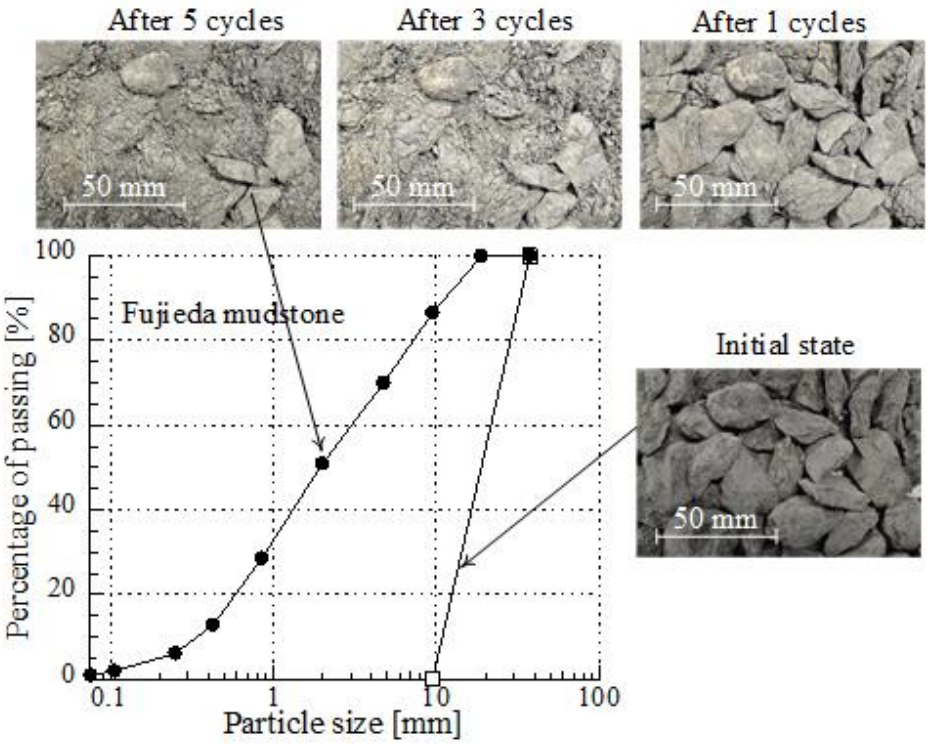

(g) Fujieda mudstone

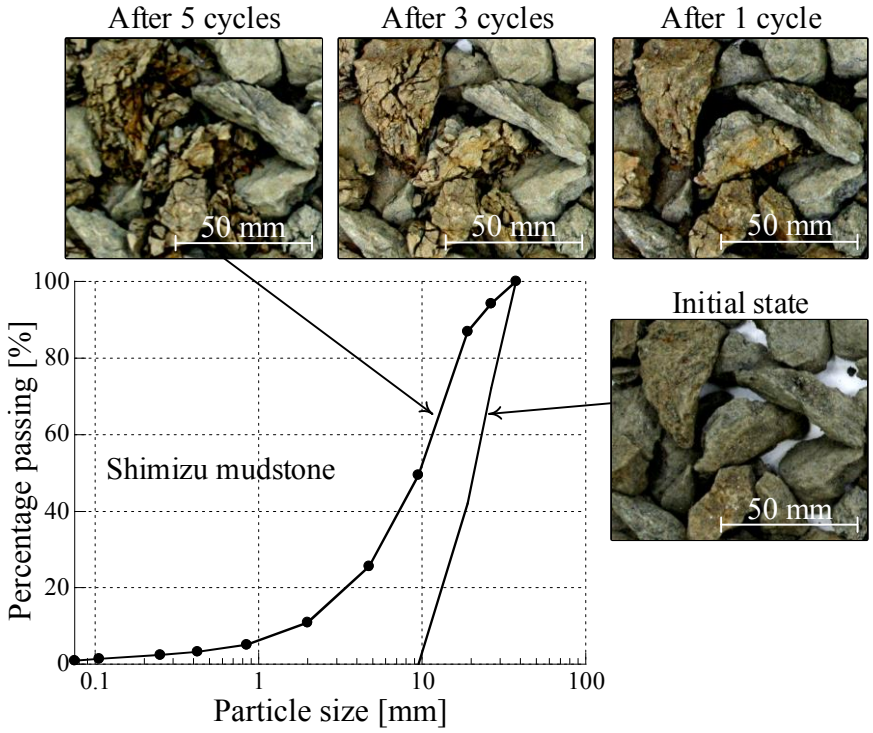

(h) Shimizu mudstone

Figure 23. (continue)

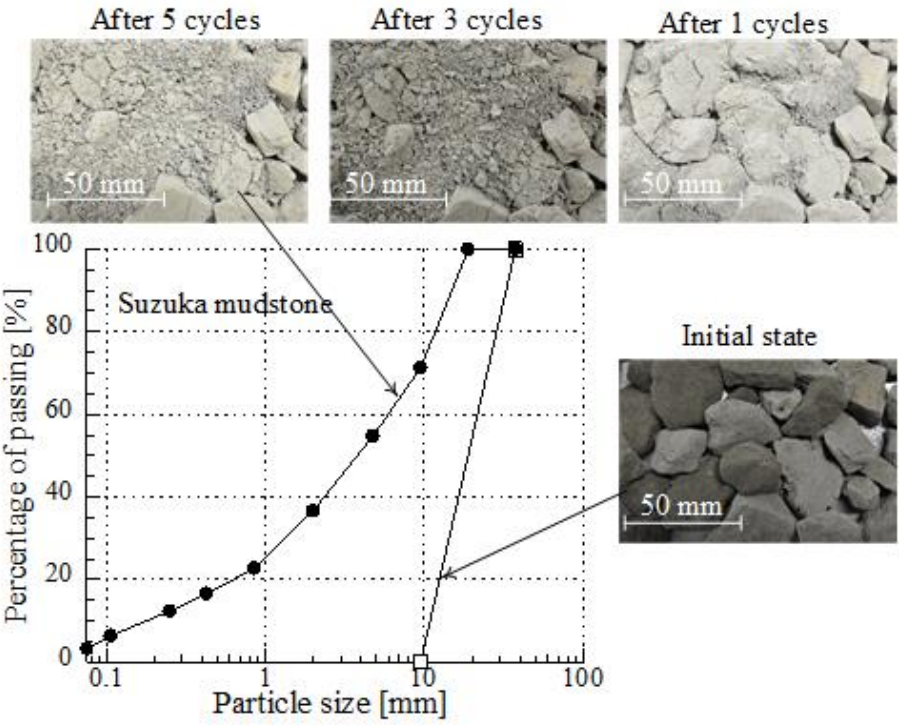

(i) Suzuka mudstone

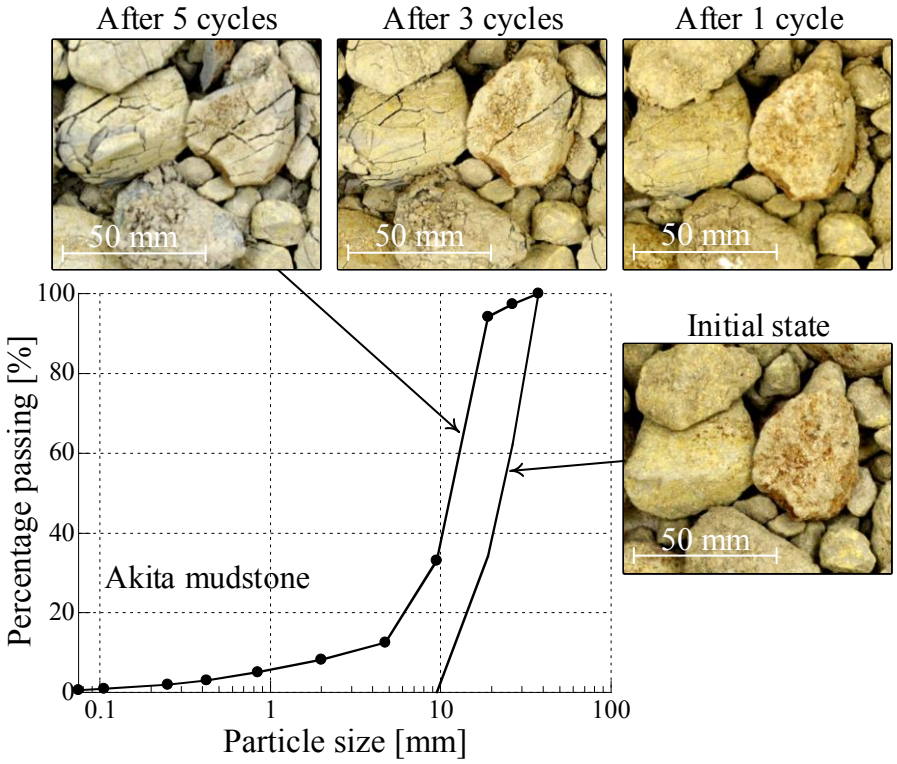

(j) Akita mudstone

Figure 23. (continue)

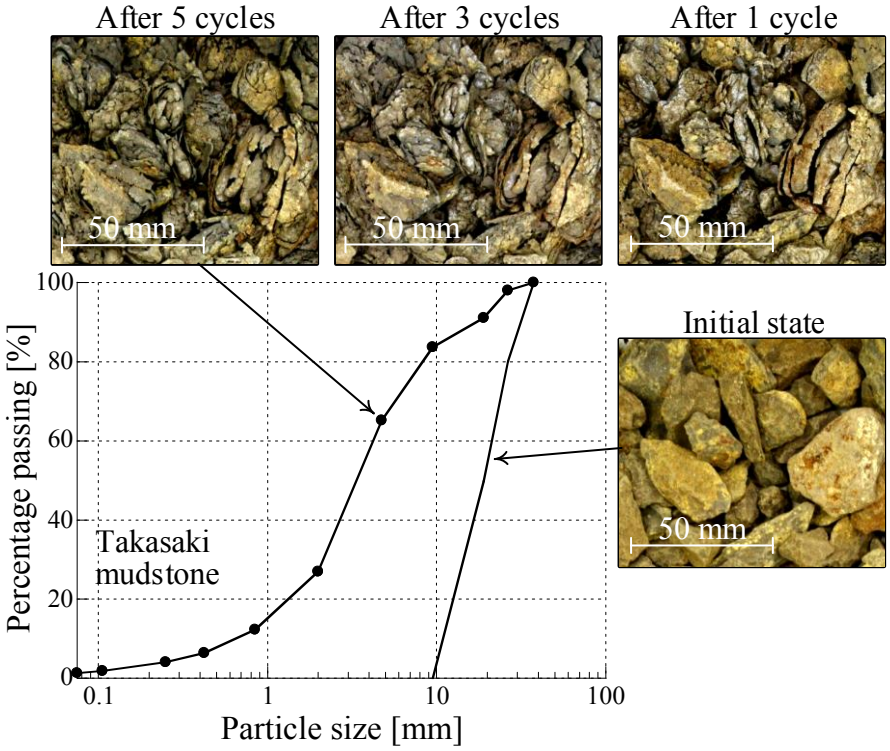

(k) Takasaki mudstone

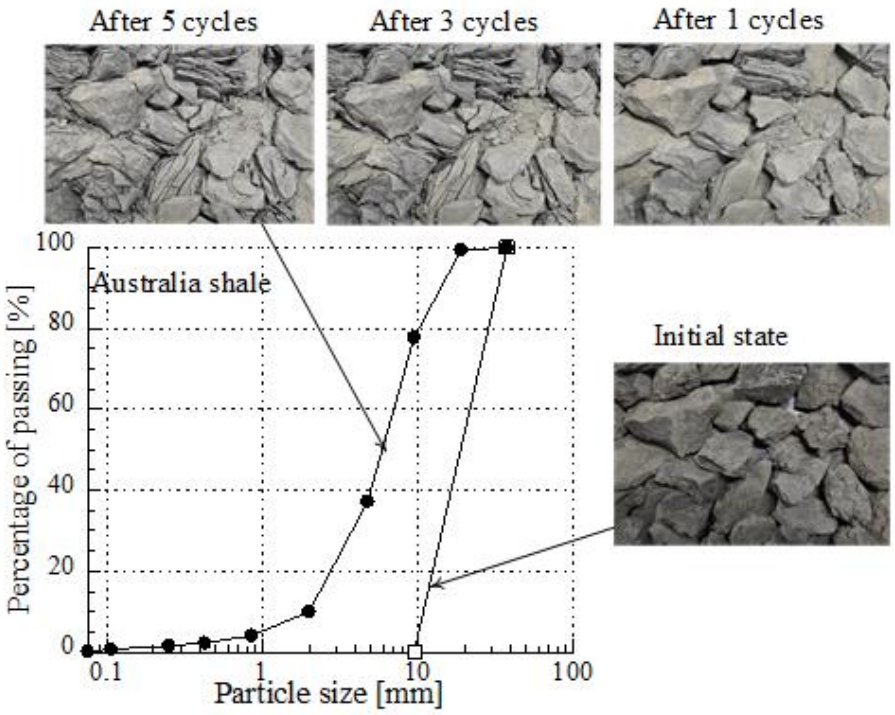

(l) Australian shale

Figure 23. Variation in particle size distribution during accelerated slaking

The particle size distributions of the crushed Kakegawa, Miyazaki, Fujieda and Okinawa mudstone, for instance, changed quite slowly after the first wetting and drying cycle, and then continued to vary with an increasing number of cycles. There is also a clear decrease in maximum particle size with these specimens, as most particles crumble during the first cycle and are only weakly aggregated after the drying process. Meanwhile, the sequential photographs in Figures 23 (h) to (l) of the crushed Akita, Shimizu, Takasaki, Suzuka and Australia shale mudstone all exhibit a similar slaking behavior, in that particles fracture while retaining their original shape, and so gradually crumble into finer grains with an increasing number of wetting and drying cycles. The fracture appeared to occur in a specific direction in the particles of the Takasaki mudstone and Australia mudstone, causing these to be crushed into thin layers.

Based on the variation of particle size distribution after accelerated slaking test, the first conclusion regarding the resistance of mudstone will be drawn. The Kobe, Nou and Jouetsu mudstone are easily to alter since the first wetting applied to both of this specimen. The Kakegawa, Miyazaki, Fujieda and Okinawa mudstone have similar variation in particle size distribution, even though the weathering or crumbling process after first cycle wetting and drying a bit late than Kobe, Nou and Jouetsu mudstone. The last criteria were presented by Akita, Takasaki, Shimizu, Suzuka and Australia, which the shape of grading size distribution almost similar, lower than 65% from cumulative distribution was smaller than 9.5 mm after fifth wetting and drying cycle applied. As an important parameter characterizing of particle size distribution, the cumulative distribution of D_{10}, D_{50} and D_{90} are necessary to identified. Particle size distribution of D_{50} is also known as median diameter or the medium value of the particle size distribution, it is physically representing of each number of particles greater or smaller than such value takes account of 50% of the total particles number. D_{50} is usually used to represent the particle size of group of particles. The span of cumulative distribution of particle would be recognized based on D_{90} and D_{10}.

Figure 24 exhibit the characteristic of mudstone specimens subjected to the volume average of particle size and the span of cumulative distribution. In accordance with the previous discussion, from D_{10} and D_{90} clearly shown that span of cumulative distribution of particle are wider for the hardest mudstone material and becomes narrower for the weakest mudstone material. Furthermore, it is known that the volume average of particle size distribution of D_{50} is an important parameter characterizing particle size. Related to the breakage parameter (B_r) after accelerated slaking test, an interesting correlation to the D_{50} and B_r shown the unique tendency (Figure 25). Next discussion is paid attention to the breakage parameter (B_r) in

accordance with the objective of this study. Related to the slaking ratio and grain crushing ratio relation in Figure 26, shows that 2/3 of all mudstone specimen has a slaking ratio more than 80%. According to the NEXCO standard, it was expected that mudstone with the high grain crushing ratio and low slaking ratio are worth it to be used as earth construction material.

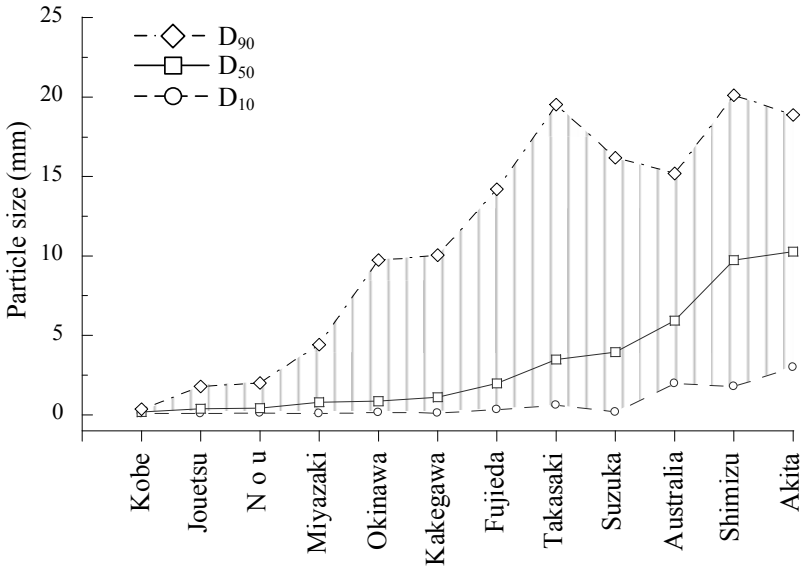

Figure 24. Particle size distribution D_{10}, D_{50} and D_{90} corresponding to the percentages 10%, 50%, and 90% of particle after accelerated slaking test

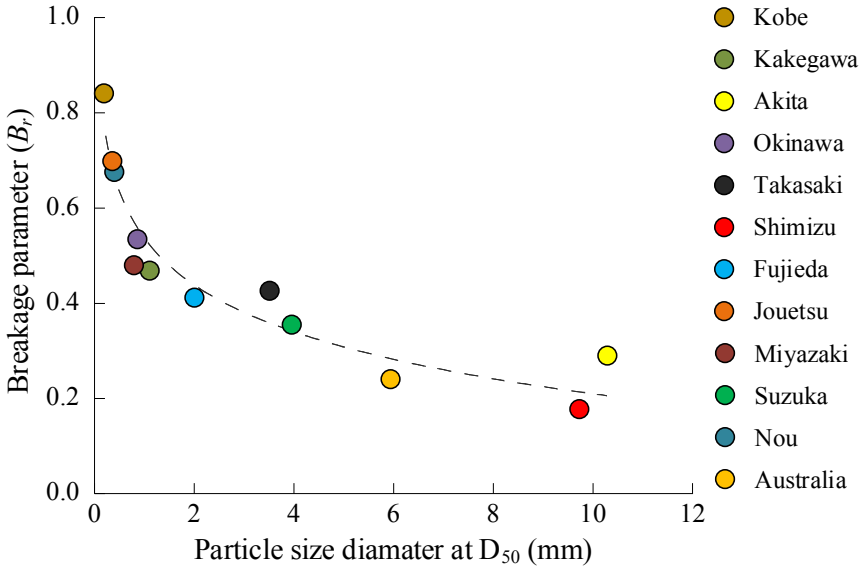

Figure 25. Correlation between Breakage parameter (B_r) and the particle size diameter at D_{50}

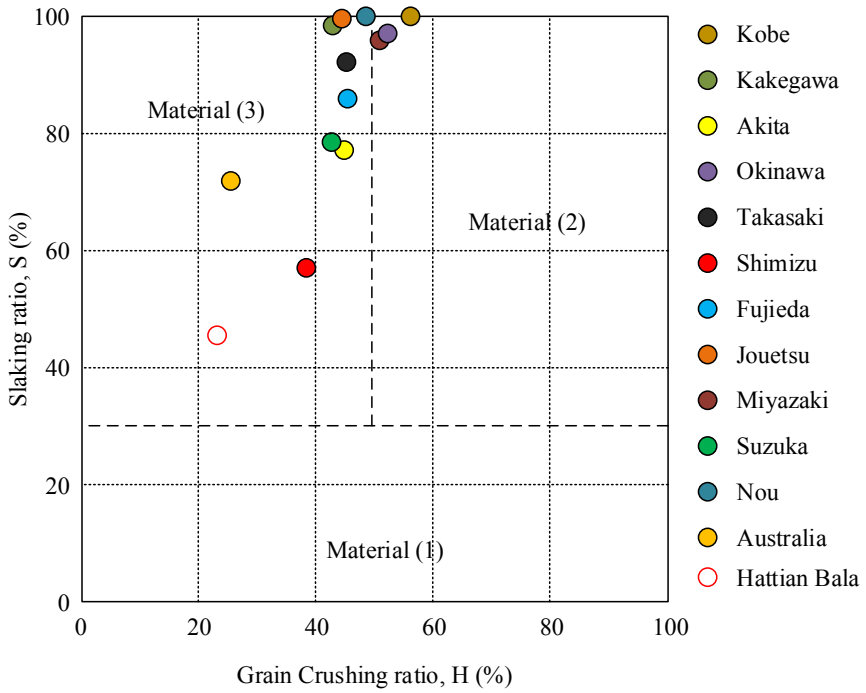

Figure 26. Grain crushing ratio (*H*) against Slaking ratio (*S*)

4.3.2. The clay minerals content after acceleration slaking test

Investigate the mineral content after the test to understand the chemical or physical weathering on the slaking of mudstone is necessary. In this subchapter, in Figure 27 shows the XRD patterns of clay mineral content of Kobe, Kakegawa and Hattian Bala mudstone. Based on those result, seems to be give an initial description that the mineral content was slightly changed. Further investigation needed regarding the percentage of mineral content. In general, the mineral content of mudstone after the test is not changed. The mineral content consists of quartz mineral group of quartz, plagioclase, K-feldspar, carbonate, pyrite and dolomite, and next is clay mineral group of illite, kaolinite, chlorite, muscovite and smectite (montmorillonite, nontronite and saponite). The weathering processes in sedimentary rocks is an important concern include the significant progress regarding the identification of chemical content, physical appearance and/or combination of physical-chemical alteration mechanisms (Taylor & Smith, 1986; Seedsman, 1986; Taylor, 1988; Olivier, 1990).

Similar to the aforementioned studies, in this subchapter, evaluate the weathering process of mudstone during accelerated slaking test by investigate the mineral content which has correlation with two kinds of weathering mechanisms. Physical weathering or disintegration is considered as the dominant process because it occurs faster than chemical decomposition and produces more diverse of surface appearance (Taylor & Cripps, 1987; Marques, 1992; Marquez, et.al, 2010). As known, the chemical reactions happen at a characteristic reaction

rate at a given temperature and chemical concentration. Typically, reaction rates increase with increasing temperature because there is more thermal energy available to reach the activation energy necessary for breaking bonds between atoms (Laidler & Meiser, 1982). Therefore, due to the temperature in accelerated slaking tests are constant room temperature during wetting cycle then it can be inferred that the chemical reaction on weathering process occurs slowly. Paid attention on the smectite content as an expandable clay mineral and the reaction to other mineral is one of purpose to explore the weathering process.

The smectite group of clays has a T-O-T structure is similar to Pyrophyllite but can also have significant amounts of Mg and Fe substituting into the octahedral layers. Thus, the smectites can be both di-octahedral and trioctahedral. The most important aspect of the smectite group is the ability for H_2O molecules to be absorbed between the T-O-T sheets, causing the volume of the minerals to increase when contacted with water contact into water.

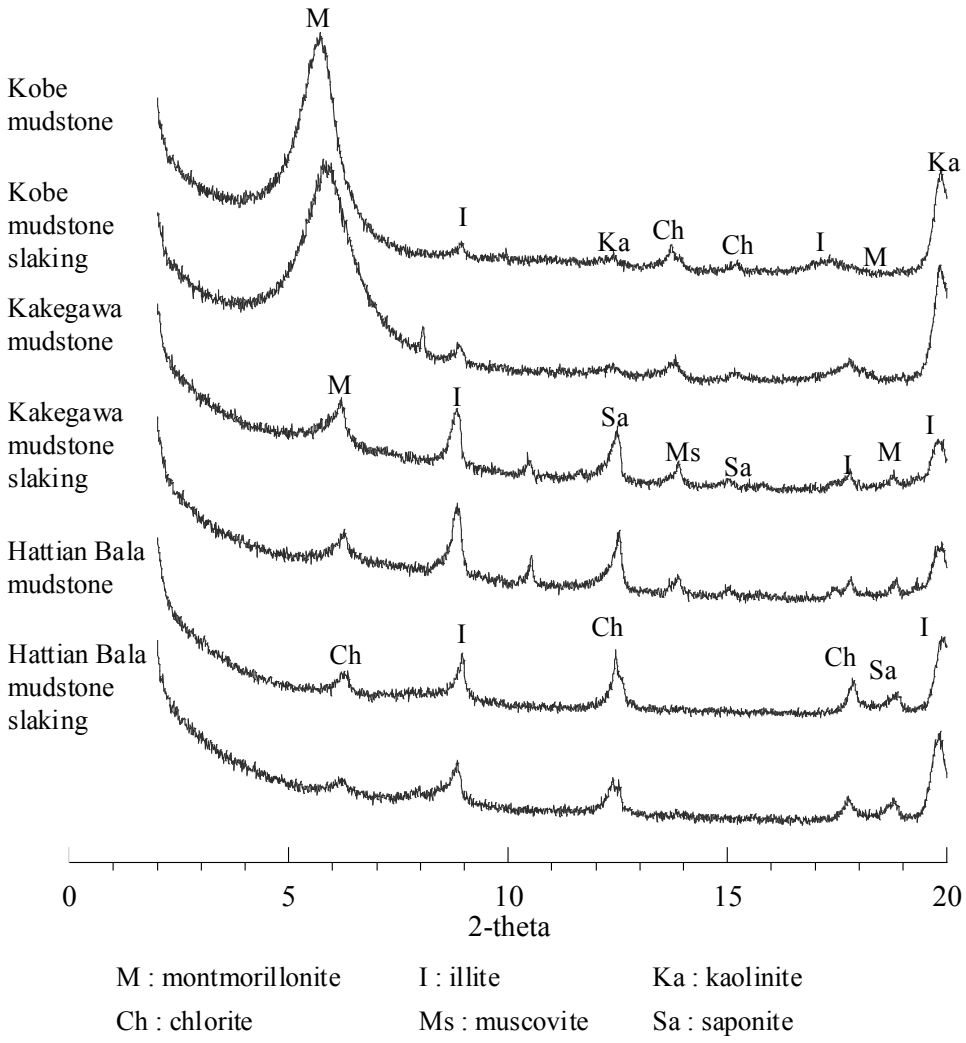

Figure 27. The XRD patterns of clay mineralogy content of Kobe, Kakegawa and Hattian Bala mudstone before and after accelerated slaking test

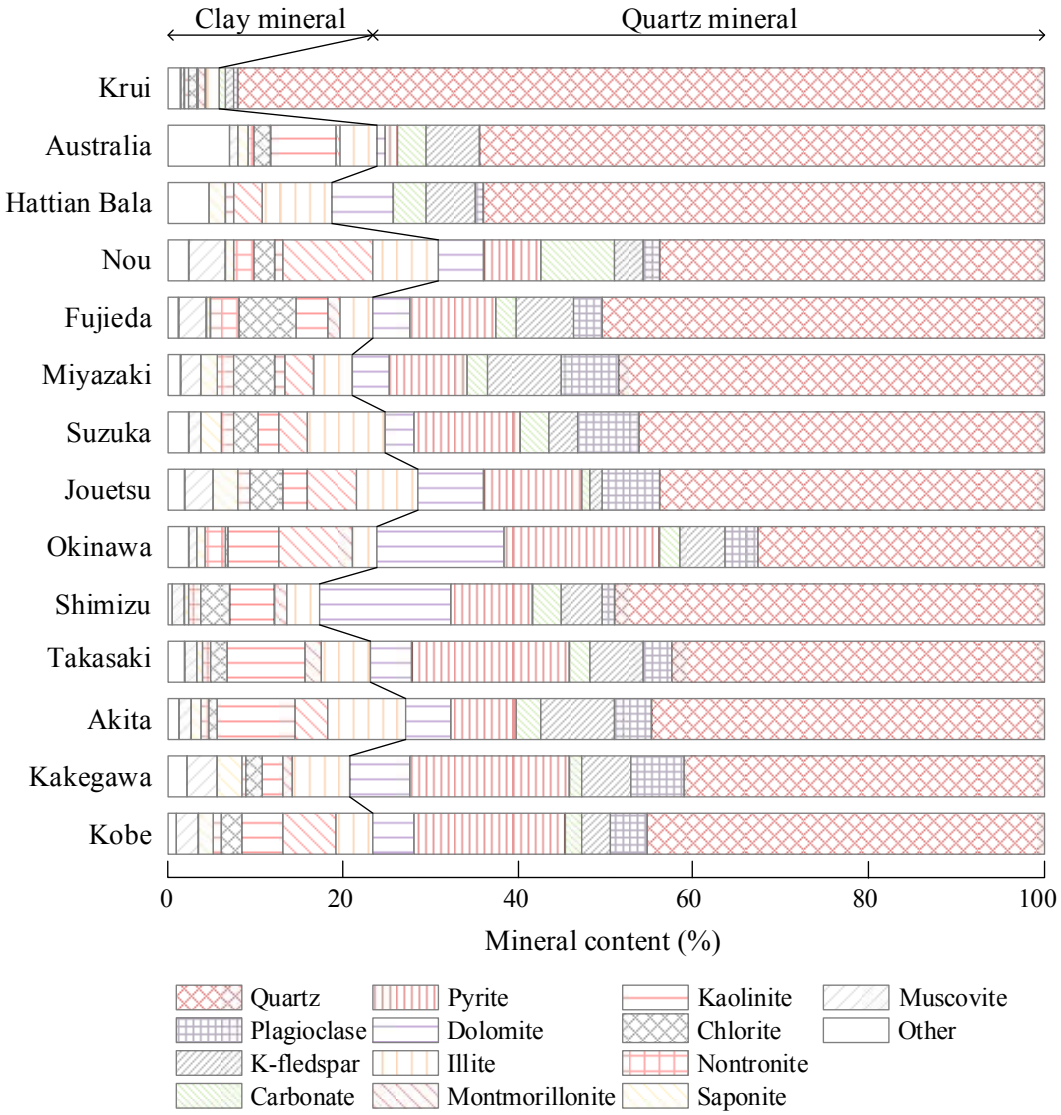

Figure 28. Changes of clay mineralogy content of mudstone and shale materials after accelerated slaking test

Thus, the smectites are expanding clays. The most common smectite is Montmorillonite. Montmorillonite is the main constituent of Bentonite, derived by weathering of volcanic ash. Montmorillonite can expand by several times its original volume when it encountered water. Montmorillonite, however, is a dangerous type of clay to encounter if it is found in tunnels or road cuts. Because of its expandable nature, it can lead to serious slope or wall failures. Other, less common, members of the smectite group include Beidellite, Hectorite, Nontronite, Sauconite, and Saponite. It is makes more confident that smectite clay mineral content is one of important role in physical weathering process. Figure 29 shows the percentage of smectite mineral during accelerated slaking test. In associated with the changes of particle size distribution due to slaking in chapter 3, Kobe mudstone, Okinawa mudstone, Jouetsu mudstone and Nou mudstone show an appropriate relationship or tendency that weathering

process after the first cycle. The physical disintegration of particle suddenly occurs from the first wetting cycle applied, it can be concluded that physical weathering plays an important role in this weathering process, instead of chemical weathering. Nevertheless, not only the four mudstones were affected by physical weathering but all mudstone and shale in this study were affected by the same mechanism. Further, the effect of smectite mineral on the physical weathering should be explained based on the relationship between the breakage parameter (B_r) and the percentage of smectite clay mineral. Figure 30 shown that the breakage parameter tends to increase due to the percentage of smectite clay mineral. It can be concluded that physical disintegration of particles is strongly influenced by the amount of smectite clay mineral content. However, it is known that mudstone is more dominated by quartz mineral content instead of smectite or clay mineral content, but in the weathering process, smectite clay minerals have more significant role impacts. Paid attention to the Kobe, Jouetsu, Kekegawa and Takasaki mudstone, the breakage parameter value slightly higher than the other mudstone which has large amount of smectite content. There are two possibilities causes these circumstances. The first, it has relation with the size of intra-granular pores. The second one is predicted to occur due to the nontronite ($Na_{0.3}Fe_2((Si,Al)_4O_{10})(OH)_2 \cdot nH_2O$) content in Kobe, Jouetsu, Kakegawa and Takasaki mudstone more than other mudstones. The other mudstone has a saponite content ($Ca_{0.25}(Mg,Fe)_3((Si,Al)_4O_{10})(OH)_2 \cdot nH_2O$) than nontronite content. It is interesting to understand since the ion Na^+ characteristics. The ion Na^+ is excellent in swelling property and suspension stability instead of ion Ca^+.

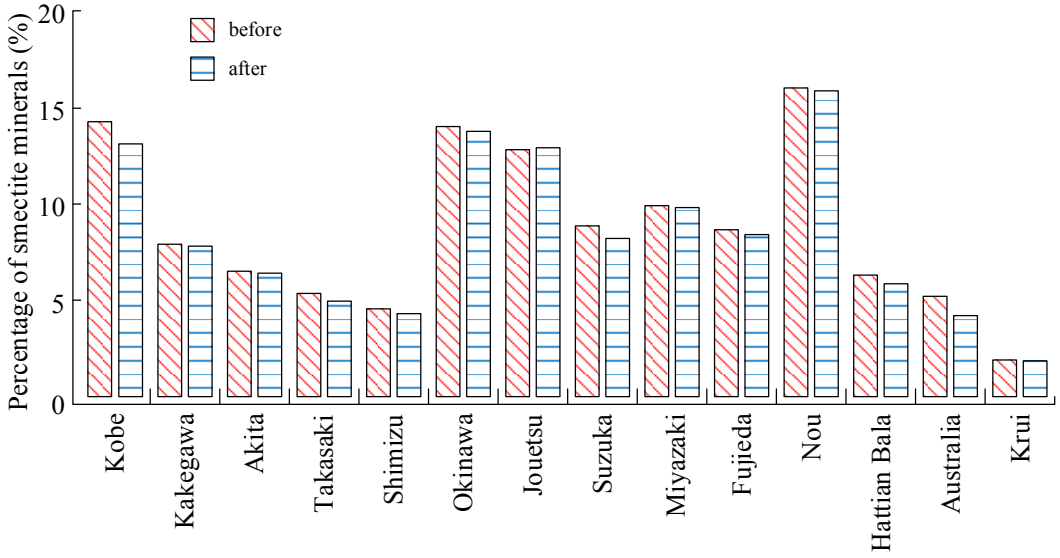

Figure 29. A variation of smectite mineral content during accelerated slaking test

In this study, the chemical reaction of other minerals caused by the smectite mineral content are also necessary to studied. Many researchers have observed that smectite clay minerals react towards illite through intermediate mixed-layer that are deeply buried in sedimentary basins (Weaver and Beck, 1971; Hower et al., 1976; Boles and Franks, 1979). This mineralogical reaction is herein termed smectite illitization.

$$Al_2Si_4O_{10}[OH]_2.\ nH_2O + KAlSi_3O_8 \rightarrow KAlSi_3O_{10}[OH]_2 + 4SiO_2 + nH_2O$$

(smectite) (K-feldspar) (illite) (quartz)

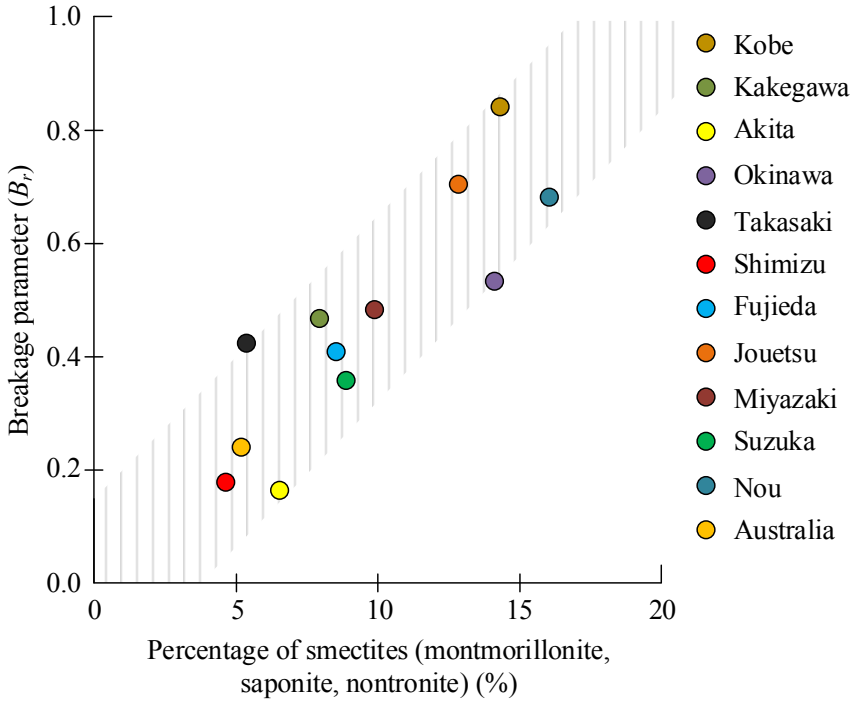

Figure 30. The effect of smectite content as an expansive clay mineral to the weathering process based on the breakage parameter (B_r)

Figure 31 shows the illite and quartz content increase caused by the reaction between smectite and k-feldspar. However, the appropriate analysis regarding the chemical reaction of smectite with K-feldspar is not yet clear enough since Kobe and Okinawa mudstone exhibit the contrary result. At least, the increase of percentage of illite and quartz minerals was confirmed the previous statement regarding the chemical reaction of smectite mineral. Next, Russel and Parker, (1979); Dixon et al., (1982); and Chigira, (1990), pointed out that such changes in mineral composition were not controlled by the original composition of the materials but were caused by weathering and oxidation. Related to the weathering and oxidation process, it was mentioned that Pyrite content is quite important in these sequential of weathering of mudstone.

Pyrite is oxidized by oxygen coming from the ground surface and sulfuric acid is generated at the base of the oxidized zone. The transformation of pyrite at the oxidation process causes the sulfuric acid is produced according to the formulae (Vear and Curtis, 1981; Berner and Berner, 1987). The crystal structures of sulfates are larger than that of pyrite, and this increase in volume can be substantial. Due to the process of oxidation pyrite, it will make the chlorite transform to be part of smectite. Combination of pyrite mineral and smectite clay mineral to observe the tendency relationship with breakage parameter was shown in Figure 32.

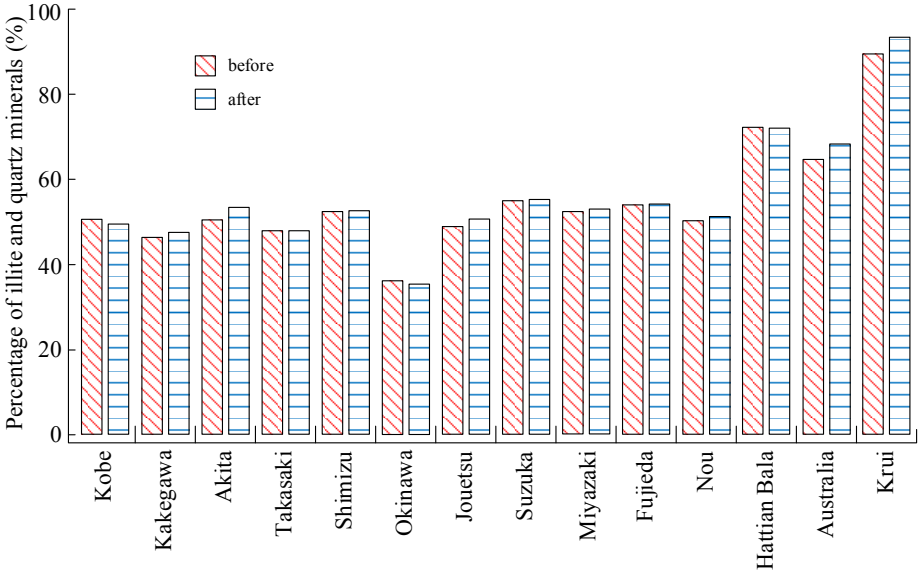

Figure 31. A variation of illite and quartz content after chemical reaction between smectite and kaolinite

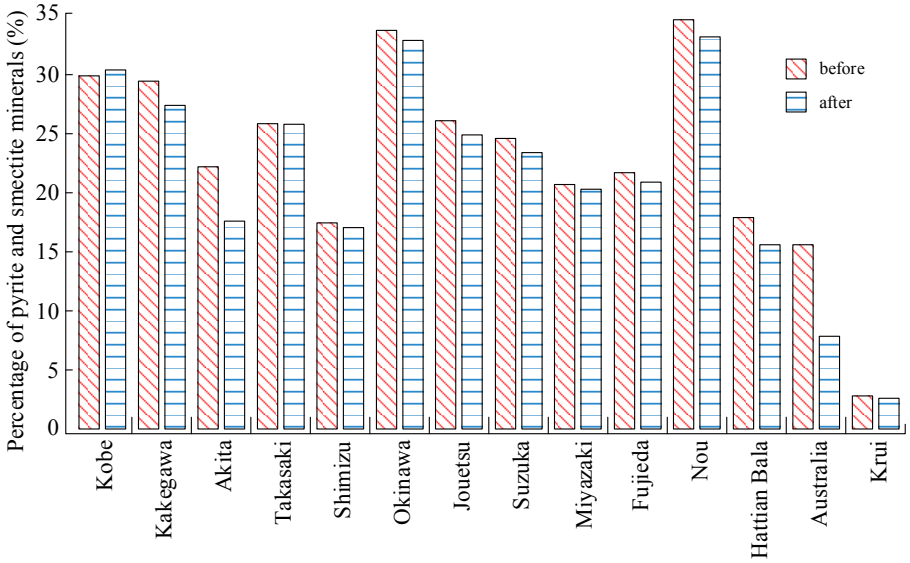

Figure 32. The combining percentage of pyrite as the main mineral on the process oxidation and smectite as an expansive clay to the weathering mechanism

Previously, it was concluded that the physical weathering mechanism is more dominant than the chemical weathering. Regardless of the change in mineral content of pyrite and smectite and the further process (Figure 33), it appears that both percentages of pyrite and smectite exhibit almost the same tendency with smectite mineral associated and the breakage parameter (B_r). But, the relationship between breakage parameter and the minerals content of pyrite and smectite seems extremely irregularly. Furthermore, the effect of smectite content against increasing of breakage parameter is more relevant and significant to describe the mudstone behavior associated with the weathering mechanism.

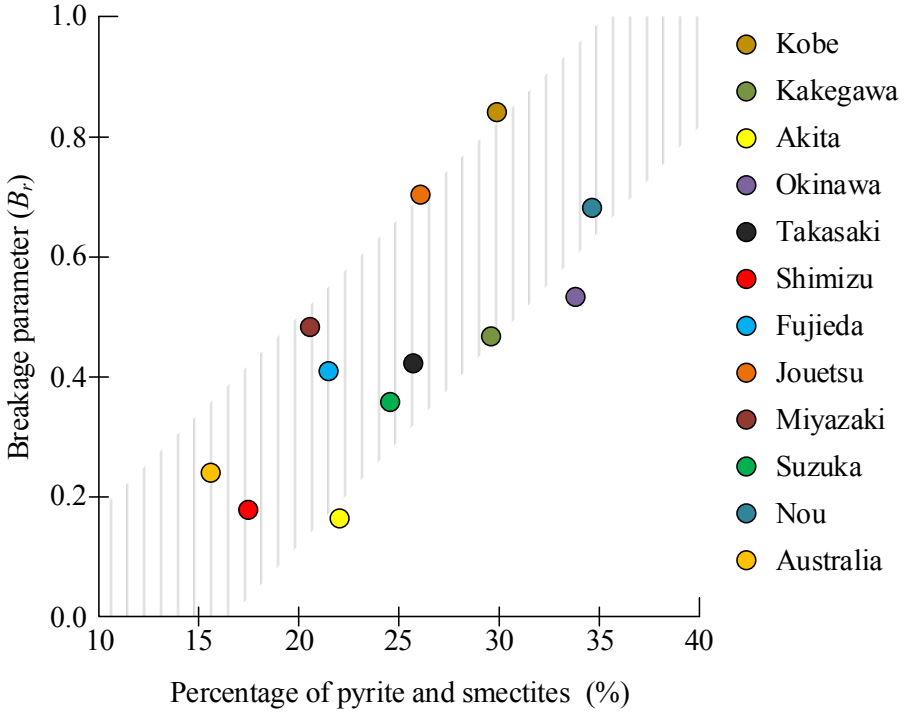

Figure 33. The effect of oxidation of pyrite mineral combining with the expansive potential of smectite content on the process of weathering of mudstone

4.3.3. The morphology appearance

The SEM photograph of morphology surface of Kobe, Kakegawa, Okinawa, Akita, Takasaki and Shimizu mudstone have been taken after a number cycles of accelerated slaking test. Santos et al. (1996) concluded that shale subjected to air drying are extremely reactive when exposed to water. Schmitt et al. (1994) explain the process of air-breakage in which trapped pore-air can lead to rock disintegration. According to these authors, when a specimen is allowed access to water, hydration by imbibition, i.e., penetration of a liquid water front within the rock, driven by capillary forces, occurs and combines with other processes such as hydration caused by condensation of gas phases in smaller pores to draw liquid into the rock.

This process can lead to entrapment and pressurization of pore air. Furthermore, because of very low permeability, pore air pressures sufficient to exert significant stress on the rock fabric may develop. During hydration of a specimen, air can be trapped in different ways, as presented on Figure 34.

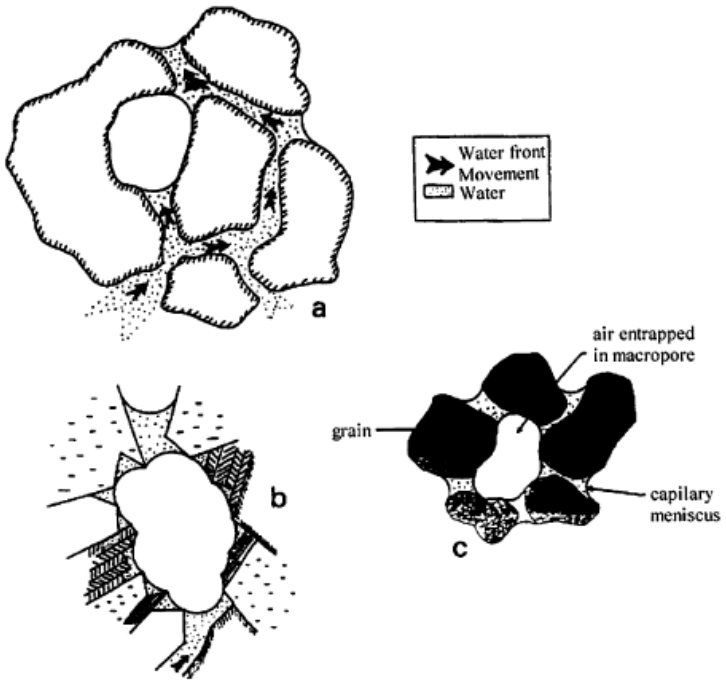

Figure 34. Air entrapment may occur by short–circuit of macro-pore (a), in a rough macro-pore (b) and by condensation of water in pore accesses (c)

In Chapter 3 had been discussed that one of the slaking mechanisms is attributed to the compression of air entrapped in the intragranular pores of the particles (Moriwaki, 1974). Vallejo et al. (1993) and Vallejo & Murphy (1999) studied the effect of the geometry of the intragranular pores and revealed that the size of the pores and the roughness of the pore boundaries have dominant effects on the resistance of particles against slaking. Figure 36 shows the morphology of mudstone specimen is seen that there is an increase in clay soil particles on all surfaces. Compare to Hattian Bala mudstone, the clay particle seen in a small amount. It means that increase of an amount of clay particle due to slaking exists even though the clay mineralogy content almost does not change. The presence of intragranular pores is still seen on Kobe mudstone and Okinawa mudstone. The small intragranular pores found in Akita mudstone. It is difficult to conclude the possibilities of disintegration particle during accelerated slaking based on morphology surface appearance. But the existence of intragranular pores and the changes of particle size distribution has revealed that physical appearance also gives a very significant effect on slaking process.

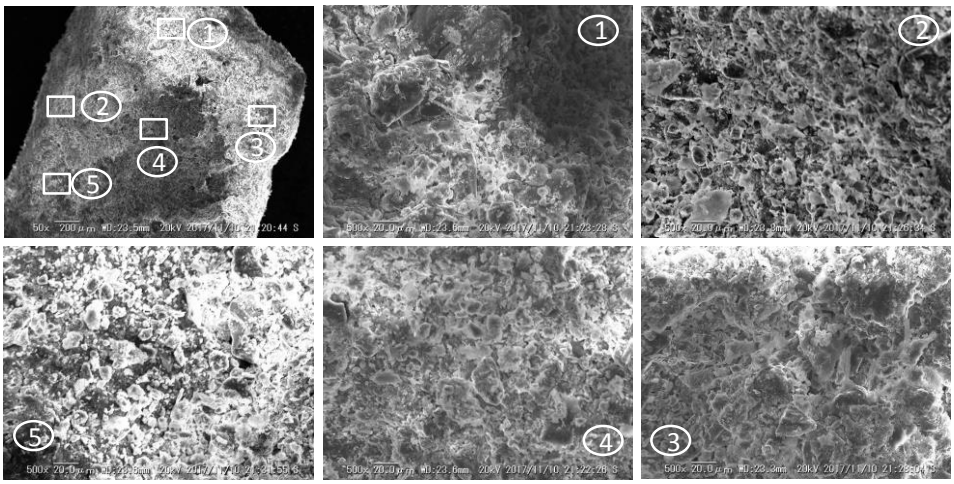

(a) Kakegawa mudstone

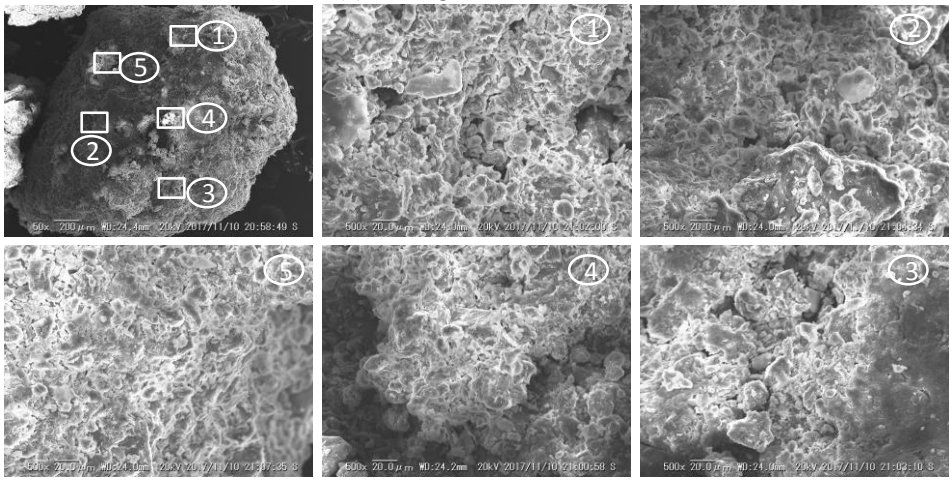

(b) Kobe mudstone

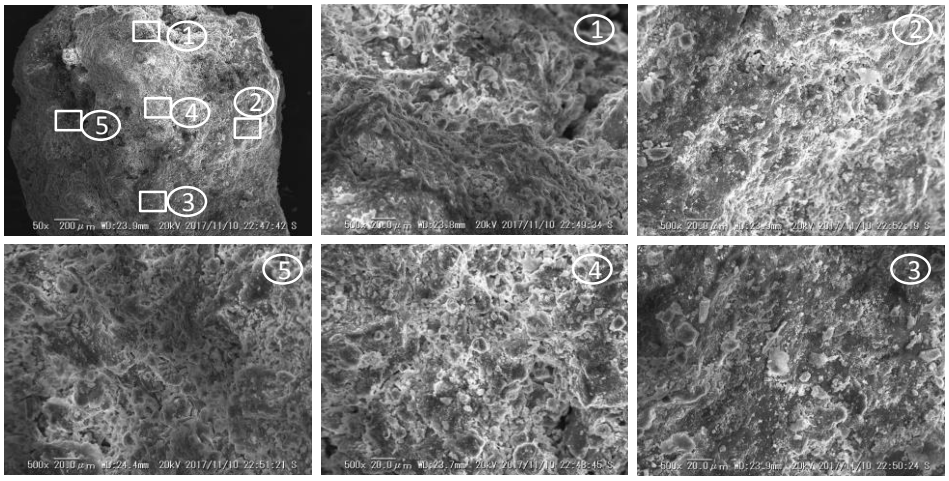

(c) Takasaki mudstone

Figure 35. (Continue)

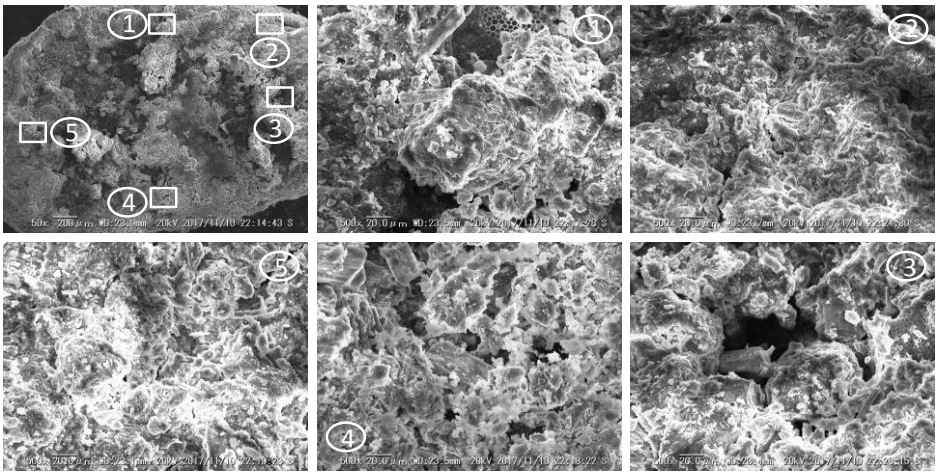

(d) Akita mudstone

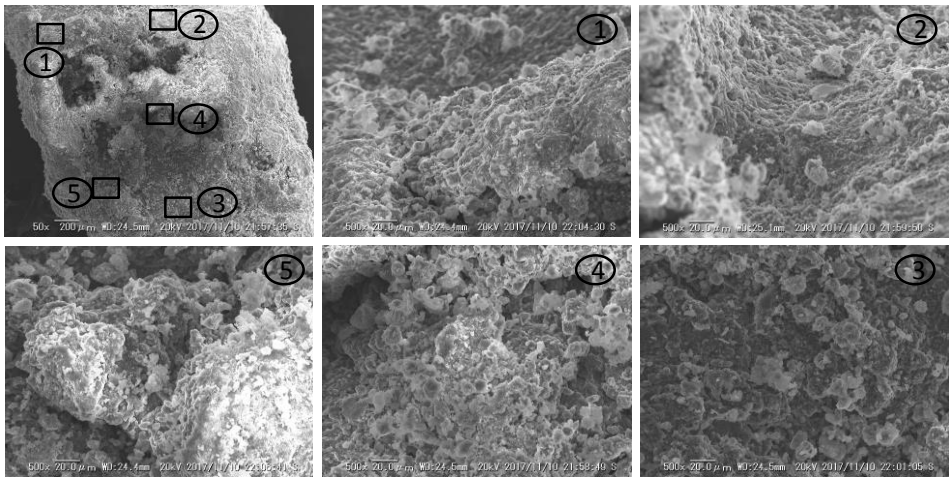

(e) Okinawa mudstone

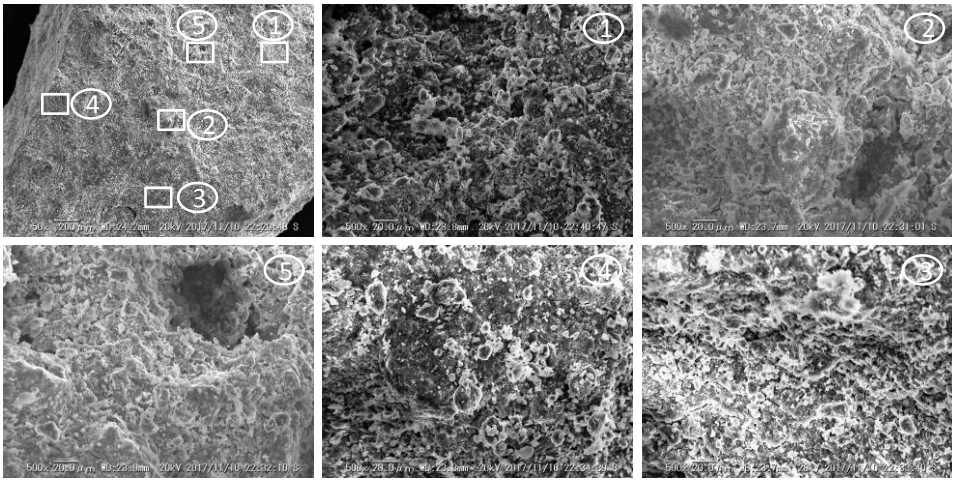

(f) Shimizu mudstone

Figure 35. (Continue)

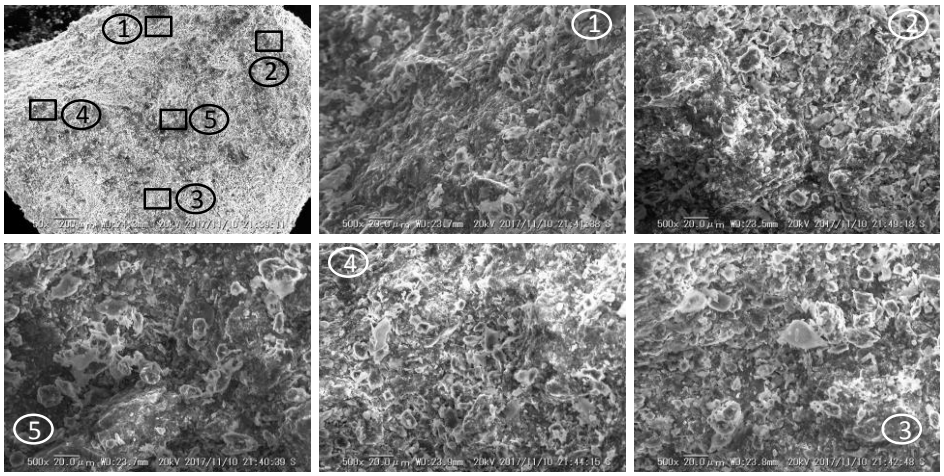

(g) Hattian Bala mudstone

Figure 35. The morphology surface appearance of mudstone specimens after slaking with magnification of x500

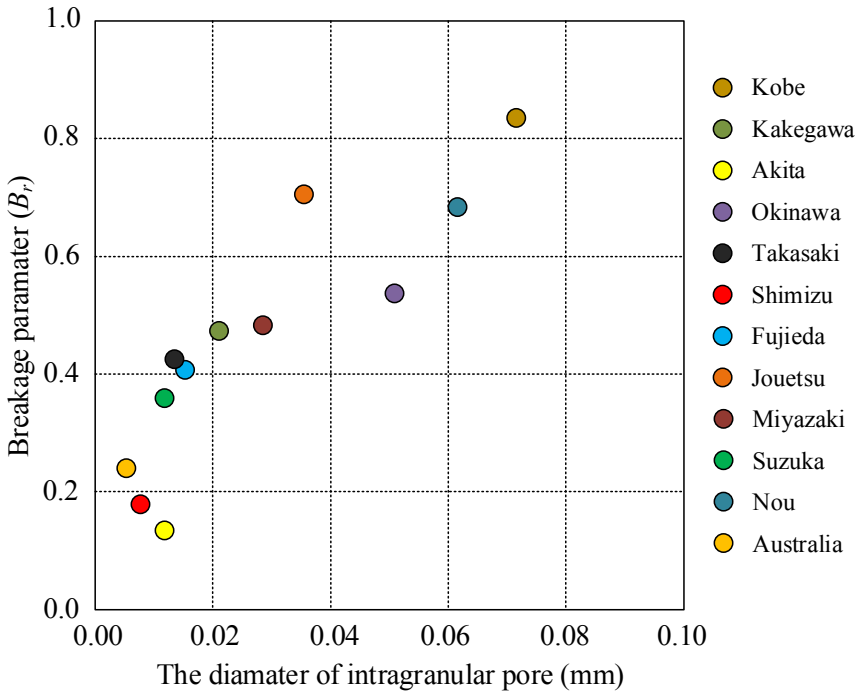

Figure 36. The tendency relationship between the diameter of intra-granular pores and breakage parameters (B_r)

Furthermore, in the previous chapter was observed and measured the diameter of intragranular pores. Figure 36 exposed the correlation between the size of intragranular pores and breakage parameter. Even though the process of determining the diameter of intragranular pores is quite arbitrary, but it can provide a reasonable understanding that the amount of intragranular pores in mudstone material extremely affects the mechanism of particle disintegration. The next studies, it is necessary to consider the relationship between the mudstone density and breakage parameter.

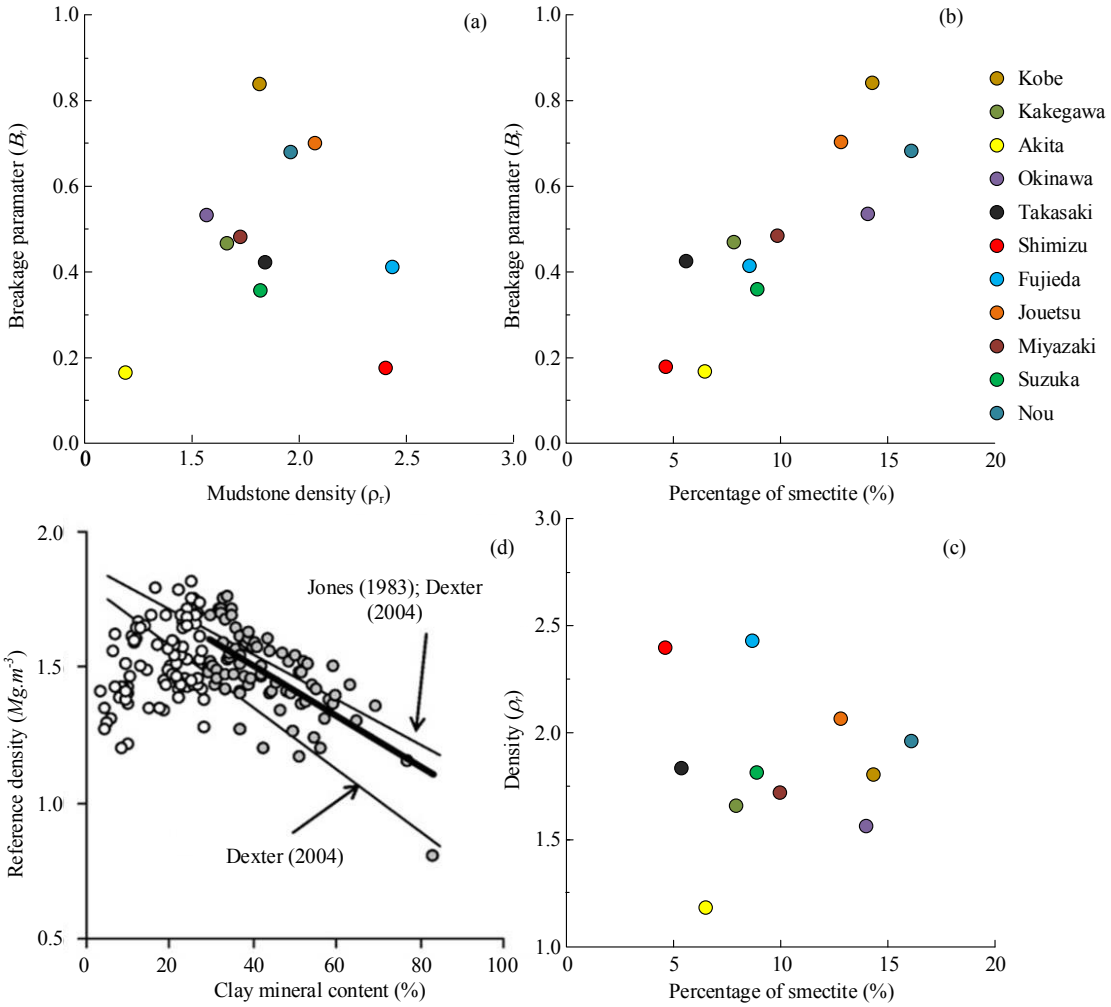

Figure 37. The relationship between mudstone density (ρ_d), smectite mineral content and breakage parameter (B_r) correspond to slaking behavior on mudstone

The correlation between the smectite mineral content, mudstone density and breakage parameter were exhibited in Figure 37. The clear linear relationship between breakage parameter (Br) and smectite content presented in Figure 37b. Increased the smectite mineral content will have an impact on increasing the breakage parameter. Meanwhile, the relationship between mudstone density and breakage parameter were not shown the clear tendency. The number of the data sample is not good enough to describe the relationship both of parameter. Based on the previous study, the relationship between the smectite mineral content as a clay mineral and the mudstone density was stated as a linear relationship. Jones (1983) and Dexter (2004) has proposed the linear relationship between the critical values of bulk density and clay content. According to the previous study and the result of this study, it can be concluded that the number of smectite mineral content will have an impact on the mudstone density. For further research, the number of samples data of mudstone specimen need to be improved or added so that the relationship of each parameter becomes understandable.

4.4. Summary

The slake resistance, mineral examinations and morphology texture appearance for mudstone specimen derived from several locations in Japan and others country were performed to observe the weathering mechanism of mudstone. Figure 38 is a summary to explain the weathering and cementation cycle on mudstone in common, but it does not neglect that cycle may also occur in other sedimentary rocks.

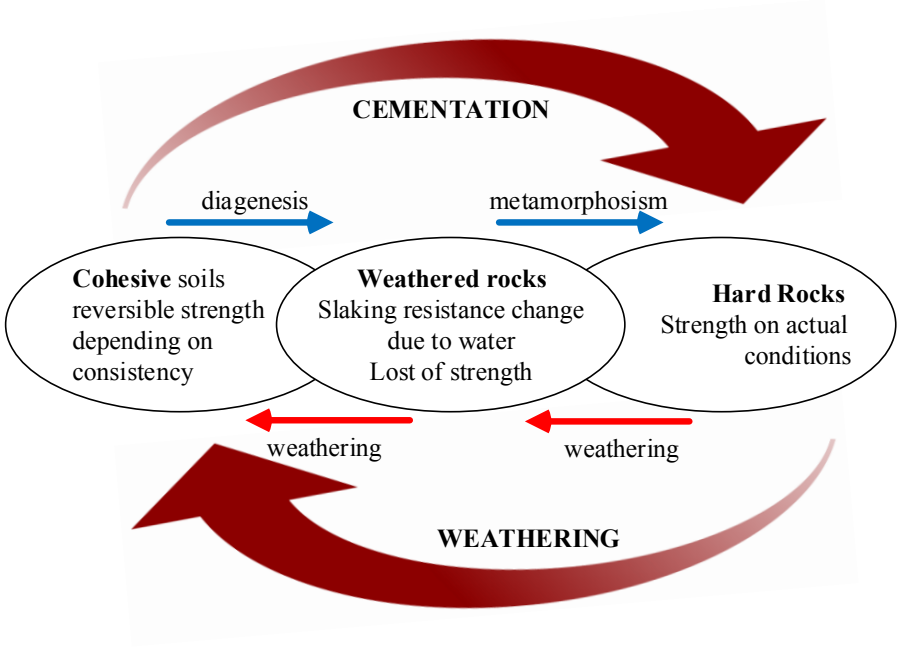

Figure 38. The mechanism of weathering and the subsequent cementation process of mudstone

The slake resistance of each material has revealed by performing of the accelerated slaking. Kobe, Jouetsu, and Nou mudstone very easy to disintegrate or break down even since the first wetting and drying cycle of accelerated slaking test applied. It was strengthened by an increase of the breakage parameter (B_r) which is representative that particle disintegration occurs during the wetting and drying cycle applied.

Based on the mineral content, the smectite mineral content as an expandable mineral plays an important role in the proses of alteration particle or known as the physical weathering. The particle size distribution of Kobe mudstone was changed rapidly. It can be happened since Kobe mudstone has a large amount of smectite mineral content. In addition, the content of nontronite which has dominant ion Na^+ was made the mudstone specimen becomes more expandable. Ion Na^+ is excellent in swelling property, thickening property and suspension stability. The physical weathering occurs becomes very fast. The linier correlation between the smectite mineral content and breakage parameter has been proven that increase of the smectite

content tends to increase the potential physical disintegration. As known, instead of physical weathering, the chemical weathering process also occurs even though it takes a times during the process. It can be concluded that the slaking phenomenon on mudstone is induced by the physical weathering mechanism that occurs during the wetting and drying cycle applied, especially due to the wetting cycle which is then gradually followed by the chemical weathering mechanism.

The relationship between breakage parameter (B_r) and smectite content was shown a clear tendency which increased the smectite mineral content will have an impact on increasing the breakage parameter. Based on the previous study, the relationship between the smectite mineral content as a clay mineral and the mudstone density was stated as a linear relationship (Jones, 1983; Dexter, 2004). It can be concluded that the smectite mineral content play an important role to understand the slaking behavior of mudstone. Furthermore, in accordance with the previous study regarding the process of air-breakage in which trapped pore-air can lead to rock disintegration (Schmitt, et.al., 1994), then the investigating of intragranular pore is needed. The intragranular pores size on mudstone material in this study shown the tendency against the physical disintegration of particle. The size of the pores will be expected to affect the process of particle disintegration.

Regarding the shape of the particle of mudstone after the accelerated slaking test applied, it can be categorized into four shapes of the mudstone aggregate: fine grain, sub-angular and tiny flakes, sub-rounded to thick flake and angular to flakes. It should be notice that particle shape has no direct effect to determine the breakage parameter of B_r. The whole category was presented in Table 3. Based on this category, is clear that the difference characteristic between mudstone and shale, mudstones break into blocky pieces whereas shales break into thin chips with roughly parallel tops and bottoms.

Table 3. Particle shape after accelerated slaking test

Initial	Final	Shape	Mudstone specimen
		Fine grain	Kobe mudstone, Jouetsu mudstone, Okinawa mudstone, Nou mudstone, Miyazaki mudstone
		Sub angular to tiny flake	Kakegawa mudstone, Fujieda mudstone, Suzuka mudstone,
		Sub-rounded to thick flake	Akita mudstone, Shimizu mudstone, Takasaki mudstone
		Angular to flake	Australia shale

Chapter 5

One Dimensional Compression Slaking: Deformation behavior

5.1. Introduction

In terms of geology, mudstone is an extremely fine grained sedimentary rock composed of clay minerals with the grain sizes generally less than 4 μm (<0.004 mm) and silt-sized quartz less than 32 μm (<0.032 mm) in size (Hallsworth & Knox, 1999). Terms such as claystone and siltstone are commonly used in place of mudstone, although these refer to weak rocks whose grain size transform within much narrower ranges and under close examination these are often technically mudstones (Dunham, 1962; Blatt & Tracy, 1996). Grain size transformation is one of the physical characteristics of mudstone. It can be happened due to mudstone is highly susceptible material to the weathered process and tends to slake and crumble into soften materials when immersed or contacted to the water. As a result, it will be lead to the swelling, disintegration and strength reduction of material (Nakano, 1970; Moriwaki, 1974; Perry & Andrews, 1984; Yoshida et.al. 1991; Vallejo, et.al., 1993; Santi & Koncagul, 1996; Dani, 1996; Botts, 1998). Regarding to these tendency, Dewhurst et.al (1998) and Broichhausen et.al (2005) stated that it can changes their mechanical behavior drastically, exhibiting 40% to 80% reductions in shear strength over periods range from 2 to 70 years.

The reason is that mudstones or shales tend to change into finer grains under repeated wetting and drying process, which is known as the slaking phenomenon. Due to this phenomenon, the stiffness and strength of the material are lowered and lead to instability. It is thus necessary to study of long-term stability problems of slopes and to clarify the mechanism of slaking and change in physical and mechanical characteristics accompanying the weathering on mudstone (Yoshida & Hosokawa, 2004; Bhattarai et.al, 2006; Aziz et.al, 2010; Yasuda et.al, 2012; O'Kelly & Zhang, 2013). Furthermore, after the Kashmir earthquake 2015, the landslide dam breached during the moderate rainfall was predicted due slaking phenomenon of mudstone as

one triggering parameter (Kiyota, et al, 2011). In order to estimate the long-term response of various natural problems and other earth structures issues, a better perception of the strength and deformation characteristics of geomaterials which affected by slaking phenomenon is crucial. As mention above, change in particle size or grain size material enables reduction in strength or stiffness. In the field, such variation in mechanical characteristics during slaking may directly affect to the deformation and failure behavior of the earth structure. However, most of the past studies focused on physical characteristics as an evolution of the particle size distribution before and after slaking cycle during weathering processes. Changes in the deformation behavior due to slaking phenomenon was not yet discussed properly. Therefore, this study attempts to address the correlation between evolution of grading size and stress-strain relationship during slaking by proposed new experimental methods such as one-dimensional compression slaking test. The experimental method has capability to exhibit the slaking phenomena and their effect on the deformation behavior.

5.2. One Dimensional compression slaking test

One-dimensional compression slaking apparatus could observe the settlement during compression and slaking cycles. Furthermore, changes in mechanical behavior induced by slaking cycles and transformation of particle size distribution will be analyzed after it. This kind of apparatus is suitable for non-cohesive soil materials. Main part of this apparatus consists of vertical stress-control system, modified confining cylinder, wetting-drying cycle path-system and automatic recording data system by time reference. A photograph of the one-dimensional compression slaking apparatus is exhibited in Figure 39.

5.2.1. Compression pressure system

Compressive stress on this apparatus was set up as a loading increment system through pneumatic air cylinder. It is applied gradually (staging) from 9.8, 19.6, 39.2, 78.5, 157, 314, 628 to 1256 kPa. Each stage was set to 30 minutes and the volumetric behavior was scarcely seen in the compression stage during the tests. After reaching a prescribed vertical stress (low compressive stress is represented by 314 kPa and high compressive is represented by 1256 kPa), wetting and drying cycle is then imposed to the specimen with keeping compressive stress constant. This system has been provided with an automatic data recording system. Similar with standard consolidation methods, during the process compression and slaking cycles, changes in vertical effective stress (σ_v') and settlements are recorded. Axial strain changes due to loading compression and slaking cycles was controlled by using LVDT to calculate void ratio (e), while vertical effective stress (σ_v') is documented through Load Cell.

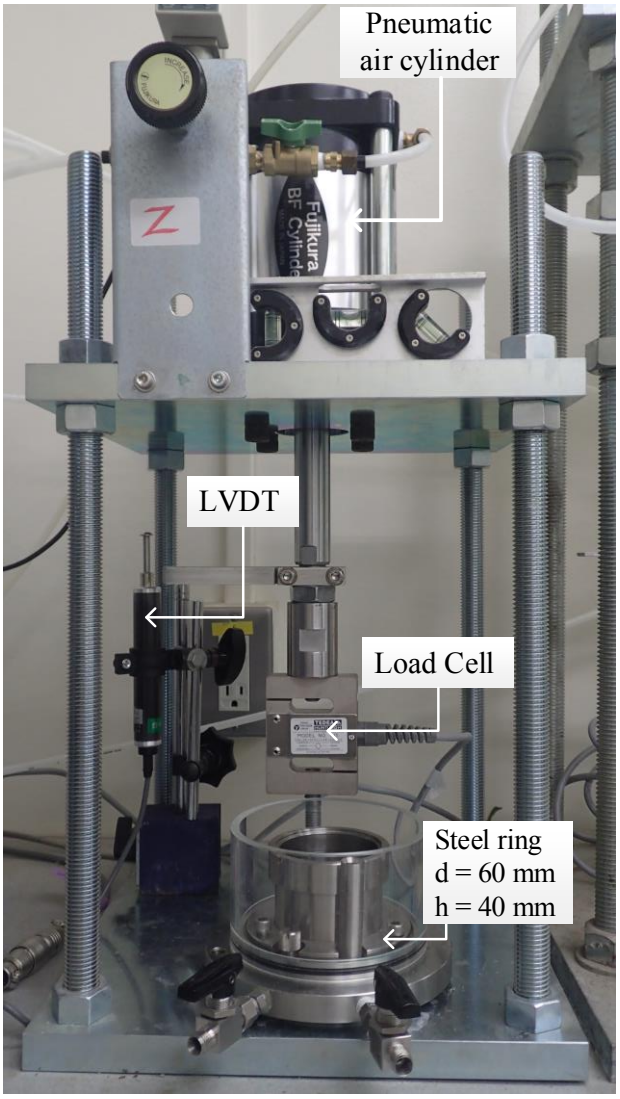

Figure 39. Photograph of One Dimensional Compression Slaking apparatus

5.2.2. Modified Confining Cylinder for slaking cycle

As we known that the common dimension of confining cylinder for consolidation test is 20 mm in height and 75 mm in diameter. To achieve the purpose of this study, it is necessary to modify the dimension of confining cylinder. The dimensions are designed with 40 mm in height and 60 mm in diameter. The height dimensions are calculated by considering the diameter maximum of particles size (20 mm) which represents 5% of the height. Similar with common consolidation confining cylinder, a circular porous stone is typically used at the interface between mudstone specimen (geomaterials) and water in the top and bottom side. The paper filters (paper membranes) are used to protect the fine particles that can fill the void of porous stone. This confining cylinder is designed from rigid steel cylinder with 5 mm in thickness and provided with ring cover to keep precisely at the center. The water flow and drainage system are permitted through a porous stone at the bottom.

5.2.3. Wetting and drying cycles

As mentioned, one of the issues is consolidation confining cylinder was provided with wetting and drying valve system. It was make a big difference with one dimensional consolidation test according to ASTM D2435/D2435M-11. As admitted that the wetting and drying cycles is one important phase to observe and evaluate the slaking phenomenon on mudstone. Compare to the previous study, Sharma (2012) was organized direct shear slaking testing under monotonic loading system. The wetting process started after stabilization of both shear and vertical displacements for 30 minutes. The drying process started after gravitational water was drained out completely, the dry air delivered to the bottom of shear box by using a dry pump. Regarding those technique, developing a wetting and drying cycle path is needed to perform the slaking cycles during compression. In this device, mechanism of wetting and drying cycle with constant pressure is very important to observe the mechanical behavior. Figure 40, the wetting process started by permeating carbon dioxide (CO_2) slowly through the specimen without changing the void pressure for 30 min to remove any air, after which distilled water was permeated through the specimen by a slight difference in water level between the water tank and specimen container h1 until the specimen was fully submerged.

After leaving the specimen submerged for 6h, the drying process was commenced by draining the void water from the specimen for 30 min through a slight difference h2 in water level. Silica gel packs were then set around the steel cylinder of the specimen container, and dried air was slowly permeated through the specimen for 48 h to ensure it was completely dried. This cycle of wetting and drying was repeated six times, during which time the volumetric behavior was observed. Following the final drying process, the specimen was oven-dried and then sieved using only horizontal circular movements without any tapping impulse being added. All of scheme is carried out in a state at room temperature.

5.3. Test Procedure of one dimensional compression slaking

The schematic of testing apparatus on Figure 40 consist of measuring system (left), loading system (center) and wetting and drying paths (right). A comprehensive description of each procedure is presented.

5.3.1. Specimens preparation

Preparing the remolded specimen into the confining cylinder for one dimensional slaking is crucial. The medium dense of mudstone specimen was determine for one dimensional compressive slaking test by divided compacted specimen into three layers. Medium dense was

obtained by following sequences procedure. Firstly, set the confining cylinder on the main pedestal and lock it. Ring cover will set on the top side before pouring the specimen. Second, place the membrane paper on the bottom side and gently pour the specimen into the confining cylinder with a low falling head as the initial layer. Then compacted by using pestle for 100 times in a circle movement. Follow this procedure for next two layers until the specimen fill the confining cylinder. Third, flatten the specimen surface by using a plat spatula to obtain a horizontal surface. Again, place the second membrane paper on the specimen. The head cover include porous stone should be set on confining cylinder. Fourth, place it in the center of measurement vessel, the process of vertical loading can be started.

Preparing the position of load cell center to the loading head and LVDT to the reference steel bar, then check it carefully. Then, load cell and LVDT should be connected to the strain amplifier and data logger after the amplifier. Turn on the PC, data logger and strain amplifier simultaneously. Setting load cell to the loading head at the precisely position so that tie rod of load cell meets the loading head and following with arrange the strain amplifier for load cell to zero value. Afterwards, setting the position LVDT to the displacement reference and arrange the strain amplifier for LVDT to zero value as well.

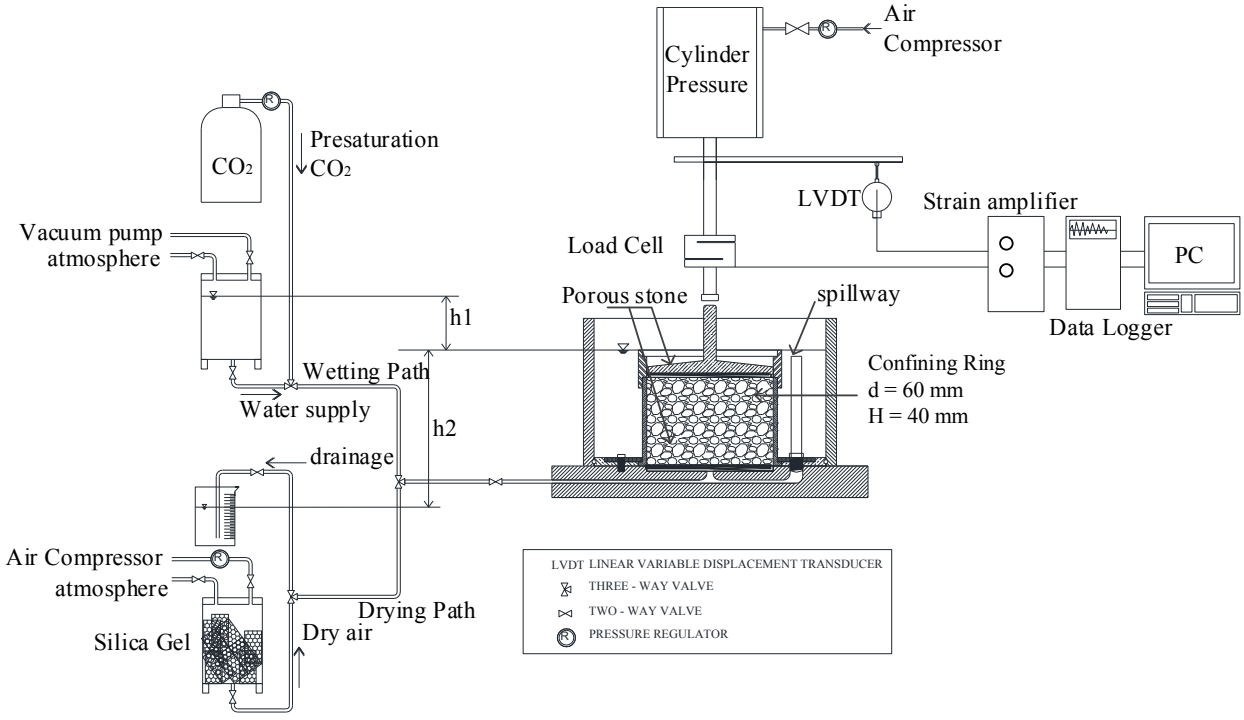

Figure 40. Schematic diagram of one dimensional compression slaking test assembly

5.3.2. Vertical loading test

As explained in the previous subchapter, the axial/vertical loading was controlled by a pneumatic cylinder and measured by load cell. Meanwhile, the displacement of the mudstone specimens measured by displacement gauge (LVDT). Vertical stress is applied gradually, starting from 9.8, 19.6, 39.2, 78.5, 157, 314, 628 to 1256 kPa via loading rod. Elapsed time of each loading stage is 30 minutes. In this paper, we conduct two types of constant axial/vertical stress, the first is 314 kPa, and the second is 1256 kPa. It has a purpose to determine the pressure which has consequences to the particle size distribution (PSD) and settlement in accordance with slaking cycles. In the end of this test, calculation of changes in particle size distribution will be introduced as particle breakage number (B_r). The particle breakage number also indicate that there are any changes in particle size distribution during the slaking cycles and compression. Whereat LVDT, load cell and confining chamber are in the right places and all recording data system are connected then the vertical loading can be immediately applied. Vertical loading will be carried out gradually with duration of loading time is 30 minutes. Vertical loading for one dimensional slaking testing had been beginning with 9.8 kPa for 30 minutes and then in consecutive forwarded to the stages of 19.6; 39.2; 78.5; 157 and 314 kPa. Every stage of adding vertical loading and decreasing of height the specimen directly recorded by strain amplifier which is transmitted to data logger in voltage unit.

5.3.3. Slaking cycles test

As explained on the previous subchapter, the wetting paths is started by permeating slowly carbon dioxide to the specimen without changing void pressure for thirty minutes and de-air water was permeated through the specimen by a gravity slight h1 in water level between the water tank and specimen container until the specimen is fully submerged into water. Specimen was then left for 6 hours. In drying paths, water was drained from the specimen for thirty minutes by a slight difference h2 in water level. The silica gel packs have set into a cylinder and ready to deliver the dry air into the specimen for 48 hours in order to ensure that the specimen was completely dried. Such cycle of wetting and drying was repeated to a prescribed number of cycles in the tests and volumetric behavior was observed. After the last drying paths, the specimen should be dried into the oven and sieved to calculate the grain size analysis.

5.3.4. Particle Size Distribution after one-dimensional compression slaking test

It was indicated that the particle crushing due to compression or shearing does not vary largest particle size and succeeded in describing such evolution of grading using a grading state index I_G (Muir Wood, 2007; Kikumoto et al., 2010). Exhibited on Figure 41(a), grading state index

or I_G is the ratio of area of S and S_o, where S_o is the whole area under a boundary of particle size distribution and S is the current state grading of particle size distribution due to crushing or slaking. The grading state index is equal to 0 for a single-sized grading or initial grading size distribution and equal to 1 for limiting fractal grading and scalar representations of the final or current grading. It will increase gradually from 0 to 1 as the particle size changes during particle crushing or slaking occurs. Based on this principle, the grading state index works as an intermediary to explain the evolutions of mechanical properties due to crushing and/or slaking. An evolution law is necessary to describe the effects of changing grading incorporating the grading state index in a proposed model. McDowell et al. (1996) discussed the existence of the limiting particle size based on the concept of fractals, but this quantity is not always a fractal. In addition, the particle size properties themselves can be defined based on another scalar quantity, but when describing constituent relationships, it is convenient to define I_G that increases monotonically from 0 to 1. Meanwhile, Hardin (1985) proposed the relative crushing ratio B_r as an index of crushing quantity that identical with I_G. B_r is, as shown in Figure 41(a), given as the ratio of the area A_0 and A, and the change in B_r increases monotonically almost proportionally to I_G. However, even when particle size crushed and slake, B_r does not reach 1 realistically, and the relative crushing ratio B_r does not consider the limiting particle size. Hence, it is inconvenient to use it for constituent modeling as a state variable of particle size. Although both indices take a value from 0 to 1, Hardin's breakage parameter *Br* does not incorporate the idea of limiting or critical grading. There is, however, considerable experimental evidence for a limit on grading before the *Br* reaches 1, with the results presented here suggesting that the change in grading during wetting and drying can be described by the grading index I_G in a similar way to particle crushing.

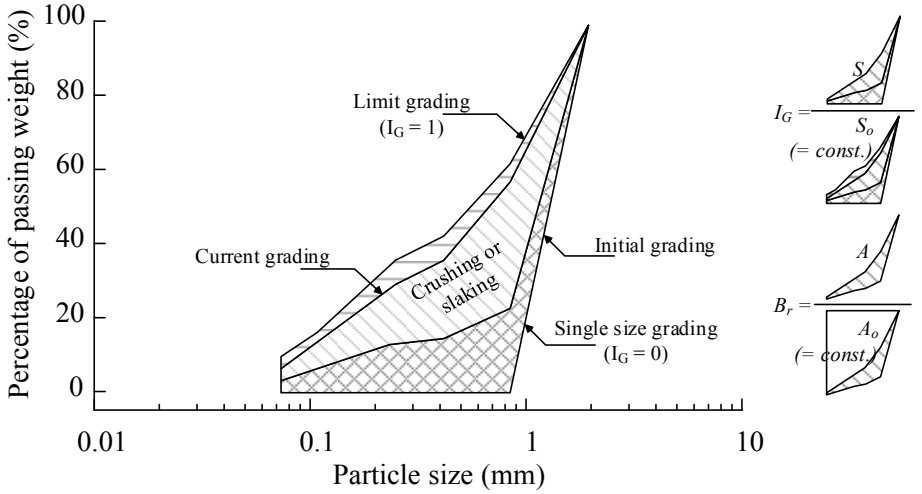

(a) Schematic diagram of grading transform and definition of grading state index (I_G)

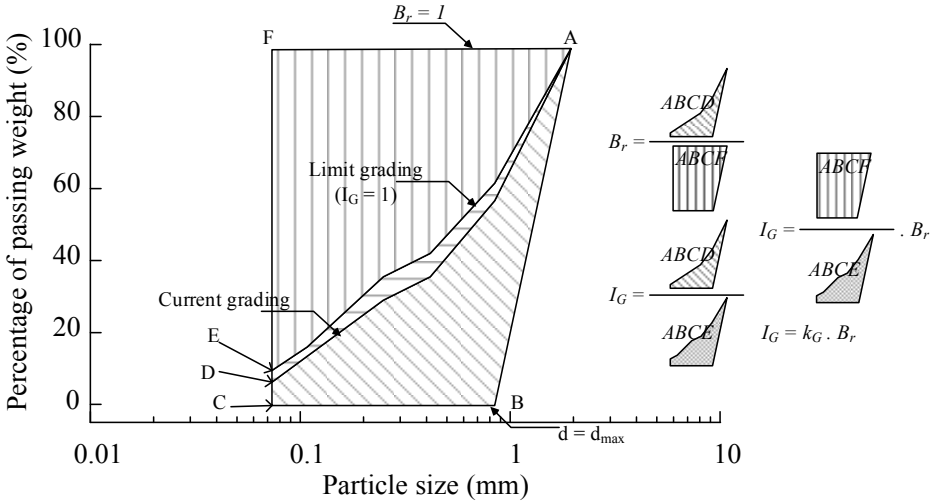

(b) Hardin's Breakage parameter (B_r) and correlation with grading state index (I_G)

Figure 41. Change in particle size accumulation curve by particle crushing and slaking and definitions of I_G and B_r parameters

5.4. Result and discussion of one-dimensional compression slaking test

The particle size distribution of the three types of crushed mudstones in their initial state, after compression and after different numbers of wetting and drying cycles, are shown in Figure 42, Figure 43 and Figure 44. The test results for the crushed Kakegawa and Kobe mudstones under a vertical effective stress σ_v' of 314 and 1256 kPa are shown in Figure 42 and Figure 43, respectively, whereas the results for the crushed Hattian Bala mudstone under a vertical effective stress σ_v' of 314 kPa are provided in Figure 44. For each specimen, magnified digital photographs taken of the initial state and after three cycles of wetting and drying under a vertical effective stress of σ_v' = 314 kPa are also provided. It is evident from this that the particle size distributions of the crushed Kakegawa and Kobe mudstones were altered after compression, and that both mudstone types experience particle breakage during one-dimensional compression. It is also clear that there is a slightly greater change in grading at 1256 kPa, and so the evolution of grading due to particle breakage is related to an increase in the stress level. The crushed Hattian Bala mudstone, however, retains its original particle size distribution, and does not seem to exhibit any particle breakage under a stress of less than 314 kPa. The crushed mudstone specimens experienced a variation in particle size distribution after wetting and drying, but the extent of this variation differed between mudstone types. The crushed Kakegawa and Kobe mudstone exhibited a significant change in particle size distribution, and from the enlarged photographs of the particles, it is evident that this is because many particles crumbled into finer particles. In contrast, the change in grading of the crushed

Hattian Bala mudstone in response to wetting and drying was relatively small, and the particles looked much the same before and after testing.

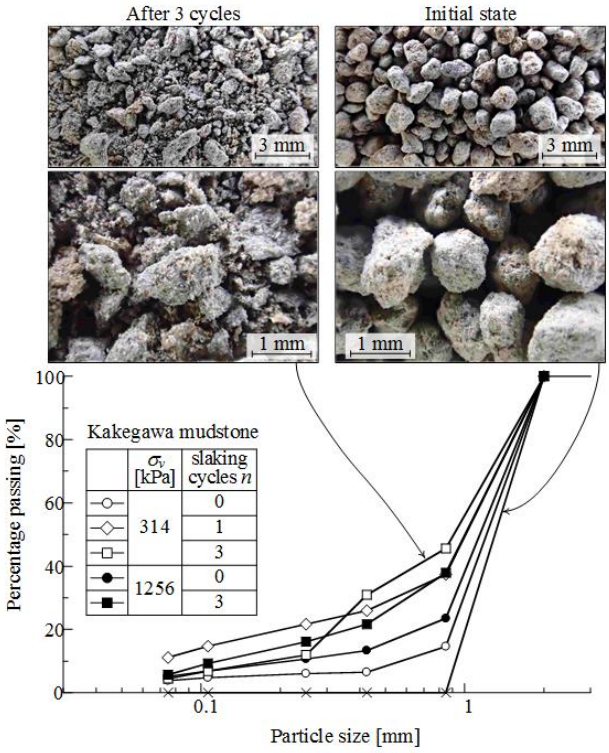

Figure 42. Change in particle size of Kakegawa mudstone during one-dimensional compressive slaking testing

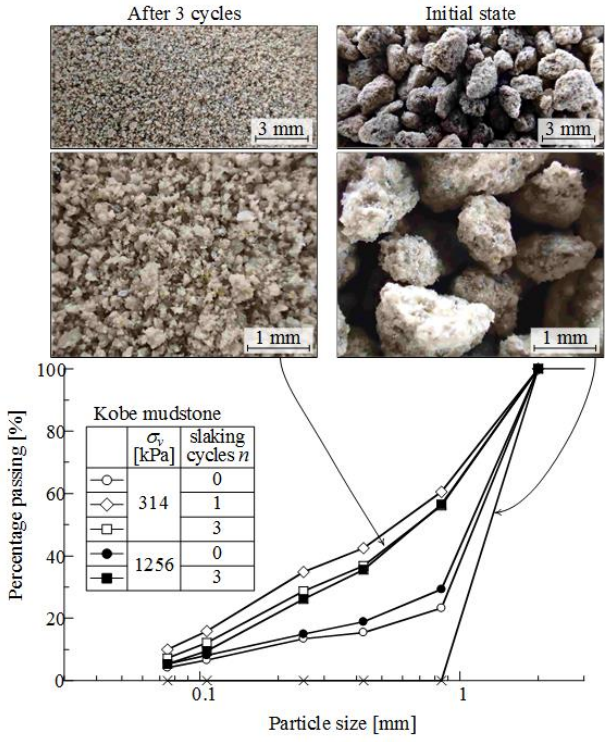

Figure 43. Change in particle size of Kobe mudstone during one-dimensional compressive slaking testing

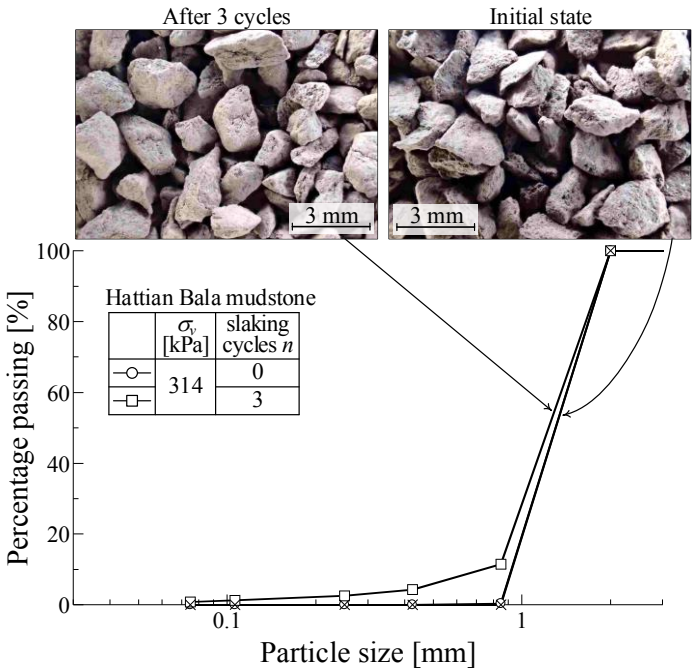

Figure 44. Change in particle size of Hattian Bala mudstone during one-dimensional compressive slaking testing

The Hattian Bala mudstone particles did not contain any intragranular pores as explained in the previous chapter, which would explain why there is so little change in particle size distribution during wetting and drying cycles. It is worth noting here that, although the maximum particle size clearly decreased in the ordinary accelerated slaking tests, in which the wetting and drying are applied under unconfined conditions, the maximum particle size of the three specimens remained almost constant in the one-dimensional compression slaking tests, in which a confining pressure is applied. It therefore seems reasonable to conclude that the breakage of soil particles occurs during compression and the wetting/drying cycles. As a result, the proportion of fine particles that are capable of filling the voids between larger particles and causing volumetric compression without noticeably changing the maximum particle size. Kikumoto et al. (2010) suggested that particle crushing due to compression or shearing does not alter the maximum particle size, and in doing so succeeded in describing the evolution of grading using a grading state index, I_G (Muir Wood, 2007; Kikumoto et al., 2010), defined by the ratio of areas ABC and ABD in Figure 41. Note that I_G is incrementally proportional to the relative breakage B_r, which is defined as the ratio of areas ABC and ABD in Figure 41(a). Although both indices take a value from 0 to 1, Hardin's breakage parameter B_r does not incorporate the idea of limiting or critical grading. There is, however, considerable experimental evidence for a limit on grading before the B_r reaches 1, with the results presented here suggesting that the change in grading during wetting and drying can be described by the

grading index I_G in a similar way to particle crushing.

Figure 45, Figure 46 and Figure 47 show the relationships between the vertical effective stress σ_v', number of wetting and drying cycles n, void ratio e and breakage parameter B_r for the crushed Kobe, Kakegawa and Hattian Bala mudstone, respectively. The upper figures (figure parts (a) and (b)) illustrate the behaviour in compression, whereas the lower figures (figure parts (c) and (d)) show the variation in grading. From the behaviour of the crushed Kakegawa mudstone shown in Figure 46, it was clear that the value of B_r (Figure 46(c)) increases to 0.07 at 314 kPa and to 0.13 at 1256 kPa, which is consistent with particle crushing.

The compression line in the semi-logarithmic plot of e and log σ_v' also becomes steeper, which further confirms that particle crushing occurred (Miura & O-Hara, 1979; McDowell et al., 1996). After the wetting and drying, the B_r value increased from 0.21 to 0.24 (Figure 46(c)) and the specimen experienced significant compression, to the extent that the decrease in void ratio was greater than 0,6. For the crushed Kobe mudstone, the results for which are summarized in Figure 45, the increase in B_r during wetting and drying and the decrease in void ratio e (volumetric compression) were more significant.

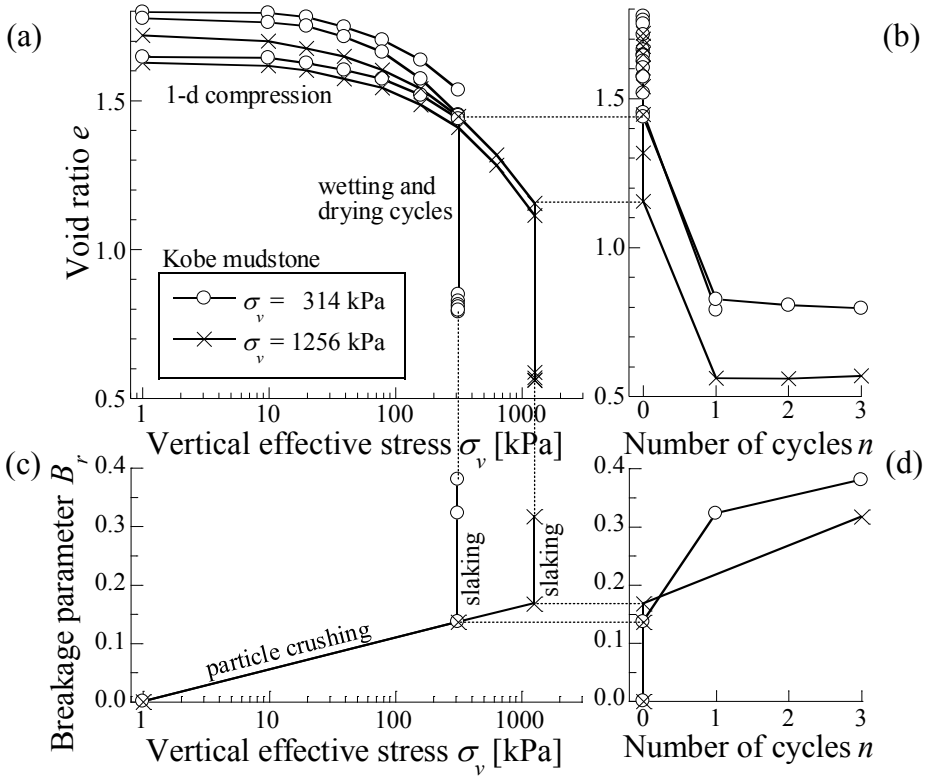

Figure 45. Change in compressive properties and particle size of Kobe mudstone during one-dimensional compressive slaking testing

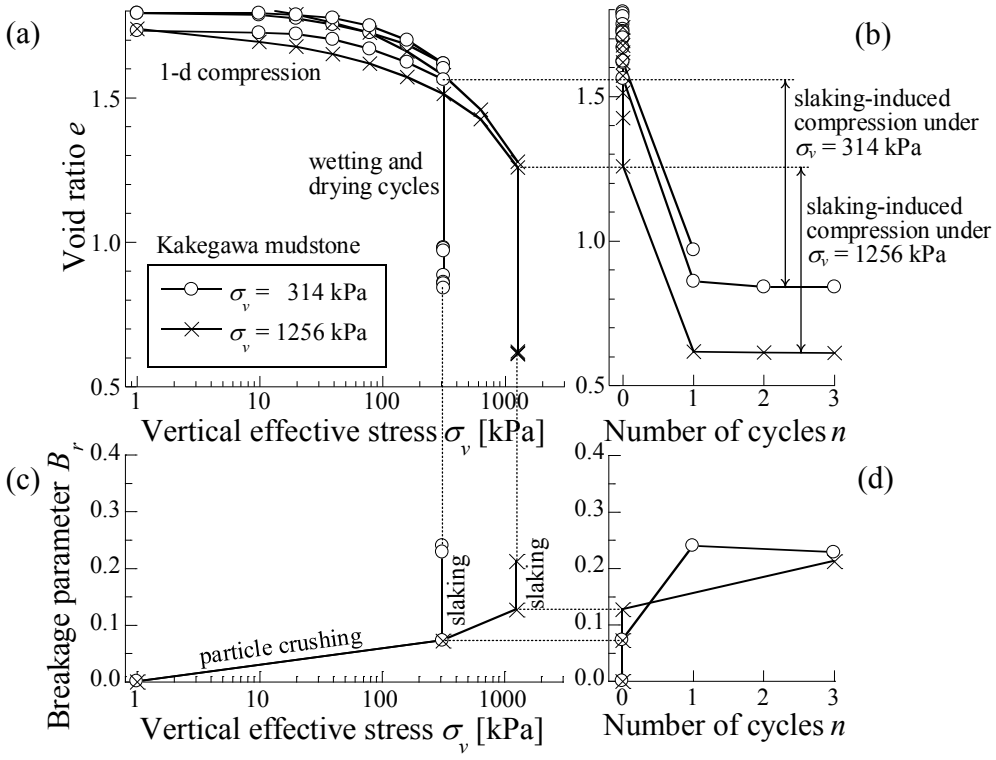

Figure 46. Change in compressive properties and particle size of Kakegawa mudstone during one-dimensional compressive slaking testing

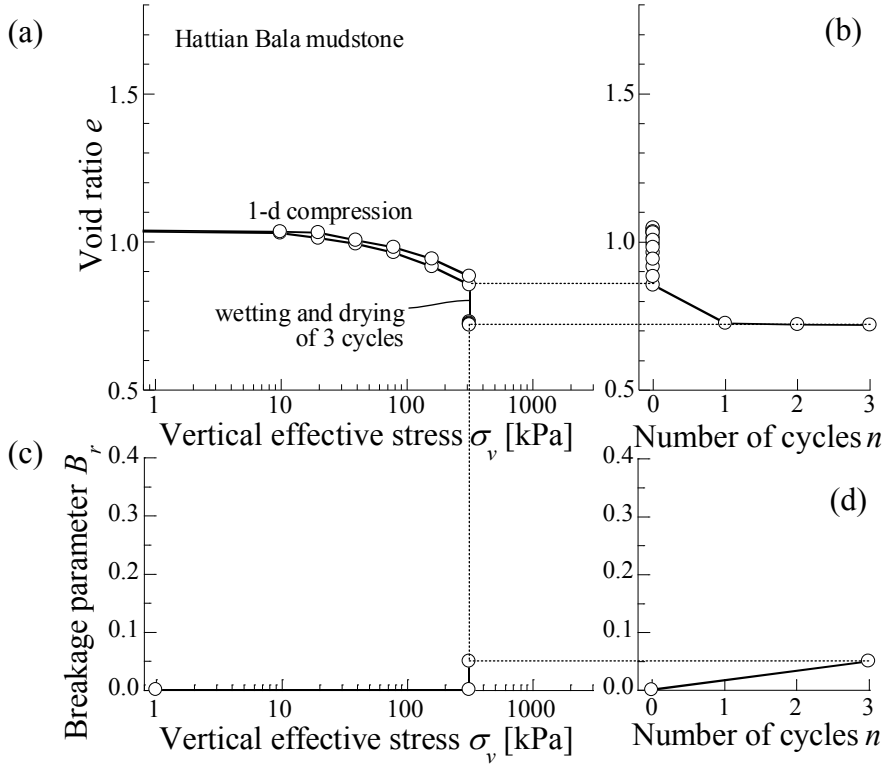

Figure 47. Change in compressive properties and particle size of Hattian Bala mudstone during one-dimensional compressive slaking testing

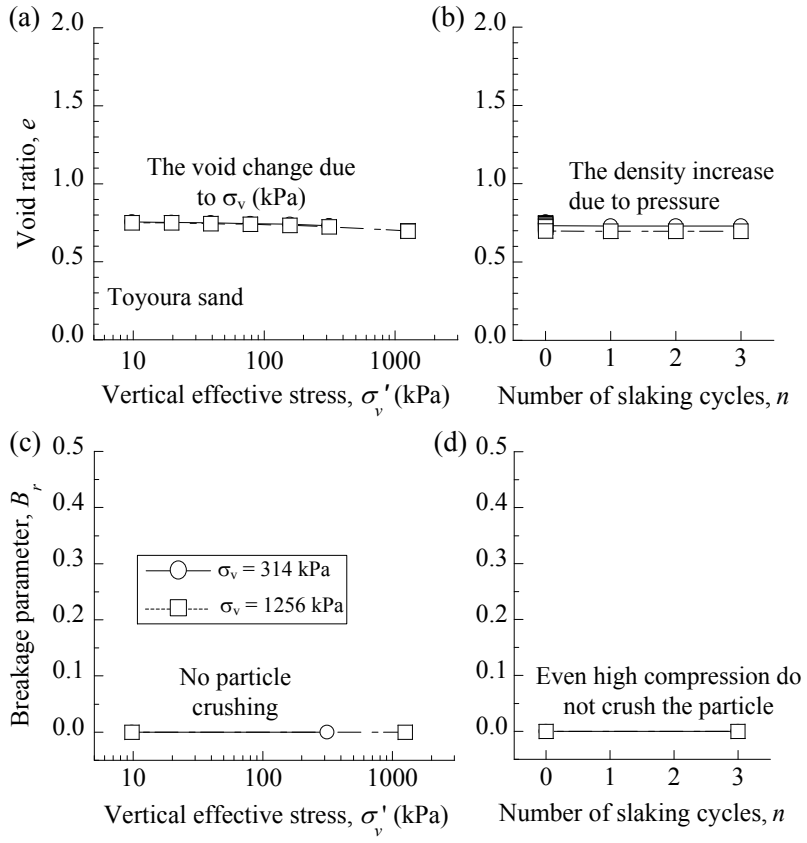

Figure 48. Change in compressive properties and particle size of Toyoura sand during one-dimensional compressive slaking testing

In contrast, the increase in B_r of the crushed Hattian Bala mudstone was almost zero during the compression stage, and the compression line in the e–ln σ_v' plane was comparatively flat. This indicates that the variation in *Br* during wetting and drying is rather small, and thus so is the volumetric compression induced by slaking. It can be concluded from this that slaking induced by cyclic wetting and drying under a constant vertical effective stress causes substantial compression of geomaterials derived from mudstone. Figure 48 is the result of Toyoura sand under one dimensional compression slaking test. As an un-slakable material, almost nothing happened during the compression and slaking. It is shown that the devices working properly as well. Furthermore, the effect that changes in grading due to slaking have on the mechanical characteristics were investigated by monitoring the maximum and minimum void ratios of the crushed Kakegawa, Hattian Bala mudstones and Toyoura sand after each cycle of wetting and drying. As seen in Figure 51, the maximum and minimum void ratios of Toyoura sand decrease by almost the same amount until the third cycle. The Hattian Bala mudstone (Figure 50), the maximum and minimum void ratios is slightly decrease, while in the small pressure of 314 kPa almost unchanged. The small compression pressure on Hattian Bala mudstone has no effect to the void.

It is similar to the Toyoura sand as an incompressible material (Figure 48). These results indicate that particle refinement occurs due to slaking, and that the mechanical characteristics (i.e. reference void ratio) are in turn altered by the change in grading. It would be set an opine that the void ratio at the critical state (void ratio at normally consolidated state) would be altered in a similar way to the maximum and minimum void ratios. Experimental studies on artificial mixtures of soil particles of different sizes (Zlatovic & Ishihara, 1995; Lade et al., 1998) investigated how the addition of finer particles affects the reference void ratio in relation to the maximum, minimum and critical state void ratio. This found that finer particles are initially able to distribute themselves within the void space of the coarser particles, meaning that the reference void ratio decreases. However, if more fine particles are added artificially, then the finer particles start to push apart the larger particles and the void ratio rises.

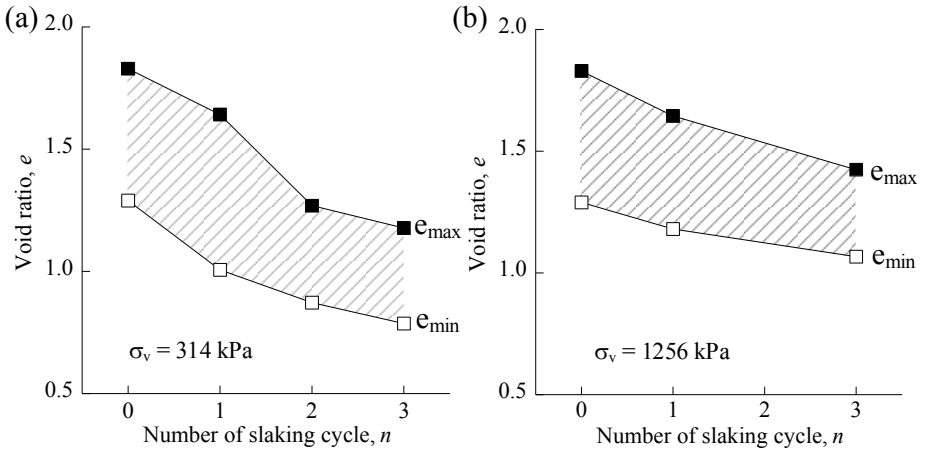

Figure 49. Relationship between wetting and drying cycles and the maximum and minimum void ratio of Kakegawa mudstone

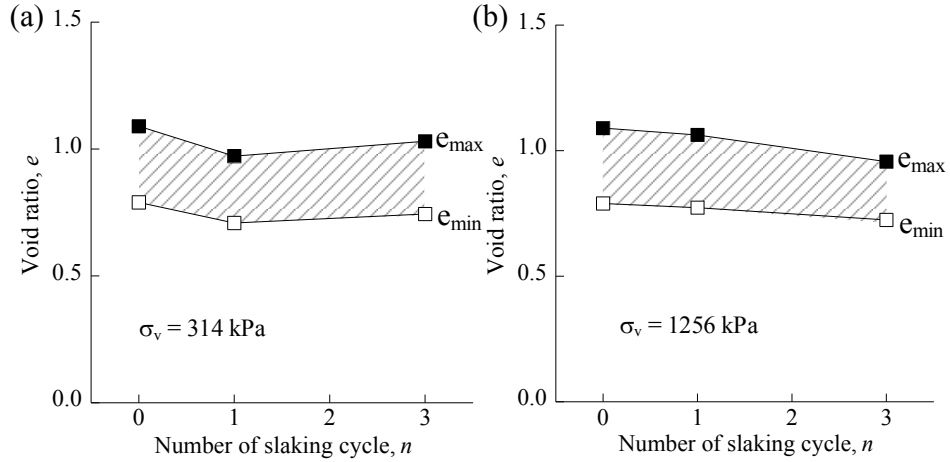

Figure 50. Relationship between wetting and drying cycles and the maximum and minimum void ratio of Hattian Bala mudstone

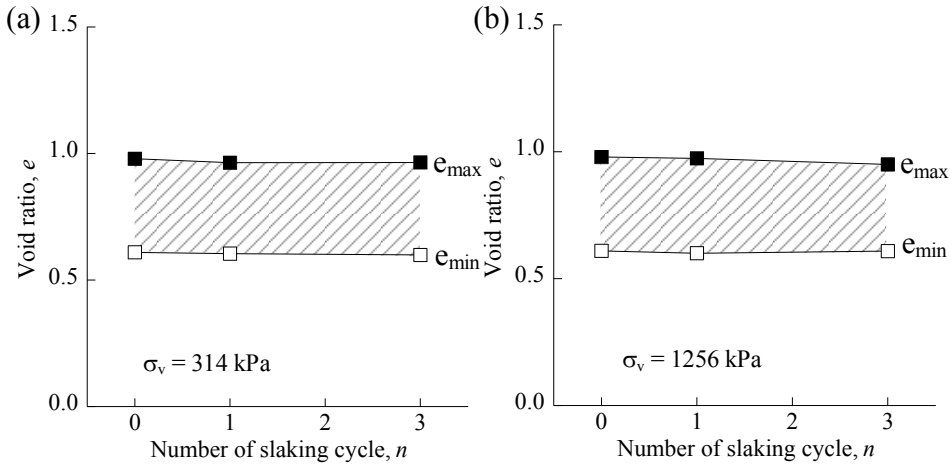

Figure 51. Relationship between wetting and drying cycles and the maximum and minimum void ratio of Toyoura sand

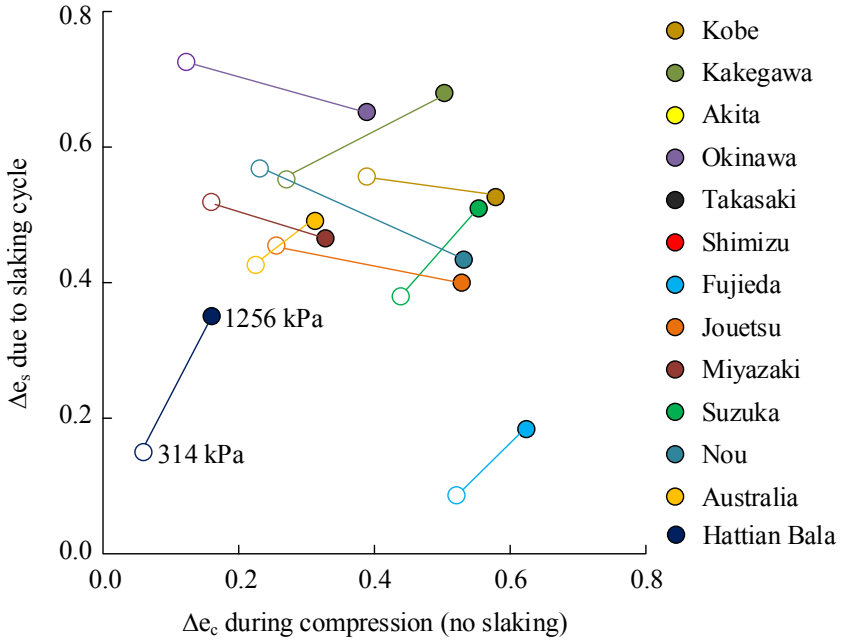

Figure 52. The variation of Δs (slaking) and Δe (compression) during one dimensional compression slaking test

According to NEXCO standard, the earth embankment material made by mudstone material should be easy to crush during the compression process, so it is expected that the fine particles from crushing process can fill the void and reduce the slaking. However, not all mudstones have properties as expected. Figure 52 shows the deformation of mudstone due to compression and slaking cycle during one-dimensional compression slaking test. Related to NEXCO standard, Fujieda mudstone might be meet the criteria as an embankment material, because the deformation induced by slaking cycle during the test is small enough. In common, the deformation due to compression has a range between 0,2 – 0,5 and the contribution of slaking cycle were made the deformation between 0,4-0,7. The mudstone with the small deformation

characteristic due to slaking cycle is a mudstone that possible to use as an embankment material. In order to provide more satisfactory results or conclusions, further experiment is required to obtain a more suitable construction method for dealing with the deformation issue of mudstone.

5.5. The Effect of Relative Density (D_r) on Slaking Characteristics

A case series of one dimensional compression slaking with different initial void ratio and relative density were performed to investigate the effect of slaking deformation behavior on earth construction or specifically road embankment. In this study, the dried Nou mudstone specimen was prepared with the diameter similar with the previous test, are 2.00-0.85mm. The properties of Nou mudstone specimen was obtained as preliminary data (Table 4).

Table 4. The Nou mudstone properties

Nou mudstone	Value
Particle density, ρs (gr/cm3)	2.687
Maximum void ratio e_{max}	1.97
Minimum void ratio e_{min}	1.40

The relative density (D_r, %) in this study was prepared with the following variations are 10, 25, 50, 75, 100. Several procedures to obtain the variation of initial void ratio and relative density was designed based on the standard procedure of JIS A 1224, JGS 0161. A slightly different with the previous one-dimensional compression slaking test, the number of slaking cycle was determined only for one cycle (n = 1) and the vertical effective stress keep constant at σ_v' = 314 kPa. Accordant with the procedure to obtain the initial void ratio and the relative density, the result of this test was presented in Table 5. The case number was representing of each case in this study. The void ratio as a result of relative density exceeds 100% (D_r, = *100%*) is lower than the minimum void ratio in physical properties of Nou mudstone. It is fine since we assumed that void ratio is more convenient and trusted. Furthermore, a series of one dimensional compressive slaking under different vertical effective stress and varying of number of slaking cycle were prepared as well. It is necessary to check and assure that the reproduce-ability of one dimensional compression slaking devices is working properly. A series of tests consists of the variation number of slaking cycle n = 0, 1 and 3 for σ_v' = 314 kPa and n = 0 and 3 for σ_v' = 1256 kPa. The result of this tests was presented in Table 6.

Table 5. The initial void ratio (e_i) and relative density (D_r) of Nou mudstone

Case	Initial void ratio, e_i	Initial relative density, D_r (%)
1	1.89	14.8
2	1.80	29.1
3	1.65	56.8
4	1.54	76.0
5	1.35	100.0

Table 6. The initial void ratio (e_i) and relative density (D_r) of Nou mudstone during one-dimensional compression slaking test

σ_v' (kPa)	Number of cycles, n	Initial void ratio, e_i	Initial relative density, D_r (%)
314	0	1.49	83.8
	3	1.35	99.9
1256	0	1.42	87.5
	1	1.43	86.5
	3	1.38	98.1

The particle size distribution changes during compression slaking test was investigated and analyzed. Figure 53 exhibit the impressive result of particle size distribution changes after the test of each case. The first, the disintegration of the particle during one-dimensional compression slaking test of each case seems similar to each other. Second, the particle size distribution curves of five cases are located between the wet and dry condition with different vertical effective stress value during one-dimensional compression slaking test, it can be inferred, the initial void ratio and density do not have an influence on the characteristics of particle size distribution changes of mudstone specimen during compression and wetting and drying cycle applied.

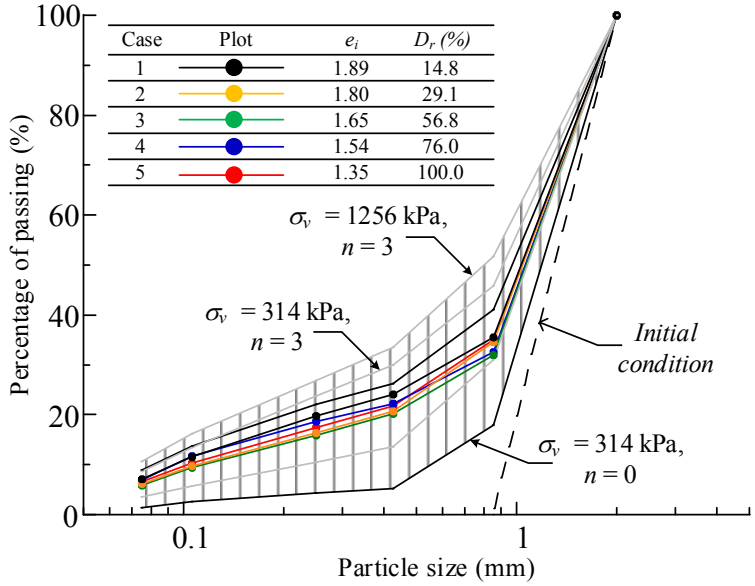

Figure 53. Changes in particle size distribution due to variation in void ratio and relative density during one dimensional compression slaking test

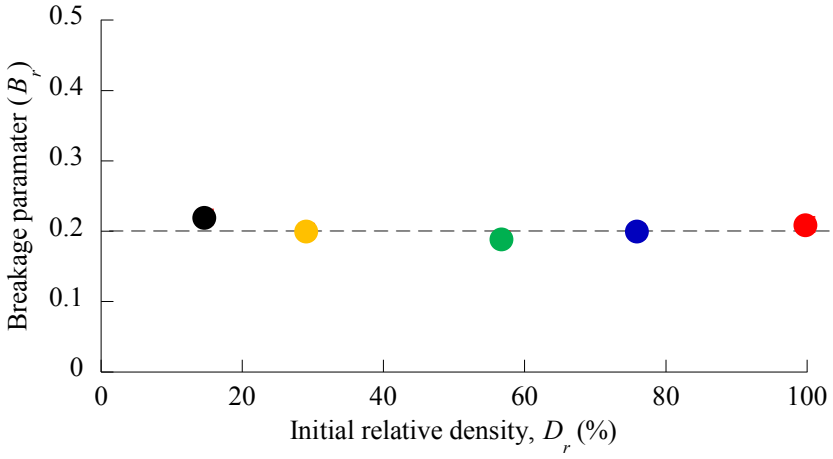

Figure 54. The breakage parameter (Br) of each case to check the effect of initial void ratio (e_i) and relative density (D_r) on slaking behavior

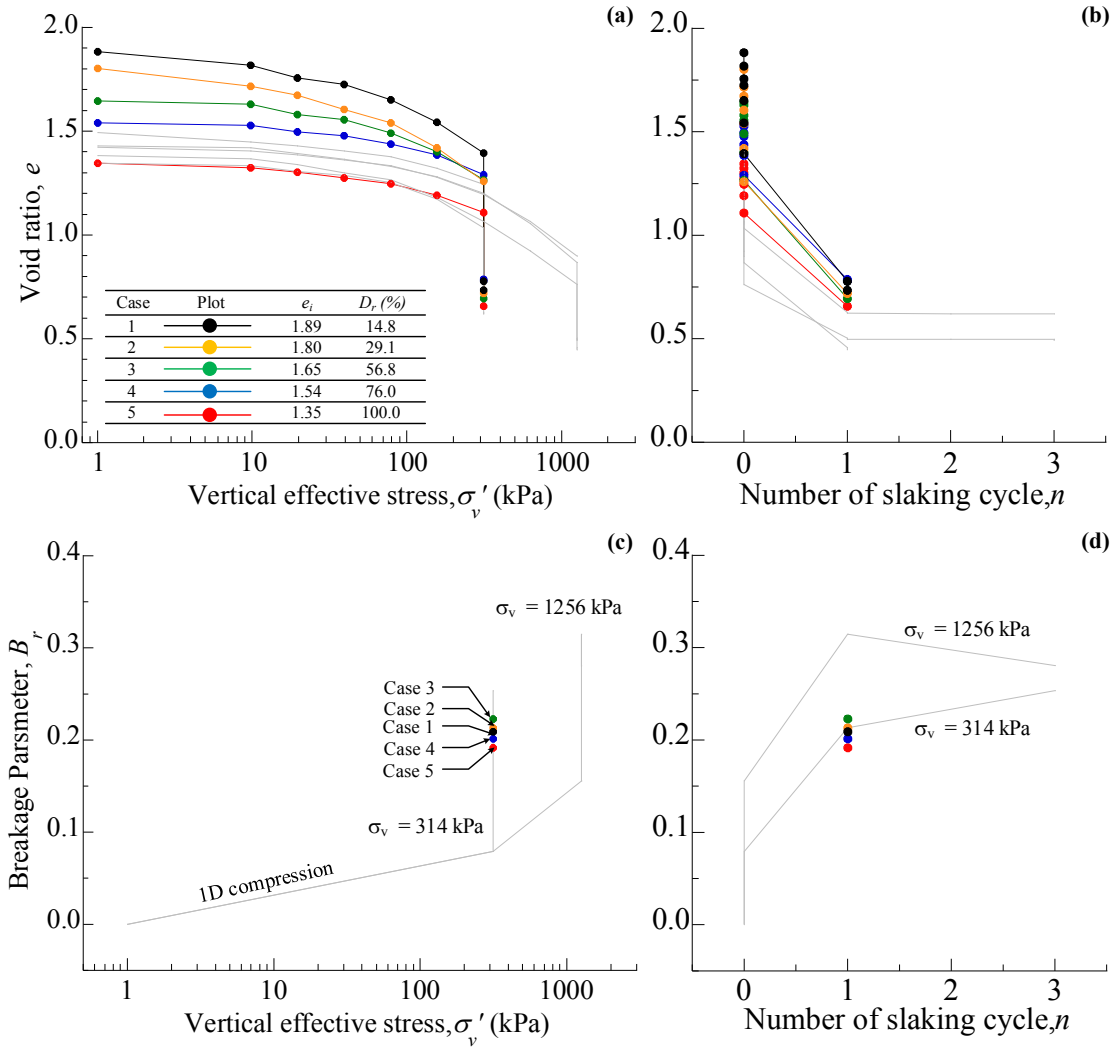

Figure 55. Change in compressive properties and particle size of each case to observe the effect of initial void ratio and relative density

The statement above is also confirmed based on the analysis of breakage parameter (Figure 54), in which the change of particle size distribution is not affected by the initial conditions of packing density. The grading size changes are more affected by the number of wetting and drying cycles and the pressure during compression process. Figure 55 show the relationships between the vertical effective stress σ_v', number of wetting and drying cycles n, void ratio e and breakage parameter B_r of each case in this chapter. The upper figures (parts (a) and (b)) illustrate the behavior in compression, whereas the lower figures (parts (c) and (d)) show the variation in grading.

In spite of the deformation during compression shown an irregular tendency but at the end of wetting and drying cycles, the deformation has reached the same result, around 0,7. The compression line in the semi-logarithmic plot of e and log σ_v' of case 1 and 2 and case 4 and case 5 shows the similar behavior except for case 3. Related to the deformation behavior of mudstone in the field work, the initial density or initial void ratio of case 4 and case 5 is more appropriate to be applied. If it is compared to another case under different constant pressure and increase in the number of wetting and drying cycle, it is inferred that the number of wetting and drying cycles are the most influential parameter to changes the particle distribution. Figure 55(c), it was clear that the value of B_r of each case increases to 0.2 after the wetting and drying cycle applied, which is consistent with particle crushing. And again, it can be concluded that slaking induced by cyclic wetting and drying under a constant vertical effective stress causes substantial compression of geomaterials derived from mudstone.

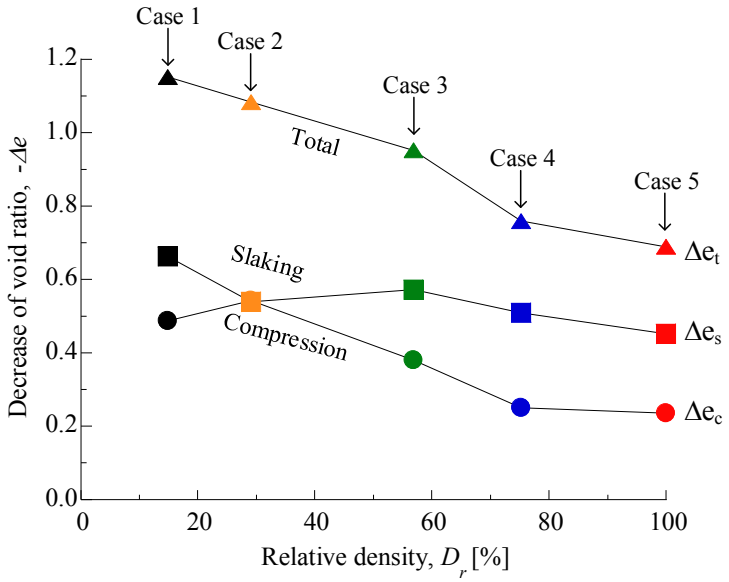

Figure 56. The volumetric compression behavior of Nou mudstone under one-dimensional compression slaking test

Related to the volumetric compression, Figure 56 exhibit the volumetric compression due to compression process (Δe_c), slaking cycle (Δe_s) and total volume compression (Δe_t) during one dimensional compression slaking test. The volumetric compression due to slaking and compression process tends to decrease while the relative density (D_r) increases. However, the large compression still occurs due to wetting and drying cycle while the relative density was 100%. Therefore, the compression phenomenon due to wetting and drying cycle is an important parameter to be paid attention. To countermeasures or minimize the potential deformation due to wetting and drying cycle of mudstone specimen, a further observation is necessary to be performed.

5.6. The countermeasure effort to minimize the potential deformation due to slaking behavior

The previous subchapter has performed several experiments related to the effect of the initial density on slaking behavior of mudstone. In this subchapter, three kinds of experimental methods have considered to be performed to countermeasure of potential deformation of mudstone specimen induced by wetting and drying cycle. The first method is performed by add some percentage of the fine grain materials to a specimen. The second method is performed by apply the initial cycle of wetting and drying and then followed by gradually increase the compression (the history of wetting and drying process). The third method is performed by load to the high pressure (1256 kPa) and unload to the small pressure (314 kPa) then cycle of wetting and drying applied (the stress history).

5.6.1. The effect of fine grain on slaking behavior

In the interest of the effect of fine particle content on the slaking behavior, the adjusting of particle size distribution needed. The fine particle with the diameter between 0.425 to 0.85mm was added to the initial particle size distribution with the diameter between 0.85-2.00mm. The tendency of particle size distribution changes and compression characteristics due to the addition of fine particles will be observed. In this study, the percentage of fine particles addition is carried 25%, 50% and 75% and represented as case 6, 7 and 8 respectively. The specimen preparation in this test was same with the previous test, in which the relative density without addition of fine particles is 75%. Meanwhile, the vertical effective stress during one cycle of wetting and drying was maintained to 314 kPa. The initial relative density of each case of fine grains presented in Table 7.

Table 7. The initial parameter to observe the effect of fine grains on slaking behavior

Case	e_i	D_r (%)	Percentage of fines (%)
4	1.54	76	0
6	1.49	69.44	25
7	1.41	67.01	50
8	1.59	65.00	75

As the exhibit in Figure 57, the initial void ratio of each case was located between maximum void ratio and minimum void ratio. The void ratio tends to decrease as the addition of fine particles increases. When the fine particle was added to the specimen, the finer particle filled the void ratio and cause the void ratio decreased. In contrary, the void ratio increased when the addition of grains more than 75%.

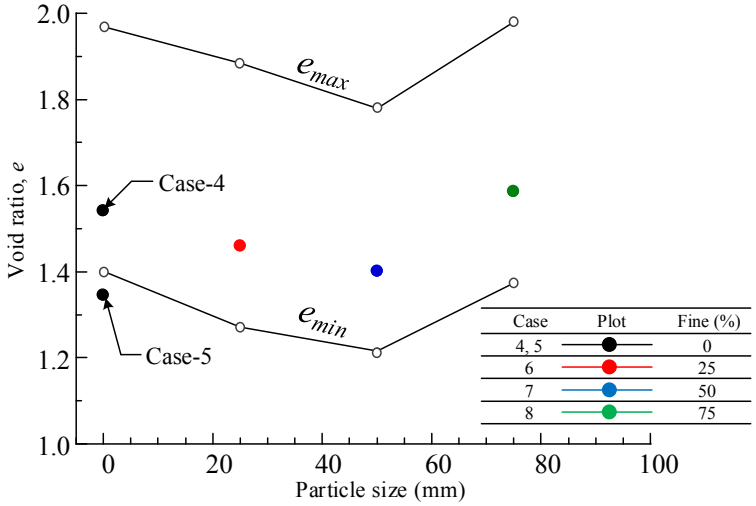

Figure 57. Effects of Non-Plastic Fines particles on Minimum and Maximum Void Ratios

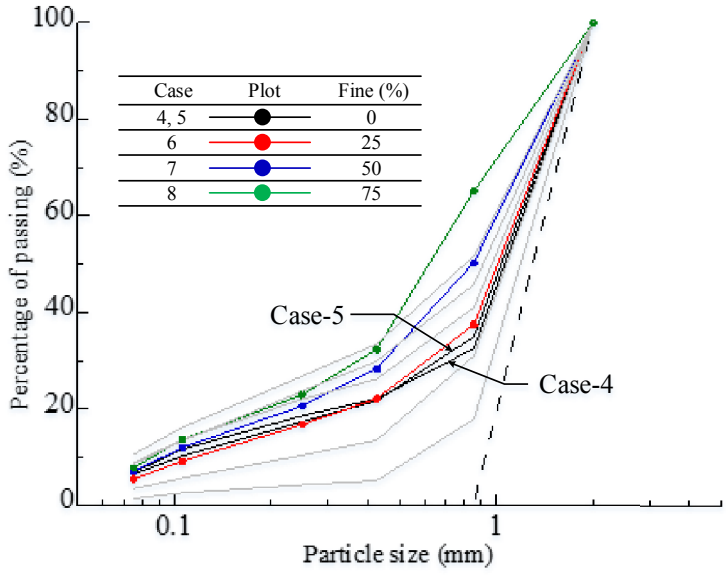

Figure 58. Changes in the particle size curve of the Nou Mudstone in the one-dimensional compression slaking test by adding fine grains material

It occurs since the fine particle has made the specimen becomes uniform condition and it is thought that the void between particle still exists then the void ratio increase. The particle size distribution after the test was analyzed to observe the evolution grading and the effect of the fine particle on the slaking behavior. Figure 58 exhibit that the particle distribution curve of case 6 (25% fine particle) has a similar pattern to the case 4 and case 5. It's mean the addition of 25% fine particle does not give any influence on the changes of particle size distribution during one-dimensional compression slaking test. Pay attention to the addition of fine particle 75 % (case 8), as mentioned before, the void ratio increase due to the particle size distribution becomes more uniform. Even though, the initial void ratio almost equal to the initial void ratio in case 4, but since the fine particle was made the specimen becomes uniform then the particle size distribution changes wider than case 4. Therefore, it is considered that the particle size and the amounts of fine particles added have given an influence the occurrence tendency of evolution grading. The correlation between vertical effective stress (σ_v'), number of slaking cycle (n), void ratio (e) and breakage parameter (Br) regarding the effect of added fine particle into the specimen was shown in Figure 59. The characteristics of compression line and the deformation due to one slaking cycle for each case was similar, the void ratio at the end of slaking process is around 0,7. Therefore, it is inferred that there is no influence on compression characteristics of mudstone due to addition of fine particles. The breakage parameter has a tendency to changes, especially for case 7 and case 8, but it doesn't give any significant conclusion regarding the effect of added fine particle to the specimen. Compare to the Figure 58 on the previous subchapter, the volumetric compression tends to decrease as the addition of fine particle. The volumetric compression due to slaking and total compression in this case (case 6, 7 and 8) were shown that the void ratio tends to decrease. On the other hand, an addition fine particle around 75% cause the specimen becomes uniform and it seems the void ratio almost reach the minimum/maximum void ratio. However, during the slaking cycle the large deformation still occur in any case in this study. It was confirmed that the volume compression due to slaking decreased until a certain addition of fine particles, but after passing a certain point (75 of fine particles), it is returned to the original tendency. It can be inferred that the optimum addition of fine particles is 50%. For further research, the variation of fine particle would be an option to get better understanding regarding the effect of fine particles to the slaking behavior of mudstone (Figure 60).

5.6.2. The effect of wetting and drying history on slaking behavior

In this subchapter, the author intends to obtain the methods to reduce the potential deformation due to slaking behavior during construction and post-construction by apply the process of

wetting and drying at the beginning. Several conditions to investigate this kind of behavior was prepared.

1. One cycle of wetting and drying cycle was applied without pressure (case 9);
2. After applied one cycle of wetting and drying, then stage loading was carried out to σ_v' = 314 kPa (case 10);
3. The initial wetting and drying cycles was applied, then stage loading was carried out until σ_v' = 314 kPa, and at the end the wetting and drying cycle applied once more (case 11).

The specimens are prepared in the same manner as in the packing method of the relative density of 75% so that the void ratio becomes approximately e = 1.54. Figure 61, shows the particle size distribution changes after the test for every case in this subchapter. It was seen, the particle size distribution of case 9 and case 10 was close to each other, and the particle size with the diameter 0.85mm crushed due to wetting and drying cycle. When the wetting and drying cycle applied in the first stage of the experiment, the material with the diameter 0.85mm has crushed to be a fine material.

The breakage parameter in Figure 62(c) revealed that the particle transformed during the wetting and drying cycle at the beginning. Compare to the conventional test (σ_v' = 314 kPa, n = 1), the amount of particle crushed due to wetting and drying cycle is larger than compression process. It can be inferred that the wetting and drying cycle is the most influential parameter to the process of particle disintegration becomes more delicate. It also emphasized the previous statement regarding the physical weathering mechanism. Nou mudstone was indicated has a smectite mineral content which is quite dominant in the process of particle destruction when encountering into the water. In case 11, the particle size distribution extremely changed due to the wetting and drying was applied once more after compression process applied gradually. Further, in case 9, the fine particles generated by wetting and drying cycle, in addition, the deformation at this stage also occurred caused by the effect of the weight of top pedestal itself. Figure 62, in case 10 and case 11, the large deformation occurs since the compression process applied. Compare to the case 5 in the previous subchapter, the final deformation of each case has reached the same condition of the void ratio as case 5. In case 5, the potential deformation due to slaking might be occur around 65% compare to the deformation in case 11 is only 1.3%. Furthermore, case 11, the deformation was not occurred even though the wetting and drying cycle was applied for the second time. In Figure 62(b) show that the deformation hardly occurs after the wetting and drying was applied for the second times. It can be concluded that the method by implementing of wetting and drying cycle at the beginning of the embankment project then followed by the compression process is one possibility to reduce the potential

deformation on the embankment related to the utilizations of mudstone as an embankment material.

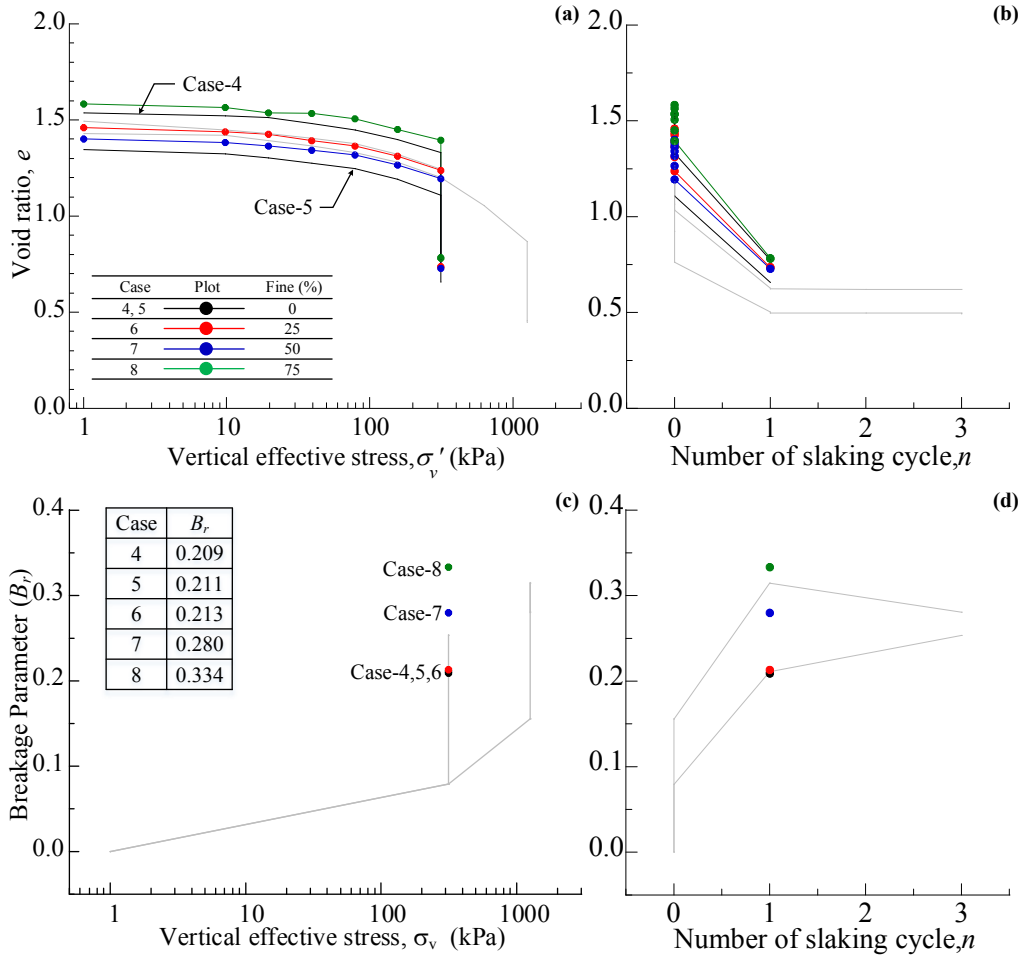

Figure 59. Compression characteristics and particle size change in Nou Mudstone one-dimensional compression slaking test (fine particle addition)

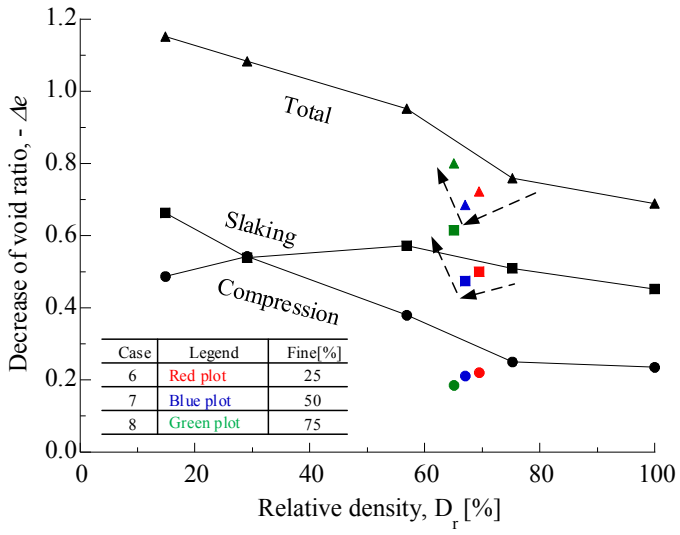

Figure 60. Decrease of void ratio due to addition of fine particle on Nou mudstone

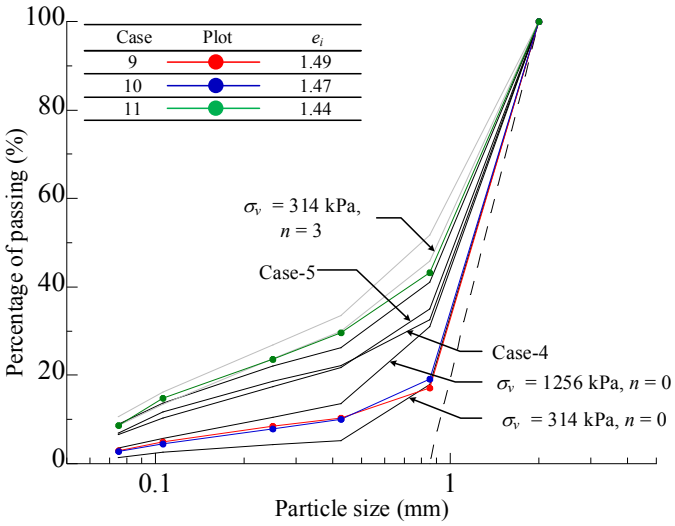

Figure 61. Changes in the particle size distribution of Nou Mudstone due to initial wetting and drying cycles (the wetting and drying history)

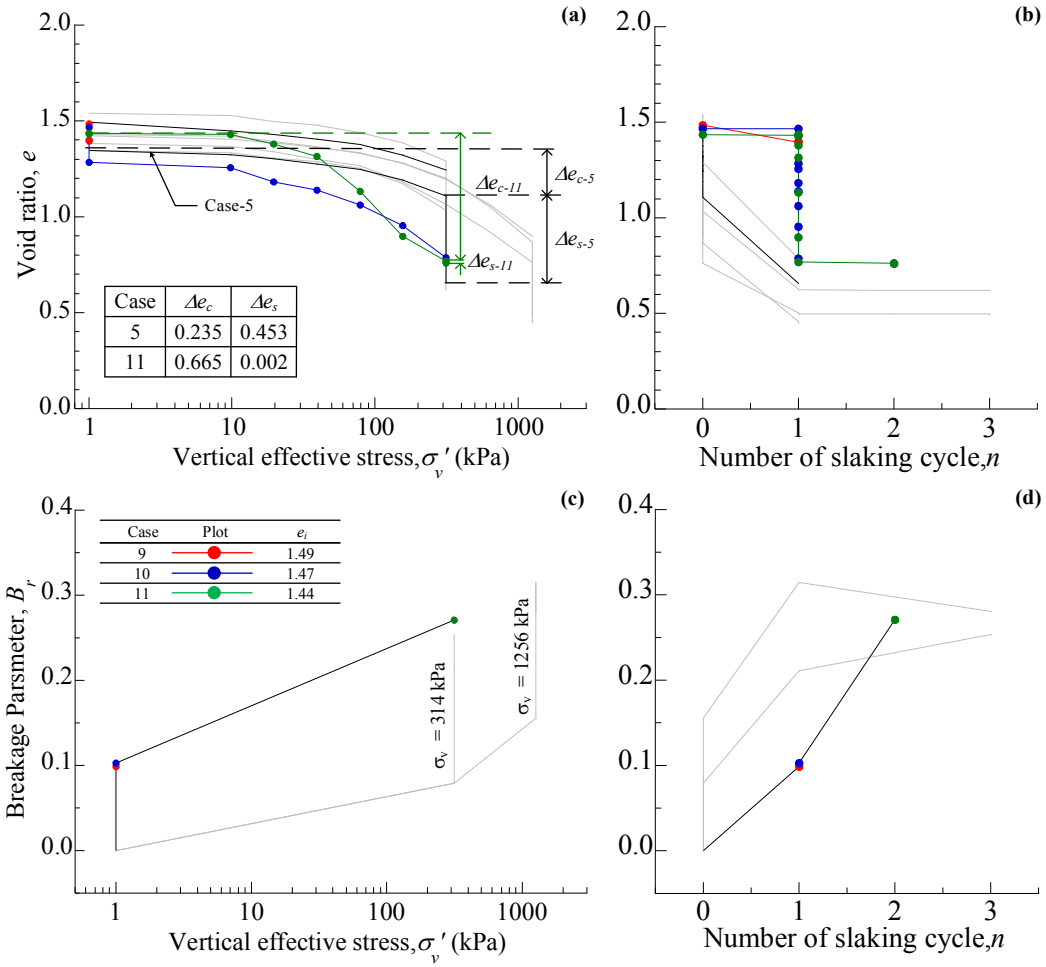

Figure 62. Compression characteristics and particle size change in one-dimensional compression slaking test of Nou mudstone under conditions of wetting and drying cycle history

5.6.3. The effect of loading/unloading history on slaking behavior

The next method is carried out by considering the effect of loading/unloading history during compression process in one-dimensional compression slaking test. The test procedure is same as the initial procedure in this study. The particle size distribution was arranged between 0.85-2.00mm and the density was prepared for the medium dense condition. The loading stage was performed by increase gradually to σ_v' = 1256 kPa, and before the wetting and drying cycle is applied, the pressure was gradually decreased to σ_v' = 314 kPa. In addition, the crushed mudstone specimen was prepared in two different initial void ratios are 1.43 for case 12 and 1.55 for case 13. It is interesting to observe the particle size distribution changes due to loading/unloading process (Figure 63). The particle size distribution change after the one-dimensional compression slaking test exhibit that the slightly different of the initial void ratio did not affect the change of distribution of particle and it was in accordance with the statement of the first methods by varying the initial void ratio. The particle size distribution after loading/unloading process and wetting and drying cycle similar with the particle size distribution of low pressure σ_v' = 314 kPa with one cycle of wetting and drying. Figure 64 shows the compression characteristics and the breakage parameter (B_r) as a representation of particle size distribution changes of Nou mudstone in one-dimensional compression slaking under the loading and unloading condition. Figure 64(a) exhibit that during the unloading process to the low pressure (σ_v' = 314 kPa) after the loading progress to reach the high pressure (σ_v' = 1256 kPa), the very small expansion seems occur due to the unloading which material try to expand but it could be ignored or just said that the void ratio after unloading is equal to the void ratio after loading to the high pressure. Compare to the case 4 and case 5, volume compression due to slaking induced by wetting and drying cycle after giving the stress history of loading/unloading process (case 12 and case 13) is slightly smaller than the conventional test in case 4 and case 5. According to the graphic correlation between the void ratio and number of slaking cycle (Figure 64(b)), exhibit that volumetric compression due to the number of slaking cycle after stress history is smaller than conventional and it has given a significant meaning to obtain the simple method for reducing the potential deformation of mudstone material. Figures 64(c) and 64(d) exhibit the breakage parameter due to loading/unloading pressure followed by the wetting and drying cycle. In addition, the dash-line is the estimation value of the breakage parameter due to stress history of loading-unloading given and the transformation of particle crushing. Related to the embankment made by mudstone, by given the stress history of loading/unloading during the process of construction might be one possibility of construction method to reducing the potential deformation.

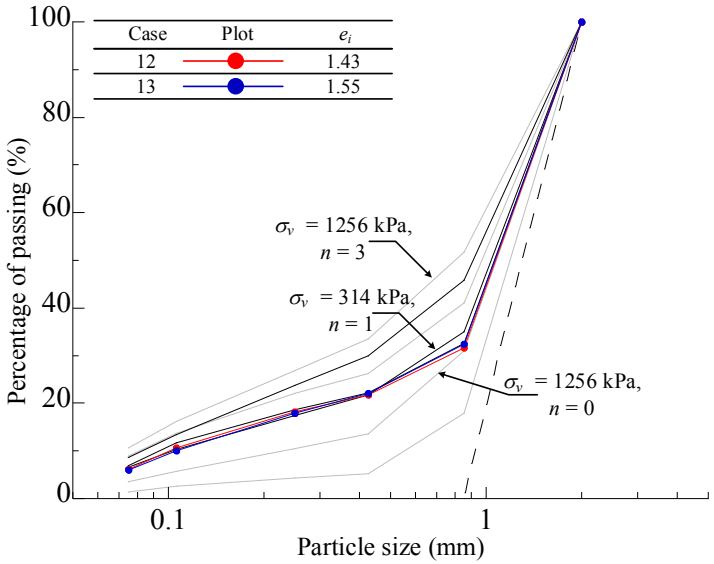

Figure 63. Changes in particle size distribution of Nou Mudstone in one-dimensional compression slaking test under stress history condition

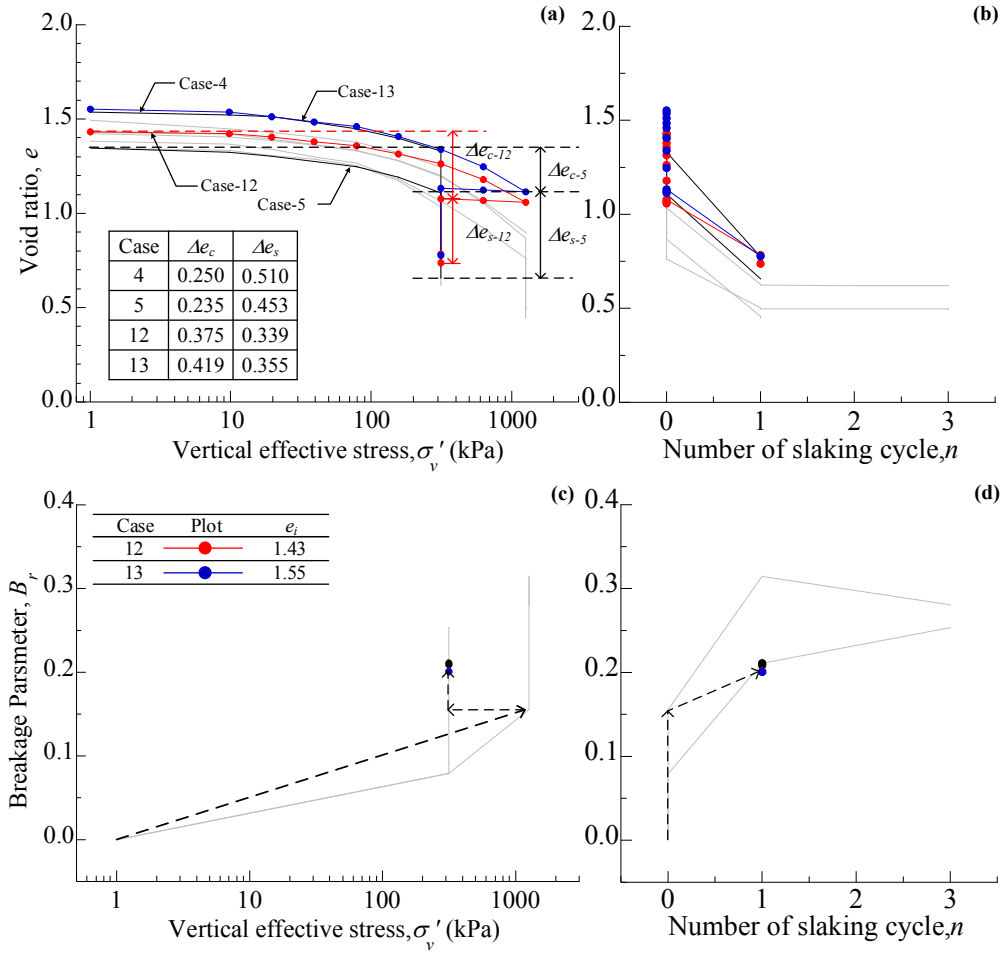

Figure 64. Compression characteristics and particle size change in one dimensional compression slaking test of Nou mudstone under stress history condition

5.7. Summary

In this study, the evolution of grading due to slaking therefore causes irreversible change in the mechanical properties of crushed mudstone attributable to variation in the packing density. Moreover, the evolution of grading during compression can increase the compressibility of crushed mudstone, with wetting and drying cycles causing significant compression despite the effective stress remaining constant. Since the evolution of particle size distribution under confined stress occurs without change in the maximum particle size, it can be described by existing indices of grading such as the grading state index I_G or breakage parameter B_r.

The author intends to acquire of the countermeasure methods of potential deformation caused by utilization of mudstone material in earth construction by perform several additional experiments. In order to investigate the effect of compaction during construction in the real field, the different initial void ratio and relative density (D_r) was applied. The deformation during compression shown an irregular tendency but at the end of wetting and drying cycles, the deformation has reached the same result, around 0,7. The breakage parameter or B_r value of each case during compression and slaking was shown the similar value, its mean that the initial density or different of compaction density does not affect the potential deformation during slaking cycle process. Some percentage of fine grain material was added to mudstone material to obtain the optimum fine grain material to reduce the deformation. It can be inferred that the optimum addition of fine grains is 50%, because when the fine grain content added more than 50% (75% of fine particles) then the volume compression returned to the original tendency. It is happened due to addition fine grain around 75% cause the specimen becomes uniform and it seems the void ratio almost reach the minimum/maximum void ratio. Considering the wetting and drying cycle in the previous test is cause the deformation, so then an initial wetting and drying cycle will be conducting at the beginning before compression. Compare to the case 5, the final deformation of each case has reached the same condition of the void ratio. It is revealed that the potential deformation due to slaking might be occur around 65% in case 5, compare to the deformation due to process of wetting and drying cycle at the beginning and followed by compression in case 11 is only 1.3%. Furthermore, in case 11, even though the wetting and drying cycle was applied for the second time, but the deformation does not occur or discontinue. It can be concluded that the method by implementing of wetting and drying cycle at the beginning of the embankment project then followed by the compression process is one possibility to reduce the potential deformation on the embankment related to the utilizations of mudstone as an embankment material. However, it is not a good idea to immerse the embankment in the real earth construction because it takes long period to drying

the embankment. Since the slaking is a weathering phenomenon, the author thought that discussion leading to practical use can be made depending on consideration such as a method of promoting weathering without releasing the water and a drying method of immersed soil. The next is the experimental methods which give the stress or compression history. It is confirmed that the deformation due to wetting and drying cycle decrease. The crushed the particle at the beginning process by applying the high compression is necessary. The crushed particle will fill the void and it will cause the deformation due to slaking decrease significantly. It makes sense to be applied in the real earth construction. Rearrangement of the size of the particle can be accompanied by this method and then followed by packing and crush the mudstone materials.

Therefore, it seems reasonable to describe the effect of slaking phenomenon on the deformation behavior represented by the evolution of grading or changes in particle size distribution. Based on the variation or several cases of one-dimensional compression slaking test, the effect of particle size distribution to reduce the deformation is an important parameter. In the future, it is necessary to study regarding the degree of saturation during and after the test. The variation of the degree of saturation (S_r) might be lead to the deformation behavior of mudstone which induced by wetting and drying cycle.

Chapter 6

Triaxial Slaking: Failure behavior

6.1. Introduction

It is necessary to carefully evaluate the deformation characteristics of sedimentary soft rocks such as mudstones. A method to evaluate the deformation behavior by conduct the triaxial test. A triaxial testing system has been modified to evaluate the deformation behavior according to the volume change of the specimen. Commonly, in triaxial testing have two conditions during the testing, the first is unsaturated condition and the second one is saturated conditions. Related to the main purpose of this study, the saturated condition is the suitable condition to be applied. Saturated soil specimen, the volume change of saturated soil specimen during consolidation or compression is equal to the volume of water in to or out to the soil specimen. It is contrary to the unsaturated soil specimen, the volume of water in to or out to the soil specimen is not equal to the volume change of the soil specimen. The different method has been proposed to measure the volume changes of unsaturated soil specimen. Wheeler (1988) modified the double cell triaxial system for checking the soils with large gas bubbles. The volume change of the inner cell was measured by using a burette. In this system, the axial load was measured the outside the cell a proving ring. The shaft of the loading piston was designed extends from the outer cell. A unique rolling diaphragm between loading piston and the inner cell was installed to minimize the leaking problem. The volume changes of the inner cell with cell pressure more than 400 kPa was nonlinear and the largest volume changes was recorded around 0.7 cm^3.

The Double Cell Triaxial System (DCTS) was improved for continuous measurement of the volume change of an unsaturated or saturated soil specimen. The main new features of the DCTS are different from the modified cells proposed by Yin (1998), and Wheeler (1988). The inner cell is totally closed within the outer cell. De-aired water is used to fill the inner cell or the outer cell. The cell pressure was applied under the same magnitude to the inner cell an

outer cell. The deformation potential during preparation the specimen could be minimize by applying the same water pressure to the wall and top cap of the inner cell. Due to the water pressure into the inner cell is equal to the outer cell, the hydraulic gradient along the piston at the cap of the inner is zero. O-ring seals was attached between the cap of the inner cell and the loading piston to be minimized the potential leakage at the gap. The error of volumetric strain calculation of soil specimen based on the double cell triaxial system are 0.2% then it can be inconsiderable (Yin, 2003). Laurenco, et.al (2000), has installed the high capacity suction probe in the pedestal of double cell triaxial system to measure the matric suction. The pedestal was designed to allow the user to remove/insert the probe while testing is running. It is possible to conduct since the suction probes can cavitate during testing. Concerning to eliminate the water absorption by the wall of the inner cell, an interior cell wall was made of glass instead of Perspex. In earlier designs a double-walled cell was trialed, where a common top cap was used for inner and outer cells. It was founded that extensions of the loading arms produced volume changes that could affect results (Mendes, et.al, 2012).

Related to the deformation characteristics, a series of test on mudstone had been conducted. Hayano, et.al (1997) was performed a series new developed triaxial test under unload-reload cycle to evaluate the deformation characteristics of soft rock material. Axial and lateral strains were measured by attaching four pairs local transducer along the surfaces of rectangular prismatic shape specimen. A series of small cyclic loading was applied to determine the elastic and plastic deformation. The critical errors at both the top and bottom specimen and at lateral surfaces during isotropic compression were observed. The local strains exhibit approximately isotropic deformation during isotropic compression. Nakano, et.al (1998), regarding the slaking on the mudstone, initially the mudstone was idealized as a heavily over-consolidated clay and the slaking is interpreted as softening behavior. Since the slaking occurs, over-consolidated mudstone particle tends to return from initial stiff solid state to normally consolidated soft clayey state.

Subjected to the purposes of this study, the triaxial with double cell system was developed to observe the volume change due to the slaking cycle on mudstone specimen. During the compression and shear-slaking stages, the volume change of mudstone specimen is observed based on the change of water level in the inner cell. In this study, the Kakegawa mudstone, Kobe mudstone, and Hattian Bala mudstone have selected to be used in the triaxial slaking test based on their accelerated slaking characteristics during the preliminary experiment. The condition of mudstone specimens was set into the dried condition and the initial particle size distribution arranged between 2.00 – 0.85 mm (ASTM D422 Standard Test Method for

Particle-Size Analysis of Soils) and it is identical size diameter with one-dimensional compression slaking test. The schematic device of triaxial slaking presented in Figure 65.

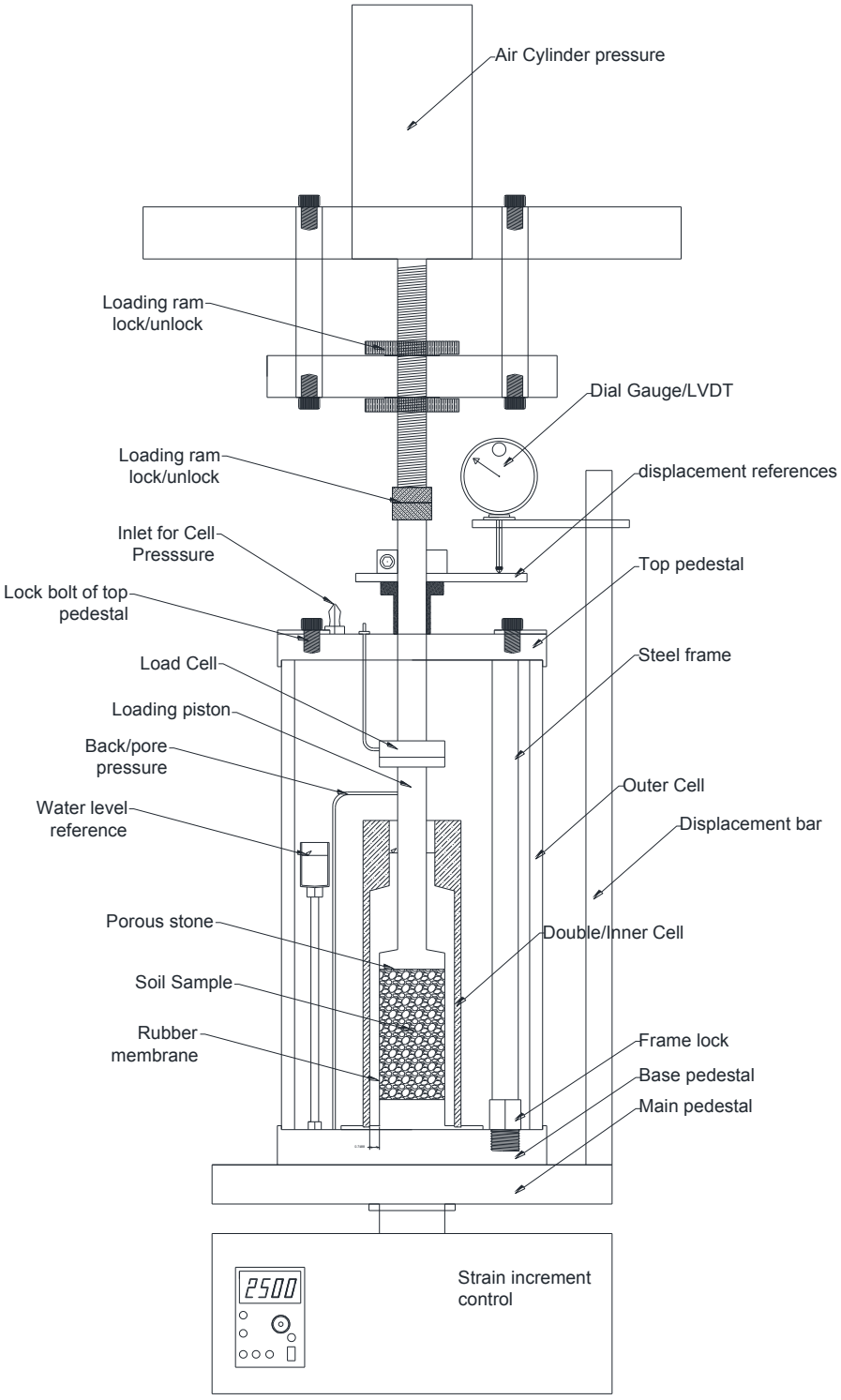

Figure 65. Schematic devices of Triaxial slaking

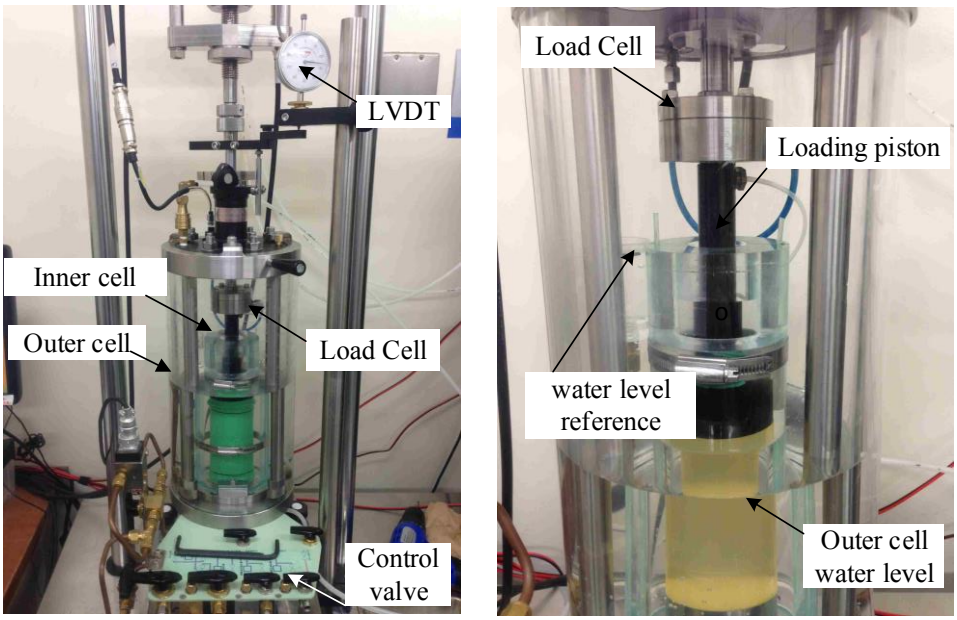

(a) Triaxial Testing machine (b) Water level changes on the Double Cell system

Figure 66. Double Cell Triaxial system devices and water level control

6.2. Double Cell Triaxial System for Slaking

Based on the result of previous study regarding the double cell triaxial system (Bishop and Donald, 1961; Wheelar, 1988 and Yin, 2003), the author has modified a double cell triaxial system for accommodate and measurement of volume change of unsaturated and saturated specimen during triaxial slaking testing on the mudstone (Figure 65). The inner cell in this system was not provided with the cap or any cover purposes and connected with the outer cell. The magnitude of cell pressure on the outer cell is same with the magnitude pressure inside the inner cell. The initial deformation of the specimen during preparation was minimized by using the EP regulator of axial pressure system. The axial loading was set to be steady when the loading piston was contacted with the top of specimen. During the compression and shear-slaking, the water level reference which has connection to the inner cell was set to be constant. The water level changes inside the inner cell are calculation of volume change of saturated or unsaturated specimen during triaxial testing (Figure 69). The outer cell has made from the acrylic glass with an internal diameter around 180 mm and height around 365 mm and wall thickness of 20 mm. The inner cell also made from the acrylic glass with high pressure capability. The dimension of inner cell has a height of 235 mm and the wall thickness of 10 mm. The diameter of the inner cell consists of two kinds of diameter, the diameter on the topside of 35 mm and the bottom side of 69 mm. The detail dimension for measure the volume changes was explained in Figure 67. The axial load piston has a diameter of 22 mm. The standard size for a soil specimen is diameter of 50 mm and height of 100 mm.

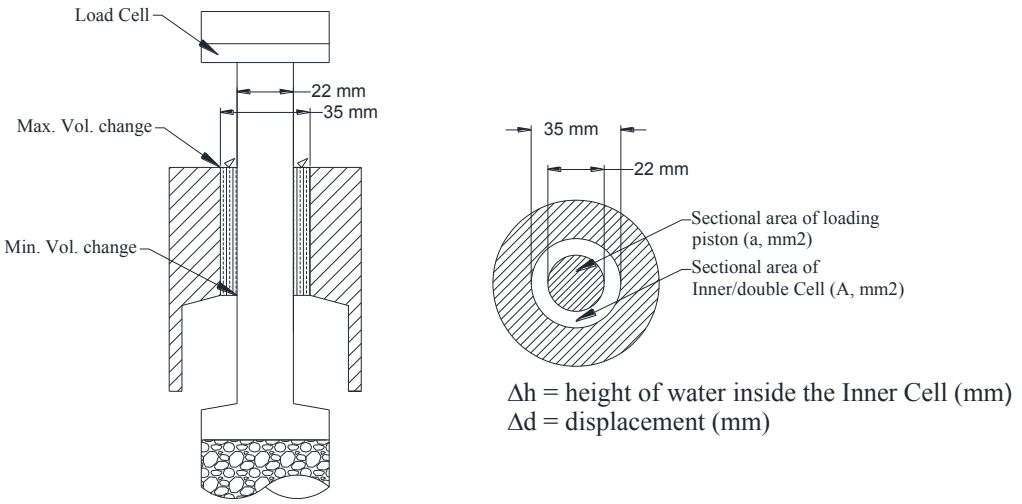

Figure 67. Principle calculation of volume change in double cell triaxial slaking system

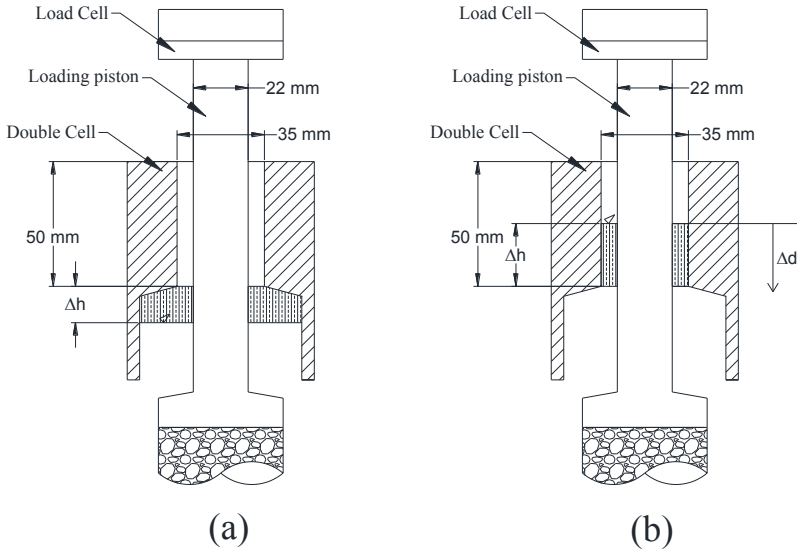

Figure 68. The water level change inside the inner cell as representative of the volume changes of soil specimen

The principle calculation of the volume change of specimen was laid on the water level change inside the double cell. Figure 67, disclose the principle calculation of volume change. The first area belongs to the inner cell (A) and the second area is the loading piston area (a). The differences between inner cell area and loading piston are the area multiply with the height up/down of water level inside the inner cell is the volume change during the triaxial testing even compression or shear process. The expansion behavior was presented by the increasing of water level inside the inner cell, and the compression behavior was presented by the decreasing of water level inside the double cell (Figure 69). The volume change measurement might error or mistaken when the water level inside the inner cell is lower than the minimum

volume change level (Figure 68a). During the triaxial testing, the initial water level position inside the inner cell was dependent on the characteristics of mudstone material. For the weakest material, the water should be filled to the nearest top of maximum volume change and for the strongest material, in the middle of the height of the inner cell is enough.

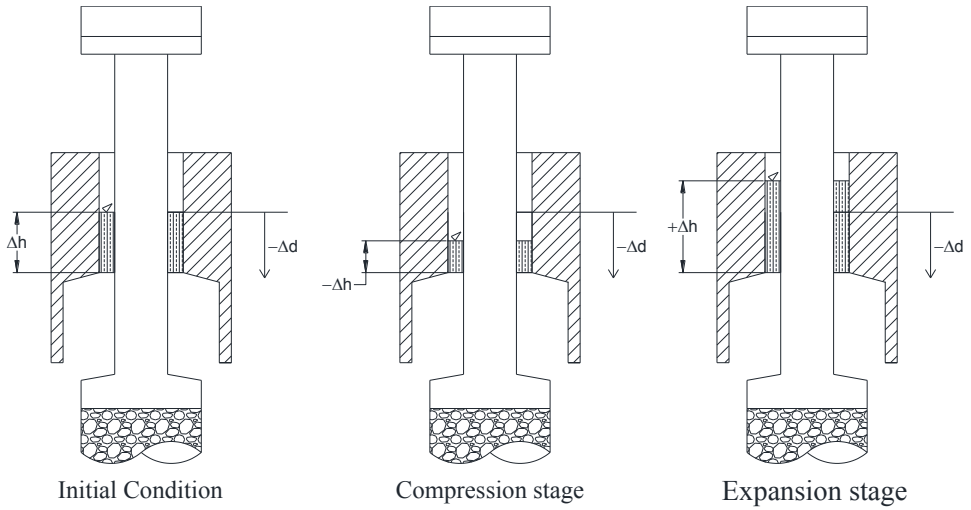

Figure 69. State reference of water level during compression and expansion stage of soil specimen

6.3. Calibration of the double cell triaxial system

The triaxial testing under fully saturated condition of Toyoura sand was prepared to calibrate the double cell triaxial system in this study. The fully saturated condition was needed throughout of calibration because the volume change result of inner cell should be same with the volume change of burette. The Toyoura sand is considered incompressible and can be used to assess the volume change of soil specimen based on the water level change into the inner cell and burette. The saturation process of Toyoura sand is very important to ensure all voids within the test specimen are filled with water, and that the pore pressure transducer and drainage lines are properly de-aired. This may be achieved by firstly applying a partial vacuum to the specimen to remove air and draw water into the transducer and drainage lines, followed by a linear increase of the cell and back pressures.

To check the degree of specimen saturation is sufficiently high before moving to the consolidation stage, a short test is performed to determine B-value. This is called a B-check and requires specimen drainage to be closed whilst the cell pressure is raised by approximately 50 kPa. Figure 70 confirmed that B-value is more than ≥ 0.95, is mean the soil specimen saturated before shearing process to observe the volume change.

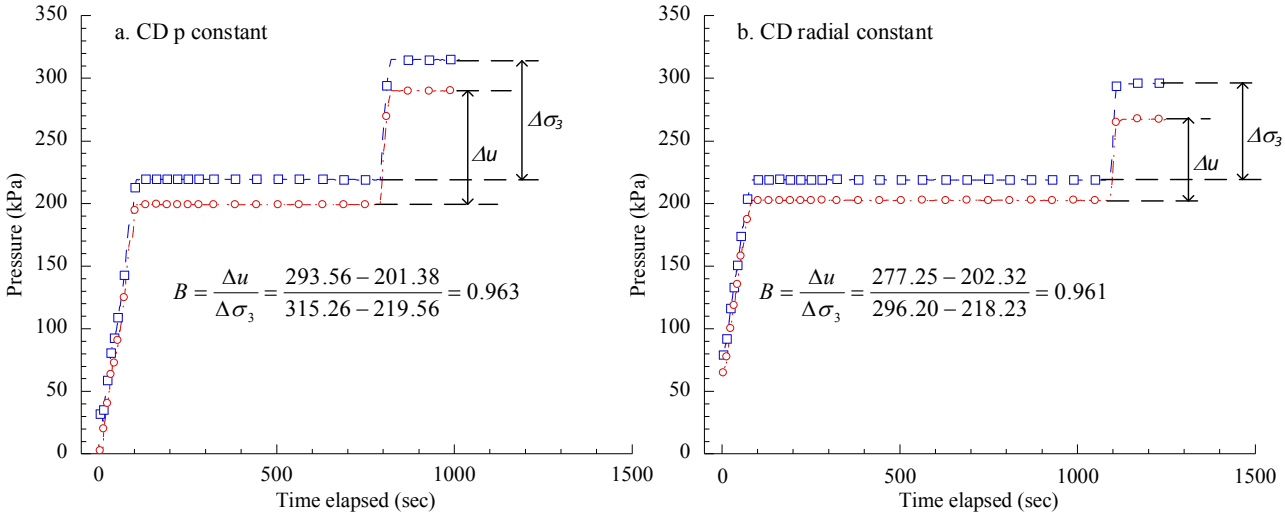

Figure 70. The result of B-check to confirm specimen saturated

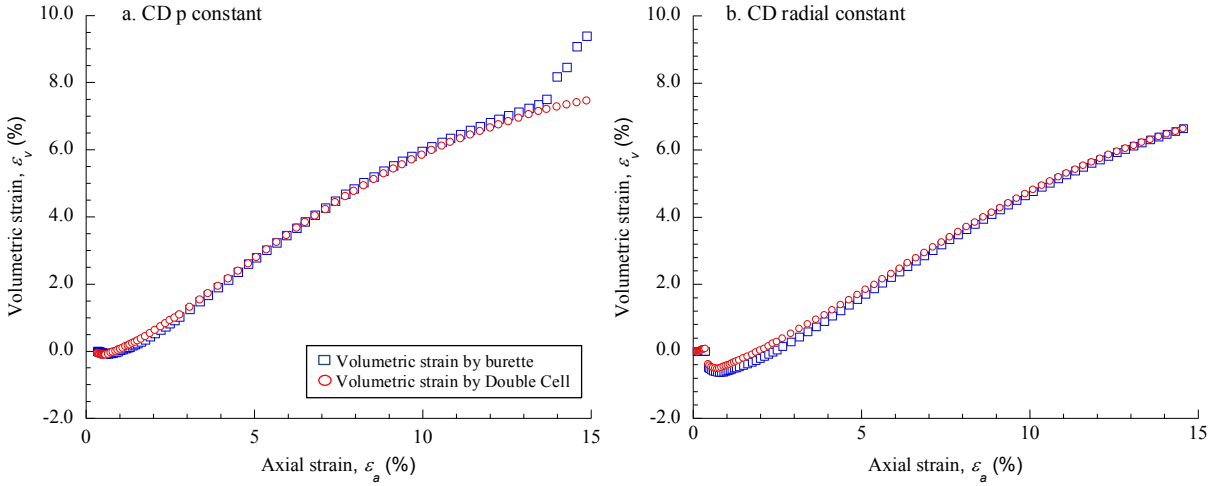

Figure 71. Calibration of volumetric strain measurement by burette and inner cell

In order to calibrate the volume change of inner cell, the triaxial CD mean effective stress constant and triaxial CD radial constant were performed. Both of this experiment result should confirm the volume change between inner cell and burette. Figure 71 exhibit the volume changes of inner cell and burette under two types of stress condition. The graphic clearly shown that volumetric strain result from inner cell or burette are almost same. The difference is not more than 5%. It was give a conclusion that the calibration of inner cell was work properly.

6.4. Triaxial Slaking

As mention in the first sub chapter, the three kinds of mudstone material were selected for triaxial slaking testing. The grain size distribution for the triaxial testing between 0.85-2.0 mm.

The whole specimen was dried and made into the crushed material. The general properties of mudstone materials are summarized in Table 8.

Table 8. General properties of geomaterials

	Particle density, ρ_s	Max void ratio e_{max}	Min void ratio e_{min}	Geological period
Kobe mudstone	2.69	1.85	1.38	Neogene Period
Kakegawa mudstone	2.65	1.83	1.29	Neogene period
Hattian Bala mudstone	2.75	1.09	0.79	Neogene period

The schematic overview of triaxial slaking test was exhibited in Figure 72. Similar to the one-dimensional compressive slaking test, the wetting and drying circulation was attached to the triaxial system. The E/P regulator was installed to control automatically the axial pressure (σ_1) and cell pressure (σ_3) during the triaxial testing (Figure 74).

The E/P regulator was controlled by the calculation code that had been written in advance. Figure 73 also disclosed the detail arrangement of manual control and automatic control in triaxial system included the wetting and drying circulation. Since the mudstone material is crushed material, the specific sample preparation is needed.

6.4.1. Sample preparation

The dimension of mudstone specimen is 100 mm in height and 50 mm in diameter. During preparation the specimen, the small negative pressure was applied to keep the rubber membrane attached to the inner side of mold. The density of specimen was arranged to the medium dense. The crushed mudstone specimen was compacted into 6 layers with 80 tamp per each layer. The filter paper mounted on top and bottom of specimen. When determining the loading ram position to the specimen, the axial pressure is controlled automatically using E/P regulator to minimize the initial deformation. Seal the rubber membrane to the loading ram and before release the mold, the negative pressure of 25 kPa was applied to keep the shape and position of crushed specimen (Figure 74).

6.4.2. Triaxial slaking

Slaking is a phenomenon on the mudstone when contacted with water. The mudstone material tends to transform into fine material during inserting into water. The triaxial slaking system is a triaxial apparatus which has been modified with the inner cell to measure the volume change and the circulation of wetting and drying path during process the slaking (Figure 72).

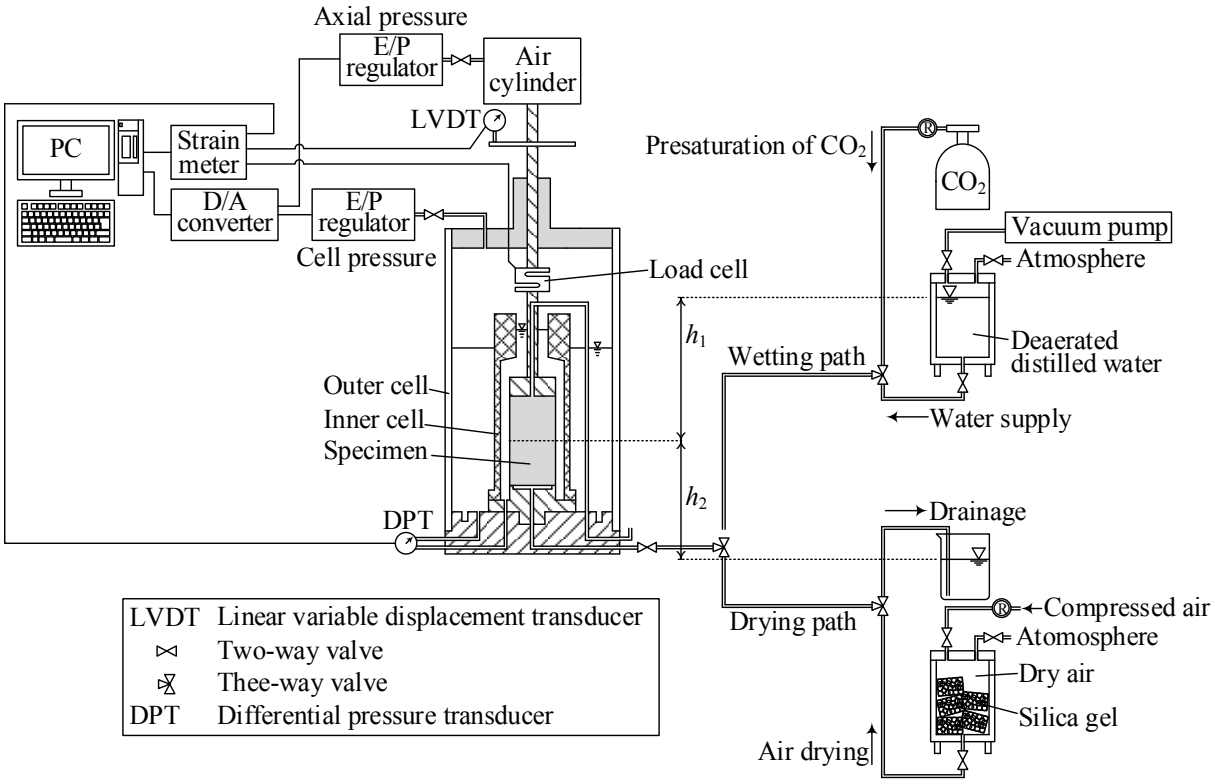

Figure 72. A schematic overview of triaxial slaking testing

Isotropic compression under consolidated drained condition tests were performed as an initial stage of triaxial slaking testing from the initial confining pressure of 25 kPa and gradually up to the 314 kPa. The volumetric strain of specimen was measured by the inner cell. Furthermore, the specimen is sheared by applying an axial strain (ε_a) to the test specimen at a constant rate of 0.5 cm/sec through upward movement of the load frame platen under mean effective stress constant (p-constant). During the test, the pore pressure is neglected. The test is focused on the volumetric compression changes during compression and shear slaking test. Specimen response during the shear stage is typically monitored by plotting the deviator stress (q) or effective principal stress ratio (q/p) against the axial strain (ε_a). The shear is continued until 20% of total axial strain has been reached, which may include identification of the peak deviatoric stress (q) or peak effective principal stress ratio. Slaking cycles in triaxial testing is performed by maintain the deviatoric stress (q) of 200 kPa and 400 kPa and mean effective stress (p) of 314 kPa. The volumetric strain during shear-CD test is measured by the inner cell. The mechanical behavior of mudstone specimen is observed by plotting the volumetric strain (ε_v) and axial strain (ε_a).

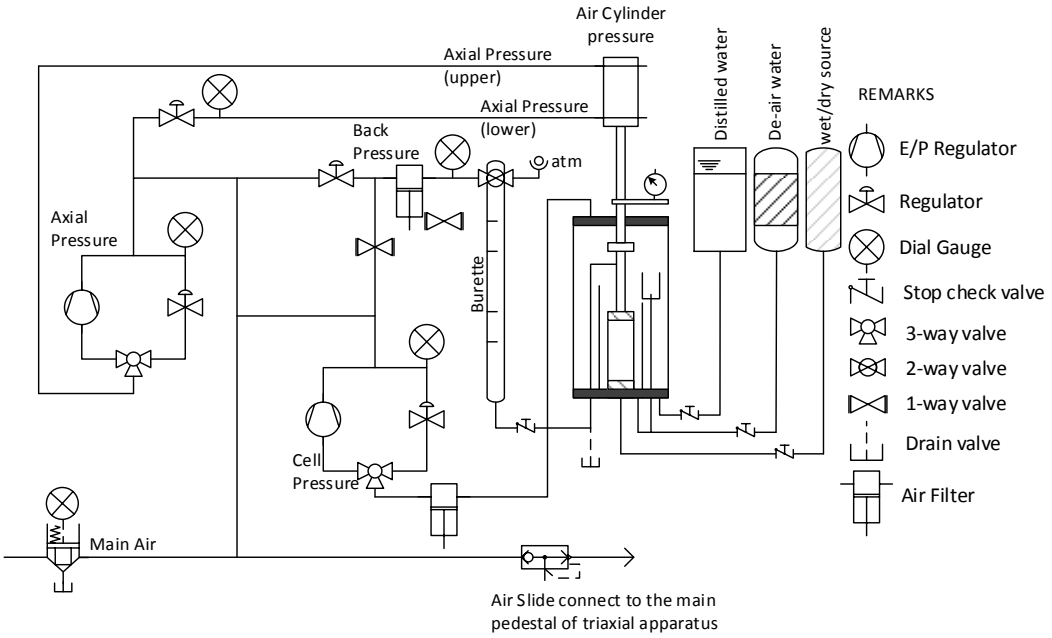

Figure 73. Schematic of E/P regulator for Axial Pressure and Cell Pressure

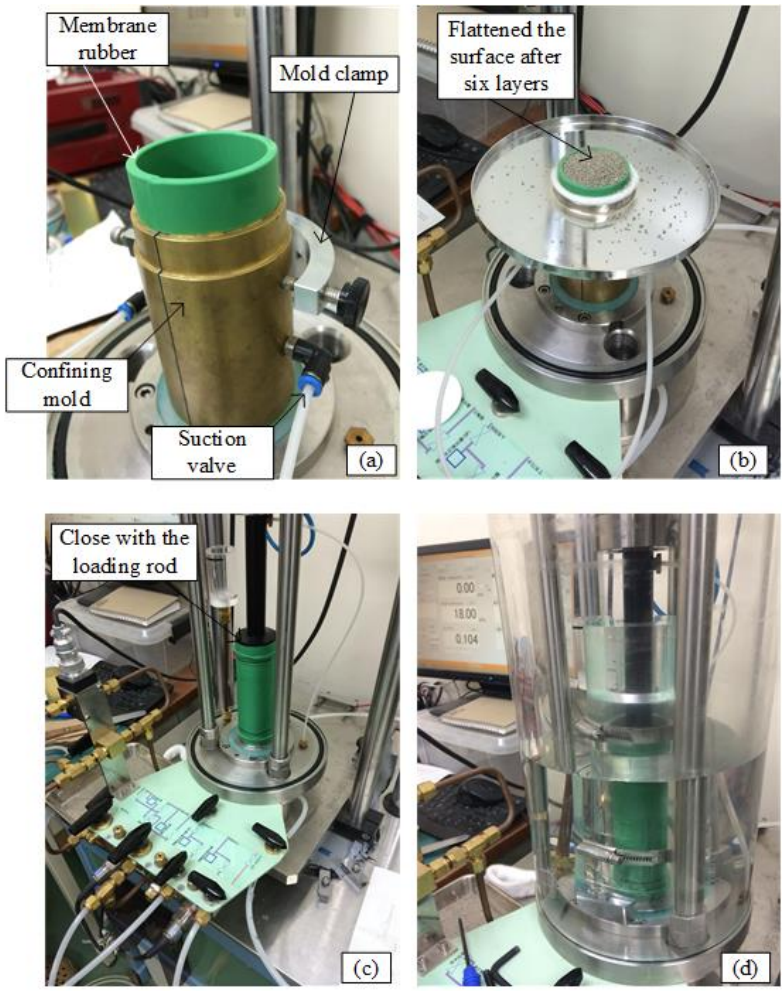

Figure 74. The photograph of triaxial specimen preparation

6.5. Result and Discussion

A series drained triaxial compression slaking test has prepared in two conditions, dry and saturated during slaking cycle. From this series of drained triaxial tests, it may be concluded that particle breakage continues to very large strains indeed, far beyond those reached in triaxial tests. That particle breakage is accompanied by volumetric compression and occurs even for tests at modest confining stresses. If an apparent critical or constant-volume state is seen in triaxial tests, as Chandler (1985) and Baharom & Stallebrass (1998) assumed, it can only be as a result of counteracting dilative strains from particle rearrangement and compressive strains from particle breakage. At very large strains a constant grading is reached, but that constant grading is dependent not only on the normal stress applied but also on the uniformity and absolute particle size of the initial grading. The mobilized strength is unaffected by the particle breakage. It is confirmed that the compressive volumetric strain is directly related to the particle breakage. Figure 75 shown the particle size distribution of the selected mudstone specimen has changed due to isotropic compression and shear under mean effective stress constant (*p-constant*) and one slaking cycle with different deviatoric stress (*q*). The particle size distribution of Kobe mudstone (Figure 75(a) was significantly changed. The triaxial slaking testing result of Kobe and Kakegawa mudstone under a deviatoric stress (q) of 200 kPa and 400 kPa had revealed that the particle size distributions of both mudstones were converted after compression and shear followed by one slaking cycle, and it's mean that the particle breakage during compression-shear-slaking occurred. Furthermore, the particle size distribution of Kakegawa and Kobe mudstone after monotonic shear almost similar, except for Hattian Bala mudstone which has slightly change from the original condition. The greater convert in grading clearly seen after slaking cycle under a constant deviatoric stress of 400 kPa, and it is also confirmed that evolution of grading due to particle breakage is related to an increase in the deviatoric shear stress and slaking cycle. During triaxial testing without slaking, the shear was performed until the axial strain has been reached 20% of total axial strain. The particle size distribution of Hattian Bala mudstone was slightly changed after triaxial CD p constant without slaking is performed. It was shown that during shearing without slaking cycle does not seem to exhibit any particle breakage. Kobe and Kakegawa mudstone has shown the similar characteristics with Hattian Bala regarding the particle size distribution change during shearing without slaking. The particle breakage in triaxial slaking testing tends to occur due to slaking cycle rather than shear itself. The failure criterion of soft rock was not deeply disclosed by a function of stresses, but the relationship between stress and the volumetric strain should be given as an essential condition (Hobbs, 1996). Related to this, the triaxial slaking devices

has been modified to explore the mechanical behavior change due to slaking on mudstone. Figure 76, Figure 77 and Figure 78 shows the relationship of (a) mean effective stress (p')-deviatoric stress (q), (b) axial strain (ε_a)-deviatoric stress (q), (c) mean effective stress (p')-specific volume (ν) and (d) axial strain (ε_a)-specific volume (ν).

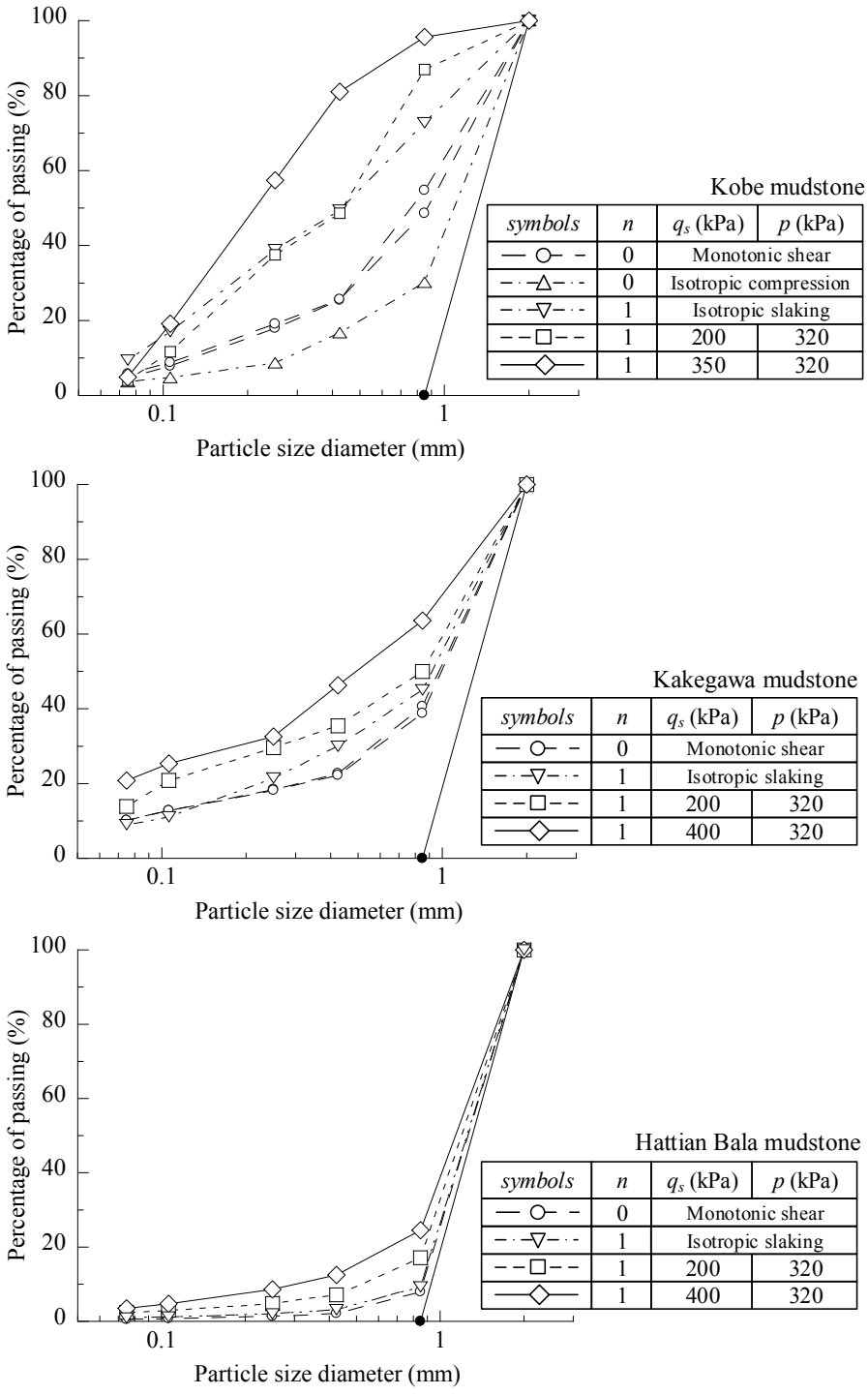

Figure 75. Changes in particle size distribution during triaxial slaking testing on mudstone

All of figures is resulted from the series of triaxial slaking testing of medium compacted mudstone material. In common, the figures (a) is shows the triaxial CD p constant characteristics. Figures (b) of each mudstone specimen has shown the stress-strain relationship of medium dense material. The maximum deviatoric stress of each mudstone specimen between 550-650 kPa and the axial strain (ε_a) reached at 20% on dry condition without slaking cycle applied. The axial strain (ε_a) of Kobe and Kakegawa mudstone in dried condition during shear is reached of 4.5% and 7.8% subjected to q = 200 kPa and q = 400 kPa, while the axial strain of Hattian Bala mudstone is reached of 1.8% and 3.9% before slaking. As known the Kobe and Kakegawa mudstone was relatively easier to crush during compression than Hattian Bala mudstone. It is the reason why the axial strain of Hattian Bala mudstone is lower than Kobe and Kakegawa mudstone subjected to the same deviatoric stress (q). The axial strain tends to increase due to slaking as the deviatoric stress increase. It is confirmed that the slaking causes increasing of the axial strain of mudstone specimen.

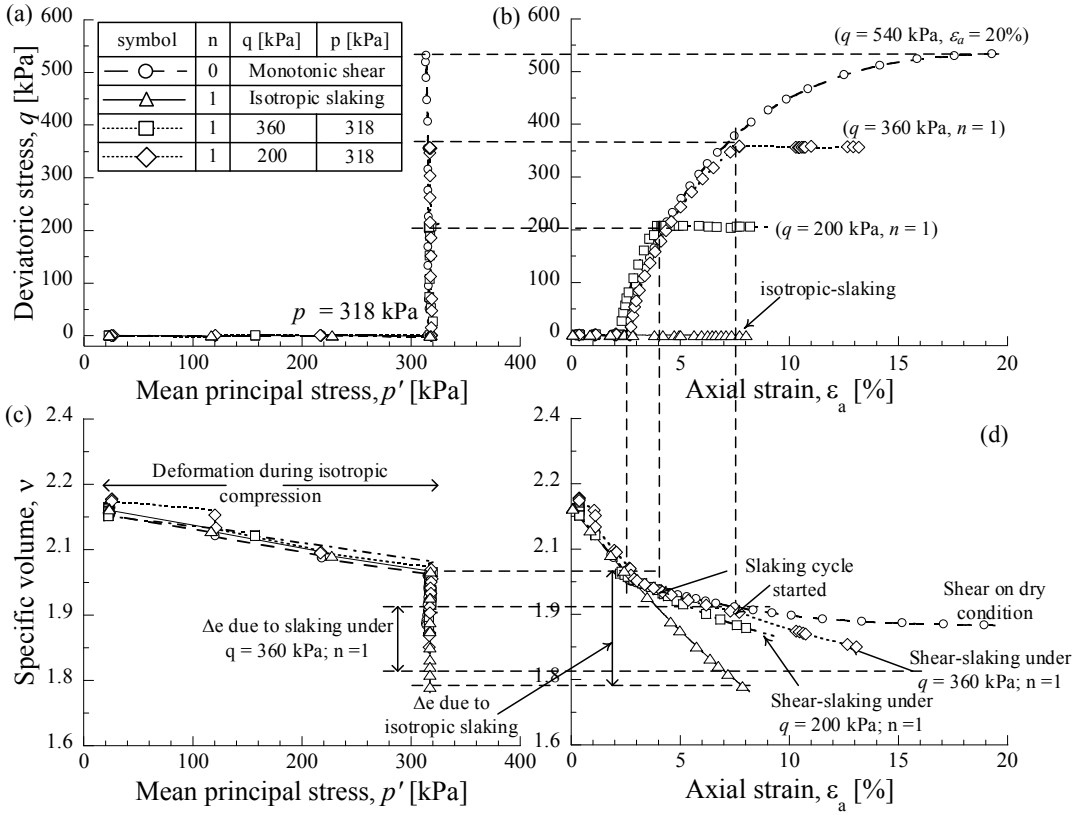

Figure 76. Change in compressive properties and strain behavior of Kobe mudstone during triaxial slaking testing

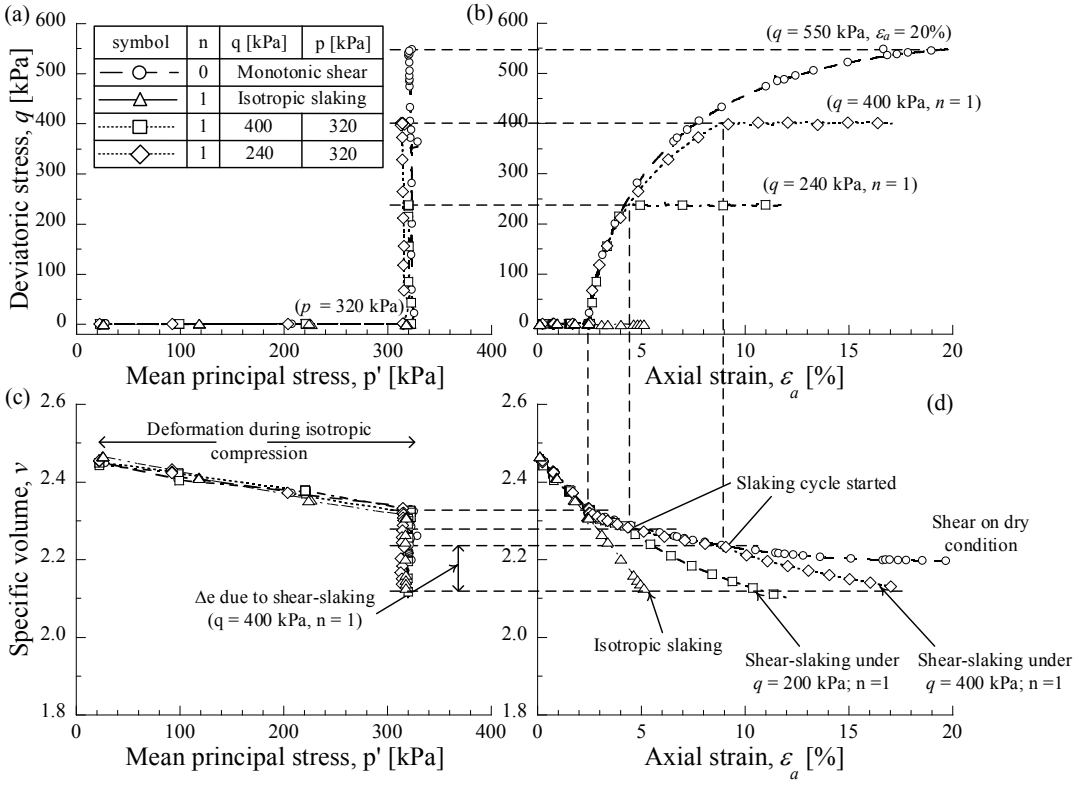

Figure 77. Change in compressive properties and strain behavior of Kakegawa mudstone during triaxial slaking testing

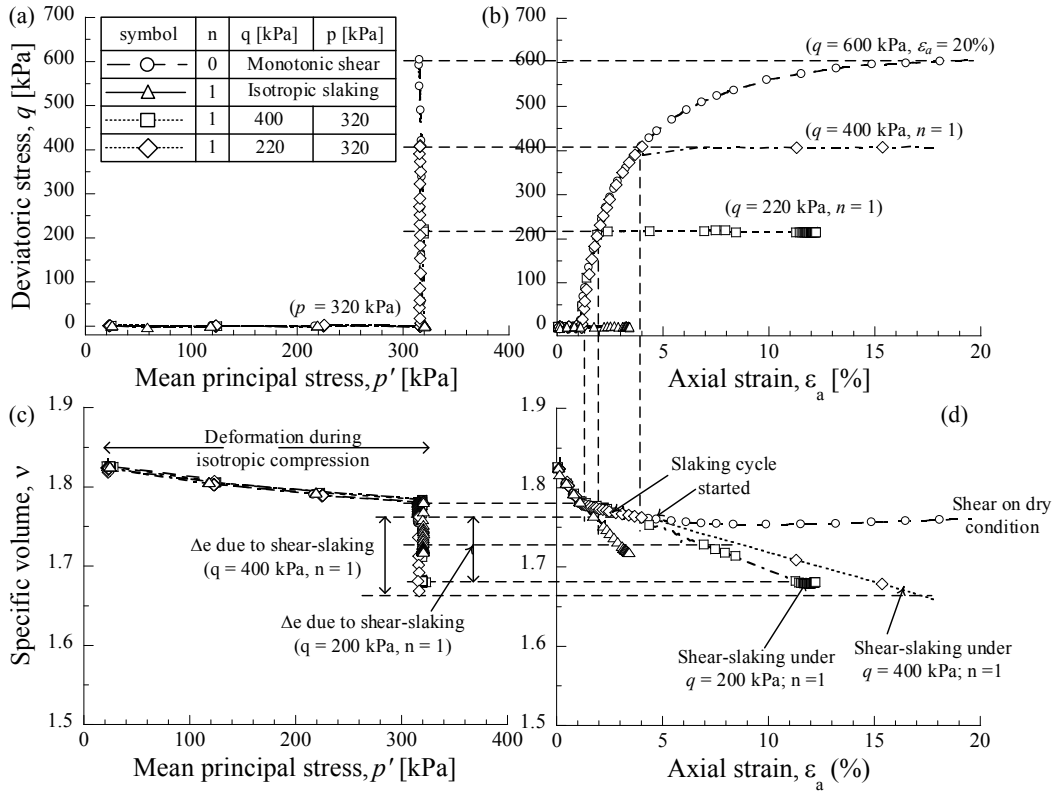

Figure 78. Change in compressive properties and strain behavior of Hattian Bala mudstone during triaxial slaking testing

Figures 77 and Figures 78 section (c) and (d) exhibit that the typical of shear strength values obtained from Kakegawa and Hattian Bala mudstone have undergone various degree of softening due to slaking cycle under p and q keep constant. The particle crushing during isotropic compression line and shear was followed the dry condition behavior lead to decrease of the specific volume. The failure deformation due to slaking cycle under high deviatoric stress (q) is smaller than the low deviatoric stress. It has been pointed out that the anisotropic behavior occurs during slaking cycle since the softening behavior appear during wetting and drying applied. The slaking cycle under isotropic compression of Kakegawa mudstone (Figure 80) seems anisotropic, after the ratio both of strain was not satisfied of $\varepsilon_v = 3\varepsilon_a$. We expected that during the isotropic slaking cycle, the volumetric compression is approximately isotropic. According to Yoshida et.al (1991), the softening behavior due to slaking will occur and reduce the shear strength of mudstone material. In this study, even though the stress has kept constant, in terms of p, but due to the wetting and drying cycle the failure deformation occurs or increase as increase the deviatoric stress. Decreasing the deviatoric will lead to changes in anisotropic behavior becomes the isotropic behavior, so then the isotropic relationship in strain ratio obtained. Figure 79 to Figure 81 shows the volumetric changes of Kobe, Kakegawa, and Hattian Bala mudstone. It confirms the previous explanation, the deformation occurred immediately after the slaking cycle started. It is provided that the compacted sample of crushed mudstone is regarded as fissured, it is reasonable to consider that the mudstone material has softened to a certain extent due to moisture arrangement in the sample preparation. The Kobe mudstone shows the approximately volumetric strain behavior due to slaking.

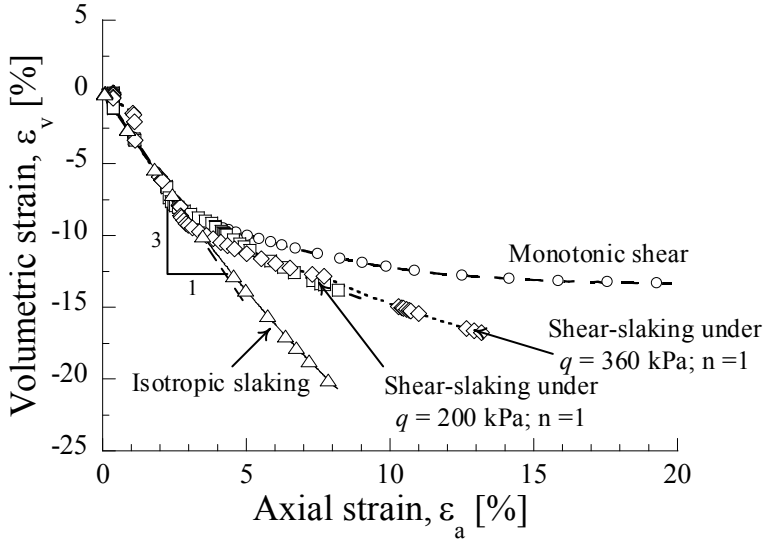

Figure 79. Volume change characteristic due to slaking cycle of Kobe mudstone with different deviatoric stress

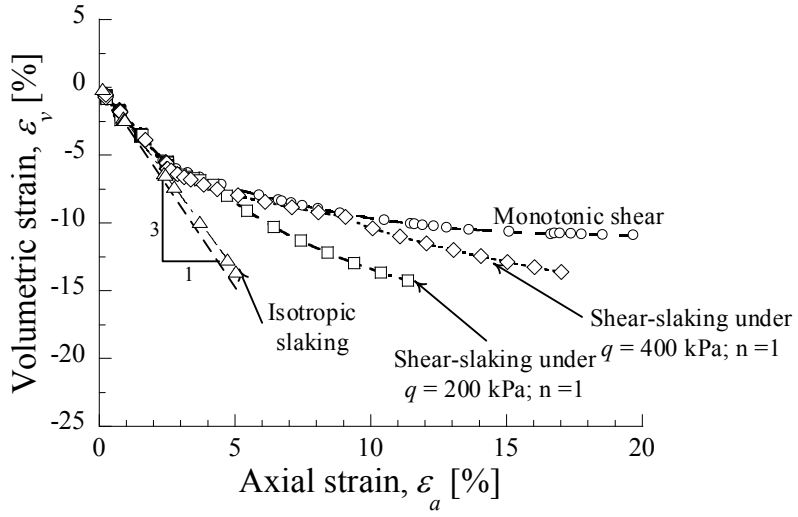

Figure 80. Volume change characteristic due to slaking cycle of Kakegawa mudstone with different deviatoric stress

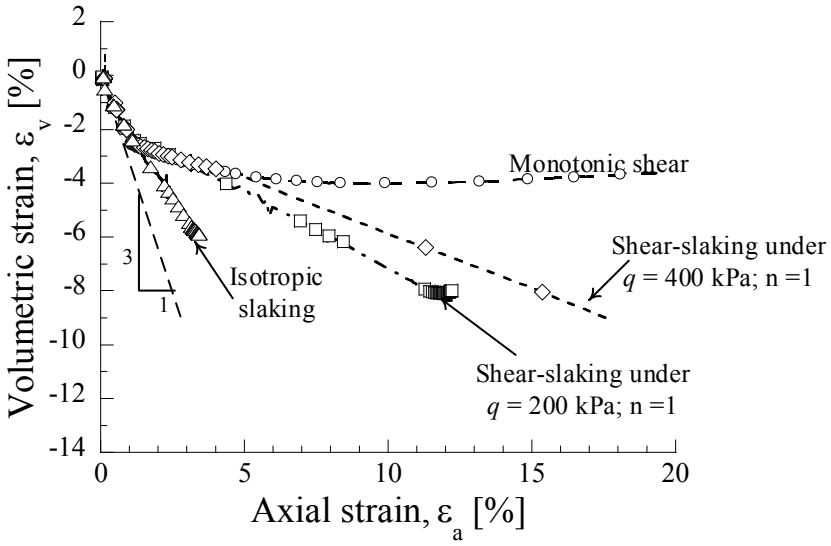

Figure 81. Volume change characteristic due to slaking cycle of Hattian Bala mudstone with different deviatoric stress

During the slaking cycle, the Kobe mudstone specimen is easy to alter when contacted into the water compare to others mudstone specimen. The particle size distribution at the end of slaking cycle shows that the grading size becomes wider compare to the initial grading. The strain relationship of Kakegawa shows an irregular condition which the axial strain rate larger than volumetric strain rate. Based on the observation during the experiment, the water on the wetting phase could not fill the specimen. However, this study attempted to observe the volumetric strain behavior due to slaking even though the result was not appropriate enough.

6.6. Summary

A series of triaxial slaking tests on the crushed mudstone specimen of Kobe, Kakegawa, and Hattian Bala mudstones were carried out to observe the failure deformation behavior due to slaking phenomenon. Based on the particle size distribution, the changes in mechanical behavior of mudstone after slaking were observed. The particle size distribution changed due to slaking is more significant than shear progress. Kobe mudstone shows the wider grading size changes after slaking cycle applied. After the early shear stage, the crushed mudstone aggregate specimens with 80% compaction degree show elastic behavior with the plastic expansion that follows the critical state line. This behavior resembles normally consolidated soil. Additionally, the number of slaking cycles as slaking progress corresponds to a constant deviator stress of crushed mudstone aggregate, and a lower hardness level accompanying plastic expansion on the effective stress path. As we expected, the deformation during isotropic slaking compression is relatively closed to the isotropic behavior. The axial strain (ε_a) of Hattian Bala mudstone before slaking was smaller than Kobe and Kakegawa mudstone and it might occur since the particle of Hattian Bala mudstone is difficult to crush during compression and shear in dry condition. The assembled crushed mudstone which is packed in medium density still exhibited the progressive deformation when the slaking cycle started, especially for the mudstone material that suspected has intra-granular pores such as Kobe mudstone. The axial strain has increased due to slaking and increase of deviatoric stress. The softening behavior clearly seen during the wetting and drying cycle applied and an anisotropic behavior suddenly occurs. Further investigation to observe the time and speed of deformation during slaking cycle applied and the effect of the number of wetting and drying cycle is needed for further study.

Chapter 7

A Constitutive model of slaking and deformation behavior

7.1. Introduction

Nowadays, geotechnical problems due to existence of mudstone material on the earth embankment are wide issues to overcome. Cost efficiency and availability of mudstone material in large amount are the reason why it is still frequent to be utilized. Mudstone is a fine grained sedimentary rock which consists of a combination of clay and silt particles. Regarding their behavior in ground engineering practices, mudstones could not be classified or categorized as rock or as soil. Mudstone tends to transform from behaving like rocks become behaving like soils in terms of particle sizes within relatively short time periods after contact with water (Botts, 1998). It became particularly interesting after several experts opine that changes in particle size distribution will affect to their behavior and characteristics of material itself (Coop and Lee, 1996; Yamamuro, 1996). Certainly, the transformation of particle size is mostly influenced by external factors. The cycles of wetting and drying combining with the compression are the potential external factor to accelerate the changes in particle size distribution. Furthermore, wetting and drying process is known as slaking cycles. Slaking cycle causes particle size changes with a significant reduction in shear strength and increases in deformation (Botts, 1986; Vallejo et. al, 1993; Sharma, et. al, 2012 and Kikumoto, et. al, 2015). Chang and Hicher (2005) and Piccolroaz et. al. (2006) stated that the deformation is a representative of materials volume which has generated by mobilizing particle contacts in all orientation and stress-strain relationship can be derived as an average of the mobilization behavior of these local contact planes. On the other hands, these studies also demonstrated that slaking cycles significantly affect the degradation process and evolution of particle size distribution in such rocks (Vallejo & Pappas, 2010; Gautam and Shakoor, 2013 and Kikumoto, et. al, 2016). Therefore, slaking in an earth embankment after a long-term period can contribute

to the deformation or large settlement. It also clarifies the characteristic of slaking and its impact on deformation and strength properties as an important challenge in geotechnical engineering practices.

Further, the direct shear test was conducted to observe slaking properties and deformation behavior under shear stress. However, strain and stress inside the specimens were unequal in these tests, making it difficult to use the test results to develop a constitutive model and more understand about mudstone behavior (Kusumi et.al., 1996 and Kiyota et.al., 2011; Sharma, 2012). The particle size changes will influence the basic constitutive properties of the soil particularly, properties such as critical states which are dependent on the available range of densities of compaction. Discrete element modeling is used to show the dependence of critical state conditions on grading and the ways in which the particle assembly seeks out new critical state conditions as the grading changes index (Gajo and Wood, 1999; Wood and Maeda, 2007). Emphasize of the previous statement, Kikumoto et.al., (2010) described that particle breakage results in an increase in the number of fine particles and broadens the particle size distribution. The primary effect of changes in particle size distribution is to shift the critical state line and other characteristics of the volumetric response in the compression plane. In this technique were assume that strength is observed as a variable quantitative, dependent on the current value of the state parameter (volumetric distance from the critical state line) which varies with changes in density and stress level. When the critical state line was shifted down as a result of broadening grading or distribution of particle size, the state parameter tends increase and the soil feels looser. Come up with this perception, Kikumoto, et.al (2016) was developed one-dimensional compression slaking tests to observe the effect of wetting and drying cycles under constant axial pressure. These data confirm that slaking in crushed mudstone is accompanied by a variation in the particle size distribution during wetting and drying cycles. The evolution of grading due to slaking, causes an irreversible change in mechanical characteristics, such as the reference packing density. Furthermore, one-dimensional compressive slaking test results were revealed that evolution of grading during compression can increase the compressibility of crushed mudstone. Meanwhile, wetting and drying cycles cause significant compression despite the effective stress remaining constant. Since the evolution of particle size distribution under confined stress did not change the maximum particle size, then it can be expressed by existing indexes of grading as the grading state index I_G or breakage parameter B_r. Therefore, it seems reasonable to describe the effect of slaking on the deformation characteristic by representing the evolution of grading as the grading index I_G and its evolution law. It also has a correlation with the reference densities such as the maximum/minimum void ratio or critical

state void ratio to I_G. In order to more comprehend of mechanical consequences and deformation behavior owing to the compression stress and slaking cycle on mudstone, the author tries to establish the constitutive model by extending the particle crushing phenomenon model (Kikumoto et.al, 2010) and validate it with the test result of one-dimensional compression slaking and triaxial slaking tests.

7.2. A constitutive model of saturated over-consolidated soil

An elastoplastic model that considers the particle-crushing phenomenon (Kikumoto, et. al, 2010) has extended to accommodate particle size changes as a result slaking phenomenon on mudstone in the same framework as the particle size crushing phenomenon was used. As mention before, the model will be validated with one-dimensional compression slaking tests result which has been done previous.

A constitutive model based on critical state condition by considering particle size changes causes particle crushing and slaking are expanded. The expanded model was incorporated with two experimental facts concerning the specific volume (ν) of normally consolidated soil. First, within the plane of the natural log of the mean effective stress p' and the specific volume $\nu\,(=1 + e)$, it is positioned on the normal consolidation line (*NCL*) which specific stress $\eta = 0$ with $\nu = N$ and inclination of $-\lambda$ in the atmosphere ($p' = Pa$).

$$\nu = N - \lambda . ln\left(\frac{p\prime}{p_a}\right) \qquad (1)$$

Second, in the critical state with the shear equal or higher than this and no change in volume or effective stress, it is positioned on the critical state line (*CSL*) which specific stress $\eta = M$ with $\nu = \Gamma$ and inclination of $-\lambda$ in the atmosphere. M is the specific stress in the critical state line.

$$\nu = \Gamma - \lambda . ln\left(\frac{p\prime}{p_a}\right) \qquad (2)$$

The specific volume of normally consolidated soil satisfies equation (1) that shows the normal consolidation line under $\eta = 0$, and equation (2) that represents the critical state line under $\eta = M$; hence, so under mean effective stress (p', η), the following equation is given.

$$\nu = N - \lambda . ln\left(\frac{p\prime}{p_a}\right) - (N - \Gamma)\xi(\eta) \qquad (3)$$

$\xi(\eta)$ is a coefficient of monotonic increase that satisfies $\xi(0) = 0$ and $\xi(M) = 1$. If equation (3) is plotted in the space of the specific volume ν, natural log of mean effective stress p', and

coefficient ξ of the specific stress η it looks resembles the plane surface shown in Figure 82. The plane surface including the normal consolidation line (*NCL*) and critical state line (*CSL*) is called the state boundary plane surface, and the normal consolidation soil is normally placed on the plane surface. $\xi(\eta)$ is the linear coefficient of the specific stress η under Original Cam clay, but for modified Cam clay, the non-linear coefficient of the next equation is used.

$$\xi(\eta) = ln\left\{1 + \left(\frac{\eta}{M}\right)^2\right\}/ln(2) \qquad (4)$$

The response to over-consolidated soil is described in accordance with the concept of the lower load surface that described the over- consolidated state after the load was removed from the normal consolidation state as the lower load state in the study of Hashiguchi and Ueno (1977); they used the reciprocal of the specific over-consolidation (*OCR*) that represented the over-consolidation density as the state variable. Nakai and Hinokio (2004) developed a model that used the difference of the void ratio *e* from the normal consolidation line (*NCL*).

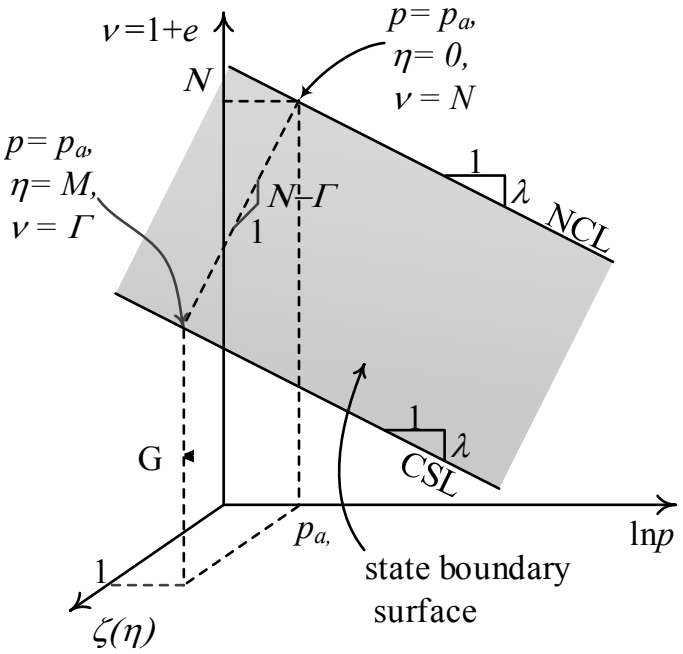

Figure 82. State Boundary Surface including Normal Consolidation Line (NCL) and Critical State Line (CSL)

On the other hand, the difference ψ of the specific volume ν from the critical state line as the state variable of sand and several models based on the reference state on the steady state line were proposed (Been & Jefferies, 1985; Gajo and Muir Wood, 1999; Nakai and Hinokio, 2004). This research focused on the loosest normal consolidation state under optional stress conditions (p', η), which is specified by the reference state surface in Figure 83, to use the

difference ρ between the specific volume on the reference state surface under present stress conditions (p', η) and the present specific volume as the state variable.

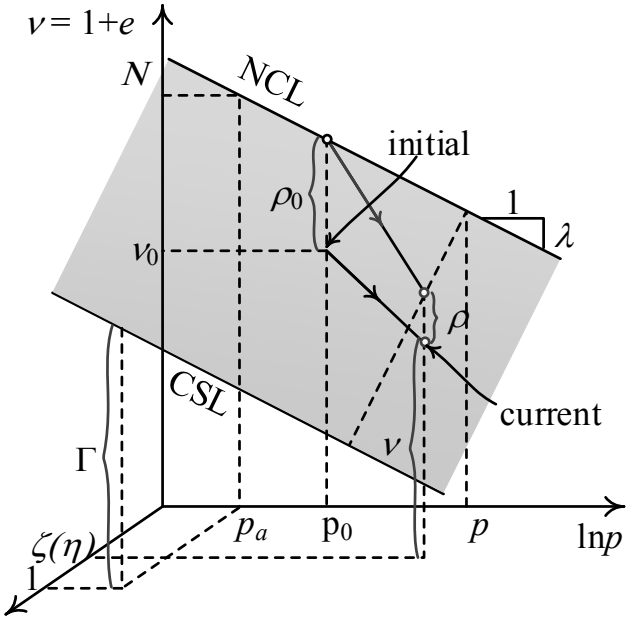

Figure 83. Description of response to Over-Consolidated Soil based on the concept of the sub-loading state boundary

$$\rho = N - \lambda . ln\left(\frac{p\prime}{p_a}\right) - (N - \Gamma)\xi(\eta) - \nu \qquad (5)$$

Figure 84 shows the definition of ρ, and the change in it caused by compression and shear. If the consolidation density soil is loaded, the state variables ρ gradually decline to converge to 0. So, when the soil in the initial state ($p = p_0$, $\eta = 0$, $e = e_0$) in Figure 84 is subjected to consolidation and shear changing it to (p, η, e), equation (4) is used to consider the change of specific volume:

$$\Delta\nu = \nu - \nu_0$$

$$\Delta\nu = \left[N - \lambda ln\left(\frac{p\prime}{p_a}\right) + (N - \Gamma)\xi(\eta) - \rho\right] - \left[N - \lambda ln\left(\frac{p\prime_0}{pa}\right) - \rho_0\right]$$

$$\Delta\nu = -\lambda ln\left(\frac{p\prime}{p_a}\right) - (N - \Gamma)\xi(\eta) - (\rho - \rho_0) \qquad (6)$$

The volumetric strain ε_v is as follows:

$$\varepsilon_\nu = -\frac{\Delta\nu}{\nu_0} = \frac{\lambda}{\nu_0} ln\left(\frac{p\prime}{p\prime_0}\right) + (N - \Gamma)\xi(\eta) + \frac{\rho - \rho_0}{\nu_0} \qquad (7)$$

Here, if the elastic volumetric strain ε_v^e is given based on the swelling index κ,

$$\varepsilon_v^e = \frac{\kappa}{\nu_0} ln\left(\frac{p\prime}{p\prime_0}\right) \tag{8}$$

the plastic volumetric strain ε_v^p is represented as shown below.

$$\varepsilon_v^p = \frac{\lambda - \kappa}{\nu_0} ln\left(\frac{p\prime}{p\prime_0}\right) + (N - \Gamma)\xi(\eta) + \frac{\rho - \rho_0}{\nu_0} \tag{9}$$

Equation (4) is substituted in equation (9) as ξ of the modified Cam clay. If the associated flow rule is hypothesized and the condition that the increase of plastic volumetric strain under the specific boundary stress M which $d\varepsilon_v^p = 0$ is considered, the following equation is obtained.

$$\varepsilon_v^p = \frac{\lambda - \kappa}{\nu_0} ln\left(\frac{p\prime}{p\prime_0}\right) + \frac{\lambda - \kappa}{\nu_0} ln\left\{1 + \left(\frac{\eta}{M}\right)^2\right\} + \frac{\rho - \rho_0}{\nu_0} \tag{10}$$

Equation (10) represents elastic change caused by stress (p, η) during loading and the elastic change caused by the state variable ρ, and hence, the same equation is used as the yield function f.

$$f = \frac{\lambda - \kappa}{\nu_0} ln\left(\frac{p\prime}{p\prime_0}\right) + \frac{\lambda - \kappa}{\nu_0} ln\left\{1 + \left(\frac{\eta}{M}\right)^2\right\} + \frac{\rho - \rho_0}{\nu_0} - \varepsilon_v^p \tag{11}$$

If the elastic constitutive model (and Poisson's ratio ν) of equation (9) and the yield function of equation (10) are used, the stress-strain relations are represented by the following equation.

$$d\varepsilon_{ij} = d\varepsilon_{ij}^e + d\varepsilon_{ij}^p = C_{ijkl} d\sigma_{kl} + \langle \Lambda \rangle \frac{\partial f}{\partial \sigma_{ij}} \tag{12}$$

C_{ijkl} is represented by the following equation using the elastic compliance tensor.

$$C_{ijkl} = \frac{1+\nu}{E} \delta_{ik}\delta_{jl} - \frac{\nu}{E} \delta_{ij}\delta_{kl} \tag{13}$$

E is Young's modulus and is given by the following equation based on the swelling index κ that represents the inclination of the swelling line on the plane of the natural log of the average effective stress p' and the specific volume ν.

$$E = 3(1 - 2\nu)\frac{\nu_0}{\kappa} p' \tag{14}$$

Λ is the plastic coefficient, and is defined as shown in equation (15)

$$\langle \Lambda \rangle = \begin{cases} \Lambda \; when \; \Lambda \geq 0 \\ 0 \; when \; \Lambda < 0 \end{cases} \tag{15}$$

When the value of Λ is established based on applicable condition $df = 0$, the evolution law of ρ needs to be known. The following equation is provided because according to Figure 84, it monotonically declines with loading.

$$d\rho = -a\rho^2 \sqrt{d\varepsilon_{ij}^p d\varepsilon_{ij}^p} \qquad (16)$$

7.3. A constitutive model by considering of grading change

The previous paper regarding the result of one-dimensional compression slaking test explained that the finer particle continuously transforms while the maximum particle size remained unchanged during the compression and slaking cycles. The transformation of particle size distribution could be described based on the scalar grading size index of I_G. Kikumoto et. al. (2010) had attempted to describe the particle size crushing phenomenon considering that the specific volume of the normal consolidation line and the critical state line that was achieved by compression and shear similarly decline. It was pointed out with reference to the results of tests by Lade et al. (1998) that the increase in the fine particle size content caused by the particle crushing phenomenon lowered the maximum void ratio e_{max} and minimum void ratio e_{min} (Kikumoto, et. al, 2012). With reference to this model, the constitutive model of the over-consolidated soil explained in an earlier section is extended in order to be able to consider the impact of change in particle size caused by particle size crushing and slaking. The proposed model represents changes in particle size caused by particle crushing and slaking cycles resulting from sub-loading state boundary surface as shown in Figure 82 and Figure 83 (including normal consolidation line and critical state line). As shown in Figure 84 with the state boundary surface of the limiting particle size that does not change any further as the standard, the degree of movement of the state boundary surface towards the specific gravity axis is represented by ψ. Then, the shift of specific volume change considering over-consolidation density changes and particle size is represented by the following equation (17) instead of equation (3).

$$v = N + \psi - \lambda ln\left(\frac{p\prime}{p_a}\right) - (N - \Gamma)\xi(\eta) - \rho \qquad (17)$$

From equation (17), the yield function f is obtained by the same procedure.

$$f = \frac{\lambda - \kappa}{1 + e_0} ln\left(\frac{p}{p_0}\right) + \frac{\lambda - \kappa}{1 + e_0} ln\left\{1 + \left(\frac{\eta}{M}\right)^2\right\} + \frac{\rho - \rho_0}{1 + e_0} - \frac{\psi - \psi_0}{1 + e_0} - \varepsilon_v^p \qquad (18)$$

The evolution law in equation 18 is used as ρ.

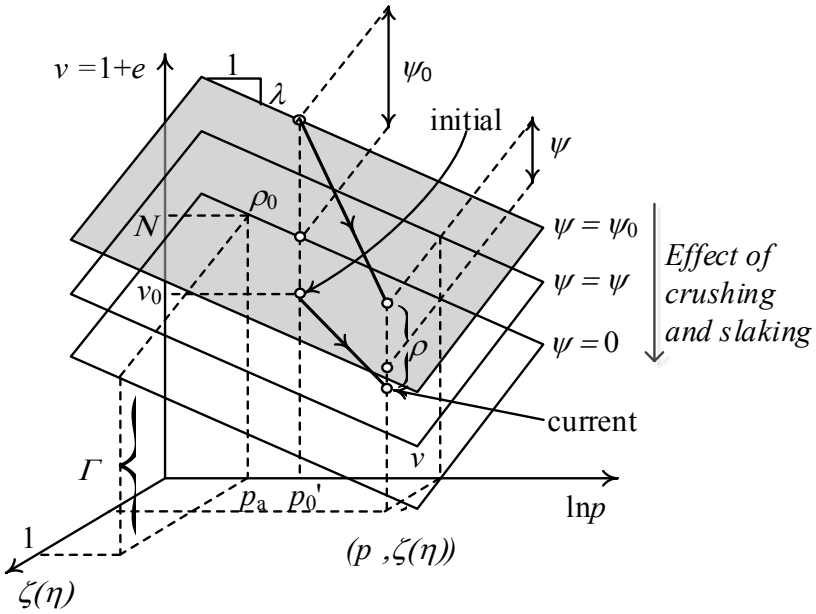

Figure 84. Change in the specific volume of over-consolidated soil considering change in particle size

ψ represents the position of the specific volume axis direction on the state boundary surface and is a negative load variable that changes with the particle size. Considering that $\psi = 0$ under the limiting particle size ($I_G = 1$), it is provided by the following linear coefficient.

$$\psi = \xi(1 - I_G) \qquad (19)$$

ξ represents the distance in the specific volume axis direction of the state boundary surface of the equal particle size (before refining) and limiting particle size (when particle crushing has advanced completely).

The evolution law of I_G that considers the particle-size crushing phenomenon that Kikumoto et. al., (2010), specified is expanded to the slaking phenomenon.

$$I_G = 1 - exp\left\{\left(-\frac{p_{cmax} - p_{c0}}{p_r}\right) + (-\lambda_s . n)\right\} \qquad (20)$$

Equation (20) is a function that increases monotonically from 0 to 1 as the stress history variable p_{cmax} and the number of wetting and drying cycles n increase. p_{c0}, p_r are constituent parameters of particle size crushing properties with the dimensions of stress, and p_{c0} is the stress level at which particles begin to fragment, and p_r represents the difficulty of advancing crushing under increase of stress. p_{cmax} is a stress history variable that represents the maximum stress level received in the past and determines the amount of crushing. p_{cmax} obtains the initial values by substituting the initial values of I_G and n in equation (20), and it increases when the stress variable pc in following equation that considers consolidation and shear exceeds the current p_{cmax}.

$$p_c = p.\left\{1 + \left(\frac{\eta}{M}\right)^2\right\} \quad (21)$$

Related to the relationship between pc to the grading state index I_G, the equation (20) is the analogy of the yield surface inside the stress space. It is nothing more than an explanation of the particle size change caused by the crushing pressure during compressive stress applied. The second terms (the exponential function of equation (20)) are the represents of slaking acceleration and changes of the particle size as the result of increasing the number of slaking cycles. λ_s is the constant parameter that determines of the accelerated slaking. It is predicted that in an actual test, the phenomenon caused by the wetting process and the drying process will differ, but to make it more simple and easy to understand then it is assumed that the number of cycles (n) as a continuous variable. The number of cycles which assume in the previous test is 1 cycle ($dn = 1$) as the process of the specimen passing through the dry state condition (degree of saturation $S_r = 0$) to the saturated state condition (degree of saturation S_r = 100), and then returning to the dry state condition as the next number of cycle. It is necessary to conduct further research regarding the relationship between the degree of saturation and the number of cycles related to applying the model to the real field.

7.4. Results and Discussion

7.4.1. Parametric studies

We have developed and validated the constitutive model by extending the particle crushing phenomenon model (Kikumoto et.al, 2010). The model will be used to investigate the slaking and deformation behavior of mudstone. The reproducibility analysis was calculated by the proposed constitutive model against the Kakegawa and Kobe mudstone, which could show of particle size change causing by particle crushing during compression stress and slaking phenomenon due to wetting and drying cycle. Considering the methods were used in this constitutive model, then some constituent parameters from the previous experiment were decided based on the parametric studies. As shown in Figure 85, the wide range parameter of p_{ci} has been simulated to understand the effect of crushing strength on index of grading (I_G). The index of grading is easy to reach 1 ($I_G = 1$) if the large value of p_{ci} was applied (Figure 85, a and c). It is concluded that the parameter of p_{ci} is a material parameter which determining the particle of mudstone reach the critical state of crushing. Furthermore, similar with the previous parameter, the large value of crushing resistance (p_r) will affect to the speed of crushing of material correspond to the crushing stress (Figure 85, b and d). The parametric studies to be involved in the proposed constitutive model listed in Table 9.

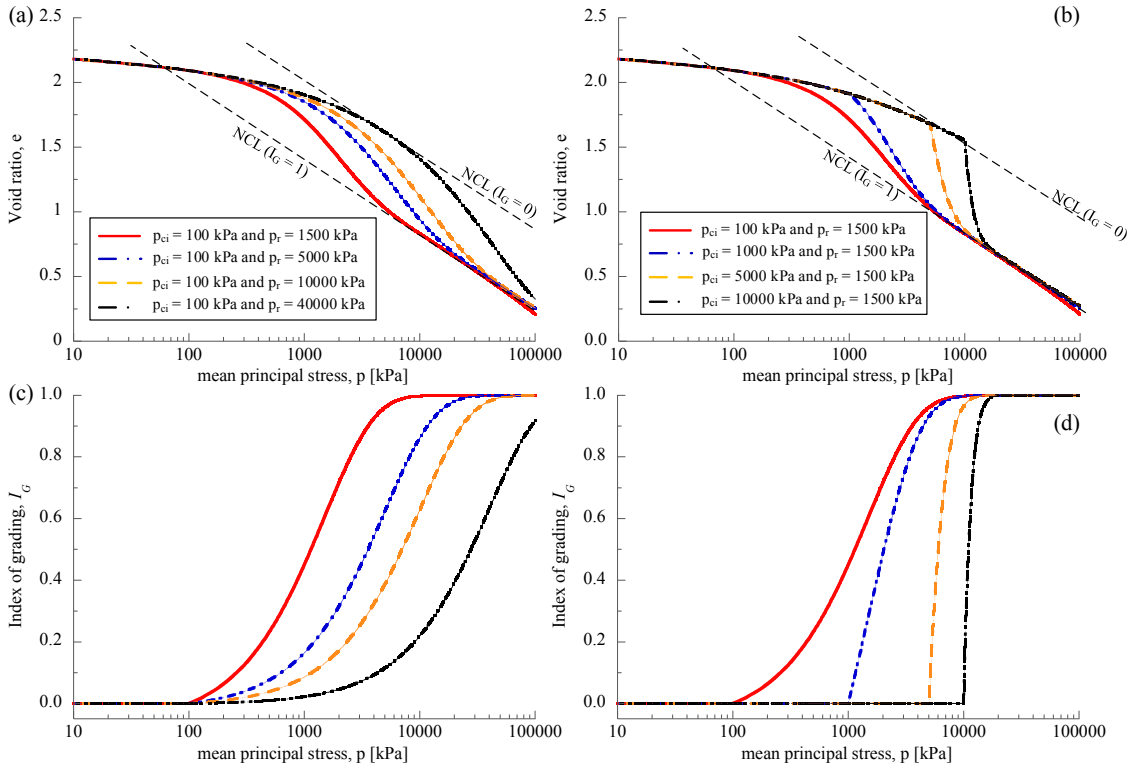

Figure 85. The effect of material parameter on the proposed model related to crushing stress (p_{ci}) and crushing resistance (p_r)

Table 9. Constitutive Parameters of the Kakegawa Mudstone and Kobe Mudstone

Constitutive parameters	Parameters	symbol	Kobe mudstone	Kakegawa mudstone
Compression index	Parameter for Cam Clay	λ	0.301	0.347
Swelling index		κ	0.010	0.010
Critical state stress ratio		M	1.5	1.5
Specific volume v on NCL at p = 98 kPa		N	2.184	2.469
Poisson's ratio		ν	0.2	0.2
Parameter of the evolution ρ	Parameter for sub loading surface	a	12	12
Crushing strength for single sized grading	Parameter for particle crushing and slaking	p_{ci}	10	10
Crushing resistance		p_r	1300	1800
Volumetric distance between state boundary surfaces for IG = 0 and 1		ξ	0.85	0.85
Slaking rate		λ_s	0.95	0.85

The constituent parameter consists of five parameters are revised based on modified cam clay model and one parameter is a parameter of the sub-loading cam clay model. Furthermore, the particle crushing properties were expressed by two parameters and one parameter for the

slaking properties. Table 9, the correlation between the particle size change and stress-strain properties were considered based on the parameter of ξ. The accelerated slaking properties was represented by the parameter of λ_s which has correlated with the number of cycles. Regarding the previous experiments, the accelerated slaking properties of Kobe mudstone are larger than Kakegawa mudstone, it is obviously described that particle of Kobe mudstone rapidly changes in diameter or size after initial wetting and drying cycles.

7.4.2. Validation of the proposed model

The simulations result of constitutive model for both mudstone specimens are shown in Figure 86 and Figure 87, respectively. As information, the white symbols plotted in these figures are experimental values and the black symbols are simulation values. The simulation results based on the constitutive model have obviously expressed that there is a tendency against the experimental result of one-dimensional compression slaking. On the left side figures for both of specimens show that the compression line gradient becomes steep gradually on the semi-logarithm axis and it also explains that the compressibility on this stage smoothly decreases due to the particle crushing. Focusing on the Figure 86(c) and Figure 87(c), it was proven that during the compression stage, the grading state index of I_G is also increased due to the particle crushing. In other words, the compressibility that occurs is not solely due to the compression process, but also due to the increasing number of fine particles. The constitutive model results have confirmed that the analysis result can accurately explain the deformation behavior of mudstone based on the one-dimensional compression slaking experimental results. Related to the triaxal slaking result, considering the particle crushing and slaking phenomenon. Applying the elastoplastic parameters for remolded mudstone specimen and evolution low parameters in calculations using a sub-loading Cam-clay model of an elasto-plastic constitutive model allowed us to reproduce the mechanical behavior of crushed mudstone aggregate. The evolution of particle sized distribution due to particle crushing and slaking cycle through a single grading index of I_G was clearly shown the mechanical behavior of mudstone (Figure 88 and Figure 89). The index of grading is easily to reach equal to 1 with small axial strain when the isotropic slaking applied compare to other case such as different deviatoric stresses. The effect of high deviatoric stress has shown the small failure deformation. After the shear stage, the particle tends to make the specimen becomes denser due to the fine particle increase and fill the gap. The volumetric strain during the slaking cycle under isotropic condition is relatively close to the expectation. After the stage of slaking cycle, the progressive failure deformation immediately occur and continue to expand.

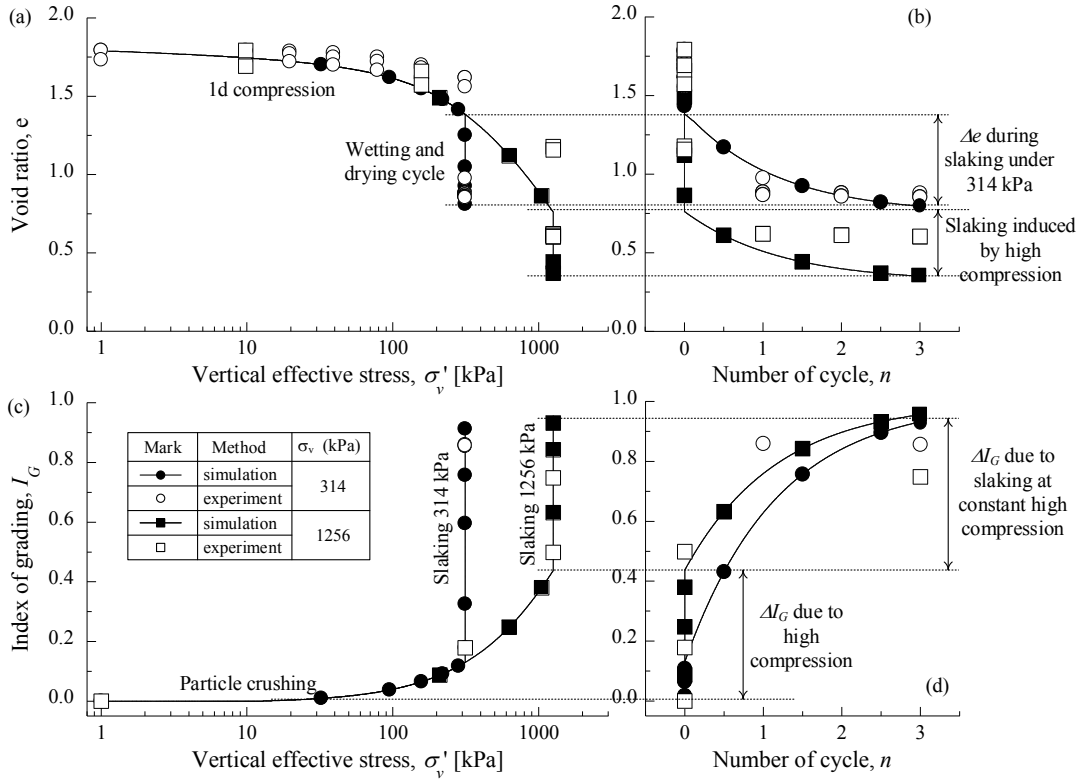

Figure 86. Validation of the proposed model based on the one-dimensional compression slaking test result of Kakegawa mudstone

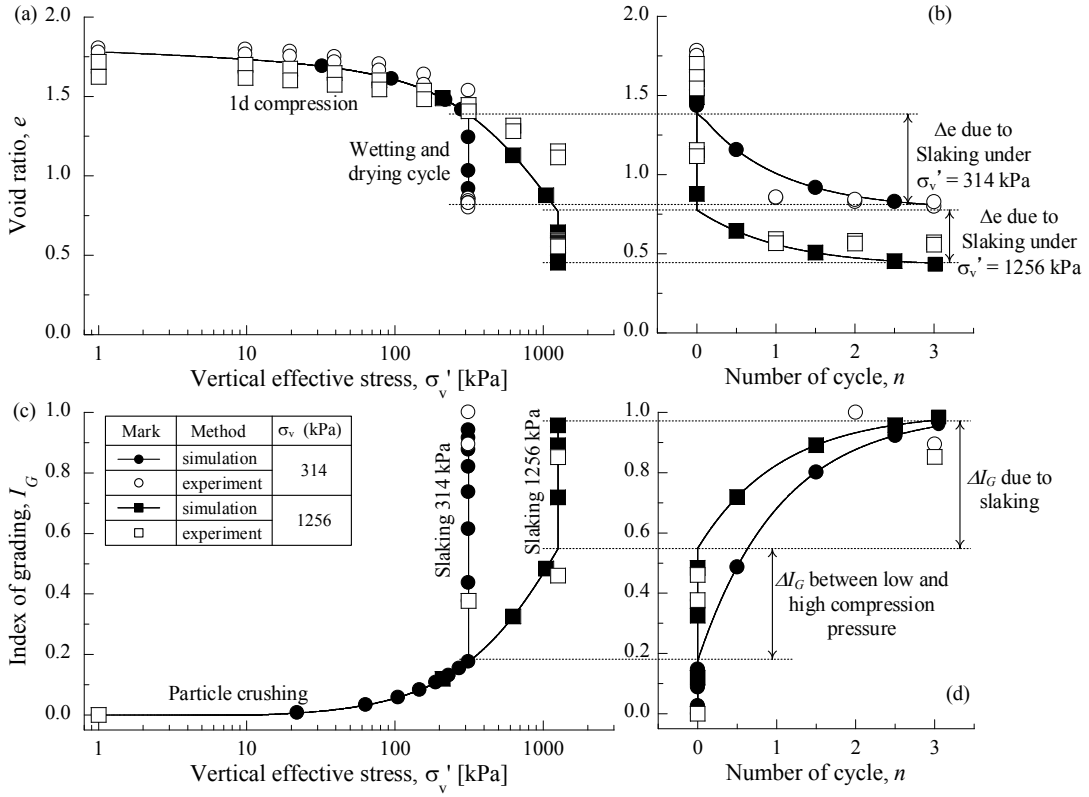

Figure 87. Validation of the proposed model based on the one-dimensional compression slaking test result of Kobe mudstone

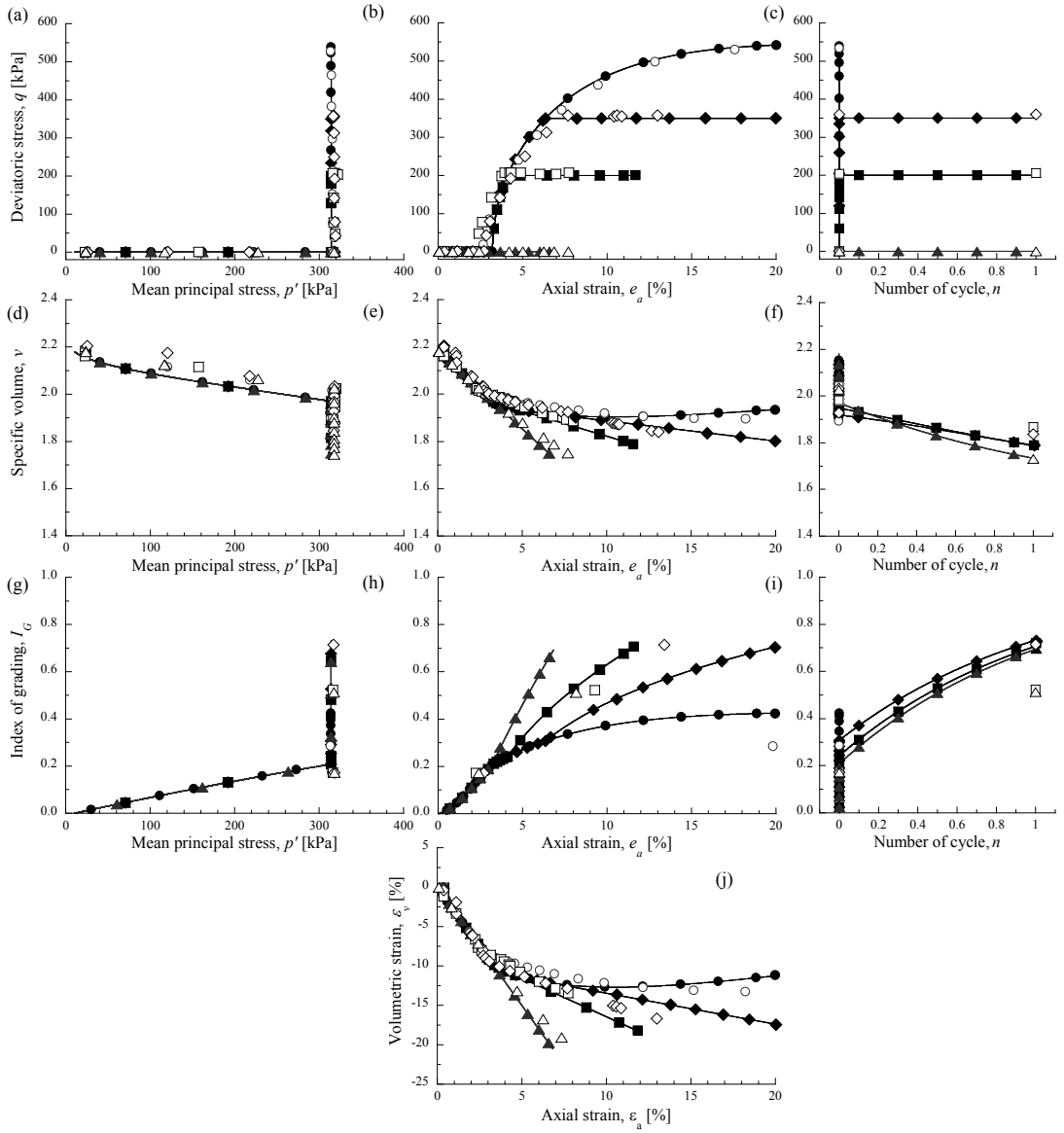

Isotropic and mean principal stress constant test (p = 320 kPa)	Monotonic shear	Number of cycle, n = 1		
		isotropic	q = 200 kPa	q = 360 kPa
Experimental on Kobe mudstone	○	△	□	◇
Simulation	●	▲	■	◆

Figure 88. Validation the model based on triaxial slaking test result of Kobe mudstone

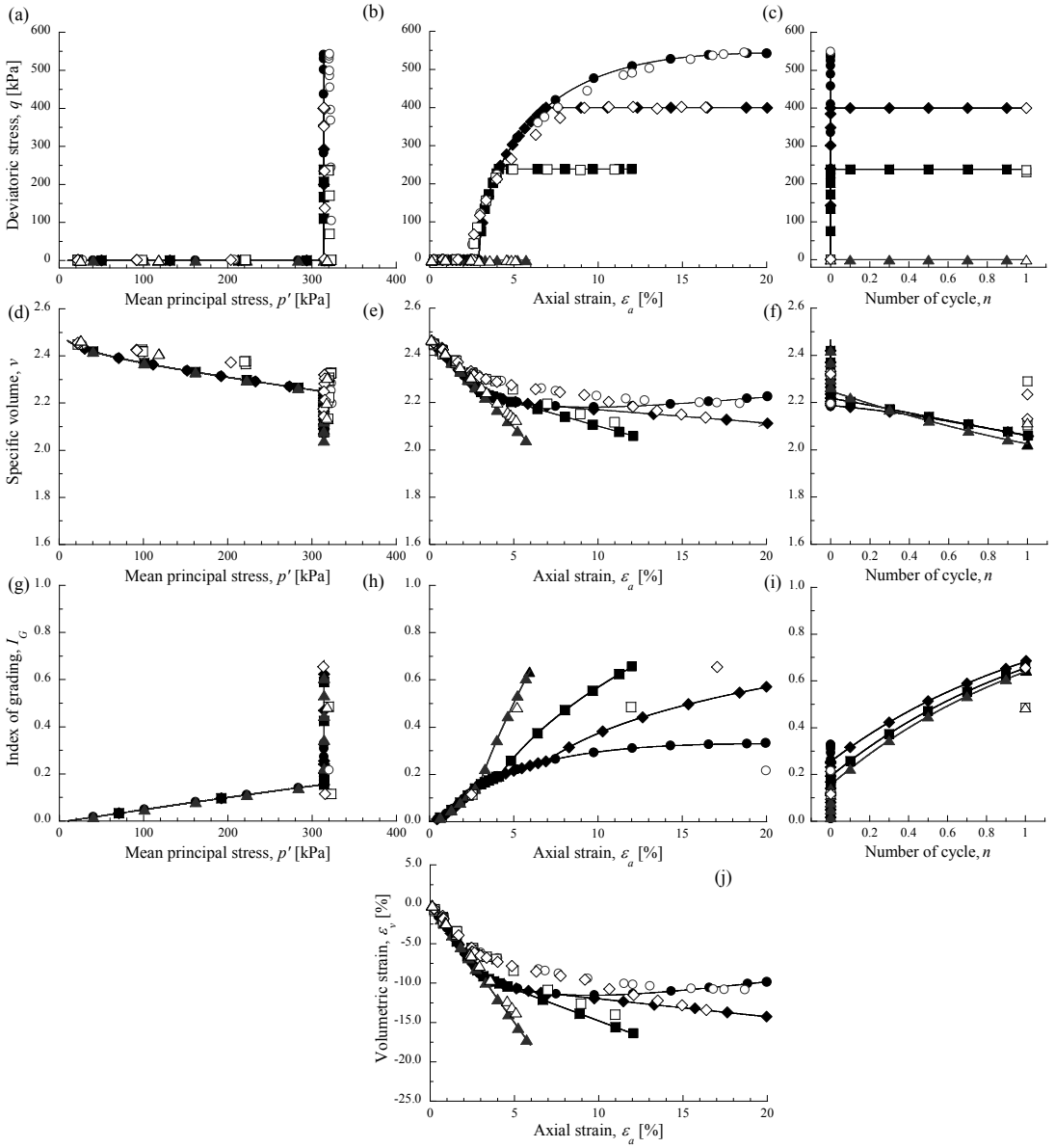

Isotropic and mean principal stress constant test (p = 320 kPa)	Monotonic shear	Number of cycle, n = 1		
		isotropic	q = 240 kPa	q = 400 kPa
Experiment	○	△	□	◇
Simulation	●	▲	■	◆

Figure 89. Validation the model based on triaxial slaking test result of Kakegawa mudstone

Further, the analysis result of the constitutive model also clearly noticed the effect of the number of slaking cycles to the compression behavior. According to the constitutive proposed model, the reduction of compressibility properties by increasing the number of slaking cycles can be expressed and the compression behavior can be reproduced. The slaking phenomenon during the slaking cycles can be described by extending the evolution law of grading state index (I_G) as in the equation (20) which is the same principle framework of particle crushing phenomenon. The influence of the stress-strain characteristics was obtained through the

grading state index of I_G as the unified equation to be considered.

Figure 90 was made on purpose to explain the correlation among the parameters on the equation (20). These figures exhibit that the accelerated slaking (λ_s) and number of cycles (n) were significant influence against changes in grading state index (I_G). As mention in the previous subchapter, the accelerated slaking parameter (λ_s) of Kobe mudstone is higher than Kakegawa mudstone. It shows that Kobe mudstone has tendency to change in the particles size rapidly, even under low compression stress (A line is 314 kPa) condition. Compared to Kakegawa mudstone, grading state index approximately the critical grading state after a high compression stress (B line is 1256 kPa) is applied on it. The number of slaking cycles (n) gives more influenced to the specimen with high accelerated slaking parameter such as Kobe mudstone. The shape of surface contour diagram on Figure 90(b) is more convex than the shape of surface contour on Figure 90(a). It also reveals that the Kobe mudstone is easier to reach the grading state index equal to 1 ($I_G = 1$) than Kakegawa mudstone. It confirms the comprehension of the deformation behavior of mudstone on the previous paper.

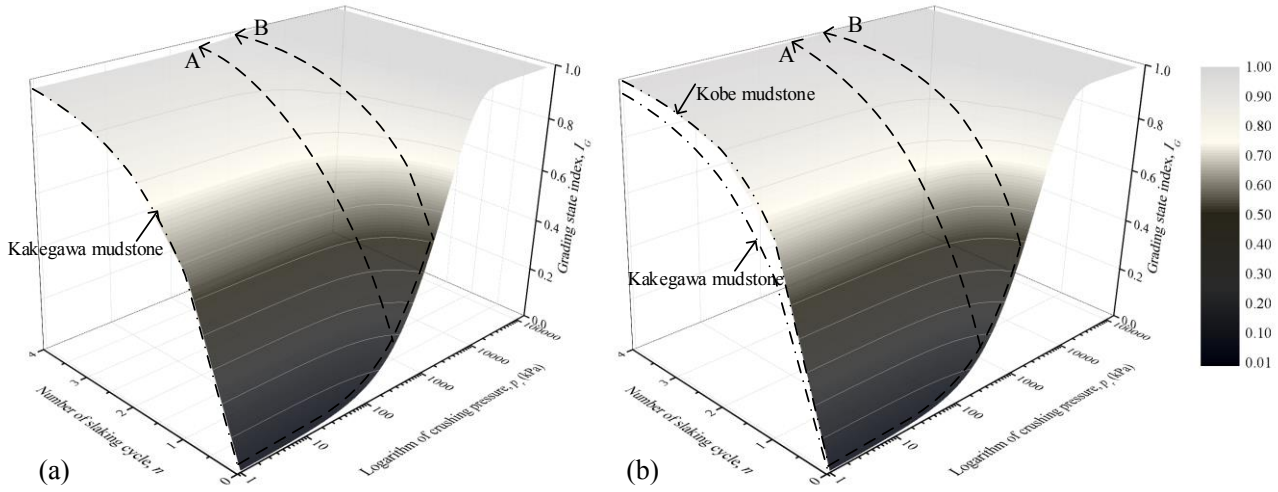

Figure 90. The diagram contour of relationship between accelerated slaking parameter (λ_s) in accordance with grading state index (I_G) and number of slaking cycle (n) for Kakegawa mudstone (a) and Kobe mudstone (b)

7.4.3. The applicability of proposed model

Another numerical parametric study was conducted to investigate the evolution law of the grading state index (I_G) considering of particle crushing (p_c) and accelerated slaking (λ_s) as explained in equation (20). According to simulation result (Figure 91(a)) during the compression pressure or crushing particle, there were no significant volumetric compression changes related to varying the accelerated slaking properties (λ_s). Here, the accelerated slaking

properties of the Kakegawa mudstone were used between four values: 0.95, 1.45, 1.95 and 2.45. The simulation results (Figure 91(a)) reveal that despite there is no change seen in response to the one-dimensional compression pressure (Figure 91(a)), but most of the compressible changes precisely occur due to the number of slaking cycles (Figure 91(b)). Much larger the accelerated slaking properties (λ_s) can cause the amount of finer particle increase (Figure 91(b)). It will affect to increase the grading state index I_G and considerable volume compression also occurred (Figure 91(d)). Variation of accelerated slaking properties (λ_s) in this way can help incorporate the differences in slaking properties of different kinds of mudstone.

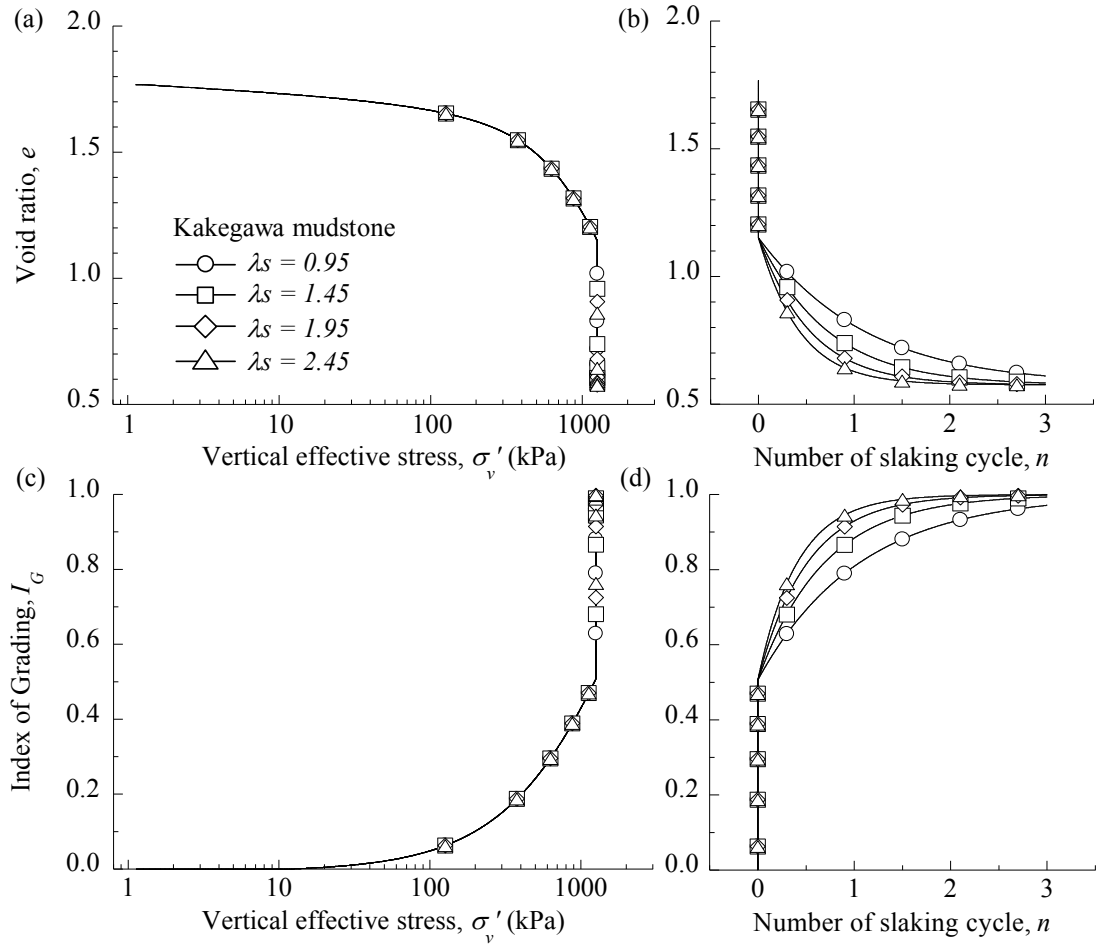

Figure 91. Parametric study of the parameter (λ_s) that represents of acceleration slaking under σ_v' = 1256 kPa

Figure 92 is expressed the distribution of compressibility parameter by applying the different vertical effective stress and gradually increase the accelerated slaking and changes in crushing pressure simultaneously. The number of cycles was equal for each vertical effective stress. As

can be seen from the Figure 92, every compressive stress shows that the volumetric compression proportionally increases, whereas the distribution of compressibility is shifted from bottom-right to the upper-left. If the distribution of compressibility was determined equal to -0.5 for every compressive stress, then clearly seen that curves shift to the left side (Figure 92(d)). It also gives some explanation that by preliminarily breaking up the particle by compressive stress, the amount of volume compression due to subsequent of the number of slaking cycles is reduced. As expressed on Figure 92(d), the contour lines in the figure move to the left as the compressive stress increases, and as a result, even if the material parameters are same, the compression decreases as the compressive stress increased. From these results, the model which has considers the particle crushing and slaking proposed in this research uniformly can express the distribution of compressibility of the vulnerable rock prescribed by NEXCO Institute of Technology as the embankment material. It is possible to express analytically the compressibility of the mudstone used as a mudstone.

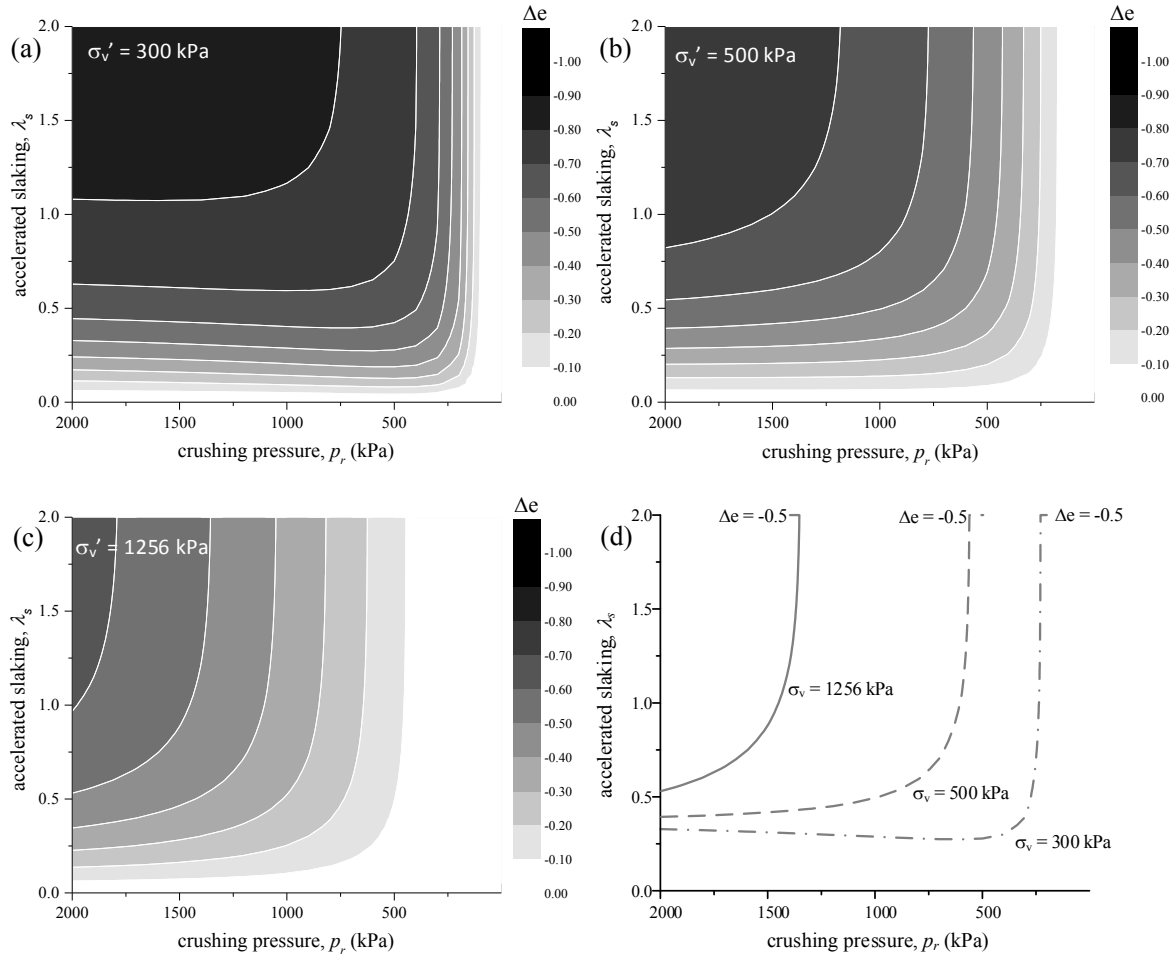

Figure 92. The Distribution of compressibility parameter (Δe) based on varying the parameter λ_s, p_r and σ_v'.

Next, let us consider the differences in the slaking properties under the test conditions. In contrast to the compressive slaking tests described above, which were only monotonic one-dimensional compression and cyclic wetting and drying. Figure 93 presents the simulation result of two different cases analysis. On the figures, the first case is the simulation of one-dimensional compressive slaking test under constant stress, representing by white circle marks and the second is the simulation by applying the loading and unloading stress, represented by white square marks. In the first case, after the compressive stress gradually increased to 314 kPa and subsequently following with the three cycles of slaking causes the grading state index of I_G (ΔI_{G1}) during slaking cycles changes around 0.745. Compare to the second case, after the high pressure up to 1,256 kPa was applied first and followed by unloading the pressure to 314 kPa, then completed by applying the wetting and drying cycles, the changes of grading state index (ΔI_{G2}) during slaking cycles around 0.45 which is almost 50% of ΔI_{G1}. It could happen due to the particles crushing has occurred during the high pressure applied and the amount of fine grain material increase represented by changes of grading state index of I_G.

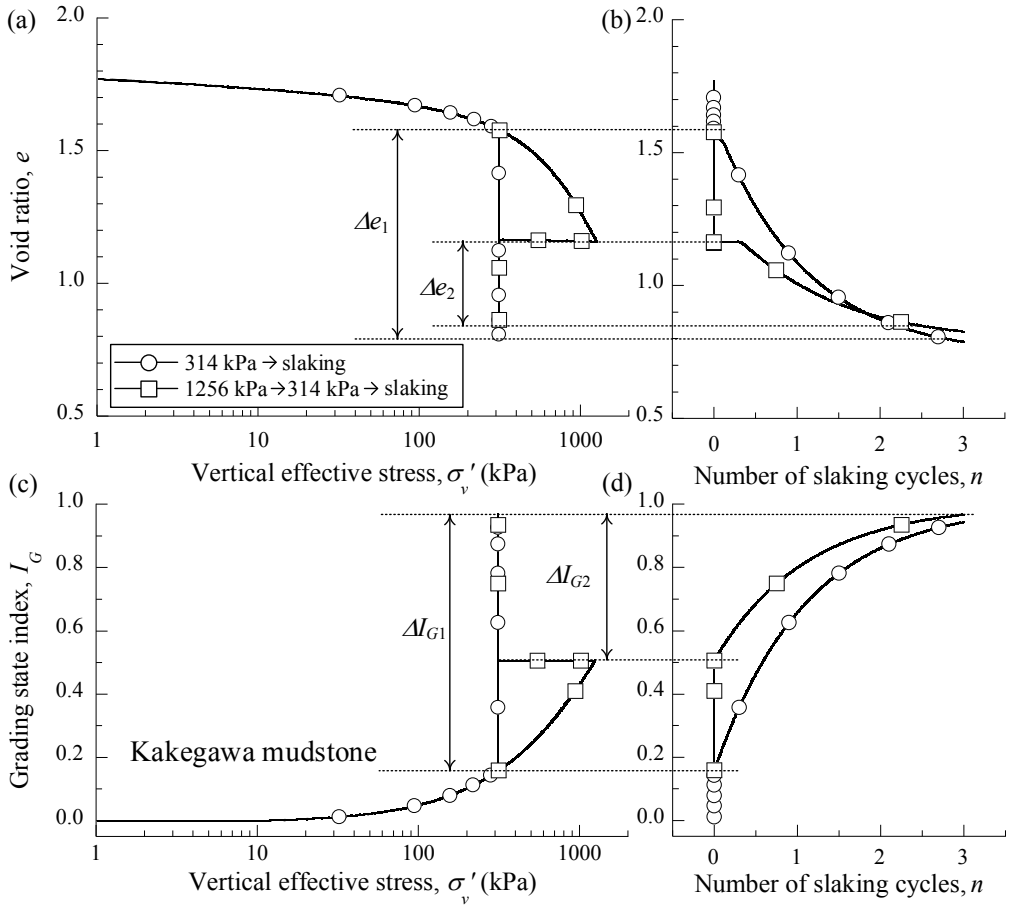

Figure 93. The volumetric compression behavior during the loading and unloading stress and followed by the three slaking cycles

The mudstone specimen becomes denser after the high compressive stress and the fine grain material fill the void, as a result, the Figure 93(a) exhibited that the volumetric compression during cyclic wetting and drying is decreased about 50% or half of simulation result of the first case ($\Delta e_2 \approx 0.5\Delta e_1$). Since the high compressive stress was given to 1,256 kPa, in addition to the fact that the compression process increased I_G to about 0.5 and reduced the change of particle size under cyclic wetting and drying (quantity of increase of I_G). Due to the process of removing a load that expanded the volumetric along the swelling line separated from the normal consolidation line to become over-consolidated. It has been pointed out that while doing the earth construction with materials with slaking properties are used, paying attention of roller compaction throughout the embanking work encourages the crushing of particles, controlling the occurrence of slaking under cyclic wetting and drying so that volumetric compression does not occur easily (Predicted and Actual Ground Behavior Editorial Committee, 1996). However, a simulation of such empirical findings based on the proposed model can be said to accurately reproduce this analytically.

7.5. Summary

In order to observe the differences in the degree of slaking mudstone tends to change during the process of slaking cycle, one-dimensional compression slaking and triaxial slaking tests were performed. Furthermore, proposed a constitutive model that uniformly considers the change in particle size accompanying particle crushing and slaking was studied. Based on the one-dimensional compression slaking and triaxial slaking tests were done to observe the effect of cyclic wetting and drying. The previous test revealed that the particle-crushing phenomenon in the compression process contributes to increase compressibility, and that slaking caused by cyclic wetting and drying causes large compression. Next, proposed a constitutive model that uniformly describes the slaking phenomenon and the particle crushing process under a critical state model. This constitutive model was considered particle size change accompanying particle crushing, by extending the evolution law of the particle size index I_G to consider the number of wetting and drying cycles. We verified the applicability of this model through simulations of the compressive slaking test. The results show that the proposed model precisely reproduces the changes in particle size and volumetric compression during the one-dimensional compression process and cyclic wetting and drying. The numerical parametric study of constitutive parameters and test conditions show that by appropriately changing the parameter of the accelerated slaking (λ_s), and other parameters of the evolution law of the particle size index I_G. It is possible to reproduce the differences between the properties of

slaking with different kinds of mudstone. Additionally, it was shown that performing compression and unloading at a high stress level can suppress the change of particle size during cyclic wetting and drying, permitting the analytical reproduction of matters, conventionally said to be based on experience when constructing the embankments.

Finally, the proposed constitutive model shows the applicability and usefulness to get better understanding of slaking behavior of mudstone. The number of wetting and drying cycles are not necessarily continuous variable. The differences in the weathering mechanisms of slaking during the wetting and drying process could not be considered. Furthermore, in the real earth construction, absolute dried and saturation are not always cyclical as they were during the compression slaking tests that was performed. Hence, in the future, it will probably be necessary to study the relationship of the degree of change of saturation under the unsaturated state dS_r and the number of wetting and drying cycles n. In the future, we will study the impact of cyclic wetting and drying on deformation failure properties of mudstone specimens under anisotropic stress, while paying close attention to the above matters.

Chapter 8

Conclusion and Recommendation

Mudstone as one of sedimentary rocks is the most encountered materials during the earth construction projects that are undertaken in certain areas. Nowadays, the existence of mudstone on earth construction is one of the current issues to understand, since the mudstone is very sensitive when contact with water, mainly the wetting and drying cycle. In Japan, the mudstone material has been used as one of the materials for highway embankment since the mudstone deposit is available in large quantities. To achieve the objectives of this study, some of laboratory experiments on mudstone material were performed. It is necessary to understand the mineral content of the mudstone to get better understanding the weathering mechanism. In addition, the slaking durability was performed to obtain the breakage parameter (B_r) of mudstone specimen and try to explore the tendency between the physical disintegration of particle induced by chemical or physical properties of mudstone. Further studies which have purposed to conceive the deformation and failure behavior of mudstone due to wetting and drying cycle were conducted by performing a series of a one-dimensional compressive slaking test and triaxial slaking test.

8.1. Conclusion

8.1.1. The chemical and physical properties effect to the slaking on mudstone

The mudstone specimen in this study was made up of Neogene to Pliocene period. The major constituent of chemical element consists of silicon (Si), iron (Fe) and aluminum (Al). It might indicate that the major constituent material of mudstone was based on crystalline element. Most of these released elements likely remain in the mudstone and crystallize to form quartz, chlorite, albite, calcite, dolomite, siderite, and ankerite, which are all minerals that occur in mudstones. Many of these minerals may in fact be products of diagenesis. It was indicated that

the major crystalline phase sand is quartz, the phase of clay is illite, while silt is represented by silica, aluminum, and calcium.

The smectite clay minerals, montmorillonite has the most dramatic shrink-swell capacity, and known as expansive. Expansive soils contain minerals such as smectite clays that are capable of absorbing water. When they absorb water, they increase in volume. The more water they absorb, the more their volume increases. Expansive soils will also shrink when they dry out. In the field, expansive clay soils can be easily recognized in the dry season by the deep cracks, in roughly polygonal patterns, in the ground surface. The Pyrite content is quite important in these sequential of weathering of mudstone. Pyrite is oxidized by oxygen coming from the ground surface and sulfuric acid is generated at the base of the oxidized zone. Oxidation of pyrite is a chemical reaction that results in crystal growth of various sulfates, expansion and volume change at or near the site of pyrite and release of mild sulfuric acid and iron. The existence of intragranular pores are indicated based on microscope photograph of mudstone specimen. It might be useful since one of the weathering mechanism was indicated by existence of pores. However, it is an arbitrary summarize regarding the existence of intragranular pore affect the weathering process. Further investigation needed by checking the rock density of mudstone specimen and compare with the size of intragranular pores.

8.1.2. The slaking resistance induced by wetting and drying cycle

The slake resistance by performing of the accelerated slaking test has revealed that Kobe, Jouetsu and Nou mudstone very easy to disintegrate or break down even since the first wetting and drying cycle of accelerated slaking test applied. It was strengthened by an increase of the breakage parameter (B_r) which is representative that particle disintegration occurs during the slaking cycle applied. Based on the mineral content, especially smectite mineral content as an expandable mineral plays an important role in the proses of alteration particle or known as the physical weathering. The particle size distribution of Kobe mudstone was changed rapidly. It can be happened since Kobe mudstone has a large amount of smectite mineral content. In addition, the content of nontronite which has dominant ion Na^+ was made the mudstone specimen becomes more expandable. Ion Na^+ is excellent in swelling property, thickening property and suspension stability. The physical weathering occurs becomes very fast. The linier correlation between the smectite mineral content and breakage parameter has been proven that increase the smectite content tends to increase the potential physical disintegration. As known, instead of physical weathering, the chemical weathering process also occurs even though it takes a times during the process. It can be concluded that the slaking phenomenon on mudstone is induced by the physical weathering mechanism that occurs during the wetting

and drying cycle applied, especially due to the wetting cycle which is then gradually followed by the chemical weathering mechanism.

Furthermore, in accordance with the previous study regarding the process of air-breakage in which trapped pore-air can lead to rock disintegration (Schmitt, et.al., 1994), then the investigating of intragranular pore is needed. The intragranular pores size on mudstone material in this study shown the tendency against the physical disintegration of particle. The size of the pores will be expected to affect the process of particle disintegration. In this study, the pores size analysis was seemed to be arbitrary but could provide sufficient explanation regarding the size of intragranular pores and the physical disintegration parameter of B_r. Regarding the shape of the particle of mudstone after the accelerated slaking test applied, it can be categorized into four shapes of the mudstone aggregate: fine grain, sub-angular and tiny flakes, sub-rounded to thick flake and angular to flakes.

8.1.3. One dimensional compression slaking test

A series of one dimensional compression slaking test were performed under the different vertical effective stress. The initial compression was applied gradually from 9.8 kPa to 314 kPa or 1256 kPa. The number slaking cycle was applied from 0, 1, 2 and 3 cycles. Based on the previous result of the preliminary experiment, Kobe mudstone, Kakegawa mudstone and Hattian Bala mudstone was selected as the object of the test. The result of this study could be concluded as follows, the evolution of grading due to slaking therefore causes irreversible change in the mechanical properties of crushed mudstone attributable to variation in the packing density. Moreover, the evolution of grading during compression can increase the compressibility of crushed mudstone, with wetting and drying cycles causing significant compression despite the effective stress remaining constant. Since the evolution of particle size distribution under confined stress occurs without change in the maximum particle size, it can be described by existing indices of grading such as the grading state index I_G or breakage parameter B_r. It therefore seems reasonable to describe the effect of slaking on the deformation characteristic by representing the evolution of grading as the grading index I_G and its evolution law, and by linking reference densities such as the maximum/minimum void ratio or critical state void ratio to I_G.

8.1.4. Triaxial slaking test

A series of triaxial slaking tests on the crushed mudstone specimen of Kobe, Kakegawa, and Hattian Bala mudstones were carried out to observe the failure deformation behavior of mudstone due to slaking cycle. In general, the particle size distribution changed due to slaking

cycle is more significant than shear. Kobe mudstone shoes the wider grading size changes after slaking cycle applied. The deformation during isotropic slaking compression is relatively closed to the isotropic behavior. The axial strain (ε_a) of Hattian Bala mudstone before slaking was smaller than Kobe and Kakegawa mudstone and it might occur since the particle of Hattian Bala mudstone is not easier to crush during compression and shear. The assembled crushed mudstone which is packed in medium density still exhibited the progressive deformation when the slaking cycle started, especially for the mudstone material that suspected has intra-granular pores such as Kobe mudstone. The axial strain has increased due to slaking and increase of deviatoric stress. The softening behavior clearly seen during the wetting and drying cycle applied and an anisotropic behavior suddenly occurs. Further investigation to observe the time and speed of deformation during slaking cycle applied and the effect of the number of wetting and drying cycle is needed for further study. And the different compaction degrees by changing the initial conditions need to observe the structure decays.

8.1.5. A propose constitutive model by considering the particle size distribution changes due to slaking cycles

In order to observe the differences in the degree of slaking mudstone tends to change during the process of slaking cycle, one-dimensional compression slaking tests were performed. Furthermore, proposed a constitutive model that uniformly considers the change in particle size accompanying particle crushing and slaking was studied. Based on the one-dimensional compression slaking and triaxial slaking tests were done to observe the effect of cyclic wetting and drying under one-dimensional compressive conditions. The previous test revealed that the particle-crushing phenomenon in the compression process contributes to increase compressibility, and that slaking caused by cyclic wetting and drying causes large compression. Further, proposed a constitutive model that uniformly describes the slaking phenomenon and the particle crushing process under a critical state model. This constitutive model was considered particle size change accompanying particle crushing, by extending the evolution law of the particle size index I_G to consider the number of wetting and drying cycles. We verified the applicability of this model through simulations of the compressive slaking test. The results show that the proposed model precisely reproduces the changes in particle size and volumetric compression during the one-dimensional compression and triaxial process and cyclic wetting and drying. The numerical parametric study of constitutive parameters and test conditions show that by appropriately changing the parameter of the accelerated slaking (λ_s), and other parameters of the evolution law of the particle size index I_G. It is possible to reproduce the differences between the properties of slaking with different kinds of mudstone.

Additionally, it was shown that performing compression and unloading at a high stress level can suppress the change of particle size during cyclic wetting and drying, permitting the analytical reproduction of matters, conventionally said to be based on experience when constructing the embankments.

The proposed constitutive model shows the applicability and usefulness of the model. The number of slaking cycles is not necessarily a continuous variable. The differences in the mechanisms of slaking during the wetting and drying process could not be considered. Furthermore, in the real earth construction, absolute dried and saturation are not always cyclical as they were during the compression slaking tests that was performed.

8.2. Recommendation

The author has some recommendation to improve the quality of the further study since several issues and limitation has been encountered. The physical disintegration seems to be important to analysis especially during the compression and slaking cycle under one-dimensional compression. It is also advised that further study should be performed on large mudstone specimen, mainly on triaxial slaking test and set the system to control temperature of drying path. The double cell in triaxial system need to be modified since the water inside the double cell is easily gone when perform the slaking cycle on the weakest mudstone such as Kobe mudstone. It will affect to result of volumetric strain due to slaking cycle applied.

Related to the constitutive model, the impact of cyclic wetting and drying on deformation failure properties of mudstone specimens under anisotropic stress is necessary to understand, while paying close attention to the above matters. in the future, it will probably be necessary to study the relationship of the degree of change of saturation under the unsaturated state dS_r and the number of wetting and drying cycles n.

REFERENCES

ASTM D6913-04. (2004) Standard Test Methods for Particle-Size Distribution (Gradation) of Soils Using Sieve Analysis, Annual Book of ASTM Standards, ASTM International, West Conshohocken, PA.

ASTM D4644-08. (2008) Standard Test Method for Slake Durability of Shales and Similar Weak Rocks, Annual Book of ASTM Standards, ASTM International, West Conshohocken, PA

ASTM D7181-11. (2011). Method for Consolidated Drained Triaxial Compression Test for Soils, Annual Book of ASTM Standards, ASTM International, West Conshohocken, PA.

ASTM D2435/D2435M-11. (2011). Standard Test Methods for One-Dimensional Consolidation Properties of Soils Using Incremental Loading, Annual Book of ASTM Standards, ASTM International, West Conshohocken, PA.

Andrews, D. E., Withiam, J. L., Perry, E. F. & Crouse, H. L. (1980) Environmental effects of slaking of surface mine spoils: eastern and central United States, Final Report, Contract No. J02855024. Denver, CO, USA: U.S. Bureau of Mines.

Been, K. & Jefferies, M. J. (1985). A state parameter for sands. Géotechnique 35 No. 1, 99–112.

Bhattarai, P., Marui, H., Tiwari, B., Watanabe, N., Tuladhar, G. R. & Aoyama, K. (2006) Influence of weathering on physical and mechanical properties of mudstone. In Disaster mitigation of debris flows, slope failures and landslides (ed. H. Marui), vol. 2, pp. 467–479. Tokyo, Japan: Universal Academy Press.

Bishop, A.W. and Donald, I. B. (1961) The Experimental Study of Partly Saturated Soils in the Triaxial Apparatus, Proceedings, Fifth International Conference on Soil Mechanics and Foundation Engineering, Paris, Vol.1: pp. 13–21

Blatt, H., & Tracy, R.J. (1996) Petrology, New York, W. H. Freeman, 2nd ed, pp.529

Botts, M. E. (1998). Effects of slaking on the strength of clayshales: A critical state approach. In Geotechnics of hard soils–soft rocks (ed. A. Evangelista), vol. 1, pp. 447–458. Rotterdam, the Netherlands: A. A. Balkema.

Broichhausen, H., Littke, R., and Hantschel, T. (2005) Mudstone compaction and its influence on overpressure generation, elucidated by a 3D case study in the North Sea, International Journal of Earth Sciences, 94(5-6), pp. 956-978.

Brooker, E. W. and Peck, R. B. (1993). Rational design treatment of slides in overconsolidated clays and clay shales, Can. Geo. Journal, 30, pp. 526-544

Chigira, M. & Oyama, T. (1999) Mechanism and effect of chemical weathering of sedimentary rocks, Eng. Geo., 55, No.1–2, pp. 3–14.

Clowes, A & Comfort, P. (1987) Process and landform: an outline of contemporary geomorphology, Conceptual frameworks in geography, Oliver and Boyd, Michigan University

Czerewko, M. A. and Cripps, J. C. (2001). Assessing the durability of mudrocks using the modified jar slake index test, Quarterly Journal of Eng. Geo. and Hydro, 34, pp.153-163

Dewhurst, D.N., Aplin, A.C., Sarda, J.P., & Yang, Y.L. (1998) Compaction-driven evolution of porosity and permeability in natural mudstones: An experimental study", Journal of Geophysical Research, 103(B1), pp. 651-661.

Dexter, A.R. (2004) Soil physical quality. Part I. Theory, effects of soil texture, density, and organic matter, and effects on root growth, Geoderma 120, pp. 201-214

Dowey, P.J & Taylor, K. G. (2016). Mineral Diagenesis in Silt- and Clay-Rich Mudstones: Macroscopic to Microscopic Characteristics. AAPG Hedberg Research Conference, Mudstone Diagenesis, Santa Fe, New Mexico, October 16-19, 2016

Dunham, R.J., (1962) Classification of carbonate rocks according to depositional texture, American Association of Petroleum Geologists Memoir. no. 1, pp. 108-121.

Chang, C.S. & Hicher, P.Y. (2005). An elasto-palstic model for granular materials with microstructural consideration, Int. Journal of Solids and Structures 42, pp. 4258-4277

Fleming, R.W., Spencer, G.S., and Banks, D.C. (1970). Empirical Study of Behavior of Clay Shale Slopes, Vol. 1, NCG Technical Report No. 15, U.S. Army Engineer Nuclear Cratering Group, Livermore, CA, December.

Franklin, J. A. & Chandra, R. (1972). The slake durability test. Int. J. Rock Mech. Min. Sci. & Geomech. Abstr. 9, No. 3, pp. 325–328.

Fukuda, K., and Kikumoto, M. (2013) Experimental study of the ground material slaking phenomenon and changes in physical and mechanical properties, the 68th Annual Conference of the Japan Society of Civil Engineers.

Gajo, A. & Muir Wood, D. (1999). Severn-Trent sand: a kinematic hardening constitutive model for sands: the q–p formulation. Géotechnique 49 No. 5, pp. 595–614.

Gautam, T. & Shakoor, A. (2013). Slaking behavior of clay-bearing rocks during a one-year exposure to natural climatic conditions. Engng Geol. 166, 17

Hallsworth, C.R & Knox, R.W O'B. (1999) Rock Classification Scheme". Volume3. Classification of sediments and sedimentary rocks. British Geological Survey Research Report, RR. pp. 99-103

Hardin, B.O. (1985). Crushing of soil particles. J. Geotech Engng. 111 No 10, pp. 1177–1192.

Hashiguchi, K. & Ueno, M. (1977). Elastoplastic constitutive laws of granular materials. Proceedings of 9th ICFSME. Spec. Sess. 9, JSSMFE, Tokyo, Japan pp. 73-82.

Hayano, K., Sato, T., & Tatsuoka, F. (1997). Defromation characteristics of a sedimentary soft mudstone from triaxial compression tests using rectangular prism specimens.

Géotechnique. 47, No 3, pp. 439-449

Hayashi, K., Fujisawa, H., Holland, H. D. & Ohmoto, H. (1997) Geochemistry of 1.9 Ga sedimentary rocks from Northeastern Labrador, Canada, Geochimica et Cosmochimica Acta 61, No. 19, pp. 4115–4137.

Hopkins, T. C. & Beckham, T. L. (1998) Embankment construction using shale, Research Report KTC-98-2. Lexington, KY, USA: University of Kentucky Transportation Center, College of Engineering.

Igarashi, T., Oyama, T & Saito, N. (2001). Experimental study on acidification potential of leachate from sedimentary rocks containing pyrite. J. Japan Soc. Eng. Geol. 42(4), pp. 214-221 (in Japan with English abstract)

JGS (Japanese Geotechnical Society). (2006) "JGS 2125-2006: Method for accelerated rock slaking test", Tokyo, Japan: JGS. See https://www.jiban.or.jp/pdf_count/JGS2125-2006E. pdf (accessed 23/11/2015).

JGS (Japanese Geotechnical Society). (2009) Test method for particle size distribution of soils, In Methods of tests of geomaterials and their explanations, ch. 4, pp. 115–136. Tokyo, Japan: JGS (in Japanese).

Jones, C. A. (1983) Effect of soil texture on critical bulk densities for root growth. Soil Sci. 58, pp. 1208-1211

Kikumoto, M., Muir Wood, D. & Russell, A. (2010). Particle crushing and deformation behavior. Soils Found. 50, No. 4, pp. 547–563.

Kikumoto, M., Putra, A.D. & Fukuda, T., (2016). Slaking and deformation behavior. Géotechnique. 66, No 9, pp. 771-785

Kiyota, T., Sattar, A., Konagai, K., Kazmi, Z. A., Okuno, D., & Ikeda, T. (2011). Breaching failure of a huge landslide dam formed by the 2005 Kashmir earthquake. Soils and Found. 51 No. 6, pp. 1179–1190.

Koncagul, E. C and Santi, P. M., (1999), The unconfined compressive strength of the Breathitt shale using slake durability, Shore hardness and rock structural properties, International Journal of Rock Mechanics and Mining Sciences 36, pp. 139-153

Ladd, C. C. (1960), Mechanism of Swelling by compacted clay, Highway Research Board Bulletin, abstract, p. 245

Lade, P. V., Liggio, C. D. Jr & Yamamuro, J. A. (1998) Effects of non-plastic fines on minimum and maximum void ratios of sand, Geotechnical Testing Journal, 21, No. 4, pp. 336–347.

Laidler, K. J.& Meiser, J.H. (1982). Physical Chemistry. Benjamin/Cummings. ISBN 0-8053-5682-7

Luzzani, L. & Coop, M. R. (2002). On the relationship between particle breakage and the critical state of sands. Soils. Found. 42, No.2, pp.71-82

Kusumi, H., Mine, Y., & Nishida, K. (1996). Research on shear behavior accompanying cyclic

wetting and drying of soft rock under constant shear loading. The annual conferences of the Japan Society of Civil Engineers, 3A No. 51, pp. 670–671.

Marques, E.A.G., Barroso E.V., Menezes Filho A.P. and Vargas Jr. E. do A. (2010) Weathering zones on metamorphic rocks from Rio de Janeiro—Physical, mineralogical and geomechanical characterization, Engineering Geology, 111 (1-4), pp. 1-18

McDowell, G. R., Bolton M. D. & Robertson, D. (1996). The fractal crushing of granular materials. J. Mech. Phys. Solids. 44, pp. 2079–2101.

Miura, N. & O-Hara, S. (1979). Particle-crushing of a decomposed granite soil under shear stresses. Soils Found. 19, No. 3, pp. 2–14.

Mochizuki, A., Kataoka, M., Sakaguchi, O. & Terashita, M. (1994). Study on speed of weathering of slate by exposure test and cyclic wetting and drying test. the Soil Engineering Society of Japan. 34 No. 4, pp. 109–119.

Moriwaki, Y. (1974). Causes of slaking in argillaceous materials. PhD dissertation, Department of Civil Engineering, University of California at Berkeley, CA, USA.

Muir Wood, D & Maeda, K. (2008). Changing grading of soil: effect on critical states. Acta Geotechnica 3, pp. 3-14

Nakai, T. & Hinokio, T. (2004). A simple elastoplastic model for normally and over consolidated soils with unified material parameters. Soils Found. 44 No. 2, pp. 53–70.

Nakano, R. (1967). On weathering and changes of properties of Tertiary mudstone related to landslide. Soils Found. Vol. 7, No. 1, pp. 1–14.

Nakano, M., Asaoka, A., & Constantinescu, D.T. (1998) Delayed compression and progressive failure of the assembly of crushed mudstones due to slaking. Soils Found. Vol 38, No. 4, pp. 183–194.

NEXCO-RI (Nippon Expressway Company Research Institute Limited). (2012) “Accelerated rock slaking test (NEXCO 110-2012)”, In NEXCO testing method, series 1: testing method on soils, 42 –45. Tokyo, Japan: NEXCO-RI (in Japanese: 岩石の促進スレーキング試験方法).

Ollier, C. D. (1969). Weathering. Science, Vol 166, Issue 3905

Ohta T, Kiya H, Hattiri, S & Asakura, T. (2003) Elution characteristics of fresh mudstone from undergoing opening, Env. Rock Eng.: Proc. of the First Kyoto International Symposium on Underground Environment, Kyoto, Japan, 17-18 March 2003, Saito & Murata (eds). pp.125-130

Pappas, D. M. & Vallejo, L. E. (1997) The settlement and degradation of non-durable shales associated with coal mine embankments, International Journal of Rock Mech. Min. Sci. & Geo., 34, No. 3 –4, pp. 779–789.

Perry, E. F. & Andrews, D. E. (1984) Slaking modes of geologic materials and their impacts on embankment stabilization, Trans. Res. Rec. 873, pp. 15-21

Pettijohn, F.J. (1975) Sedimentary Rocks. 2nd Edition, Harper and Row Publishers, New York

Piccolroaz, A., Bigoni, D. & Gajo, A. (2006). An elastoplastic framework for granular materials becoming cohesive through mechanical densification. Part I-small strain formulation. European J. of Mech. A/Solids 25, pp. 334–357

Predicted and Actual Ground Behavior Editorial Committee. (1996). Predicted and Actual Ground Behavior (Geotechnology, Working Series 2), Japanese Geotechnical Society.

Roberts, J. E. & de Souza, J. M. (1958). The compressibility of sands. Proc. of the American Society for Testing and Materials. 58, pp. 1269–1277.

Rocchi, I. & Coop, M. R. (2015) The effects of weathering on the physical and mechanical properties of a granite saprolite, Géotchnique, 65, No. 6, 482–493, http://dx.doi.org/10.1680/ geot.14. pp..177.

Sadisun, I. A., Shimada, H., Ichinose, M. & Matsui, K. (2005). Study on the physical disintegration characteristics of Subang claystone subjected to a modified slaking index test. Geotech. Geol. Engng 23, No. 3, pp. 199–218.

Santi, P. M. (2006) Field methods for characterizing weak rock for engineering, Env. & Eng. Geo., XII, No. 1, pp. 1–11.

Santi, P. M. & Koncagul, E. C. (1996) Predicting the mode, susceptibility, and rate of weathering of shales, In Design with residual materials in geotechnical and construction considerations (ed. G. Matheson), ASCE Geotechnical Special Publication No. 63, pp. 12–27. Reston, VA, USA: ASCE.

Santos, H., Diek, A., Roegiers, J.C., & Fontoura, S. (1996). Can shale swelling be (easily) controlled. ISRM International Symposium, Italy,

Sattar, A., Konagai, K., Kiyota, T., Ikeda, T. & Johansson, J. (2011) Measurement of debris mass changes and assessment of the dam-break flood potential of earthquake-triggered Hattian landslide dam, Landslides, 8, No. 2, 171–182.

Sato, T., Itabashi, I. & Kawamura, M. (1994). Method of organizing mudstone particle refinement by cyclic wetting and drying and test results. Reports of the Japan Society of Civil Engineers. 487, pp. 69–77.

Schaefer, V. R. & Birchmeir, M. A. (2013) Mechanisms of strength loss during wetting and drying of Pierre shale, Proceedings of the 18th international conference on soil mechanics and geotechnical engineering, Paris, France, pp. 1183–1186.

Schmitt, L., Forsans, T & Santarelli, F.J. (1994). Shale testing and capillary phenomena. Int. J of Rock Mech. & Min.Sci. & Geomech. 31 pp. 411-427

Seedsman, R. W. (1986), The Behavior of Clay-shales in water, Canadian Geotechnical Journal, 23, pp. 18-22.

Shamburger, J. H., Patrick, D. M. & Lutten, R. J. (1975) Design and construction of compacted shale embankments, Vol. 1 Survey of problems areas and current practices, Interim Report, Washington, DC, USA: Federal Highway Administration, Offices of Research and Development.

Sharma, K. (2012). Slaking characteristics of geomaterials in direct shear test. A Thesis for Master of Engineering, Department of Civil Engineering, Graduate School of Engineering, The University of Tokyo, Japan.

Shinjo, T. & Komiya, Y. (1978). Decline of strength of Shimajiri layer mudstone by cyclic wetting and drying. Technical Report of the University of the Ryukyus, Faculty of Agriculture. 25, pp. 307–323.

Shima, H. & Imagawa, S. (1980) The settlement of compacted soft rock-fragment sands the counter measure, Tsuchi-to-Kiso, JGS28, No. 7, pp. 45–52 (in Japanese).

Surendra, M., Lovell, C. W. & Wood, L. E. (1981) Laboratory studies of the stabilization of nondurable shales, Trans. Res. Rec. Journal 790, pp. 33 –40.

Taira A., Ohara, Y., Wallis, S., Ishiwatari, A & Iryu, Y. (2016). Geological evolution of Japan: an overview. In the Geology of Japan (ed. Moreno et.al), Geological Society, London pp. 1-24

Taylor, R. K. and Spears, D.A. (1970), The Breakdown of British Coal Measures Rocks, International Journal of Rocks Mechanics, Mineral and Sciences, 7, pp. 481 – 501

Taylor, R.K. and Cripps, J.C. (1987) Mineralogical Controls on Volume Change, pp. 268–301

Taylor, K. G & Macquaker, J. H. S. (2014). Diagenetic alterations in a silt- and clayrich mudstone succession: an example from the Upper Cretaceous Mancos Shale of Utah, USA. Journal of Clay minerals. Vol. 49. Pp. 213-227

Vallejo, L. E., Welsh, R. A., Lovell, C. W. & Robinson, M. K. (1993) The influence of fabric and composition on the durability of Appalachian shales, In Rock for erosion control (eds C. H. McElroy and D. A. Lienhart), ASTM Special Technical Publication (STP) 1177, pp. 15–28. Philadelphia, PA, USA: American Society for Testing and Materials.

Vallejo, L. E. & Murphy, S., A. (1999) Fractal pores and the degradation of shales, In Fractals: theory and applications in engineering (eds M. Dekking, J. Levy-Vehel, E. Lutton and C. Tricot), chapter 15, pp. 229–243. London, UK: Springer.

Vallejo, L. E. & Pappas, D. (2010) Effect of nondurable material on settlement of embankments, Trans. Res. Rec. Journal 2170, pp. 84 –89.

Walkinshaw, J. L. & Santi, P. M. (1996) Shales and other degradable materials. In Landslides: investigation and mitigation (eds A. K. Turner and R. L. Schuster), Special Report 247, ch. 21, pp. 555–576. Washington, DC, USA: Transport Res. Board, National Research Council, National Academy Press.

Welsh, R. A., Vallejo, L. E., Lovell, C. W. & Robinson, M. K. (1991) The U.S. Office of Surface Mining (OSM) proposed strength-durability classification system. In Detection of and construction at the soil/rock interface (eds W. F. Kane and B. Amadei), ASCE Geotechnical Special Publication No. 28, pp. 125–140. New York, NY, USA: ASCE.

Yamaguchi, H., Yoshida, K., Kuroshima, I. & Fukuda, M. (1989). Slaking phenomenon of Tertiary mudstone. Soils Found. 37 No. 4, pp. 5–10.

Yasuda, S., Yokota, S., Nakamura, H. & Inou, K. (2012) Reduction of static and dynamic shear strength due to the weathering of mudstones, Proceedings of the 15th world conference on earthquake engineering, Lisbon, Portugal, pp. 4–11.

Yoshida, N., Enami, K. & Hosokawa, K. (2002). Staged compression-immersion direct shear test on compacted crushed mudstone. J. Test. Evaluation 30, No. 3, pp. 239–244.

Yoshida, N. & Hosokawa, K. (2004). Compression and shear behavior of mudstone aggregates. J. Geotech. Geoenviron. Engng, ASCE 130, No. 5, pp. 519–525.

Yamaguchi, H., Yoshida, K., Kuroshima, I. & Fukuda, M. (1990). Triaxial shear properties of Triassic mudstone crushed by slaking. Soils Found. 38 No. 1, pp. 59–66.

Yasuda, S., Yokota, S., Nakamura,H &Inou, K. (2012). Reduction of static and dynamic shear strength due to the weathering of mudstones. Proceedings of the 15th world conference on earthquake engineering, Lisbon, Portugal, pp. 4–11.

Zlatovic, S. & Ishihara, K. (1995) On the influence of non-plastic fines on residual strength in Earthquake geotechnical engineering (ed. K. Ishihara), vol. 1, pp. 239–244. Rotterdam, the Netherlands: Balkema.